Design and Synthesis of some CYP26 and CYP24 Inhibitors as Indirect Differentiating Agents for Prostate and Breast Cancer

A Thesis submitted to the University of Wales for the Degree of

Doctor of Philosophy

by

Mohamed Sayed Mohamed Gomaa

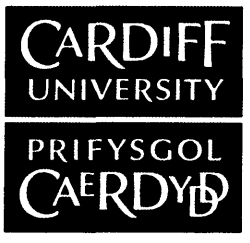

February 2008

Medicinal Chemistry Division, Welsh School of Pharmacy,
Cardiff University

Supervisors: **Dr. Claire Simons**
Dr. Andrea Brancale

ProQuest LLC
789 East Eisenhower Parkway
P.O. Box 1346
Ann Arbor, MI 48106-1346

Declaration

This work has not previously been accepted in substance for any degree and is not being concurrently submitted in candidature for any degree.

Signed. Mohamed Osman (candidate)

Date.....26/02/2008

STATEMENT 1

This thesis is being submitted in partial fulfillment of the requirements for the degree of PhD.

Signed. Mohamed Osman (candidate)

Date...26/02/2008.

STATEMENT 2

This thesis is the result of my own independent work/investigation, except where otherwise stated. Other sources are acknowledged by explicit references.

Signed Mohamed Osman (candidate)

Date....26/02/2008

STATEMENT 3

I hereby give consent for my thesis, if accepted, to be available for photocopying and for inter-library loans after expiry of a bar on access approved by the Graduate Development Committee.

Signed. Mohamed Osman (candidate)

Date....26/02/2008..

Acknowledgments

I dedicate this work to all people in the UK and back home who have contributed in different ways to the development and progress of this piece of work with their help, support and kind attention.

First and foremost I would like to thank my supervisor, Dr. Claire Simons, for her guidance, encouragement and support throughout my work during the past three years and for giving me all the opportunities to experience and to work in her group.

I am also indebted to my supervisor, Dr. Andrea Brancale, for his Knowledge, advice and constant support throughout my thesis.

I would like to thank the Egyptian Ministry of Higher Education especially the Mission department for financial support and funding of this work. I am also grateful to the Egyptian Embassy and Culture Bureau in London for their continuous support and supervision.

I would like to thank all members at the Welsh School of Pharmacy, Cardiff University, including Scientific staff, Technical staff, Friends and Colleagues for their kind help and pleasant company.

Finally, the greatest appreciation goes to my Wife, Son, Mother and Father. Their constant love, inspiration and encouragement are immeasurable.

Abstract

Prostate and breast cancer are a leading cause of death all over the world. Retinoic acid and vitamin D_3 play an important role in cellular proliferation and differentiation and as such have potential therapeutic value as differentiating agents in the treatment of cancer and hyperkeratinising diseases.

The focus on the development of differentiation agents for the treatment of solid tumours, e.g. prostate and breast cancer, was stimulated by the ability of ATRA to inhibit cellular growth and restore normal differentiation of neoplastic cells, ATRA was also shown to be successful in the treatment of acute promelocytic leukemia. The use of differentiating agents to suppress prostate and breast cancer cell proliferation is now one of the new therapeutic strategies. However, the use of ATRA and vitamin D_3 as differentiating agents is limited by their rapid metabolism through the self induction of the cytochrome P450 enzymes that are involved in their catabolism. The P450 enzymes responsible for the metabolism of ATRA and 1α, 25-$(OH)_2$-D_3 (calcitriol) are cytochrome P450 26 (CYP26A1) and cytochrome P450 24 (CYP24A1) respectively. Therefore the use of potent and selective inhibitors of CYP26A1 or CYP24A1 with ATRA or 1α, 25-$(OH)_2$-D_3 respectively may be a new strategy for the treatment of prostate and breast cancer.

To date, the crystal structures of human CYP26A1 or CYP24A1 have not been resolved and there is no single theoretical model published.

Homology models of cytochrome P450 RA1 (CYP26A1) and cytochrome P450 24 (CYP24A1) were constructed using three human P450 structures, CYP2C8, CYP2C9 and CYP3A4 as templates for the model building. Using MOE software the lowest energy CYP26A1 and CYP24A1 models were then assessed and showed good stereochemical quality and side chain environment comparable with the templates. Further active site optimisation of the CYP26A1 and CYP24A1 models built using the CYP3A4 template was performed by molecular dynamics using Gromax software to generate final CYP26A1 and CYP24A1 models.

The docking studies carried out on the final models showed that the models accommodated the natural substrates ATRA and vitamin D_3 as well as the potent inhibitors R115866 and (*R*)-VID-400 for CYP26A1 and CYP24A1 respectively.

To design inhibitors as potent as R115866 and VID-400, for CYP26A1 and CYP24A1 respectively, the virtual screening of a designed library of compounds based on the structure of potent inhibitors, natural substrate and intuition was performed. The results revealed good interaction with the active site of several compounds and therefore potentially good CYP26A1 and CYP24A1 inhibition activity.

Two series were synthesised for CYP26A1 inhibition, including α substituted 4-(1,2,4)triazol- and imidazol-1-ylmethylphenylaryl and heteroarylamine and aryl and heteroaryl substituted 3-(4-aminophenyl)-3-imidazol-1-yl-2,2-dimethylpropionic acid methyl ester derivatives. The synthesised compounds were biologically evaluated using a MCF-7 breast cancer cell assay, from which some have shown potent inhibitory activity, with IC_{50} in the low nanomolar range (20 nM), and others less active but still much more active then the well known inhibitor liarozole.

A series of 4 or 5 substituted 1-(3-benzenesulfonylpropyl)-1*H*-indoles was synthesised and biologically tested for CYP24A1 inhibition. The series showed moderate inhibition activity with a good structure-activity relationship, for further evaluation.

List of papers

The following publications have arisen from this thesis. The full articles are referred to in Appendix.

1. Yee, S.W.; Jarno, L.; Gomaa, M.S.; Elford, C.; Ooi, L.; Coogan, M.P.; McClelland, R.; Nicholson, R.I.; Evans, B.A.J.; Brancale, A. and Simons, C. Novel tetralone-derived retinoic acid metabolism blocking agents: Synthesis and *in vitro* evaluation with liver microsomal and MCF-7 CYP26A1 cell assays. *Journal of Medicinal Chemistry*, **2005**, (48), 7123-7131.

2. Gomaa, M.S.; Yee, S.W.; Milbourne, C.E.; Barbara, M-C., Simons, C. and Brancale, A. Homology model of human retinoic acid metabolising enzyme cytochrome P450 26A1 (CYP26A1): active site architecture and ligand binding. *Journal of Enzyme Inhibition and Medicinal Chemistry*, **2006**, (21), 361-369.

3. Gomaa, M.S.; Simons, C. and Brancale, A. Homology Model of 1,25-dihydroxyvitamin D_3 24-hydroxylase Cytochrome P450 24A1 (CYP24A1): Active Site Architecture and Ligand Binding. *Journal of Steroid Biochemistry and Molecular Biology*, **2007**, (104), 53-60.

4. Gomaa, M.S.; Armstrong, J.L.; Bobillon, B.; Veal, G.J.; Brancale, A.; Redfern, C.P.F. and Simons, C. Novel azolyl-(phenylmethyl)aryl/heteroarylamines: potent CYP26 inhibitors and enhancers of all-*trans* retinoic acid activity in neuroblastoma cells. *Bioorganic and Medicinal Chemistry*, **2008**, in Press.

Abbreviations

Abbreviation	
AP-1	Activator protein-1
APL	Acute promyelocytic leukaemia
ATRA	All-*trans* retinoic acid
BLAST	Basic local alignment search tool
BRCA	Breast cancer antigen
CDI	Carbonyldiimidazole
CRABP	Cellular retinoic acid binding protein
CRBP	Cellular retinol binding protein
CYP	Cytochrome P450
3D	Three-dimensional
DBD	DNA binding domain
DCM	Dichloromethane
DCIS	Ductal carcinoma *in situ*
DES	Diethylstilbestrol
DNA	Deoxyribonucleic acid
DRE	Digital rectal examination
EBI	European bioinformatics institute
EIC	Extensive intraductal component
EMBL	European molecular biology laboratory
ER	Oestrogen receptor
EtOAc	Ethyl Acetate
EXPASY	Expert protein analysis system
HPLC	High performance liquid chromatography
4-HPR	*N*-(4-hydroxyphenyl)-retinamide
HRMS	High resolution mass spectroscopy
LH	Leutinizing hormone
LHRH	Luteinizing hormone-releasing hormone
LRAT	Lecithin retinol acyl transferase

MOE	Molecular operating environment
MeOH	Methanol
MS	Mass spectroscopy
NADPH	Nicotinamide-adenine dinucleotide phosphate (reduced form)
NCBI	National centre for biotechnology information
NMR	Nuclear magnetic resonance
25-(OH)-D_3	25-hydroxyvitamin D_3
1α,25$(OH)_2D_3$	1α,25-Dihydroxyvitamin D_3 (Calcitriol)
PDB	Protein data bank
PSA	Prostatic specific antigen
PSMA	Prostatic specific membrane antigen
PTH	Parathyroid hormone
RA	Retinoic acid
RAMBAs	Retinoic acid metabolism blocking agents
RARE	Retinoic acid receptor response element
RARs	Retinoic acid receptors
RE	Retinyl esters
ROH	Retinol
RP	Radical prostectomy
RXRs	Retinoid X receptors
SERMs	Selective oestrogen receptor modulators
SHBG	Sex-hormone binding globulin
SIB	Swiss institute of bioinformatics
t.l.c.	Thin layer chromatography
TRUS	Transrectal ultrasound
VDR	Vitamin D receptor
VDRE	Vitamin D receptor response element
v/v	volume/volume
WHO	World health organization

Table of Contents

Chapter 1

Introduction

1 Introduction

1.1 Prostate cancer

1.1.1 Incidence

Prostate cancer is a leading cause of cancer-related deaths in many countries. Premalignant lesions and invasive cancer occur more frequently in the prostate than in any other organ other than the skin (Jemal *et al.*, 2005). Prostate cancer is the most common malignancy among males in the US, with 230,110 new cases and 29,900 deaths for the year 2003-2004 alone (Jemal *et al.*, 2004). Prostate cancer was the third most common cancer in men in Europe (Bray *et al.*, 2002), and in the USA (Ferlay *et al.*, 2001; Powell, 2007). Prostate cancer is the most common cause of death among men after lung cancer and before large bowel and rectum cancers (WHO, 2003). 10% of men over 50 years old will develop prostate cancer and 3 - 4 of every 100 men will die from prostate cancer, with 40,000 deaths per year in the USA (Lynn *et al.*,1999). Yet, the incidence of clinically detected prostate cancer is much lower than the histopathological incidence.

1.1.2 Unique features of prostate cancer

Prostate cancer, perhaps more than any other type of cancer, has features that lend themselves to control of progression. Autopsy studies show that cancer begins to arise in the prostate as early as the 3rd decade of life (Sakr *et al.*, 1993), yet most men are not diagnosed with clinically evident prostate cancer until they are in their 60's (Abbas and Scardino, 1997). This fact shows that prostate cancer progresses slowly and therefore should offer a wide window of opportunity for control strategies. Men over 50 have about a 40% chance of having cancer in the prostate regardless of nationality, race or ethnicity (Abbas and Scardino, 1997). Therefore, the initiation of prostate cancer probably occurs somewhat similarly around the world as far as is known, but progression to a clinically detectable state differs. The discrepancy between the frequency of latent and clinically manifest cancer is presumably due to some variation in factors that control progression. An examination of the natural history of the natural histopathogenesis of prostate cancer also shows several points at which progression could be controlled. The initial event in the conversion of normal prostatic epithelium to

cancer is considered to be the development of dysplasia, also known as prostatic intraepithelial neoplasia (PIN) (McNeal and Bostwick, 1986). Dysplasia occurs very frequently in the prostate and first appears in men in their 30's (Sakr *et al.*, 1993). Invasive prostate cancer has been observed emerging directly from dysplastic lesions (McNeal *et al.* 1991). This then is one point of potential control, if progression of normal epithelium to dysplasia could be prevented, then presumably the incidence of invasive prostate cancer would be decreased. Well-differentiated invasive prostate cancer is classified as grade 3 in the widely used Gleason grading system (Gleason, 1977). Cancer at this stage is seemingly curable. If however, grade 4 or 5 (poorly differentiated cancer) was present then the rate of recurrence was directly proportional to the percentage of grade 4/5 cancer (Stamey *et al.*, 2000). Therefore, another point of control would be prevention of progression of grade 3 cancer (curable) to grade 4 (not curable by surgery).

1.1.3 Risk factors

There are a number of acknowledged and potential risk factors. Clinical research concerning these risk factors has been well documented and include:

1) Age (Chan *et al.*, 1998; Peehl and Feldman, 2003; Vickers, 2007).

2) Race (Hsing *et al.*, 2000; Narod, 1999; Boring *et al.*, 1992; Pienta and Esper, 1993; Peehl and Feldman, 2003).

3) Family history (Carter *et al.*, 1992; Cotter *et al.*, 2002).

4) Diet (Cohen *et al.*, 2000; Giovannucci, 1999; Heinonen *et al.*, 1998; Schwartz and Hulka, 1990; Adlercreutz, 2002; Jacobsen *et al.*, 1998; Shirai *et al.*, 2002; Wang *et al.*, 2002; Vickers, 2007).

5) Hormones (Wilding, 1995; Gann *et al.*, 1996; Pienta and Esper, 1993; McLeod, 2003; Vickers, 2007).

1.1.4. Diagnosis, staging and clinical evaluation of prostate cancer

The prostate gland is a small organ situated at the base of the penis just below the bladder and in front of the rectum (**Figure 1.1**).

In the past prostate cancer was diagnosed based on the development of symptoms caused by progression of the disease. This included invasion of the cancer to

local tissues or metastasis to other areas of the body such as the bone (Kirby *et al.*, 1998; Kirby, 2002). Today, however, new diagnostic measures allow the disease to be detected at an asymptomatic stage much earlier in the course of the disease (Kirby, 2002; Linton and Hamdy, 2003).

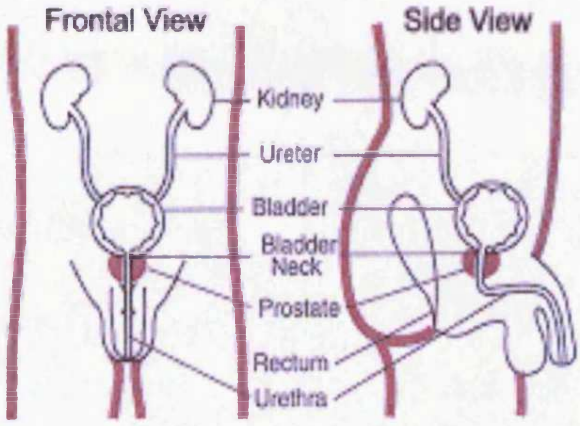

Figure 1.1: The location of the prostate gland in males (South california prostate cancer institute, 2003, http: www.scprostatecancer.com/prostate_cancer/antomy.htmL)

Early diagnosis of prostate cancer is important, when the disease is detected at an early stage, the prognostic factors, the rate of mortality and morbidity can be greatly improved (Wink *et al.*, 2007). The presenting features for prostate cancer is a result of urinary tract obstruction due to the enlarged prostate gland. The patient will be complaining of nocturia, increase in urination frequency and urgency. Patients can by asymptomatic during the early stage; therefore screening for prostate cancer by the Prostate-Specific Antigen (PSA) testing is very important.

The first stage of diagnosis of prostate cancer is to carry out a Digital Rectal Examination (DRE) and to measure serum PSA levels. If there are suspicious findings from either of these tests, transrectal ultrasound technology will be used to allow histological confirmation of the presence of prostate cancer (Wink *et al.*, 2007).

1.1.5 Treatment and management of prostate cancer

Patients with newly diagnosed prostate cancer as well as their doctors need to make a very difficult decision regarding the treatment. This is due to variable course, unpredictable prognosis and limited choices (Onel *et al.*, 1998). A practical approach to management of the disease is to adapt treatment to the individual patient (Wang *et al.*, 2007). In each case, therapy will be decided by considering the patients age, co-

morbidity, life anticipation, personal preference, clinical stage, tumour grade and the potential benefits and risks of any treatment modality (Henry *et al.*, 1999).

Table 1.1: (Kirby *et al.*, 1998): the clinical stage of prostate cancer and the corresponding presenting symptoms.

Stage of prostate cancer	Presenting symptoms
Local disease	Elevated PSA, weak urine stream, sensation of incomplete emptying of bladder, frequency of urination, urgency of urination and urinary tract infection
Locally invasive disease	Haematuria, dysuria, perineal and suprapubic pain, impotence, incontinence, symptoms of renal failure haemospermia and rectal symptoms including tenesmus.
Metastatic prostate cancer	Bone pain, paraplegia secondary to spinal cord compression, lymph node enlargement, anuria due to obstruction of the ureters by lymph nodes, lethargy, weight loss and cutaneous and bowel haemorrhage.

There are four main methods to manage prostate cancer (Small, 1998) which are being used depending on previous mentioned conditions:

1.1.5.1 Radical prostectomy (RP)

This surgical operation is to remove the entire prostate gland plus some of the surrounding tissue. The main advantage of radical prostatectomy (RP) is to allow the surgeon to assess pathological disease of the patient, *i.e.* to assess the extent to which the cancer has spread. This could guide the physician as to whether to give any other adjuvant therapy to the patient (Ohori *et al.*, 1995).

RP is being performed more frequently on younger men with earlier stage disease. The operation is now performed more rapidly with less blood loss, and the surgical pathology outcome end points and early disease-free survival are improved (Moul *et al.*, 2002). Currently, radical prostatectomy should only be offered to fit, physically active men with early stage prostate cancer and at least 10 years life expectancy (Zincke *et al.*, 1994). These patients should have a negative bone scan and tumours confined to the prostate gland (stages 1 and 2) (Catalona, 1990; Fletcher - andtheodorescu, 2005).

1.1.5.2 Radiotherapy

High-energy rays or particles are used in radiation therapy to kill cancer cells. There are two main types of radiation therapy:

- External-beam radiotherapy and
- Brachytherapy

External-beam radiation therapy

Studies on the use of external-beam radiation therapy have been carried out extensively for early-stage prostate cancer (Hanlon and Hanks, 2000; Shipley *et al.*, 1999; Zagars *et al.*, 1997; Zietman *et al.*, 1995). External-beam radiation therapy has undergone a technological revolution, and as a result, it appears promising in increasing success rate and reduction of side effects (Fletcher andtheodorescu, 2005). Various randomised trials have been carried out in various centres using external-beam radiation, the results were positive (Koper *et al.*, 1999).

Brachytherapy

This technique uses small radioactive pellets and these are implanted directly into the prostate gland (The Prostate Cancer Charity, 2003). Transrectal ultrasound, CT scans or MRI is used to guide the placement of the radioactive material. The exact dose of radiation needed will be calculated by a special computer programme (The Prostate Cancer Charity, 2003).

Overall advantages of radiation therapy – It is a non-invasive method, with no anaesthesia risk. It could be available to a wide spectrum of patients with prostate cancer, and especially to those who would not be able to tolerate prostatectomy (Jani and Hellman, 2003). Radiation therapy allows localised dose distribution and brachytherapy provides a more localised dose distribution compared with external-beam radiation therapy (Vicini *et al.*, 1999)

1.1.5.3 Hormone therapy

Treatment for locally or advanced disease rely on hormonal therapies to suppress testosterone production (Scherr *et al.*, 2003; D'Amico *et al.*, 2007).

Randomised trials have been carried out to evaluate the effect of neoadjuvant hormonal therapy on prostate cancer treated with radical prostatectomy (Yu and Oh, 2003) as well as with radiotherapy (Laverdiere *et al.*, 1997; Pilepich *et al.*, 2001).

The available hormonal therapies could be divided into 4 groups

Oestrogen therapy

Oestrogen therapy in the form of diethylstilbestrol (DES) (**Figure 1.2**) was the earliest form of treatment for advanced prostate cancer in the 1980's (Scherr *et al.*, 2002). Diethylstilbestrol was among the first non-steroidal compound with potent oestrogenic activity (Dodds *et al.*, 1938).

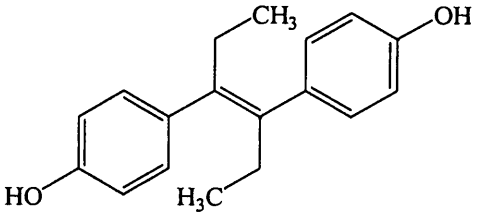

Diethylstilbestrol (DES)

Figure 1.2: The chemical structure of Diethylstilbestrol.

DES has an effect on suppressing the production of testosterone. The use of DES has fallen out of favour due to the unfavourable side-effects (Zagars *et al.*, 1988).

Luteinizing Hormone-Releasing Hormone (LHRH) Agonist

Luteinizing Hormone-Releasing Hormone (LHRH) was first isolated by Schally and his co-workers (Schally *et al.*, 2000) from porcine hypothalamic extracts. They demonstrated that this decapeptide is responsible for the release of luteinizing hormone (LH). The mode of action of a LHRH agonist is to down regulate the LHRH receptors at the pituitary level, thus decreasing the release of testosterone (Limonta *et al.*, 2001). A review has anticipated that LHRH may exert direct anti-proliferative and apoptotic effects in prostate cancer cells (Kraus *et al.*, 2005). LHRH analogues have an increasing role in locally advanced and metastatic prostate cancer (Scherr *et al.*, 2003).

Anti-androgen therapy

Anti-androgen drugs, for example, flutamide, bicalutamide (Casodex®) and cyproterone acetate (**Figure 1.3**), are used in patients with locally advanced disease (Kolvenbag *et al.*, 2001). The function of anti-androgens is to block the androgen receptor and thus prevent the natural androgen substrate from binding to the androgen receptor (D'Amico *et al.*, 2007). Androgen plays an important role in the pathology of

prostate cancer by inducing growth of the prostate cancer cells (Debes and Tindall, 2002).

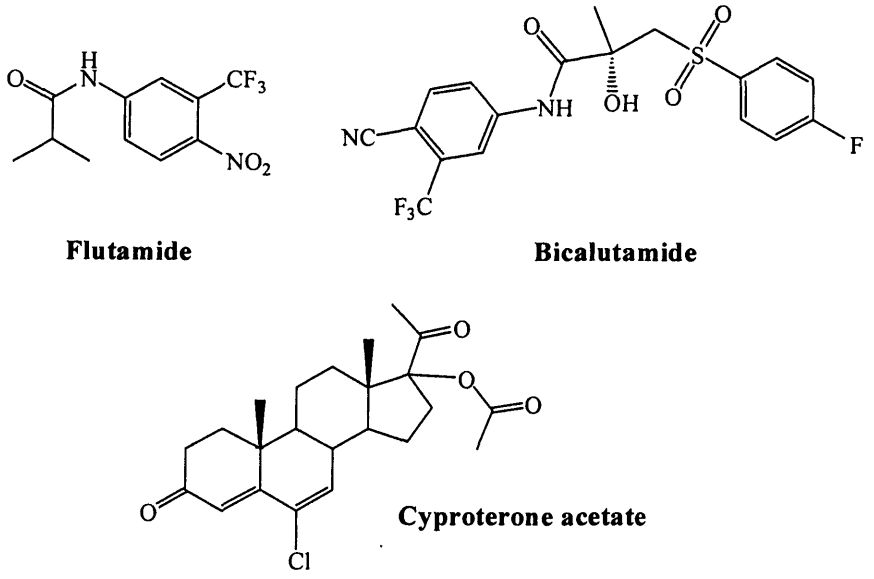

Figure 1.3: The chemical structure of anti-androgen therapy used in locally advanced prostate cancer.

Monotherapy with 150 mg bicalutamide (Casodex®) has shown an equivalent effect to castration in patients with non-metastatic disease (Abrahamsson, 2001; Chodak *et al.*, 1995; Iversen *et al.*, 2000; Kolvenbag *et al.*, 2001). However, anti-androgens are not recommended in conjunction with surgical castration (Eisenberger *et al.*, 1998). The side-effects profile for bicalutamide is better in terms of quality-of-life related to sexual interest and physical capacity (Seidenfeld *et al.*, 2000).

Combined androgen blockade

This therapy involves the combination of an anti-androgen with a LHRH agonist to block androgen synthesis as well as preventing the binding of circulating androgen to the receptors. The use of LHRH analogues alone cannot block the androgen produced by the adrenal gland as the androgen produced from the adrenal gland is controlled by andrenocorticotropic hormone (ACTH). Therefore the use of the combined androgen blockade is to stop the action of the adrenal androgens (Chamberlain *et al.*, 1997; Dalesio *et al.*, 2000).

1.1.5.4 Chemotherapy

Although more than 85 % of patients with metastatic disease will respond to hormonal therapy, unfortunately, the prostate tumours eventually develop into

hormone-independent type. During the long term androgen deprivation, the tumour cells lose the capacity to undergo apoptosis and do not depend on androgen for survival (Brinkmann, 2001; Feldman and Feldman, 2001). In this situation, patients will not respond to hormonal therapy, and this is manifested by increasing PSA levels, worsening of symptoms and progressive disease on imaging studies.
One of the options for patients with hormone-independent prostate cancer is to use cytotoxic therapy (Oh and Kandoff, 1998; Scherr *et al.*, 2003).

The commonly used chemotherapy agents are mitoxantrone with prednisolone and estramustine (Skladanowski and Konopa, 2000; Dyrstad, *et al.*, 2006). More recent agents have progressed to phase (II) clinical trials including sorafenib for patients with progressive hormone-refractory prostate cancer (Steinbild *et al.*, 2007) and bortezomib combined with prednisolone for castration resistant metastatic prostate cancer (Morris *et al.*, 2007).

1.2 Breast cancer

1.2.1 Epidemiology

Breast cancer is an extremely important and common disease in the world especially in western countries. According to the World Health Organization (WHO) report updated in June 2003, there are nearly 1,000,000 new cases of breast cancer each year with 370,000 deaths among them (Ferlay *et al.*, 2001; WHO, 2003). In the United States, breast cancer accounts for over 180,000 new cases each year and approximately one quarter of them die of breast cancer (Key *et al.*, 2001). While, in 2005, an estimated 211,240 new cases of breast cancer will be diagnosed with 40,410 women expected to die from breast cancer (Jernal *et al.*, 2005). However, a report from the American cancer society finds that the breast cancer death rate in the United States continues to drop more than two percent per year, a trend that began in 1990 and is credited to progress in early detection and treatment (American cancer society, 2007). Breast cancer affects more than 41,000 women in the UK every year with 16,000 deaths each year (anonymous, 2007). Until the late 1980's the mortality rates were increasing by about 1% per year. Since then however the mortality rates have fallen by over 10% and improvements in adjuvant therapy and in screening for early detection of breast cancer

are believed to be the two main causes of this decline (Bundred, 2001; Brewster and Helzlsouer, 2001). The incidence and mortality rates from breast cancer vary significantly around the world, presenting 5-10 fold variation (Hulka *et al.*, 2001). Breast cancer is far more common in the United States, Canada and Europe than in Asia and in black Africa (Key *et al.*, 2001). In the developed countries, the risk of breast cancer is very high with a lifetime risk of developing the disease of one in eight (ECCO 11, 2000). A report of WHO represents 5 fold variation between the incidence of breast cancer in more developed countries and those in less developed countries (WHO, 2003). These facts would suggest that there is possibly some genetic or environmental causes for the disease (Hopper, 2001).

1.2.2 Risk factors

The two most important identified risk factors for breast cancer are gender and age (Hayes, 2000; Okobia *et al.*, 2006). Of course breast cancer is uncommon in men and accounts only for 0.8 percent of all breast cancers (Giordano *et al.*, 2002). Moreover, the incidence of breast cancer increases with age (Kessler, 1992). Unfortunately, more than 70 percent of women over the age of 50 who have breast cancer do not have any other remarkable risk factor (Hayes, 2000; Hulka *et al.*, 2001). Therefore, although risk factors other than age and gender have been investigated, they account for only a few percent of patients with breast cancer (Uauy and Solomons, 2005). Risk factors:

Family history/genetic factors (Thompson, 1994; Bergfeldt *et al.*, 2002; Miki *et al.*, 1994; Schwab *et al.*, 2002; Hopper, 2001; Hulka *et al.*, 2001; Okobia *et al.*, 2006), endogenous oestrogens (Key *et al.*,1997 and 2001; Rang *et al.*,1995; Buzdar, 2001; Parker and Franks, 1997; Jonat, 2001; Wakeling, 2000; Kuller *et al.*, 1997; Hulka *et al.*, 1995; Rao, 2000; Helewa *et al.*, 2002; Newcomb *et al.*, 1994; Helewa *et al.*, 2002; Okobia *et al.*, 2006), diet (Hunter *et al.*, 1996; Wu *et al.*, 2002; Franceschi 1997; Bohlke *et al.*, 1999; Uauy and Solomons, 2005) and other factors such as alcohol consumption and cigarette smoking (Lenz *et al.*, 2002; Uauy and Solomons, 2005).

1.2.3 Development and progression

It is probable that the origin of breast cancer is multifactoral, with genetic (Hopper, 2001; Okobia *et al.*, 2006), natural metabolic (Chajes *et al.*, 1999; Uauy and Solomons, 2005; Okobia *et al.*, 2006) and environmental components (Silva Idos, 2002; Uauy and Solomons, 2005). A reasonable model might include an inherited genetic weakness resulting in the development of breast cancer for example, inheritance of one or more abnormal recessive oncogenes such as BRCA1 and 2 (Warmuth *et al.*, 1997) which, when coupled with exposure to a particular environmental factor such as diet, alcohol or smoking (Silva Idos, 2002, Uauy and Solomons, 2005), leads to the development of a malignant clone of cells (Hayes, 2000). Subsequent uncontrolled growth, invasion and metastases might then be the result of further exposure to factors that are not the only reason but rather support these behaviours on already transformed cells. These might include substances with growth-stimulating potential, such as endogenous oestrogens (Britton *et al.*, 2002).

1.2.4 Types of breast cancer and staging

The female breast (**Figure 1.4**) is composed of 15-20 sections, called lobes, with each lobe ending in many smaller lobules. These lobules further end in dozens of tiny bulbs which produce milk during lactation. The three components, lobes, lobules, and bulbs, are all linked together by thin tubes called ducts (mammary ducts) running throughout the breast. All the small ducts eventually come together to form larger ducts named as collecting ducts which empty to the outside through the nipple (Anonymous, 2005).

Staging of cancer disease is one of the most important tasks of clinical oncologists. It allows the preliminary diagnosis of the disease, starting the proper treatment on time and a prognostic evaluation of survival (Ravaioli *et al.*, 2000).

Although there are a number of types of breast cancer, they can be conveniently divided into two types:

- those that show no evidence of invasion (non-spreading types, stage 0).
- those that show signs of invasion or spread (spreading types, stages I-IV) (Ravaioli *et al.*, 2000)

It is thought that breast cancer starts as the non-spreading type, and later develops the ability to spread and invade as the cancer cells become more abnormal.

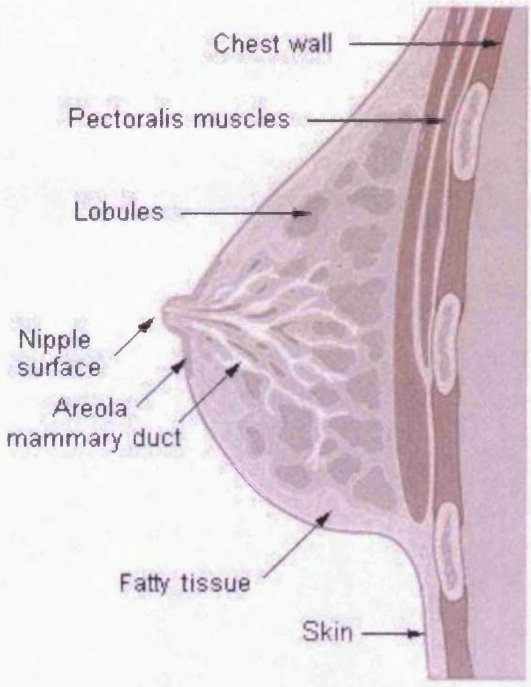

Figure 1.4: Diagram of breast anatomy (Anon, 2005)

Ductal Carcinoma *in situ* is the most well-known of the non-spreading cancers (Harris *et al.*, 2000). It is normally found during routine mammography or during breast screening. Of the invading types, (*i.e.* those cancers that can spread), the most common is Ductal Carcinoma. Not only is this the most common form of breast cancer but it also has the worst prognosis (Skinner, *et al.*, 2001). There are other forms of invasive breast cancers, typically described as the special types which are mostly benign.

1.2.5 Treatment of breast cancer

1.2.5.1 Surgery

Breast conservative surgery in order to remove a part of or whole of the breast in the case of breast cancer, so-called mastectomy, is considered in the following cases and being performed for the early stages of the breast cancer (i.e. stages I and II) (Hayes, 2000; Moulder and Hortobagyi, 2008):

1 Patient preference

2 Medical contraindication to radiotherapy

3 Pregnancy

4 Anticipated poor cosmetic result

5 Diffuse or multi-focal disease

Breast surgery requires careful evaluation of the prebiopsy mammogram, the presence or absence of extensive intraductal component (EIC) and the position of the tumour with respect to the margins of excision (Coburn *et al.*, 1995). When EIC is present, larger resections achieve smaller recurrence rate (Felippe *et al.*, 2007). When the tumour is EIC-negative, simple excision is quite satisfactory (Kurtz, 1992).

1.2.5.2 Radiotherapy

The breast-preserving treatment of early-stage invasive or non-invasive breast carcinoma at present uses a combination of conservative surgery for resection of the primary tumour with a close margin of totally normal breast tissue and radiation therapy for the eradication of remaining subclinical disease (Anonymous, 1998).

The radiation oncologist should optimise techniques and doses of radiotherapy in order to minimise the risk of local return and achieve excellent cosmetic results (Harris, 2001).

1.2.5.3 Chemotherapy

Chemotherapeutic agents interfere with essential cell processes, leading to cell death. None of these agents is specific for cancer cells and therefore all are toxic to normal cells as well. However, most of these agents work only when cells are in the active stages of the cell cycle. The most frequently associated side effects of chemotherapy are seen in normal organs with high cellular growth fractions such as suppression of bone marrow and gastrointestinal mucosal function and hair loss (Moulder and Hortobagyi, 2008).

Not all chemotherapeutic agents are active against breast cancer. The most active and therefore most commonly used chemotherapeutic drugs for breast cancer are listed in table **1.2** (Goodman *et al.*, 2001; Buzdar, 2007) (**Figure 1.5**).

Table 1.2: Active chemotherapeutic agents in breast cancer.

Class	Agent
Alkylating agents	Cyclophosphamide, L-phenylalanine mustard, Thiotepa, Mytomycin-C
Intercalators	Doxorubicin, Epirubicin, Mitoxantrone
Antimetabolies	Methotrexate, 5-Fluorouracil, Capecitabine

Tubulin interaction	Vinblastin, Vinorelbine, Paclitaxel, Docetaxel
Other	Gemcitabine

1.2.5.4 Endocrine therapy

Since hormone manipulations are relatively non-toxic when compared with alternative therapies, such as cytotoxic chemotherapy, they have become widely established as a preferred first-line therapeutic choice in many cancer management programs (Nicholson, 1993; Murta and Nomelini, 2007; Yu *et al.*, 2007). Among the numerous types of endocrine therapies available for the treatment of breast cancer, the majority of work has focused on anti-oestrogens, compounds designed to block the action of oestrogen in breast cancer cells through binding to oestrogen receptors present in hormone dependent tumours (Wakeling and Bowler, 1991). The most powerful reason for the response of breast cancer to hormonal therapy is the existence of oestrogen receptors in the tumour cells. Oestrogen receptors are present in approximately 35-55% of all breast tumours and in up to 80-90% of tumours of women older than 55 years (Kuerer *et al.*, 2001).

Of the antihormonal drugs currently widely employed in breast cancer therapy, the partial antioestrogen, now named selective oestrogen receptor modulator (SERM), tamoxifen is used (**Figure 1.5**). Tamoxifen was introduced in 1971 and has been for the past 30 years the most widely used anti-oestrogen for breast cancer treatment (Aapro, 2001; Yu *et al.*, 2007). It is most frequently used as first-line treatment in postmenopausal women (Bentrem *et al.*, 2002). More recently, the antiestrogenic effect of other antihormonal agent, 20s-protopanaxadiol and it's synergy with tamoxifen on breast cancer cells has been studied and has shown promising results (Yu *et al.*, 2007). Tamoxifen was found to block oestrogen binding to human oestrogen receptor (ER) (Jordan *et al.*, 1975) which might explain its mechanism against breast cancer where blockage of ER could play an important role in the therapy.

Use of tamoxifen in advanced breast cancer showed 30% response in unselected patients and 40-60% in patients with ER+ tumours (Osborne, 1998). Its use as an adjuvant to surgery on presentation of breast cancer has been demonstrated to improve breast survival rates by 25% in patients with ER+ disease (Tan and Swain, 2001).

Although it is clear that partial antioestrogens (SERMs) have been used with great success in the treatment of breast cancer, there is not evidence whether or not their

clinical activity is in any way limited by their oestrogen-like properties. Wakeling and Bowler carried out extensive structure–activity experiments that led to the discovery of a new drug class, the pure antioestrogens (Wakeling *et al.*, 1987). The principal compound ICI 164,384 was antioestrogenic in all target tissues and seemed to produce its effects by premature destruction of the ER (O'Regan *et al.*, 2002). These promising preliminary data were subsequently confirmed with the pure antioestrogen ICI 182,780 which was selected for clinical development (O'Regan *et al.*, 2002) but does not appear to be progressed.

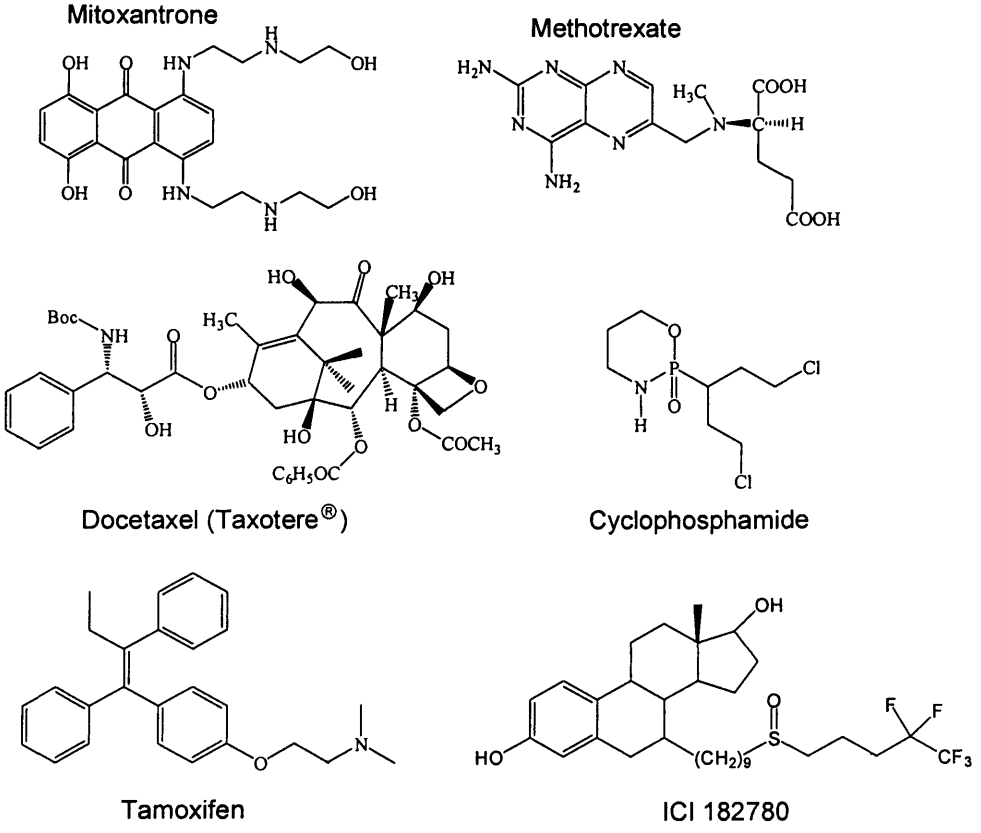

Figure 1.5: The chemical structure of the most commonly used chemotherapeutic and endocrine drugs for breast cancer

Another trend in endocrine therapy of breast cancer is inhibition of steroid production using cytochrome P450 aromatase inhibitors. P450 aromatase is the key enzyme in the conversion of androgens (androstene-3,17-dione and testosterone) to oestrogens (oestradiol and oestrone) *via* the loss of the C19 methyl group and the aromatisation of steroidal ring A (Brodie, 1985; Skinner and Akhtar, 1969; Steele *et al.*, 2006). Currently aromatase inhibitors are most frequently used as endocrine therapy in patients with locally advanced or metastatic disease in postmenopausal women (Assikis

et al., 2002; Briest and Davidson, 2007). Tamoxifen is still used as the first-line hormonal therapy for breast cancer of all stages. However, the aromatase inhibitors are becoming an important treatment alternative (Kuerer *et al.*, 2001; Steele *et al.*, 2006). According to clinical experiments, aromatase inhibitors have become established as the second-line therapy for postmenopausal women with advanced breast cancer progressing during tamoxifen therapy (Goss *et al.*, 2001; Howell, 2005). In addition, other clinical studies support the use of these agents as first-line therapy instead of tamoxifen (Assikis *et al.*, 2002).

Aromatase inhibitors are divided into two groups:

- Type I inhibitors which are steroidal and derivatives of androstenedione eg., exemestane (Clemett *et al.*, 2000; Steele *et al.*, 2006). These are irreversible inhibitors and have a long duration of action.
- Type II inhibitors (*e.g.*, animide) which are non-steroidal, largely phenylamines, imidazoles and triazoles, which are reversible competitive inhibitors of the enzyme (Smith *et al.*, 2001; Le Borgne *et al.*, 2007)

1.3 Retinoids

1.3.1 Biosynthesis and metabolism of retinoids

Retinoids are a group of compounds that refer to the natural forms of vitamin A as well as synthetic analogues. The main sources of vitamin A are dietary and are derived from provitamin A (carotenoids) found in vegetables or retinyl esters (RE) primarily obtained from animal sources (fish-liver oil) or by dietary supplements (Underwood, 1996). A number of the carotenoids can be converted in the intestine and liver to vitamin A, also known as retinol, after a central oxidative cleavage to retinal followed by reduction to retinol (Blaner and Olson, 1994). On the other hand, the retinyl esters are hydrolysed into retinol (ROH) by lipases or esterases in the intestine prior to absorption (Curely and Robarge, 1997). Retinol is then bound to the cellular retinol binding protein (CRBP). The resulting CRBP-retinol complex serves as a substrate for two different microsomal enzymes:

- Lecithin retinol acyl transferase (LRAT), which catalyse the esterification of retinol to retinyl esters. Retinyl ester is the storage form of retinol in

many tissues *e.g.* small intestine, liver, skin, eye, testis (Napoli, 1996).

- Retinol dehydrogenase, which catalyses the oxidation of retinol to retinaldehyde. This is the rate limiting step in the oxidative formation of RA (Napoli, 1996).

Retinal is then metabolised to all-*trans* retinoic acid (ATRA) by cytochrome P450 enzymes, namely the CYPs 1A1, 1A2 and 3A4 in human (Zhang *et al.*, 2000). The major pathway of metabolic deactivation of ATRA starts with the hydroxylation at C-4 to form 4-hydroxy ATRA and 4-oxo ATRA which is then oxidised into more polar and less bioactive metabolites (Blanner and Olson1994). This bio-oxidative reaction of ATRA is catalysed by the cytochrome P450 enzyme, ATRA 4-hydroxylase, cytochrome P450RAI (Retinoic Acid Inducible) (designated as CYP26) which is highly specific for the catabolism of ATRA (Sonneveld *et al.*, 1998). Other isoforms of all-*trans* retinoic acid generated *in vivo* include 13-*cis*-RA (Tang and Russell, 1990) and 9-*cis*-RA (Heyman *et al.*, 1992) (**Figure 1.6**).

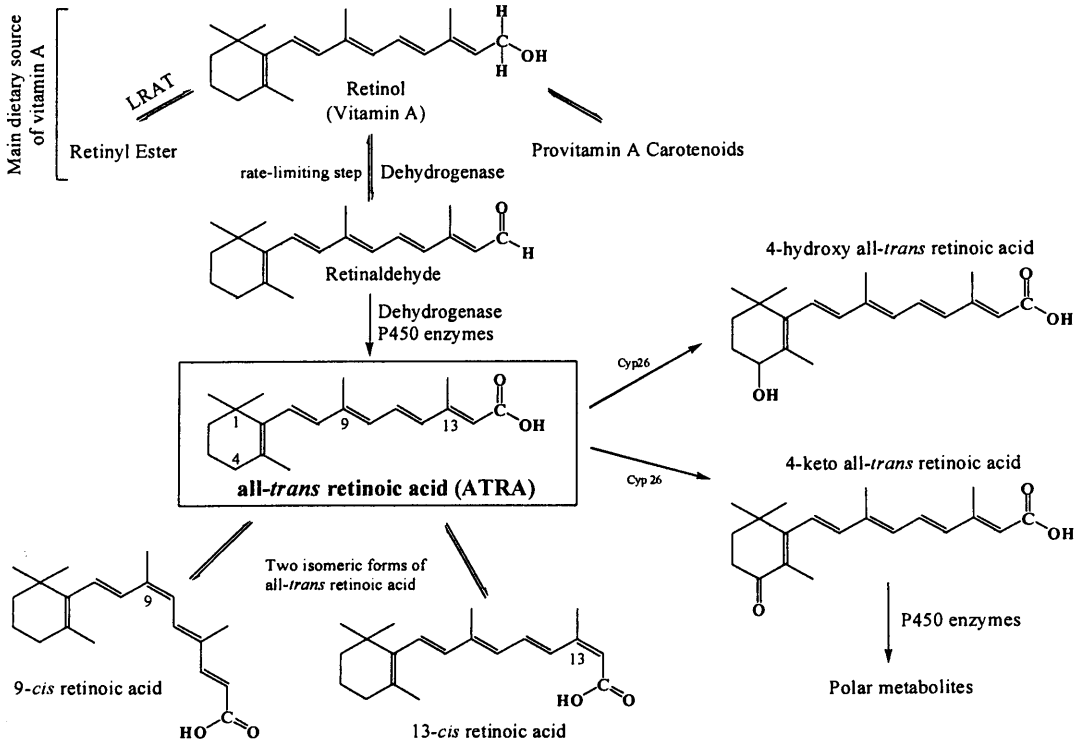

Figure 1.6:. Biosynthesis and metabolism of all-*trans* retinoic acid.

CYP26 appears to be the novel cytochrome P450 hydroxylase enzyme expressed in numerous tissues, and is rapidly induced by ATRA (White *et al.*, 1997).

CYP26 has been cloned from zebra fish (White *et al.*, 1996), mouse (Abu-Abed *et al.*, 1998) and man (White *et al.*, 1997).

After the discovery of P450RAI-1 (CYP26A1) by the White group (White *et al.*, 1997), they identified another two members of CYP26, namely the P450RAI-2 (CYP26B1) and P450RAI-3 (CYP26C1) (Taimi *et al.*, 2004). ATRA is the preferred substrate for all the three members of CYP26, except for CYP26C1 which can metabolise both ATRA and 9-*cis* RA (Taimi *et al.*, 2004).

1.3.2 Biological action of vitamin A

Retinoids play a major role in pattern formation during embryogenesis, they are also essential for biological processes including vision, reproduction, differentiation and bone development (Sporn *et al.*, 1994). Vitamin A deficiency is a significant health problem especially among children in developing countries where it is the leading cause of severe visual impairment such as xerophthalmia (progressive disease of the eye) and blindness (Underwood and Arthur, 1996). Moreover vitamin A deficiency leads to hyperkeratosis of the skin and to hyperplastic and metaplastic changes in the epithelia of mucous membranes (Bollag, 1996). Thus, there is no doubt that vitamin A is involved in maintaining differentiation of skin cells. Therefore considerable efforts have been made to use retinoic acid (RA) and its derivatives in the treatment of disorders of skin keratinisation.

1.3.3 General mechanism of action of retinoids

Retinoids are small hydrophobic molecules and thus are able to cross biological membranes and enter cells where they can bind specific receptors (Giguere, 1994). Retinoid receptors belong to the nuclear receptor superfamily which includes the steroid, thyroid and vitamin D receptors (Petkovich, 1987). Cellular retinoic acid uptake is made through binding to the cellular retinoic acid binding protein (CRABP). RA once bound to CRABP is translocated to the nucleus where it can bind to nuclear receptors.

There are two families of nuclear receptors, the retinoic acid receptors (RARs) and retinoid X receptors (RXRs). Each receptor is composed of three subtypes (α, β and γ). The RAR family (RAR α, β and γ) is activated by both ATRA and by 9-*cis* RA (Mangelsdorf *et al.*, 1995), whereas, the RXR family (RXR α, β and γ) is activated only by 9-*cis* RA (Heyman *et al.*, 1992).

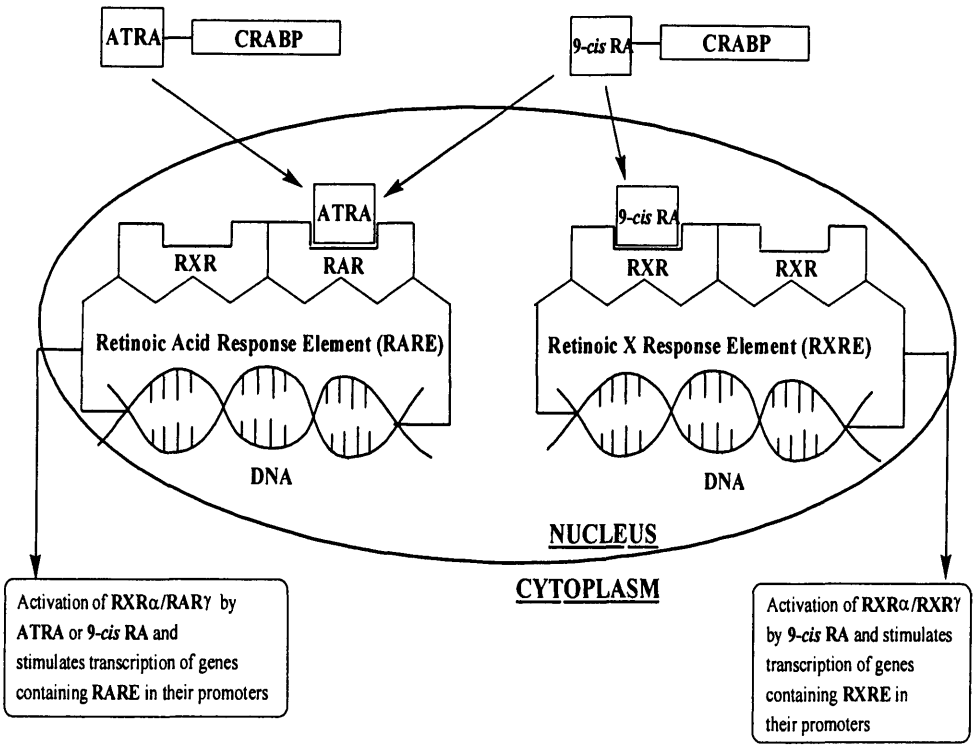

Figure 1.7: The binding of ATRA and 9-*cis* RA to the RAR and RXR nuclear receptor respectively in the nucleus.

Once the complex ligand-receptor has formed, it binds to its response element, either retinoid X response element (RXRE) or retinoic acid response element (RARE) and induces transcription. (**Figure 1.7**).

Both RARs and RXRs can bind RA response elements as homodimers, although heterodimers have been shown to be more efficient in binding than homodimers (Bugge *et al.*, 1992). Indeed, it has been suggested that RAR/RXR heterodimers are the dominant functional unit in activation of the retinoid signal (Chambon, 1996). Significantly, although RAR can only form heterodimers with RXR, RXR is able to heterodimerise with other receptors such as the vitamin D_3 receptor (VDR) and the thyroid receptor (TR) to improve the recognition of VDR, TR and RAR with their respective DNA response elements (Yu et al., 1991).

1.3.4 Therapeutic uses of retinoids

For a long time now, Vitamin A has been known as a critical regulator of growth and differentiation of developing and adult mammalian skin. Studies demonstrated that ATRA is the major biologically active form of vitamin A in the skin (Fisher and Voorhees, 1996). A number of pharmaceutical agents have thus been

developed to treat dermatological diseases such as psoriasis and acne (Njar, 2002; Cunliffe, 2002; Njar *et al.*, 2006).

Of the many synthesised retinoids, there are only three retinoids that have become prescription-only medicine in the United Kingdom: Tretinoin, isotretinoin and acitretin (Anon, 2004) (**Figure 1.8**).

The synthetic retinoids such as isotretinoin (13-*cis*-RA) and etretinate show less toxicity than the natural compound (Peck and Digiovanna, 1994). The use of these synthetic retinoids in dermatology has been beneficial and was reviewed by Peck (Peck, 1982; Peck and DiGiovanna, 1994). The drug of choice for severe cystic acne is isotretinoin, whereas, acitretin is the drug of choice for the treatment of psoriasis and related disorders of keratinisation (Gollnick *et al.*, 1990; Goodman, 1984) (**Figure 1.8**). A synthetic retinoid Tazarotene, which is a selective ligand for RARβ and γ, has been approved as a topical therapy for the treatment of mild to moderate plaque psoriasis, which constitute the majority of psoriasis cases (Disepio *et al.*, 1997; Thacher *et al.*, 2001; Weindl *et al.*, 2006).

Moreover, synthetic retinoids have been shown to be useful and effective in the prevention of carcinogenesis in laboratory animals as supported by a substantial body of literature (Hill and Grubbs, 1992; Lotan, 1980; Moon *et al.*, 1994). The most compelling and thoroughly documented results have been obtained with ATRA in the treatment of acute promyelocytic leukaemia (APL) (Hong and Itri, 1994; Fenaux *et al.*, 2007). ATRA, which induces differentiation of the leukaemic cells into mature granulocytes, represents an important advance in the field of successful differentiation therapy of APL (Tallman *et al.*, 2002).

One of the retinoids, *N*-(4-hydroxyphenyl)-retinamide (4-HPR), also know as fenretinide, has been studied for its effect in tumourigenic (DU145) and non-tumourigenic (RWPE and WPE) prostate cancer cell lines at different stages of prostate carcinogenesis. Sharp *et al.* (Sharp *et al.*, 2001) found that 4-HPR inhibits the growth of DU145 cells in a dose-dependent manner. 4-HPR has also demonstrated a benefit in both prevention and progression in prostate cancer rat models (Pienta *et al.*, 1993; Pollard *et al.*, 1991; Huynh *et al.*, 2006).

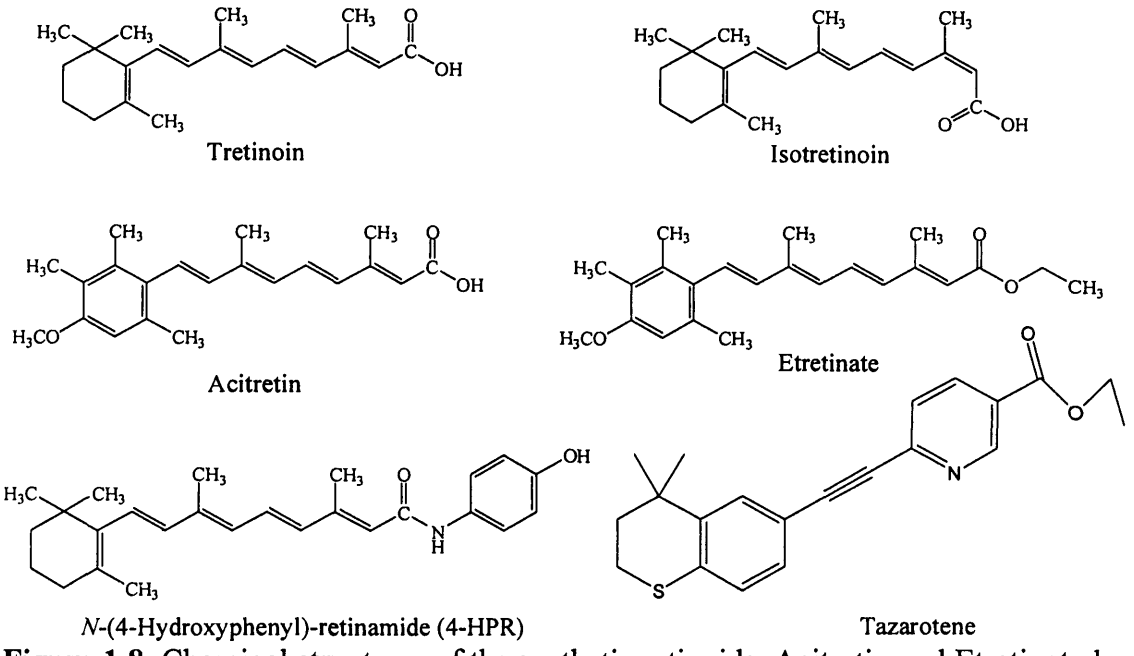

Figure.1.8: Chemical structures of the synthetic retinoids. Acitretin and Etretinate have aromatic ring structure.

1.4 Vitamin D_3

1.4.1 Biosynthesis and metabolism

In the presence of ultraviolet light, 7-dehydrocholesterol is converted into previtamin D_3 in the human skin. This precursor is rapidly transformed by a rearrangement of double bonds to form vitamin D_3 **(Figure 1.9)**.

The next step that occurs in the liver, involves hydroxylation of vitamin D_3 at carbon 25 to give 25-hydroxyvitamin D_3 (25-(OH)-D_3) by vitamin D_3-25-hydroxylase (CYP27A1). Further processing occurs in the kidney which involves the enzyme 25-hydroxyvitamin D_3-1α-hydroxylase (CYP1α) that introduces a hydroxyl group at the α-position of carbon 1 of the A ring to produce 1α,25-dihydroxyvitamin D_3 (1α,25-$(OH)_2$-D_3) also known as calcitriol which is the hormonally active metabolite. The enzyme 25-hydroxyvitamin D_3-24-hydroxylase (CYP24) in the kidney, is involved in the catabolism of 25-(OH)-D_3 and calcitirol to 24,25-dihydroxyvitamin D_3 (24,25-$(OH)_2$-D_3) and 1α,24,25-trihydroxyvitamin D_3 (1α,24,25-$(OH)_2$-D_3) respectively **(Figure 1.9)**.

The degradation of calcitriol to form calcitrioic acid, involves several steps catalysed by the CYP24 enzyme via the C-24 oxidation pathway **(Figure 1.9)**.

The three vitamin D_3 hydroxylases mentioned above have been isolated and cloned. Based on their sequence-alignment (Chen *et al.*, 1993; Guo *et al.*, 1993;

Monkawa et al., 1997), they were found to contain haem-binding and functional domains typical of cytochrome P450 haem protein enzyme (Ghazarian *et al.*, 1974).

1.4.2 Biological action

Vitamin D metabolites are involved in a wide array of biological responses, including calcium homeostasis, immunology, cell differentiation and regulation of gene transcription (Bouillon *et al.*, 1995; Ylikomi *et al.*, 2002). The principal mediator in this host of cellular processes, is the hormone 1α,25-dihydroxyvitamin D_3 (calcitriol).

The classical role of calcitriol is to maintain normal development of the skeleton and maintenance of calcium homeostasis. Since the discovery of the physiological action of vitamin D in preventing bony diseases such as rickets and osteomalacia (DeLuca, 1988), it became clear that the essence of calcitriol action is to increase plasma calcium and phosphorus to mineralise skeleton to prevent bone diseases. Calcitriol does this by (Ettinger and DeLuca, 1996; Reichel *et al.*, 1989) :-

- Stimulating intestinal transport of calcium and phosphorus
- Mobilising calcium from bone
- Reabsorption of calcium in the renal distal tubule

1.4.3 Mechanism of action

Vitamin D exerts its action through binding to the vitamin D receptor (VDR). Baker *et al.* successfully cloned and isolated the human VDR in 1988 (Baker *et al.*, 1988). VDR is a member of the nuclear receptor superfamily. These nuclear receptors are characterised by a DNA-binding domain (DBP), which targets the receptor to specific DNA sequences known as the nuclear receptor response element. The VDR-complex binds to its response element (VDRE) and induces gene transcription.

VDR functions as a heterodimer with RXR (Kliewer *et al.*, 1992). Alterations in RXR would therefore affect both Vitamin D and retinoid signalling pathways. Degradation of RXR has been shown to influence the sensitivity of cells to the antiproliferative effects of calcitriol (Prufer *et al.*, 2002).

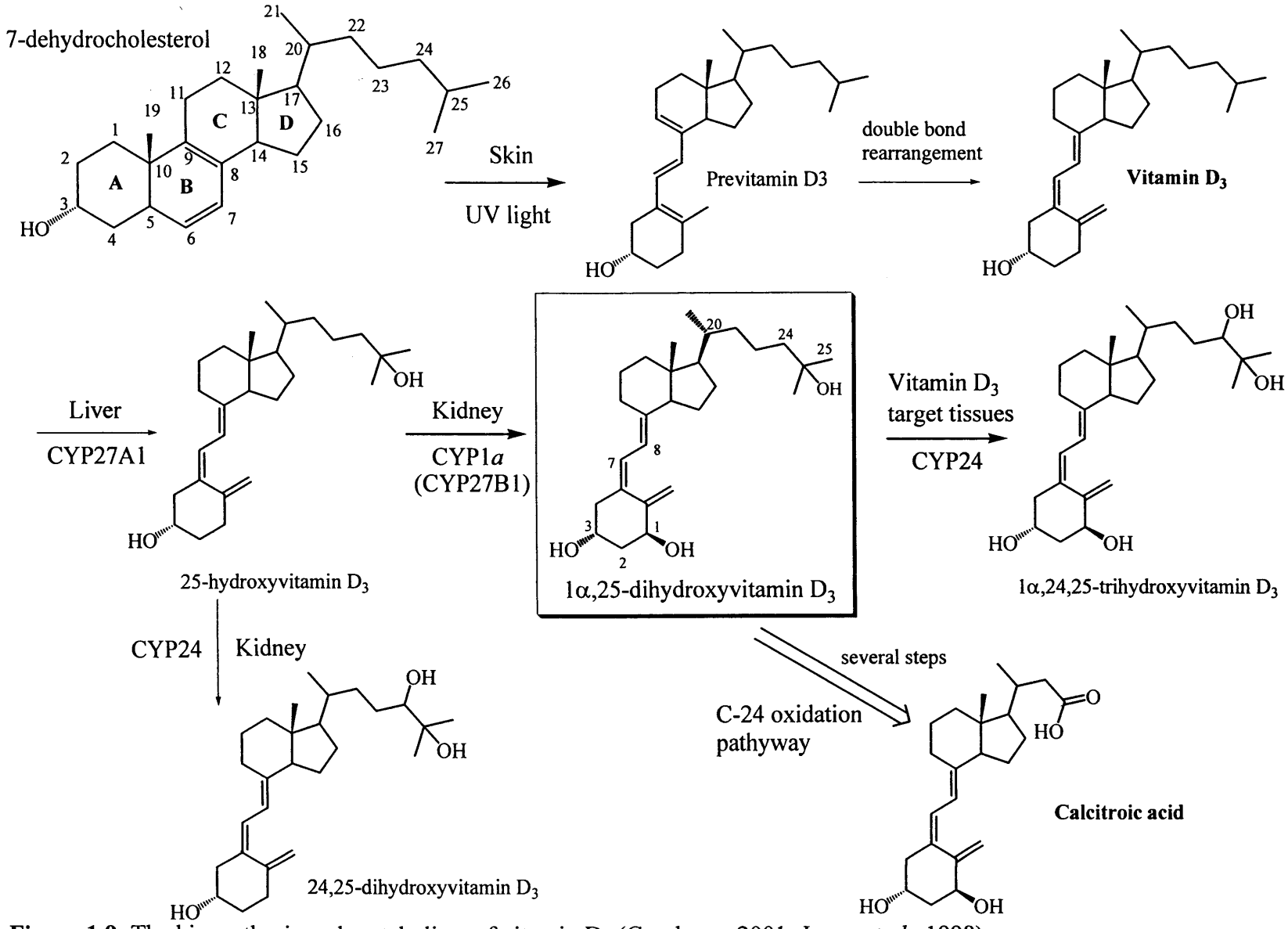

Figure 1.9: The biosynthesis and metabolism of vitamin D_3 (Goodman, 2001; Jones *et al.*, 1998).

1.4.4 Therapeutic uses

Hundreds of vitamin D analogues have been synthesised and biological activity has been evaluated (Bouillon *et al.*, 1995; Jones *et al.*, 1998). These analogues show alterations to the A, B and/or CD ring of $1\alpha,25(OH)_2D_3$. These vitamin D analogues have been selected to target diseases such as bone disease (osteoporosis), skin disease (psoriasis) and hormonal therapy (hypoparathyroidism) (Tong, *et al.*, 2006).

Vitamin D compounds are formulated either on their own or with calcium carbonate, used as a supplement product for patients with vitamin D deficiency due to intestinal malabsorption or chronic liver or kidney disease (Tong, *et al.*, 2006). The products ergocalciferol (vitamin D_2), alfacalcidol (1α-hydroxyvitamin D_3), calcitriol ($1\alpha,25$-dihydroxyvitamin D_3), cholecalciferol (vitamin D_3) and dihydrotachysterol (**Figure 1.10**) are listed in the British National Formulary 2004 (Anon, 2004). Calcitriol is also licensed for the management of postmenopausal osteoporosis (Anon, 2004).

It is desirable to develop vitamin D_3 analogues as effective chemopreventive agents, as these analogues should possess desirable anti-proliferative and pro-differentiating activities rather than undesirable calcaemic activity (Campbell and Koeffler, 1997).

1.5 Retinoids, vitamin D and cancer

1.5.1 Prostate cancer

Retinoids and vitamin D have emerged as leading candidates both to prevent and to treat prostate cancer. Many of the activities of these compounds established from epidemiological studies, research with cell cultures, animal models and clinical trials are consistent with tumour suppressor effects (Peehl and Feldman, 2003; Fichera *et al.*, 2007).

Epidemiologic studies have indicated a strong link between incidence of prostate cancer and RA and vitamin D. Examples of such studies are as follows:

- Vitamin A intake is inversely related to the risk of prostate cancer (Kolonel *et al.*, 1987; Pasquali *et al.*, 1996)

- Low level of circulating calcitriol was co-related with the risk of prostate cancer (Schwartz and Hulka, 1990)
- An inverse correlation between mortality due to prostate cancer and exposure to ultraviolet light, which is the principal source of vitamin D (Hanchette and Schwartz, 1992; John *et al.*, 2004).
- Given the correlation between vitamin D deficiency and prostate cancer risk, and the fact that age is the strongest risk factor known for prostate cancer, it is noteworthy that hypovitaminosis D is epidemic among the elderly (Lips, 2001).

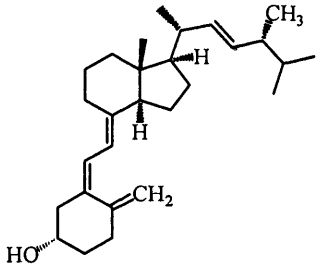

Ergocalciferol (Vitamin D_2)

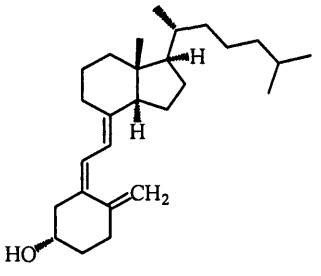

Colecalciferol (Vitamin D_3)

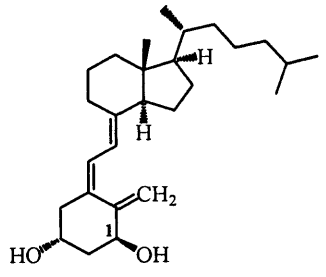

Alfacalcidol
(1α-hydroxycholecalciferol or
1α-hydroxyvitamin D_3)

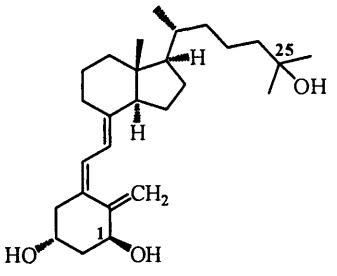

Calcitriol
(1α,25-dihydroxycholecalciferol or
1α,25-dihydroxyvitamin D_3)

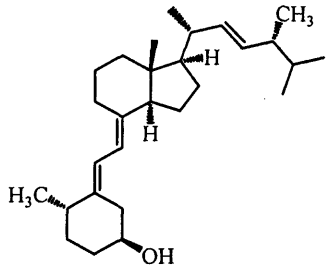

Dihydrotachysterol

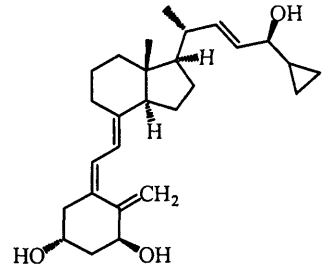

Calcipotriol (Dovonex®)

Figure 1.10: Chemical structures of vitamin D analogues.

The mechanism of action by which retinoids and vitamin D exert their anticancer activity can be summarised as follows:

Anti-proliferative effects.

It is now well established that vitamin D compounds inhibit the growth of normal prostatic epithelial cells, primary cultures of prostate cancer cells and many prostate cancer cell lines (Reviewed in Miller 1998; Blutt and Weigel 1999; Konety *et al.*, 1999; Feldman *et al.*, 2000) and that this growth suppression occurs via the induction of cell cycle arrest (Pelczynska *et al.*, 2006).

Similarly, retinoids also have antiproliferative effects on normal prostatic epithelial cells and primary cultures of prostate cancer cells (Peehl *et al.*, 1993, Igawa *et al.*, 1994, Liang *et al.*, 1999, *Pasquali et al.*, 1999) as well as on prostate cancer cell lines (Fong *et al.*, 1993, De Vos *et al.*, 1997, Pili *et al.*, 2001; Huynh *et al.*, 2006) and other cancer cell lines (Njar *et al.*, 2006).

Proliferating cells continuously undergo the process of the cell cycle as illustrated in **Figure 1.11**, whereas, non-proliferating cells will leave the cell cycle in G_1 phase and will enter the resting/quiescent phase. There are many types of proteins/genes that help control cell growth and proliferation, to name a few, tumour suppressor gene (*e.g. Ras*, *Rb* gene), apoptotic protein (*e.g. bcl-2*) and cyclin and cyclin-dependent kinases (CDK).

It has been shown by a few research groups that calcitriol and RA inhibit the growth (anti-proliferation effect) of normal prostatic epithelial cells, primary cultures of prostate cancer cells, and many different types of prostate cancer cell lines, by:

- Increasing the expression of CDK inhibitor p21 (Johnson *et al.*, 2002) and p27 (Campbell *et al.*, 1997).
- Decreasing CDK2 activity leading to a decrease in phosphorylation of retinoblastoma protein (*Rb*) resulting in the prostate cancer cell to arrest in the G_0/G_1 phase (Kobayashi *et al.*, 1993; Zhuang and Burnstein, 1998).

Apoptotic effects

The apoptotic effect of RA and its analogues have been examined in androgen-dependent and androgen-independent prostate cancer cell lines (Gao *et al.*, 1999; Liang *et al.*, 1999; Shen *et al.*, 1999; Sun *et al.*, 1999). Retinoids have also been shown to induce apoptosis in different cancer cell lines including, ovarian carcinoma cells, breast cancer cells, oesophegal carcinoma cells, hepatoma cell lines, mast cell tumor cell lines, leukemia cells and neuroblastoma cells (Hormi-carver, *et al.*, 2007; Czeczuqa-Semeniuk, *et al.*, 2004; Santos, *et al.*, 2007; Lopez-Pedrera, *et al.*, 2004).

Furthermore, a combination of melarsoprol (an organic arsenical) and all-*trans* retinoic acid induced a high level of apoptosis in PC-3 and DU-145 cells (Koshiuka *et al.*, 2000).

RA induces apoptosis in prostate cancer cell lines by downregulation of Bcl-2 and Bcl-X_L, the two anti-apoptotic proteins (Blutt *et al.*, 2000; Guzey *et al.*, 2002).

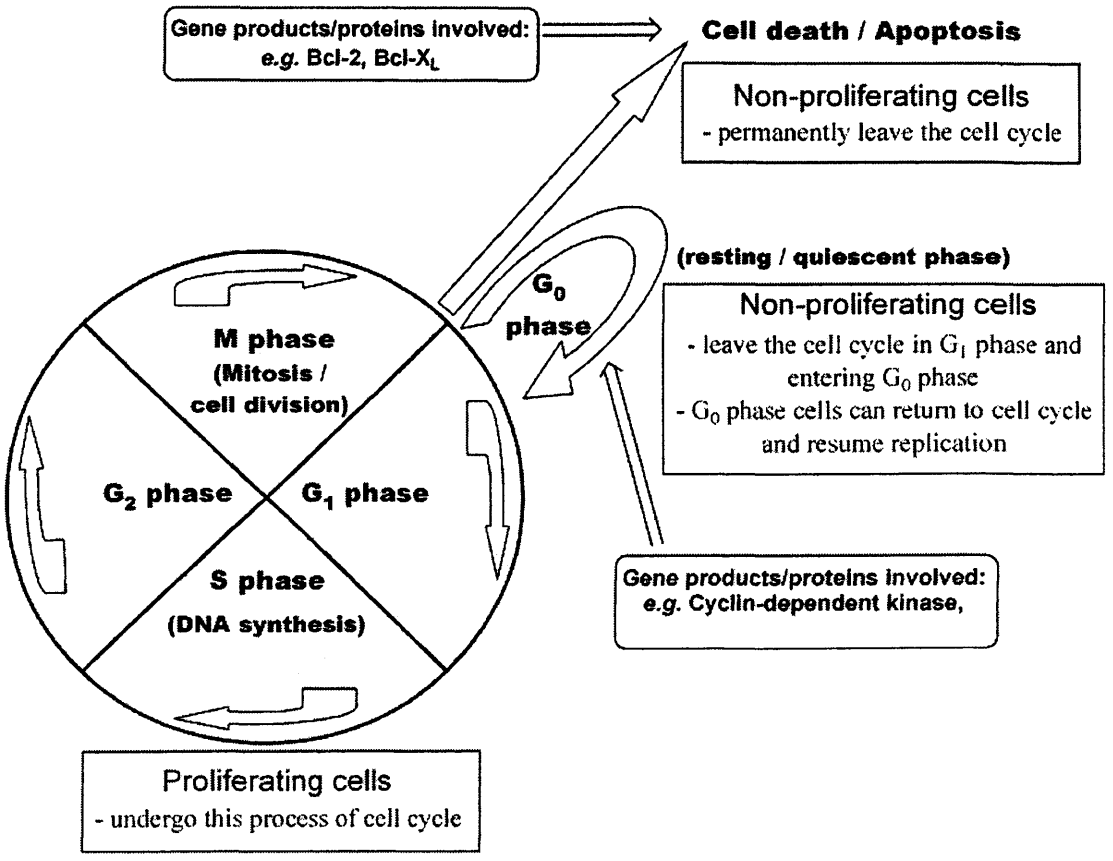

Figure 1.11: The cell cycle of the proliferating cells. The gene products/proteins that are involved in apoptosis and cell-cycle arrest (G_0 phase) are shown here.

The apoptotic and the differentiation effect of endogenous calcitriol on prostate cancer cell lines Du-145 and PC-3 was greatly enhanced by the use of CYP24 inhibitors, that reduced the metabolism of calcitriol resulting in greater inhibition of proliferation of the cancer cells (Yee *et al.*, 2006). In vitro studies with genistein, a soy isoflavone that is able to inhibit calitriol metabolizing enzyme (CYP24), have shown induction of apoptosis and inhibition of cell growth in androgen-sensitive (LNCaP) and androgen-independent (PC3 and VeCaP) prostate cancer cell lines (Vaishampayan, *et al.*, 2007).

Differentiation effect

Several lines of evidence also suggest differentiating effects of retinoids and Vitamin D on prostate cells, in addition to cell cycle arrest or apoptosis (Huynh *et al.*, 2006). Levels of keratin 8 and 18, expressed in the differentiated secretory cells of the luminal prostatic epithelium are increased by retinoic acid in cultured prostatic epithelial cells (Peehl *et al.*, 1993). Upregulation of tissue transglutaminase by retinoic acid in primary cultures of normal and malignant prostatic cells is also consistent with differentiating effects (Pasquali *et al.*, 1999). Kelly *et al.* (Kelly *et al.*, 2000) investigated the histological changes of the tumour biopsy specimens of androgen-independent patients who were treated with ATRA. The increase in prostate-specific membrane antigen (PSMA) expression that occurred after treatment with ATRA indicated the tumour cells changed from metastatic to a high-grade phenotype.

PSA, a differentiation marker of prostatic epithelial cells is increased in androgen-responsive prostate cancer cells by vitamin D compounds (Zhao and Feldman, 2001, Zhao *et al.*, 1999; Beer *et al.*, 2006.) or retinoids (Fong *et al.*, 1993; Pasquali *et al.*, 2006).

Antimetastatic activity

In addition to antiproliferative activities, retinoids and vitamin D have properties consistent with antimetastatic behaviour. Treatment of several androgen independent prostate cancer cell lines with vitamin D compounds *in vitro* decreased invasion, adhesion and migration to laminin (Sung and Feldman, 2000; Schwartz *et al.*, 1997).

Retinoids have also been shown to reduce adhesion, motility, invasion and expression of proteinases, particularly plasminogen activator, by prostate cells (Dahiya *et al.*, 1994; Kim *et al.*, 1995; Webber and Waghray 1995).

Chemopreventive activity

Chemopreventive activity of retinoids in animal models of prostate cancer has been shown. Dietary retinoic acid reduced the incidence of prostate cancer in rats treated with androgen and a carcinogen (McCormick *et al.*, 1999) and decreased the development of prostate cancer in Noble rats, which spontaneously develop prostate cancer (Christov *et al.*, 2002).

In an approach to show the chemopreventive effect of vitamin D, investigators fed rats a diet with high fat and low calcium and vitamin D (Xue *et al.*, 1999). These animals exhibited hyperproliferation of the epithelium of the dorsal prostate. Increased levels of calcium and vitamin D in the diet blocked this hyperproliferation. If hyperproliferation is considered to promote tumourigenesis, then this experiment provides evidence for potential antitumour activity of calcium and vitamin D. Also relevant to chemoprevention strategies are the synergistic activities that vitamin D shows with other putative chemopreventive agents. For example, vitamin D synergistically inhibited the growth of human prostatic epithelial cells with genistein (Rao *et al.*, 2002; Vaishampayan, *et al.*, 2007), the component in soy believed to have chemopreventive properties (Moyad, 1999; Vaishampayan *et al.*, 2007). Very recently, a vitamin D analogue showed a chemopreventive effect both in models of colon cancer and colon cancer cell lines (Fichera *et al.*, 2007).

1.5.2 Breast cancer

Retinoids have been shown to have anti-proliferative effect on the growth of various tumour cells *in vitro*, including breast carcinoma cells (MCF-7, ZR-75.1) (VanHeusden *et al.*, 1998; Toma *et al.*, 1997; Czeczuqa-Semeniuk *et al.*, 2004) and human leukaemia cells (HL 60) (Fontana *et al.*, 2000; Lopez-Pedrera *et al.*, 2004).

The mechanism of action by which retinoids and vitamin D exert their anticancer inhibitory activity can be summarised as follows:

Antiproliferative activity

Retinoic acid treatment has been shown to be capable of stopping the progression of cells through the cell cycle, particularly at the G0/G1 phase interface (Dragnev *et al.*, 2001; Huynh *et al.*, 2006). Indeed, the downregulation of cyclin D1 and CDK2 protein levels have been associated with the growth inhibitory effect of retinoic acid (Teixeira and Pratt, 1997). Other studies have suggested that RA mediates its effects via CD3/CDK4 inhibition in MCF-7 breast cancer cells, which acts to stop the passage of cells through the G1 phase (Zhu *et al.*, 1997). It has been shown that induction of RARα, by treatment with ATRA, increases the endogenous level of RARβ (Rosenauer *et al.*, 1998; Liu *et al.*, 1996) to higher levels in ER+ breast cancer cells than in ER- cells, correlating with their increased growth inhibition (Sheikh *et al.*, 1994; Vander Burg *et al.*, 1993; Roman *et al.*, 1992).

Apoptotic activity

As well as inhibiting cell cycle passage, RA has also been shown to induce apoptosis in several different breast cancer cell types (Niu, *et al.*, 2001; Liu *et al.*, 1996; Shao, *et al.*, 1995; Lopez-Pedrera *et al.*, 2004). The induction of apoptosis represents a major mechanism used by retinoids to exert their anti-growth effects on cancer cells and has been demonstrated not only in breast cancer cells but also in various models of leukaemia (Delia *et al.*, 1993), neuroblastoma (Ponzoni *et al.*, 1995) and lung carcinoma (Kalemkerian *et al.*, 1995).

Several studies have demonstrated that the growth inhibition induced in breast cancer cells by ATRA requires the activation of RAR but not RXR and that RARβ should be considered the main mediator of apoptosis and growth inhibition by ATRA (Seewaldt *et al.*, 1995; Liu *et al.*, 1996). This was confirmed by blocking RAR with selective antagonists which, results in its inhibitory effects on cell growth and apoptosis being reduced (Li *et al.*, 1999).

Significantly, RARs, especially RARβ, possess anti-activator protein-1 (AP-1) activity (Li *et al.*, 1999; Lin *et al.*, 2000) and this may also contribute to their anti-tumour properties. Retinoids have been reported to inhibit the expression of a number of genes containing activator protein-1 (AP-1) response elements within their promoters and are thus capable of repressing the activity of several protooncogenes (Wu *et al.*, 2002).

1.5.3 Synergistic effect of Retinoids and Vitamin D in cancer

VDR acts as a heterodimer with RXR, mediating cross-talk between the vitamin D and retinoid signal pathways. This interaction of VDR with RXR is related to synergistic or additive activity of vitamin D and retinoids on prostatic and other types of cells (Peehl *et al.*, 1995; Zhao *et al.*, 1999). Disruption of this heterodimer has an effect on both pathways. RXR degradation can cause resistance to both vitamin D and retinoids (Prufer *et al.*, 2002). Despite these positive results, there are no studies showing synergistic or beneficial effects using both vitamin D and retinoids *in vivo*.

1.5.4 Clinical uses of Retinoids and Vitamin D in cancer

A small trial in 14 men with hormone-refractory metastatic prostate cancer failed to show an objective response in any patient, but in two there were declines in PSA levels of 25 % and 45 % (Osborne *et al.*, 1995). In another study (Gross *et al.*, 1998), 7 patients with early recurrent prostate cancer after radical prostatectomy or radiotherapy were treated with calcitriol, 6 showed a statistically significant decline in the rate of PSA increase. In both of these studies doses of calcitriol were limited by hypercalcemia and hypercalciuria.

A review by Trump *et al.* (Trump *et al.*, 2004) discussed the use of combination therapy of calcitriol and other chemotherapeutic agent(s), *e.g.* dexamethasone, carboplatin or taxanes in androgen-independent prostate cancer. Intermittent use of calcitriol to reduce toxicity has shown positive results in Phase I and Phase II clinical studies for androgen-independent prostate cancer (Trump *et al.*, 2004). However, the major drawback of using calcitriol for prostate cancer is hypercalcemia and hypercalciuria (Gross *et al.*, 1998; Osborne *et al.*, 1995). Another element controlling the activity of vitamin D is metabolism. The P450 enzyme 25-hydroxyvitamin D-24-hydroxylase (CYP24) initiates the degradation of calcitriol to inactive compounds. Treatment of prostate cancer cell line (DU145) with liarozole, an inhibitor of P450 enzymes, blocks activity of CYP24 and restores sensitivity of DU145 cells to calcitriol (Ly *et al.*, 1999). Other CYP24 inhibitors developed by (Yee *et al.*, 2006) reduced the metabolism of calcitriol resulting in greater inhibition of proliferation of the cancer cells. The use of calcitriol with other agents as genistein showed positive results *in vitro* in androgen-sensitive and androgen-independent prostate cancer cells (Vaishampayan *et al.*, 2007).

ATRA has been used successfully in differentiated therapy of acute promyelocytic leukemia, skin cancer, Kaposi's sarcoma, and cutaneous T-cell lymphoma, and also in the treatment of acne and psoriasis (Sporn *et al.*, 1994; Njar *et al.*, 2006).

Clinical studies of RA have demonstrated moderate efficacy, despite the anti-proliferative, pro-differentiative and apoptotic effects shown *in vitro* (Culine *et al.*, 1999; Hammond *et al.*, 2002; Trump *et al.*, 1997). Beside their use in the treatment of several epithelial cancers and APL, retinoids are being evaluated as possible therapeutic agents for other types of cancer. Retinoids have also been shown to induce apoptosis and differentiation in different cancer cell lines including, ovarian carcinoma cells, breast cancer cells, oesophegal carcinoma cells, hepatoma cell lines,

mast cell tumor cell lines, leukemia cells and neuroblastoma cells (Hormi-Carver, *et al.*, 2007; Czeczuqa-Semeniuk, *et al.*, 2004; Santos, *et al.*, 2007; Lopez-Pedrera, *et al.*, 2004). RA may also improve the efficacy of other treatments such as radiation, cisplatin and interferon therapies (Wiess *et al.*, 1998; Petterson, *et al.*, 2001). However, current systemic therapy and clinical success with ATRA in the treatment of cancer is limited due to toxicity and rapid metabolism in the body which results in underdosing. The rapid metabolism is due to its self induction of oxidative metabolism mediated by the P450 enzyme ATRA-4-hydroxylase (CYP26). ATRA is able to induce its own metabolism which suggests that CYP26 is implicated in an auto-regulated feedback by ATRA (Petkovich, 2001; Van Heusden, *et al.*, 2002). Actually, this accelerated metabolism of ATRA has been proved to be a disadvantage in the use of ATRA as an anti-proliferative compound on breast cancer cells. Its breakdown occurs rapidly with a short half-life of only 6-7 h (Napoli, 1999).

1.6 Retinoic acid and Vitamin D hydroxylase enzymes

1.6.1 The cytochrome P450 enzyme system

The hydroxylase enzymes that are involved in the metabolism of 25-hydroxyvitamin D_3 (CYP1α and CYP24) and retinoic acid (CYP26) are members of the cytochrome P450 superfamily (Leo and Lieber, 1985; Marill *et al.*, 2000; Omdahl *et al.*, 2002).

On addition of carbon monoxide (CO) to the P450 enzyme, it forms a complex which gives a major absorption band at about 450 nm wavelength, and hence the name P450.

The P450 enzymes consist of a large family of single polypeptide chains in the order of 45000 to 55000 Da. All these proteins contain a single iron protoporphyrin IX prosthetic group coordinated to the four pyrrole nitrogen atoms as a haem (DeMatteis, 1980).

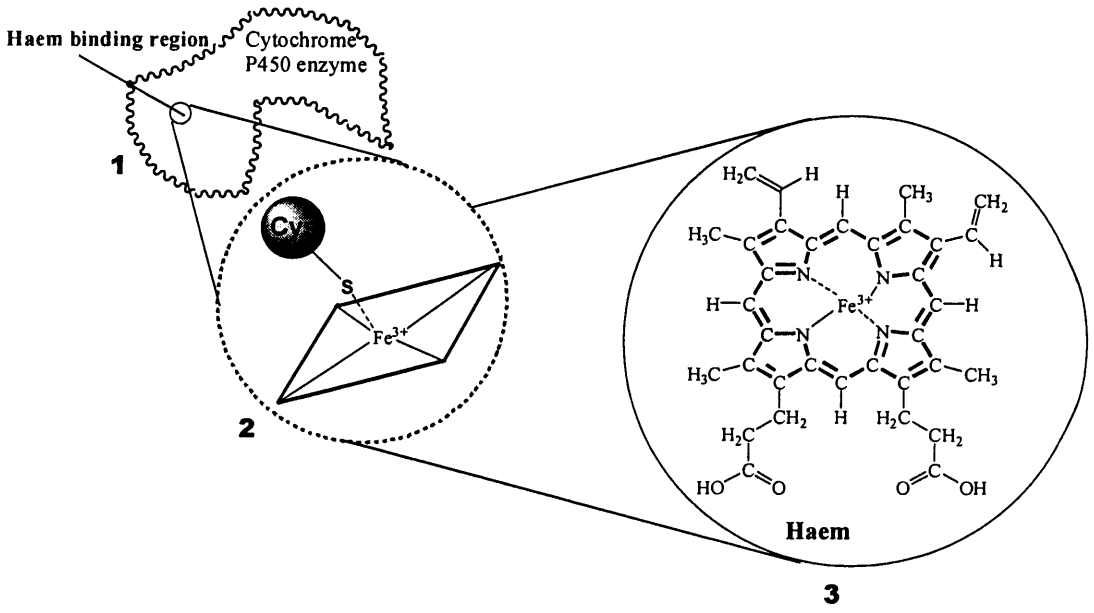

Figure 1.12: The haem sits in the haem binding region within the P450 enzyme (**1**). The sulphur atom of the P450 enzyme cysteine residue is ligated to the iron of the haem (**2**). The haem has a porphyrin ring structure (**3**).

The haem (**Figure 1.12**) sits in the interior of the P450 enzyme. The iron atom of the haem is involved in the enzyme catalytic reaction. The sulphur atom of the P450 enzyme cysteine residue is ligated to the iron of the haem, whereas, the dioxygen (O_2) is bound to the sixth coordination site of the haem iron (Lewis, 1986; Williams *et al.*, 2000) during the P450 catalytic cycle.

In mammals, we can find P450 enzymes in most tissues, except the muscles, neurones and red blood cells (Waterman *et al.*, 1986). These enzymes are located in the endoplasmic reticulum and are highly concentrated in the liver and small intestine (Nerbert and Gonzalez, 1987). CYP1α, CYP24 and CYP26 can be found in other tissues, *e.g.* skin, colon, breast and prostate as well as in the kidney and liver as reviewed by Gudas *et al.* (Gudas *et al.*, 1994) and Bouillon *et al.* (Bouillon *et al.*, 1995).

These enzymes are monooxygenases, able to insert one oxygen atom of the oxygen molecule (O_2) into a large number of substrates, while reducing the other oxygen atom by two electrons to form water (Dawson, 1988).They are involved in the synthesis or the degradation of a large number of endogenous compounds such as steroids and fatty acids, and can also transform new synthesised compounds such as drugs (Simmons *et al.*, 1985)

1.6.2 Vitamin D hydroxylase (CYP24)

The important role of vitamin D in many physiological and pathological processes (Bouillon *et al.*, 1995; Ettinger and DeLuca, 1996; Jones *et al.*, 1998) has attracted many researchers in developing new drugs for targeting the key enzymes in the synthesis or metabolism of the active vitamin D_3 hormone, $1\alpha,25(OH)_2$-D_3:-

- 25-Hydroxyvitamin D-1α-hydroxylase (CYP27B1 or CYP1α) – the key enzymes in the synthesis of the biological active metabolite, calcitriol.
- 1α,25-Dihydroxyvitamin D 24-hydroxylase (CYP24) – a multicatalytic enzyme, that causes side-chain oxidative cleavage of $25(OH)_2$-D_3 resulting in calcitroic acid formation (Akiyoshi-Shibata *et al.*, 1994). This multicatalytic sequence is also known as the C-24 oxidation pathway **(Figure 1.9)**.

Although there have been successes in cloning the rat 24-hydroxylase enzyme and in determining the enzyme's derived sequence (Ohyama and Okuda, 1991), structural information from X-ray crystallography or NMR analyses is still missing.

1.6.3 CYP24 inhibitors

Various azole compounds have been shown to inhibit CYP24. The azole compounds bind directly to the prosthetic haem iron via a lone pair of electrons from the heterocyclic nitrogen and through interaction with other sites in the binding pockets (Schuster *et al.*, 2003). A few standard azole compounds from other companies have been shown to inhibit CYP24, *e.g.* ketoconazole and liarozole (**Figure 1.13**). The use of CYP24 inhibitors could potentially slow down the metabolism and depletion of the active vitamin D hormone, calcitriol.

However, selectivity is a crucial demand in designing CYP24A1 inhibitors in order to avoid impairment of $1\alpha,25(OH)_2$-D_3 synthesis by 1α-hydroxylase, a distinct, but related mitochondrial CYP.

SDZ 89-443 and VID400 (**Figure 1.13**) have been identified as potent CYP24 inhibitors and also very selective for CYP24 compared with CYP27B (Schuster *et al.*, 2001). These selective inhibitors of CYP24 were used by Schuster group to study vitamin D metabolism in human keratinocytes.

Other compounds that have been described as potent, selective and low-calcemic inhibitors of CYP24 include some 24-sulfone (Posner *et al.*, 2004) and 24-sulfoximine (Kahraman *et al.*, 2004) analogues of the hormone $1\alpha,25(OH)_2$-D_3.

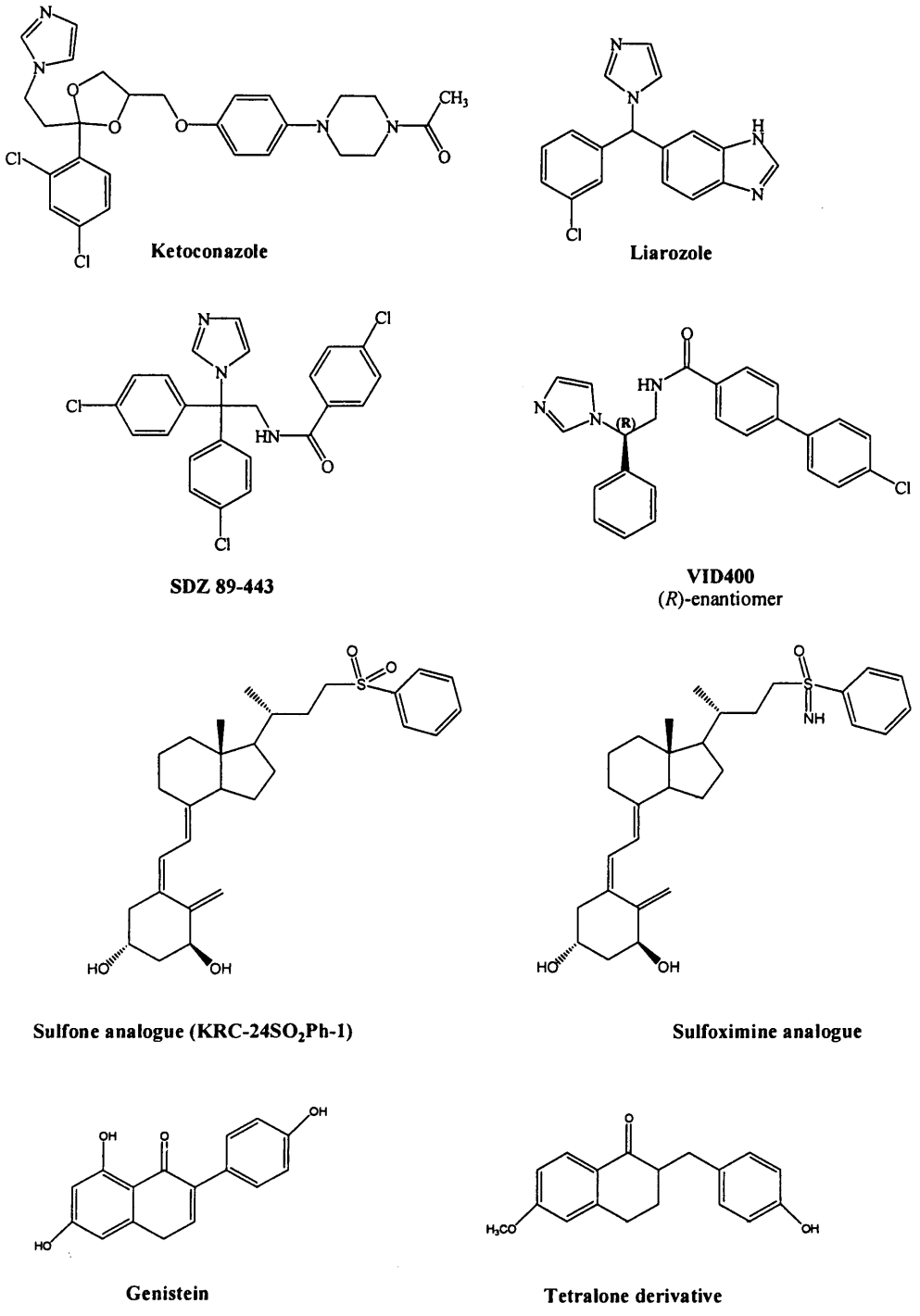

Figure 1.13: Azole and calcitriol analogues compounds which show inhibition of CYP24.

It has been postulated from *in vivo* studies, that CYP24 inhibitors can be useful agents for the treatment of androgen-independent prostate cancer (Farhan *et al.*, 2002; Farhan *et al.*, 2003).

Ly and co-workers (Ly *et al.*, 1999) have added liarozole to calcitriol in an androgen-independent DU145 cell line, this resulted in an increase in the half-life of

calcitriol and enhanced up-regulation of the vitamin D receptor. Liarozole, a CYP24 inhibitor was also used in Phase II trials for hormone-refractory prostate cancer (Seidmon *et al.*, 1995). There are also promising results from preclinical studies carried out in prostate cancer cells to study the combination of ketoconazole (CYP24 inhibitor) with calcitriol (Peehl *et al.*, 2001; Peehl *et al.*, 2002). It was shown in rat osteosarcoma cells that ketoconazole can inhibit the self-induced metabolism of calcitriol (Reinhardt and Horst, 1989).

An enhancement of antiproliferative activity of calcitriol analogues by P450 enzyme inhibitors has been demonstrated in different cell lines. For example, Zhao and co-workers showed that ketoconazole and liarozole (P450 enzyme inhibitors, including CYP24 inhibitor) enhanced the antiproliferation of MCF-7 and T47-D breast cancer cell lines, this combination therapy might synergise the anticancer properties (Zhao *et al.*, 1996).

More recently, tetralone derivatives (**Figure 1.13**) synthesised by the Welsh School of Pharmacy group greatly enhanced the apoptotic and the differentiation effect of endogenous calcitriol on prostate cancer cell lines Du-145 and PC-3 by reducing the metabolism of calcitriol resulting in greater inhibition of proliferation of the cancer cells (Yee *et al.*, 2006). In vitro studies with genistein (**Figure 1.13**), a soy isoflavone that is able to inhibit calitriol metabolizing enzyme (CYP24), have shown induction of apoptosis and inhibition of cell growth in androgen-sensitive (LNCaP) and androgen-independent (PC3 and VeCaP) prostate cancer cell lines (Vaishampayan, *et al.*, 2007).

CYP24 inhibitors could be a promising combination therapy together with calcitriol vitamin D, as indirect differentiation therapy for hormone-refractory (androgen-independent) prostate cancer by sustaining the level of calcitriol and allowing the dose of calcitriol to be reduced thus reducing the side-effects of calcitriol. The combination have been shown to slow the growth of the prostate cancer cells and restore normal responses to hormonal signaling (Zhao and Feldman, 2001; Yee *et al*, 2006).

1.6.4 Retinoic acid hydroxylase enzyme (CYP26)

The specific P450s responsible for 4-hydroxylation of ATRA in the human liver are CYP2C8 as a major contributor, as well as 3A7, 3A5, 3A4, 2C9 and 1A1 (Zhang *et al.*, 2000). However, in living tissues, ATRA administration induces

another RA-metabolising enzyme, CYP26 (CYP26A1 and CYP26B1) which recognises only ATRA as its substrate, and the expression of this isozyme can be induced by ATRA both *in vitro* and *in vivo* (Stoppie *et al.*, 2000). Another isozyme, CYP26C1 may have a role in the specific metabolism of both all-*trans* and 9-*cis* isomers of RA

Structural information of CYP26 from X-ray crystallography is still missing despite the fact that there have been successes in cloning CYP26 by White's group (White *et al.*, 1997). However, the cloning of the cDNA of CYP26 allow it to be expressed in *Candida albicans* and other mammalian expression systems to investigate the ATRA metabolism *in vitro* (Chithalen *et al.*, 2002; Stoppie *et al.*, 2000).

1.6.5 Retinoic acid metabolism blocking agents (RAMBAs) (CYP26 inhibitors).

Due to the rapid metabolism of retinoic acid in cells, ATRA shows a decrease in plasma concentrations after repeated dosage (Muindi *et al.*, 1994). An alternative approach of potentiating endogenous ATRA can be through inhibition of CYP26 and may avoid the frequency and severity of complications associated with intensive high dose ATRA therapy and may provide an effective means of treatment following relapses in cases where resistant emerges due to CYP26 up regulation. As a result inhibitors of CYP26, also known as retinoic acid metabolism blocking agents (RAMBAs) have emerged and proven to be effective in blocking the catabolic effects on ATRA and have demonstrated an increase in endogenous ATRA levels (Miller *et al.*, 1994). Liarozole and ketoconazole are capable of inhibiting the CYP-dependent metabolism of RA by hamster (Van Wauwe *et al.*, 1990) and rat (Ahmad *et al.*, 2000) liver microsomes respectively. With liarozole, the first generation CYP26 inhibitor, *in vitro* studies showed suppression of the metabolism of ATRA in MCF-7 cells (Debruyne *et al.*, 1998). Aditionally, liarozole in conjuction with exogenously administered ATRA, displayed growth inhibition in MCF-7, T47D and AT6.1 cells. In *in vivo* studies, liarozole (30 mg/Kg, b.i.d.) showed 90% growth inhibition in both AT-6 androgen independent prostate adenocarcinoma (R3227 line) and AT-6 androgen independent prostate tumours in rats (Mark *et al.*, 2005).

Njar's group (Njar *et al.*, 2000) and the group at Welsh School of Pharmacy (Kirby *et al.*, 2003; Kirby *et al.*, 2002) have identified compounds which showed interesting activities against RA metabolism enzyme(s) (**Figure 1.14**).

Another series of benzofurantriazoles (**Figure 1.14**) were synthesised at the Welsh school of pharmacy and showed comparable activity with liarozole (Pautus *et al.*, 2006).

A more recent CYP26 inhibitors, is a series of [2-imidazol-1-yl-2-(6-alkoxy-naphthalen-2-yl)-1-methyl-ethyl]-dimethyl-amines designed and synthesized by Mulvihill et al (Mulvihill *et al.*, 2005; Mulvihill *et al.*, 2006). Some of these compounds have been shown to have potent inhibitory activity with an IC_{50} of 125 nM in T47D tumour cells.

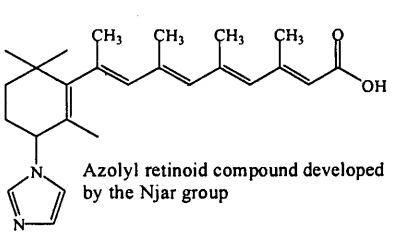

Azolyl retinoid compound developed by the Njar group

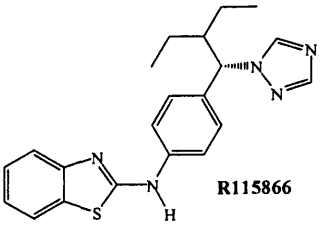

R115866

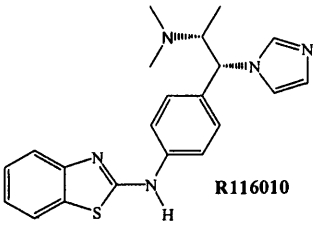

R116010

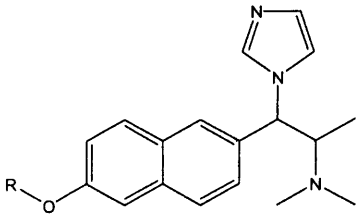

Compounds synthesized by Mulvihill *et al.*

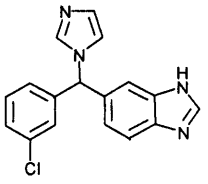

Liarozole

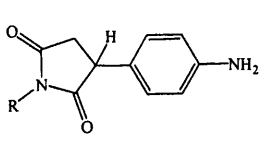

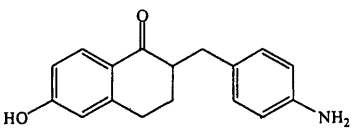

Compounds developed by the group at Welsh School of Pharmacy

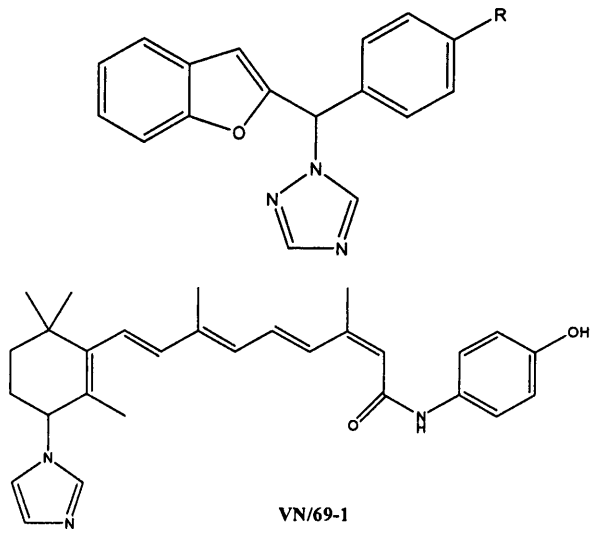

Figure 1.14: Examples of some Retinoic Acid Metabolism Blocking Agent (RAMBA).

Very recently, Njar group developed a series of RAMBAs that showed strong inhibitory effect on the catabolism of ATRA and the growth of human prostate cancer cells (Njar *et al.*, 2006). *In vivo*, treatment of LNCaP tumours growing in SCID mice with VN/66-1 and VN/69-1 (**Figure 1.14**) resulted in modest but statistically significant tumour growth inhibition of 44 and 47%, respectively.

The most selective and potent CYP26 inhibitor reported so far is R115866 (**Figure 1.14**) as reported by Stoppie *et al.* (Stoppie *et al.*, 2000). In an *in vitro* system (*i.e.* human CYP26 expressed in yeast), R115866 showed an IC_{50} of 4 nM. In an *in vivo* study, R115866 was able to enhance endogenous RA levels and also to mimic the effects of RA (Stoppie *et al.*, 2000). *In vivo* in rats after a single oral dose, R115866 increased endogenous tissue RA levels and mimicked RA in several others of its biological actions, R115866 has also shown to be beneficial when administered topically to skin. A more recent derivative, R116010, has shown potent and selective inhibitory activity of retinoic acid metabolism in human T47D breast cancer cells (Van Heusden et al., 2002). R116010 increased the intacellular availability of all-trans retinoic acid in neuroblastoma cells (Armstrong *et al.*, 2005). The rationale behind the use of ATRA with CYP26 inhibitors in the treatment of acute promyelocytic leukemia (APL) was that the remission duration for patients treated with ATRA was very brief (Chen *et al.*, 1991; Miller *et al.*, 1994). *In vivo* studies have shown that the use of CYP26 inhibitor with administered retinoic acid, *e.g.* ketoconazole or liarozole,

increased plasma half-life of retinoic acid and enhanced endogenous retinoic acid plasma levels in rats (Van Wauwe *et al.*, 1990; Van Wauwe *et al.*, 1992). In androgen-dependent and androgen-independent prostate cancer (AIPC) mouse models (R3327 Dunning prostate adenocarcinomas), liarozole, which inhibits the catabolism of ATRA, was shown to contribute to its anti-tumoural effect (De Coster *et al.*, 1992; Djikman *et al.*, 1994). In order to achieve sufficient and non-toxic levels of ATRA in target tissues, the use of a CYP26 inhibitor could be a new strategy. This allows ATRA to play its role as a differentiation agent at lower doses to achieve effectiveness in the treatment of prostate, breast and other types of cancer.

Chapter 2

Aims and Objectives

2 Aims and Objectives

The aim of this project is to develop new, potent and selective inhibitors of CYP26 and CYP24 that can be used in the differentiation therapy of prostate and breast cancer. We are looking for inhibitors as potent as R115866 and *R*-VID400 for CYP26 and CYP24 respectively. The X-ray crystal structures of CYP26 and CYP24 are unknown and there are no models published, therefore, the first step is to develop a theoretical model for each of the studied enzymes. This will be done through homology modelling based on the most homologous templates followed by docking studies to validate the model including the docking of the natural substrate as well as the best known inhibitors, which may aid in the rational design of potent and selective inhibitors. The developed models will be used in the design of potent inhibitors through virtual screening of a designed library of compounds based on the structure of the potent inhibitors, natural substrates and intuition. MOE QuaSAR-CombiGen will be used used to generate a fully-enumerated combinatorial library from a scaffold database and a set of substituent R-group databases. This will be followed by docking the generated library of compounds in the enzyme active site using the FlexX program. Scaffold and substituents used for building of the combinatorial library in case of CYP 26 and CYP 24 are shown in **Figure 2.1**.

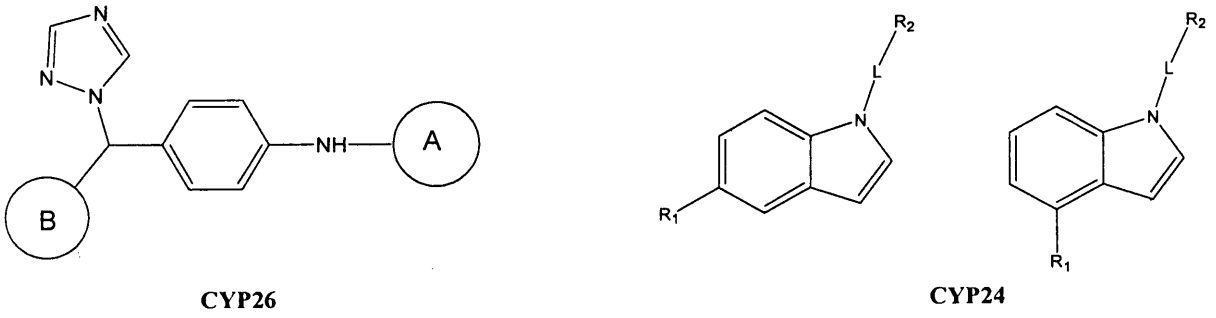

Figure 2.1: Scaffold and substituents used for building of the combinatorial library in case of CYP 26 and CYP 24.

This work will also include the chemical synthesis of some of the promising compounds for CYP26 and CYP24 inhibition. The synthesis will also include some of the non-promising compounds to further validate the constructed models. Based on the structure of the scaffold and substituents used in building of the combinatorial library 2 series of compounds are proposed for CYP26 (**Figure 2.2**). The methods will

be described in Chapter **5**. **Series 1** compounds are (1,2,4)triazol- and imidazol-1-yl-methylphenylaryl and heteroarylamine derivatives. **Series 2** compounds contain an ester group that could be hydrolysed *in vivo* to give a carboxylate group and thereby, mimic the natural substrate ATRA. **Series 2** compounds are designed to be *N*-aryl and heteroaryl substituted 3-(4-aminophenyl)-3-imidazol-1-yl-2,2-dimethylpropionic acid methyl ester. A series of 4 or 5 substituted 1-(3-benzenesulfonylpropyl)-1*H*-indole is proposed for CYP24. The methods will be described in Chapter **9**.

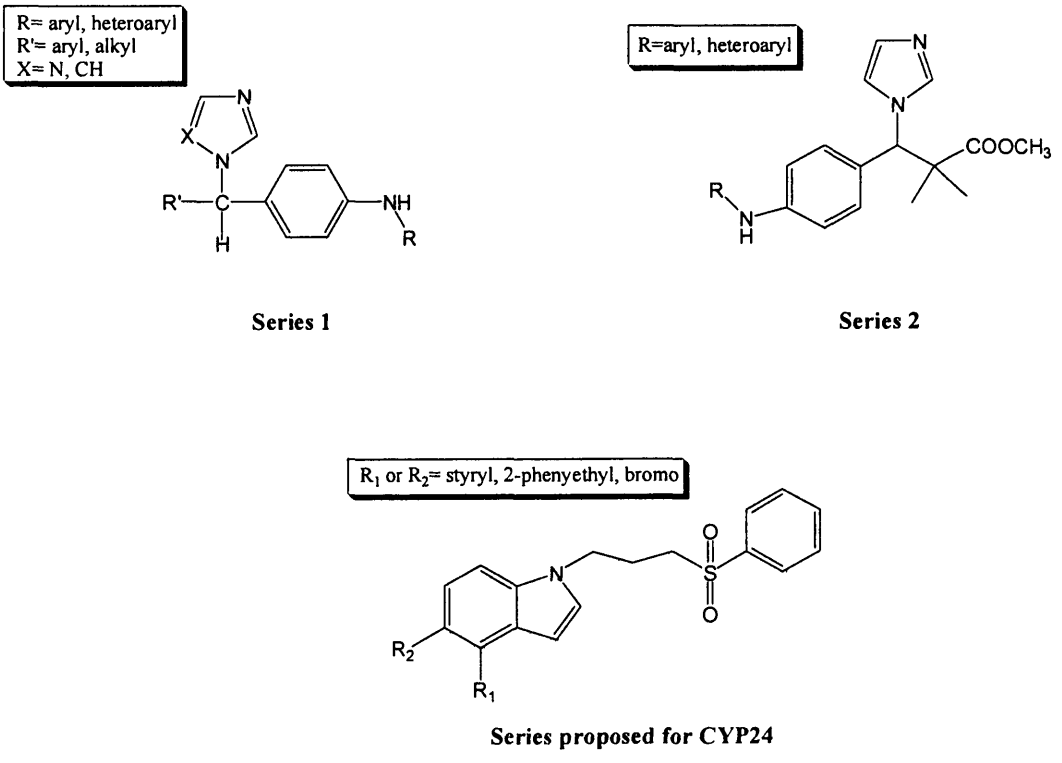

Figure 2.2: Series of compounds proposed for CYP26 and CYP24.

The last step is to test the synthesised compounds for enzyme inhibitory activity, analyse the results and compare with the results of the docking studies. The compounds will be biologically evaluated for CYP26 inhibitory activity using a MCF-7 breast cancer cell assay previously described by our group (Yee *et al.*, 2005). The inhibitory activity of the novel compounds versus CYP24 will be performed by Professor Glen Jones, Queen's University Kingston, Ontario, Canada.

Chapter 3

Homology modelling of CYP26A1

3 Homology modelling of CYP26A1

3.1 Introduction

Proteins are essential to life as they play crucial roles in almost all known biological processes. As such the ability to elucidate how they work based on their 3D structures is of great interest. Experimental techniques such as X-ray crystallography and nuclear magnetic resonance (NMR) spectroscopy, are able to determine the three-dimensional structure of proteins to a relatively high degree. Unfortunately the vast majority of proteins are currently not amenable to these techniques as they are difficult to crystallize, and/or insufficiently soluble or too large for NMR studies.

The rapid expansion and success of the various genome projects has resulted in an abundance of amino acid sequence information becoming readily available. As scientists are unable to determine the structures of proteins at a similar rate there is a large deficit between the knowledge of protein amino acid sequence and the ability to relate this to its 3D structure. Due to this deficit, alternative methods are required to help understand the functional roles a protein adopts in terms of its 3D structure. One such technique is comparative (or homology) modelling.

It has been shown that proteins which display a high degree of similarity between their amino acid sequences tend to adopt similar three-dimensional protein folds (Chothia *et al.*, 1986) and this premise underpins comparative modelling. It is therefore possible to predict the 3D structure of a protein based solely on knowledge of its amino acid sequence and the 3D structures of proteins that have similar sequences.

Homology, or comparative, modelling thus uses experimentally determined protein structures to predict the conformation of another protein that has a similar amino acid sequence. The method relies on the observation that in nature the structural conformation of a protein is more highly conserved than its amino acid sequence and that small or medium changes in sequence typically result in only small changes in the 3D structure (Lesk *et al.*, 1986).

Although the protein data bank (PDB) (Berman *et al.*, 2000; PDB, 2004) is growing rapidly (about 13 entries daily), the 3D structure of only 1-2% of all known proteins has as yet been experimentally characterised (Hillisch *et al.*, 2004).

However advances in sequence comparison, fold recognition and protein-modelling algorithms have enabled the partial closure of the so-called sequence structure gap and the extension of experimental protein structure information to homologous proteins. The equality of these homology models, and thus their applicability to, for example, drug discovery predominantly depends on the sequence similarity between the protein of known structure (template) and the protein to be modeled (target). Despite the numerous uncertainties that are associated with homology modelling, recent research has shown that this approach can be used to significant advantage in the identification and validation of drug targets, as well as for the identification and optimization of lead compounds.

The aim of comparative or homology protein structure modelling is to build a 3D model for a protein of unknown structure (target) based on the sequence similarity to proteins of known 3D structures (template) (Marti-Renom *et al.*, 2000). All current comparative modelling methods consist of five sequential steps (Sanchez *et al.*,1997).

a) fold assignment and template selection
b) template-target alignment
c) model building
d) model refinement
e) model evaluation

If the model is not satisfactory, then template selection, alignment and model building can be repeated until a satisfactory model is achieved. Thus, the process of comparative modelling is an iterative process with validation possible at almost every level (**Figure 3.1**). This is used to ensure that the resulting model gives as true and accurate a representation of the 3D structure of the target protein as is possible.

After the discovery of CYP26 in 1997 little work has been done to elucidate the secondary structure of CYP26. A better understanding of the structure of CYP26 will aid the rational design of compounds to help control therapeutic levels of ATRA in treating retinoid sensitive diseases such as cancer. As yet no one has published a crystal structure for CYP26, possibly due to the fact that most proteins are sensitive to the techniques used. CYP26 is hard to crystallise, as it is a membrane bound enzyme. On the other hand, there is no single model published for it.

In this work, we report on the use of comparative modelling to predict the 3D structure of CYP26A1 based on knowledge of its amino acid sequences plus the 3D structure of other P450s.

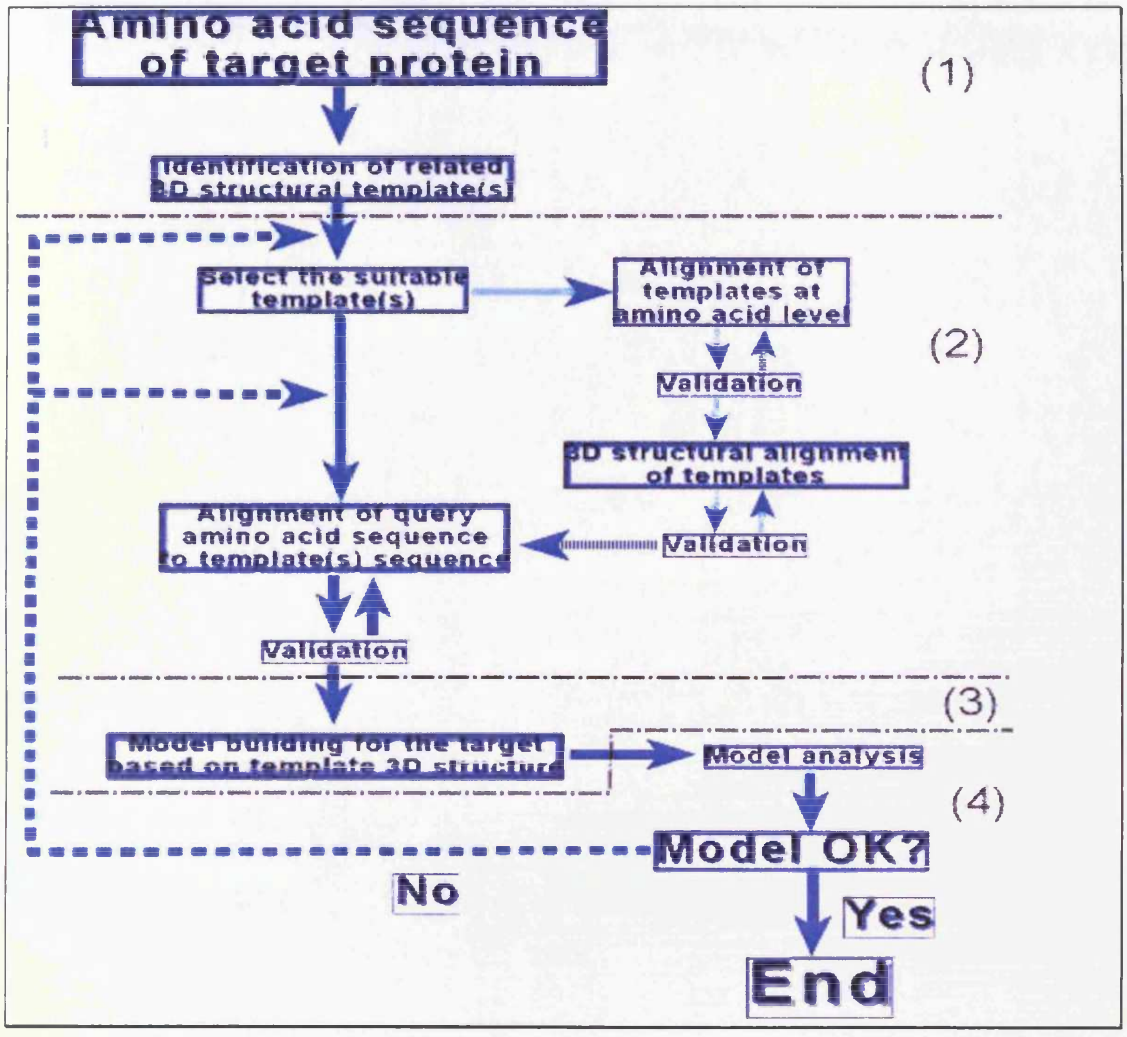

Figure 3.1: Flowchart of comparative protein structure modelling. Four steps are involved as described above (Marti-Renom *et al.*, 2000; Kirton *et al.*, 2002).

3.2 Computational approaches.

All molecular modelling studies were performed on a RM Innovator Pentium IV 2.4GHz running either Linux Fedora Core 3 or Windows XP using Molecular Operating Environment (MOE) 2004.03 (MOE, 2004.03) and FlexX module in SYBYL 7.0 (Tripos SYBYL, 7.0) molecular modelling software.

Molecular dynamics simulations were performed with GROMACS 3.2 (Berendsen *et al.*, 1995; Lindahl *et al.*, 2001) and the Gromacs force field in a NVT (canonical) environment. Individual ligand/protein complexes obtained from the docking results were soaked in a triclinic water box and minimised using a steepest descent algorithm to remove unfavorable van der Waals contacts. The system was then equilibrated via a 20 ps MD simulation at 300°K with restrained ligand/protein complex atoms. Finally, a 800 ps simulation was performed at 300°K with a time step of 2 fs and hydrogen atoms constrained with a LINCS algorithm. Visualisation of the dynamics trajectories was performed with the VMD software package, version 1.8.3. (Humphery *et al.*, 1996)

All the minimisations were performed with MOE until RMSD gradient of 0.05 Kcal mol^{-1} $Å^{-1}$ with the forcefield specified and the partial charges were automatically calculated.

3.3. Homology searching

Information on the amino acid sequence of human CYP26A1 was obtained from the EXPASY server (Berman *et al.*, 2000; Expasy server, 2004; Gasteiger *et al.*, 2003). The EXPASY (Expert protein analysis system) proteomics server of the Swiss institute of bioinformatics (SIB) is dedicated to the analysis of protein sequences and structures.

Search in Swiss-Prot/TrEMBL for CYP26A1 reveals matches to 6 out of 164201entries in Swiss-Prot and matches to 7 out of 1503829 entries in TrEMBL.

The human CYP26A1 in Swiss-Prot database, code (O43174), synonyms (retinoic acid metabolising cytochrome, P450 retinoic acid-inactivating1 and retinoic acid 4-hydroxylase) was selected.

The protein sequence was first entered in the Swiss-Prot database in December 1998. The protein has a molecular weight of 56162 Daltons and a chain length of 497 amino acids with the iron of the haem directly attached to cysteine 442 (Sonneveld *et al.*, 1998; Expasy, 2004a; White *et al.*, 1997).

Homologous proteins with known crystal structures were found by performing a PSI-BLAST search (comparison matrix, BLOSUM62; E-threshold, 10), using the ExPASy server, aligning the query sequence (CYP26A1) against sequences in the Protein Data Bank (PDB) (PDB, 2004) The alignment parameters and thresholds used

for screening candidate homologues were used with their default values and BLOSUM62 comparison matrix.

The alignment yielded 28 similar sequences isolated from different species with % identity of 27%-22%, scores of 252-57 and E values of $2e^{-22}$ - 8.8. The results showed that the template having the highest BLAST score had a 25% sequence identity and none of the templates identified is one of the human P450s recently deposited in the PDB, CYP3A4, CYP2C9 and CYP2C8. Therefore, an advanced WU-BLAST2 search at the European molecular biology laboratory (EMBL) (EMBL, 2004) was performed for the query protein against the PDB database.

The BLAST search returned the amino acid sequence of different P450s isolated from different species including the three human P450s recently deposited in the PDB database. This included more than one structure for the same protein, different resolutions and those derived from mutagenesis studies. Only the one with the highest resolution for each protein is included in the table. The sequences are ranked in **Table 3.1** in order of BLAST score. The score is calculated for each hit sequence aligned to the sequence of CYP26A1 by looking at aligned positions and gaps (Altschul *et al.*, 1997).

Any alignment with E-value above 0.05 (Lesk, 2002) was regarded as a non-reliable entry. An important parameter, which must be taken into account, is the length of the protein applied in the alignment. The fewer the residues included in the alignment the less reliable the template even though a high identity may be observed. On the other hand, it is necessary to consider both identity and the number of residues participating in the alignment in order to choose the best template. The server itself considered the above criteria and gave a score to each entry. The higher the score the more reliable is the alignment. Models derived from crystallography experiments rather than theoretical models should be considered.

The fourth column in the table lists the percentage of sequence identities of the structure to the target. They all have a sequence identity of about 25%. Studies have shown that the active site region of the microbial P450s is conserved across the entire family despite low overall sequence homology (Kirton *et al.*, 2002). This can also be expected for human P450s since the structural conformation of a protein is more highly conserved across the family than its amino acid sequence (Ravichandran *et al.*, 1993).

Table 3.1: The P450 structures recovered by a WU-BLAST search at the EMBL server using the sequence of P45026A1.

Protein[a]	**WU BLAST score**[b]	**Sequence identity**[c]	**% sequence identity**	**Chain length**	**E-Value**
1EA1-A	275	115/447	25	455	$1.3e^{-22}$
1JPZ-A	253	113/432	25	473	$5.7e^{-20}$
1TQN-A	**249**	**111/437**	**26**	**486**	**$1.8e^{-19}$**
1R90-A	**171**	**52/203**	**25**	**477**	**$3.8e^{-13}$**
1PO5-A	164	71/285	24	476	$6.9e^{-16}$
1PQ2-A	**156**	**67/277**	**24**	**476**	**$1.1e^{-11}$**
1DT6-A	153	53/219	24	473	$4.5e^{-12}$
1CPT	153	42/133	31	412	$4.0e^{-10}$

[a] The PDB code of the cytochrome P450

[b] The PSI-BLAST score for an alignment is calculated by summing the score for each aligned position and the scores for gaps

[c] (The number of identical residues) / (the length of sequence fragment identified by PSI-BLAST).

In this respect, CYP3A4 (1TQN), CYP2C9 (1R90) and CYP2C8(1PQ2) were identified as the best templates. They are all human P450s, they all have good BLAST score, % sequence identity and E-value (**Table 3.1**). They have chain length similar to that of CYP26A1 and they are all crystal structure determined by X-ray crystallography to a high resolution.

CYP3A4, (synonyms, quinine 3-monooxygenase, nifedipine oxidase) is a membrane bound human P450 involved in a NADPH- dependant electron transport pathway. It is an oxidoreductase that performs a variety of oxidation reactions such as caffeine 8-oxidation, omiperazole sulfoxidation). It is mainly expressed in prostate and liver. The crystal structure of CYP3A4 was published in July 2004 with a resolution of 2.05Å (Yano *et al.*, 2004).

CYP2C9, (synonyms, limonene 6-monooxygenase, mephenytoin 4-hydroxylase) is a membrane bound human P450 involved in a NADPH-dependant electron transport pathway. It is an oxidoreductase that oxidises a variety of structurally unrelated compounds, including steroids, fatty acids and xenobiotics. The crystal structure of CYP2C9 was published in June 2004 with a resolution of 2.0Å (Wester *et al.*, 2004).

CYP2C8, (synonyms, P450 form 1), is a membrane bound human P450 involved in a NADPH-dependant electron transport pathway. It is an oxidoreductase that oxidises a variety of structurally unrelated compounds, including steroids, fatty acids and xenobiotics. The crystal structure of CYP2C8 was published in January 2004 with a resolution of 2.70Å (Schoch *et al.*, 2004).

3.4 Sequence and structure alignment

The aim of this step is to match each residue in the target sequence to its corresponding residue in the template structure, allowing for insertions and deletions (Barton, 1996). An underlying assumption is that the chains to be aligned are all related. The alignment procedure can use sequence only (i.e. residue identities) and sequence-derived information (i.e. predicted secondary structure) as well as structure-based information when computing a multiple sequence alignment. MOE-Align implements a modified version of the alignment methodology originally introduced by Needleman and Wunsch (Needleman and Wunsch, 1970). In this approach, alignments are computed by optimising a function based on residue similarity scores obtained from applying an amino acid substitution matrix to pairs of aligned residues and gap penalties. Penalties are imposed for introducing and extending gaps in the sequence with respect to another. The final optimised value is referred to as the alignment score.

The sequence alignment was performed using MOE with an alignment constraint between the target and the template active site. All the default settings in the MOE-Align panel were used for the sequence alignment.

The secondary structure of the CYP26A1 models together with the templates were determined using Swiss-PDB viewer 3.7 (.Guex and Peitsch, 1997) The query sequence was then aligned against the most homologues template, CYP3A4, CYP2C9, CYP2C8 and CYP2C5 using Clustal W (Thompson *et al.*, 1994) for identification of specific α-helices, β-sheets, coils and loops and model validation.

3.5 Building the homology model

Once the sequence alignment was produced, the next step was to derive a 3D model using comparative modelling. Programs for comparative modelling use one of

two approaches either a fragment based stepwise approach or a single step approach. Both methods produce models of equally good quality. However, the single step approach enables experimentally derived restraints (*e.g.* from NMR-derived distances) (Modi *et al.*, 1996) to be added during the modelling process, rather than in a post hoc fashion as with the fragment based approach.

The fragment-based approach divides parts of the structural templates into three groups: the well-defined regions of the polypeptide backbone (or structurally conserved regions), the poorly-defined regions of the polypeptide backbone (or structurally variable regions), and the amino acid sidechains. The first step is to build the polypeptide backbone of the structurally conserved regions of the model, which are either defined automatically by the program or entered manually by the user. This results in a disjointed set of structural fragments. The next stage is to join these with the structurally variable regions of the polypeptide backbone (often loops joining secondary structural elements) or, where no suitable fragments exists in the templates, to scan a database of protein structures to identify a suitable fragment. The third stage is to change the atoms in the amino acid sidechains, where necessary. The final step is energy minimisation of the model. For example, the program COMPOSER (Sutcliffe *et al.*, 1987; Tripos SYBYL, 2004) or the SWISSMODEL web server (SWISSMODEL, 2004) can be used for fragment- based comparative modelling.

The single-step approach represents the individual structural features in the model (e.g. mainchain conformation and the position of hydrogen bonds) by probability distribution functions based partly on the structure of the templates and partly on known stereochemistry. These probabilities are used as restrains when the model is constructed. Since each feature is represented as a probability distribution function, a family of models consistent with this set of distributions, each with a different conformation, is produced. Production of a family of models, rather than a single model as in the fragment-based approach, enables the significance of different interactions and conformations in the final models to be evaluated. If steric problems (particularly with bond lengths and, to lesser extent, bond angles) occur consistently across the family of models, these are indicative of an error in the sequence alignment. The sequence alignment is therefore checked against the three-dimensional alignment of the template structures with the models using interactive molecular graphics (e.g. InsightII and Quanta, Accelrys (Accelrys, 2004)), and the sequence alignment updated accordingly. The major advantage of this approach is that restraints

derived from both experimental observations and analysis of previous models can be included in the modelling process in the form of distance restrains. For example the program Modeller (Sali *et al.*, 1993; Modeller, 2004) and Molecular operating environment (MOE) (Kharkar *et al.*, 2003; MOE, 2004) use the single step approach.

MOE was first chosen over Modeller and Swiss-Model owing to its ease of use and superior rendering facilities.

Different force fields built in MOE were tried to construct the homology models including AMBER 94 (Weiner *et al.*, 1984; Weiner *et al.*, 1986), CHARMM22 (Ilson *et al.*, 2003) and MMFF94X (Halgren, 1996) in an attempt to find the best model in term of stereochemical properties and sidechain environment.

MOE folds the residues of CYP26A1 in a similar manner to the template. It generates ten intermediate models for each run which are the results of the permutational selection of different loop candidates and sidechain rotamers. Ten intermediate models were generated and the final model was taken as the cartesian average of all the intermediate models. The haem was positioned using the same coordinates as in the template and the complex model was energy minimised.

The models obtained after docking the haem and doing energy minimisation, showed that the distance between the thiolate of the cysteine residue at the active site and the iron of the haem was 2.77 Å in the homology model based on CYP 3A4 as a template, 2.84 Å in the homology model based on CYP2C9 as a template and 2.92 Å in the homology model based on CYP2C8 as a template. This distance is very suitable for the interaction between the thiolate of the cysteine and the iron of the haem to occur.

3.6 Model validation

Once the homology modelling procedure has finished, the final model should be inspected using Stereochemical Quality Evaluation tools in order to confirm that the model's stereochemistry is reasonably consistent with typical values found in crystal structures. Persistent problems may suggest a problem with the alignment used to build the model; manual adjustments to the alignment may be necessary, particularly in the loop areas, followed by a rebuilding of the model. The process of comparative modelling is an iterative process with validation possible at almost every

level. This is used to ensure that the resulting model gives as true and accurate a representation of the 3D structure of the target protein as is possible.

Two types of checks are generally used for this: stereochemical quality and sidechain environment. For all these checks, we use the results returned for the templates as a baseline against which to compare the models. The results of the model validation are summarised in **Table 3.2**, the corresponding values from the templates, the baseline against which these values were compared, are summarised in **Table 3.3**.

The Biotech Validation Suite for Protein Structure (Biotech, 2004) makes available a wide range of stereochemical checks. These assess how well the stereochemistries of the residues in a given protein structure compare with those in well-refined, high-resolution crystal structures. We use the Ramchandran plot to assess the quality of the polypeptide backbone and sidechains. The Ramachandran plot was obtained using the RAMPAGE server at Cambridge (Rampage, 2004; Lovell *et al.,* 2002). The Ramachandran plot shows the Phi-Psi torsion angles for all residues in the structure (except those at the chain termini). Glycine residues are separately identified by crosses as these are not restricted to the regions of the plot appropriate to the other sidechain types. The colouring/shading on the plot represents the different regions and correspond to the "core" regions representing the most favourable combinations of Phi-Psi values.

The glycine and proline residues are represented in different plots because they have different Phi/Psi combination.

In the Ramchandran plot a model is validated "OK" if about 80-90% of the residues lie in the most favoured region of the plot.

The compatibility between the amino acid sequence and the environment of the amino acid sidechains in the model is another validation criterion. We use Verify 3D (Luthy *et al.,* 1992; Verify 3D, 2004) and Errat (Colovos *et al.,* 1993; Errat, 2004) for this. It appears that these two approaches are complementary. Verify3D assesses the environment of the sidechain based on the solvent accessibility of the sidechain and the fraction of the sidechain covered by polar atoms. Compatibility scores above zero correspond to acceptable sidechain environments while the total average of the Verify3D score should be above 90 for a reasonable model. Errat assesses the distribution of different types of atoms with respect to one another in the protein models. Average confidence limits of about 50% correspond to acceptable sidechain environment. Errat is a sensitive technique which is good for identifying incorrectly

folded regions in preliminary protein models. It is a protein structure verification algorithm that is especially well-suited for evaluating the progress of crystallographic model building and refinement. The program works by analysing the statistics of non-bonded interactions between different atom types. A single output plot is produced that gives the value of the error function versus position of a 9-residue sliding window. By comparison with statistics from highly refined structures, the error values have been calibrated to give confidence limits, which is useful in making decisions about reliability. 5% of a good protein structure is expected to have an error value above the 95% confidence level. However it is limited in that it does not contain any parameterisation regarding surface polarity shown to be an important factor in determining whether or not folds in proteins are valid (Novotny *et al.*, 1988). Hence, any misfolded proteins, which display volumes comparative to their native forms, will not be identified by Errat as having been misfolded.

It was found that models using CHARMM22 force field for energy minimisation have the best stereochemical properties together with a good sidechain environment, those using AMBER94 do not have as good stereochemical properties

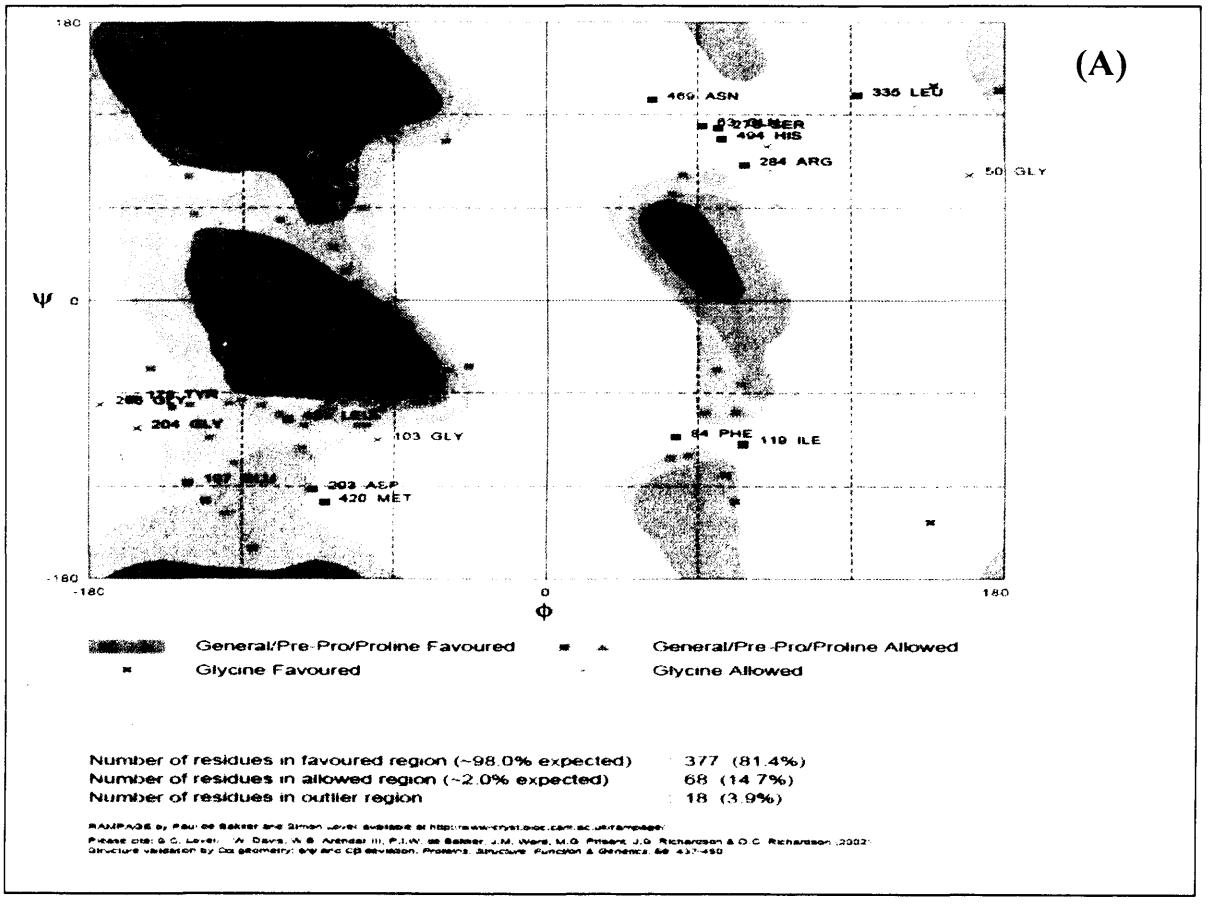

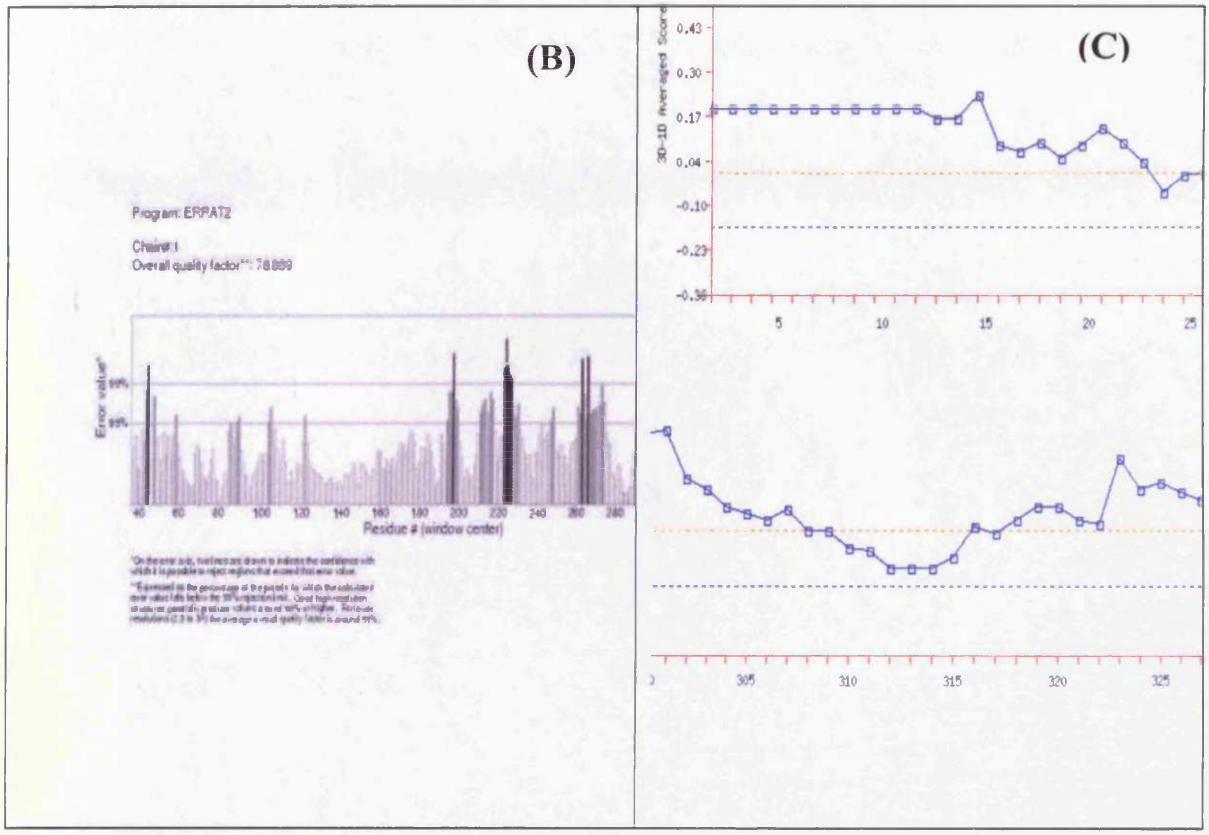

Figure 3.2 (A): Ramachandran Plot for CYP26A1 model based on CYP3A4. The dark blue areas correspond to the most favoured regions, the light blue areas to the allowed regions, the white areas to the disallowed regions, dark yellow to the glycine favoured regions and light yellow to the glycine allowed regions.

Figure 3.2 (B): Errat plot for the CYP26A1 model based on CYP3A4 as a template. The black columns identify problem areas.

Figure 3.2 (C): Verify3D result for CYP26A1 model based on CYP3A4 as template. The graph shows only residues having a low score.

as those with CHARMM22 but they show good sidechain environment. Models using MMFF94X have good stereo chemical properties but not good sidechain environment.

In the final model based on CYP3A4, the percentage of residues in the Ramchandran plot in the most favoured regions has increased to 81.4 %, 14.7% in the allowed regions and 3.9% in the disallowed area (**Figure 3.2a**).

Thus, a total of 96.1% of the residues of the modeled structure after minimisation were in the allowed region, which indicate that the backbone dihedral angles Phi and Psi in the model were reasonably accurate. The model also showed a good sidechain environment represented in its high Errat score (84.5) (**Figure 3.2b**). Areas of potentially unfavourable interactions are indicated by the dark bands, notable in the residue regions: 45-47, 200-205, 225-230, 265-270 and 320-325.

In Verify3D, a good quality crystal structure of a protein of this size should score 200 and a score less than 90 would indicate an incorrect structure. The model has a score of 121, below that expected for a crystal structure of the same size and above the score that would indicate an incorrect fold. As seen in **Figure 3.2c**, the model suffers in the regions of residues 30-35 and residues 310-320.

The final model of CYP26A1 based on CYP2C9 had 82.4 % of its residues in the most favoured regions of the Ramachandran plot, 15.2% in the allowed regions and 2.4% in the disallowed regions. Thus, a total of 97.6% of the residues of the modelled structure after minimisation were in the allowed region, which indicate that the backbone dihedral angles Phi and Psi in the model were reasonably accurate.

The number of residues in normal non-bonded environment (Errat) increased to 82.3%. The main problem areas that are seen are at the C-terminal, residues 80-85, 160-170, 200-205 and 290-295.

The average of compatibility score in Verify3D was 136 suggesting proper solvent accessibility for the sidechains. The model is good except in the areas that dip below the baseline and are likely to exhibit unsuitable sidechain environment. These were residues 240-250 and residues 300-310.

The final model of CYP26A1 based on CYP2C8 had 82.3 % of its residues in the most favoured regions of the Ramachandran plot, 15.1% in the allowed regions and 2.6% in the disallowed regions. Thus, a total of 97.4% of the residues of the modeled structure after minimisation were in the allowed region, which indicate that the backbone dihedral angles Phi and Psi in the model were reasonably accurate.

The Errat score was 84.5% indicating that most of the residues are in a good non-bonded environment. The main problem areas were at residues 70-75, 80-85, 100-105, 120-125, 145-155 and 190-200.

In Verify3D, the model has a score of 127 and suffers in residues 130-140 and 295-305.

The results of the validation checks performed on the final lowest energy model for each template are listed in **Table 3.2**.

For comparison, the validation checks have also been performed on the template crystal structures, the results are shown in **Table 3.3**.

Table 3.2: Results of validation studies performed on the CYP26 models produced from the homology modelling with the three templates.

Model	Ramachandran plot[a] (%)	Errat[b] (%)	Verify3D[c] (total score)
Based on 3A4 as template	81.4	84.5	121
Based on 2C9 as template	82.4	82.3	136
Based on 2C8 as template	82.3	84.5	127

[a] percentage of residues with Phi and Psi conformation in the most favoured regions of the Ramachandran plot.

[b] the percentage of residues in normal non-bonded environment.

[c] The total Verify3D score summed overall residues.

Table 3.3: Validation results for the crystal structures used as templates for the modelling studies.

Crystal structure (PDB code)	Resolution (Å)	Ramachandran plot[a] (%)	Errat[b] (%)	Verify3D[c] (total score)
CYP3A4 (1TQN)	2.05	91.2	93.7	178
CYP2C9 (1R90)	2.00	92.3	89.6	183
CYP2C8 (1PQ2)	2.70	93.8	90.8	161

[a] percentage of residues with Phi and Psi conformation in the most favoured regions of the Ramachandran plot.

[b] the percentage of residues in normal non-bonded environment.

[c] The total Verify3D score summed overall residues.

From **Table 3.3** it is apparent that the templates have more than 90% of their residues in the most favoured region of the Ramachandran plot and Errat scores greater than 90% (i.e. 90% or more of their residues are in normal sidechain envioronment). The theoretical models of CYP26A1 have more than 80% of their residues in the most favoured region (i.e. 10% or less than the values of the templates) and acceptable Errat and Verify3D scores indicating good sereochemical quality and non-bonded atom environment compared with the template crystal structures (**Table 3.2**).

Validation results would suggest that all three models performed equally well in terms of mainchain stereochemistry and amino acid environment, therefore substrate and ligand docking was required for further validation of the active site architecture.

3.7 Docking studies

In general, there are two strategies for docking a ligand into a macromolecule. The first one is to use the whole molecule of a ligand as a starting point and then performs a particular search algorithm to explore the energy landscape of the ligand at the binding site, looking for optimal solutions (local energy minima). The search algorithms include molecular dynamics and genetic algorithms. The programs AutoDock (Morris *et al.,* 1996), Gold (Jones *et al.,* 1997) and MOE Dock (Kharkar *et al.,* 2003) are some examples in this group.

The second strategy, called fragment-based docking, is to start by placing one or several base fragments of the ligand into a binding pocket, and then to build the rest of the molecule in the site. DOCK4.0 (Ewing *et al.,* 1997), FlexX (Rarey *et al.,* 1996a; Rarey *et al.,* 1996b), LUDI (Bohm, 1992), Hammer-head (Welch *et al.,* 1996), GROWMOL (Bohacek *et al.,* 1997) and HOOK (Eisen *et al.,* 1994) are programmes in this group, although some of these algorithms are mainly used in the area of de novo ligand design.

The fragment-based approach is faster than the whole molecule-based docking method. However, only the local interactions between the protein binding site and the ligand fragments under construction are taken into account during the docking procedure. Thus it is difficult to evaluate if the global energy minimum has been found. The results from the fragment-based approach are also sensitive to the choice of the base fragment and its placement. Indeed, if the binding site has a deeply buried pocket with hydrogen bond donors or acceptors, this approach gives good results. However, if the pocket is dominated by lipophilic residues or characterised by a shallow pocket, not only the placement of the base fragment is not definite, but also it is difficult for the program to decide where to add the next fragments. Consequently, the resulting docking structures can deviate from the real binding mode significantly. While the docking results from whole-molecule-based methods are not dependant on the choice of the base fragment, they require much more computation to find an optimal solution in general. For a large flexible ligand, the whole molecule-based docking approaches may not find a good binding mode due to the vast space to be searched (Wang *et al.,* 1999).

The docking methods were developed in association with scoring functions in order to rank docked compounds. These scoring functions should be able to

distinguish active from inactive compounds independently of the docking method used. The docking methods have typically been validated on the basis of their ability to reproduce the geometries of high-affinity protein-ligand complexes.

Ligands were docked within the active site of the homology model using the FlexX docking programme of SYBYL, performed with the default values. The active site was defined by all the amino acid residues within a 6.5 Å distance from TRP112, VAL116, THR304, VAL370 and GLY373, including the haem in a heteroatom file. The output of FlexX docking was visualised in MOE and the scoring.svl script (Code, scoring.svl) was used to identify interaction types between ligand and protein.
ATRA was found to dock satisfactorily in the active site of all three models, with ATRA orientated in a position that favours 4-hydroxylation at C-4. Considerable hydrophobic interactions are formed between the substrate and the active site holding the substrate into a lipophilic tunnel and with C-4 at a distance of 4.83Å in the model based on CYP3A4, 6.06Å in the model based on CYP2C9 and 5.93Å in the model based on CYP2C8.

However, only the CYP26A1 model built using the CYP3A4 template was able to accommodate the inhibitor ligand (*S*)-R115866 (Stoppie *et al.*, 2000) in an orientation that would allow coordination between the nitrogen of the triazole heterocycle and the haem iron transition metal. However, docking studies had indicated that TRP112 was partially obstructing coordination between the triazole nitrogen of the ligand R115866 and the transition metal resulting in a distance of 5.50 Å (**Figure 3.3a**). Docking studies do not take into account protein flexibility therefore molecular dynamics were performed on the active site containing (*S*)-R115866. For that, a molecular dynamics of the active site containing the docked inhibitor was performed. Molecular dynamics addresses the problem of solving the classical equations of motion for a system of *N* atoms in an effort to generate a conformational search in space, or *trajectory*, under specified thermodynamic conditions (e.g. constant temperature or constant pressure). Such a trajectory is important for two reasons. Firstly, it provides configurational and momentum information for each atom, from which thermodynamic properties of the system can be calculated. Secondly, the trajectory represents an exploration, or search, of the conformation space available to a particular system.

The principle underlying conformation search using dynamics is that a molecule in a dynamics simulation will eventually search the entire conformation

space. The obvious problem with this approach is that the search space may be huge, and thus, it may take many thousands, millions, or even billions of steps to adequately sample the conformation space.

This resulted in an optimised active site architecture and the TRP112 residue positioned in a more favourable conformation with respect to ligand binding (**Figure 3.3b**) with the triazole nitrogen perpendicular to the haem iron at a distance of 2.6 Å. Furthermore, (*S*)-R115866 establishes a hydrogen bond between the benzothiazole nitrogen and the NH of SER115, as well as several hydrophobic interactions with the side chains of TRP112, PHE374, PHE84, PHE299, VAL116, PRO371 and other residues (**Figure 3.4**)

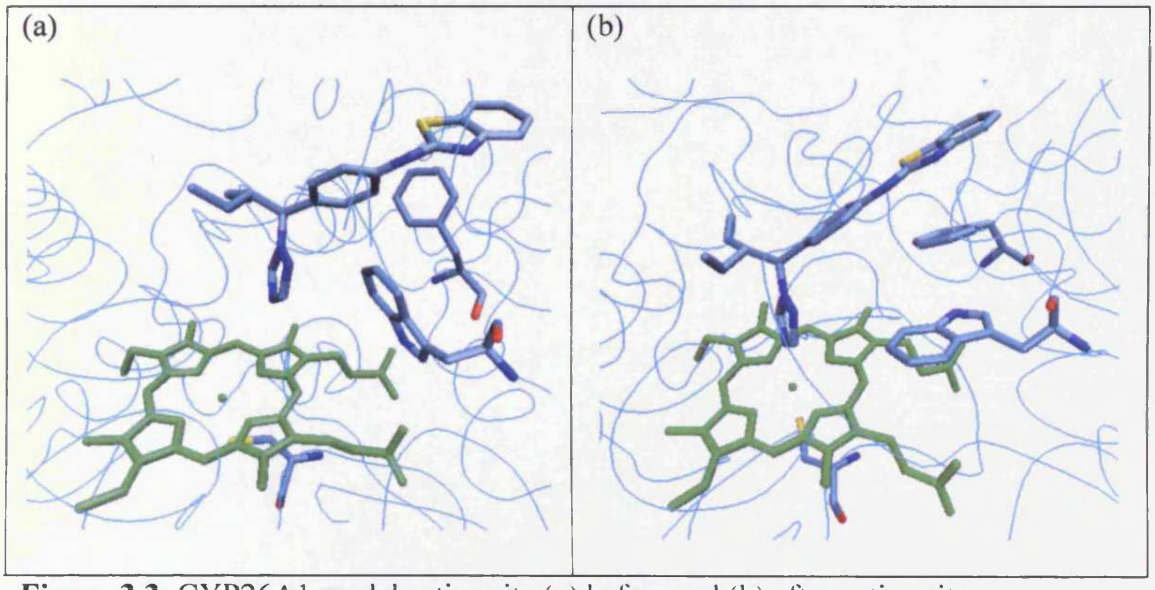

Figure 3.3: CYP26A1 model active site (a) before and (b) after active site optimisation with the (*S*)-R115866 bound inhibitor.

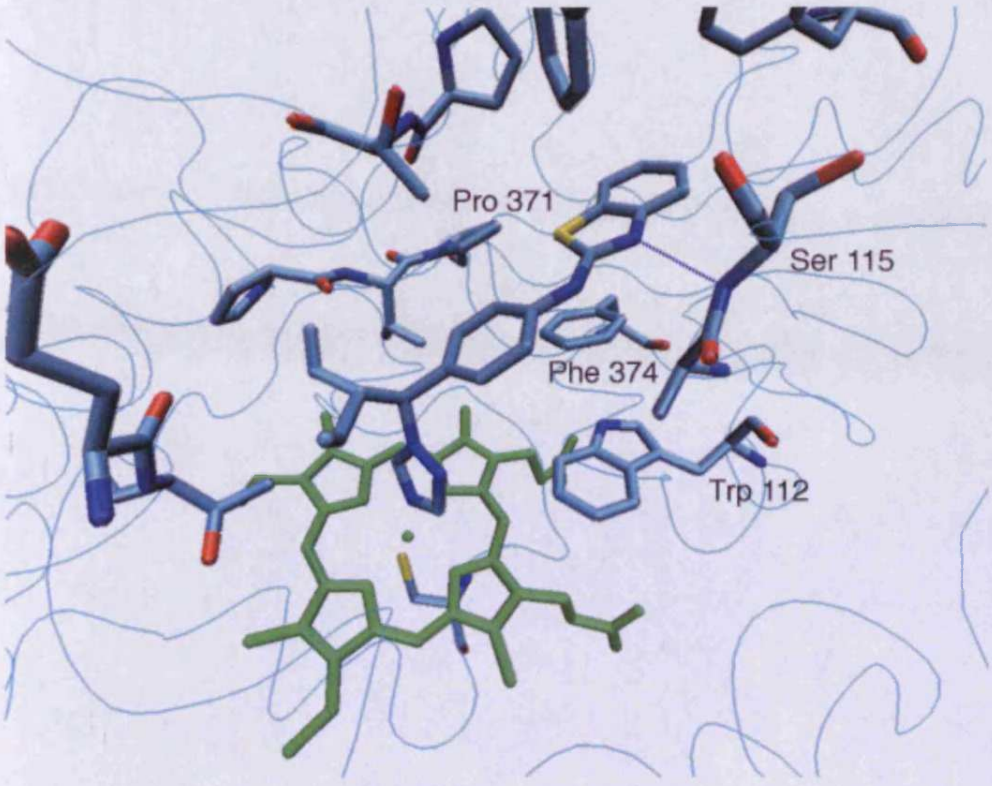

Figure 3.4: Interactions between (*S*)-R115866 and the CYP26A1 active site.

The natural substrate ATRA was docked in the optimised active site. **Figure 3.5** shows the putative active site of CYP26A1 containing the bound substrate orientated for 4-hydroxylation with the C4 atom positioned in proximity of the haem iron at a distance of 5.3 Å, a distance that would accommodate a water molecule between the 4-position of ATRA and the haem iron. ATRA interacts with amino acid residues at the active site by multiple hydrophobic interactions, including the side chains of TRP112, PHE299, PHE222, PHE84, PHE374 and PRO371. Hydrogen bonding interactions between the carbonyl group of ATRA and ARG86 hold the molecule within the hydrophobic tunnel.

3.8 Model explanation and discussion

The secondary structure of the CYP26A1 models together with the templates were determined using Swiss-PDB viewer 3.7 (Swiss-PDB, 2004) with identification of α-helices, β-sheets, coils and loops.

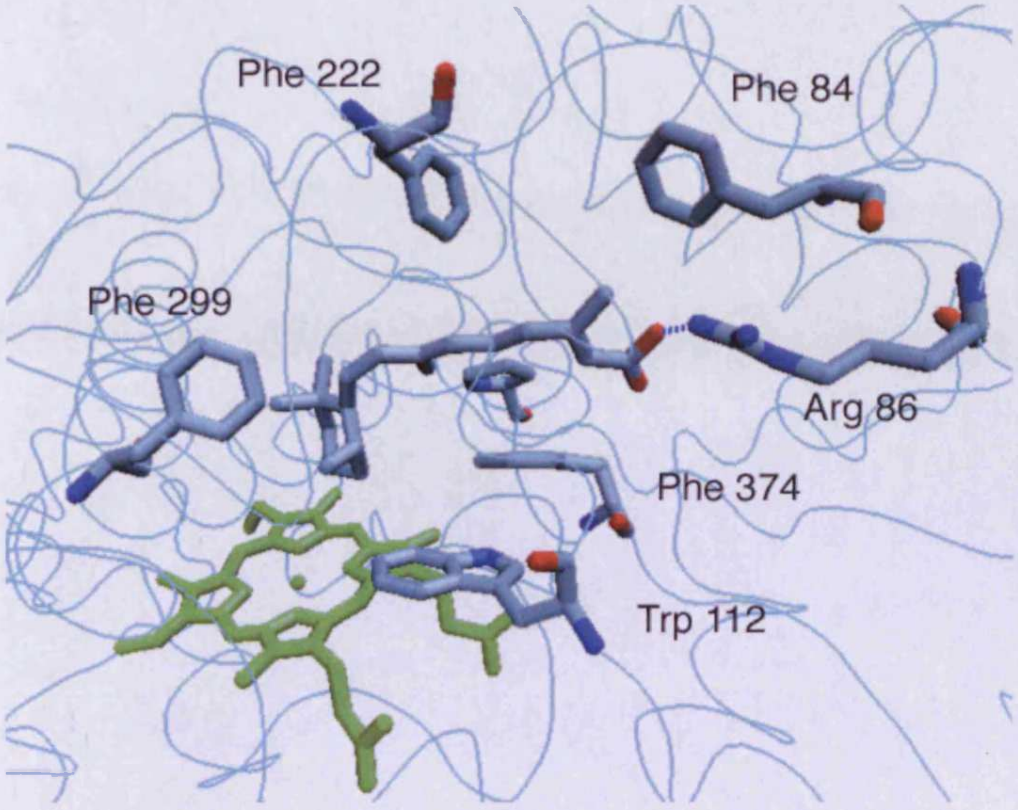

Figure 3.5: ATRA docked in CYP26A1 active site

Structural alignment of the CYP26A1 with the most homologus human P450s allowed the assignment of substrate recognition sites and P450 binding motifs (ETLR, PERF and haem binding domains) and identification of specific α–helices, β-sheets, coils and loops (**Figure 3.6**). The alignment was performed using ClustalW (Thomson *et al.,* 1994) on the EBI server (Clustal W). Then, by the aid, of a multiple sequence alignment of 20 CYP2 family P450s produced using the GCG package (Genitcs Computer Group, Modison, WI, USA) in which the location of substrate recognition sites (Gotoh, 1992) together with the position of α-helices and β-sheets are identified (Lewis, 1998 a; Lewis, 1998b), the specific helices and sheets for the models and templates for comparison were identified.

The resultant alignment was subsequently checked to ensure that any residues identified experimentally as being crucial to catalytic activity such as the proximal cysteinate ligand that occupies the fifth co-ordination site of the haem and is responsible for stabilisation of the high energy oxy-ferryl species generated during the catalytic cycle of the P450 (Lewis, 1986), were matched.

Studies have shown that the active site region (**Figure 3.6**) of the P450s is conserved across the entire family and the middle section of the I-helix (**Figure 3.6**) is also well conserved despite low overall sequence homology (Hasemann, 1995). However, although similarities do exist across the family, there are flexible regions in each P450 which have significantly different amino acid composition, such as the β'-helix, which may or may not be present, and F-G loop regions.

The resultant alignment was subsequently checked to ensure that highly conserved and functionally important residues in the CYP superfamily are correctly aligned with each other.

```
CYP2C8    HDDKEFPNPNIFDPGHFLDKNGNFKKSDYFMPFSAGKRICAGEGLARMELFLFLTTILQN 455
CYP3A4    RDPKYWTEPEKFLPERFSKKNKDNIDPYIYTPFGSGPRNCIGMRFALMNMKLALIRVLQN 461
CYP26A1   DVAEIFTNKEEFNPDRFMLPHPEDASRFSFIPFGGGLRSCVGKEFAKILLKIFTVELARH 462
             : :.: : * * :*     :  .   : **..* * * *  :* : : :    : ::

                        | SRS6  |
CYP2C9    FNLKSLVDPKNLDTTPVVNGFASVPPFYQLCFIPV------ 490
CYP2C8    FNLKSVDDLKNLNTTAVTKGIVSLPPSYQICFIPV------ 490
CYP3A4    FSFKPCKETQIPLKLSLGGLLQPEKPVVLKVESRDGTVSGA 502
CYP26A1   CDWQLLNGPPTMKTSPTVYPVDNLPARFTHFHGEI------ 497
             . :          . .   .   .
```

Figure 3.6: CYP26A1 sequence and ClustalW (1.82) alignment with CYP2C9, CYP2C8 and CYP3A4. The colour coding of amino acid type: red, small + hydrophobic (AVFPMILWY); blue, acid (DE); magenta, basic (RHK); green, hydroxyl + amine + basic (STYHCNGQ). Substrate recognition sites (SRS) and conserved P450 domains (ETLR, PERF and Haem binding domain) are indicated. "*" means that the residues are identical, ":" means that conserved substitutions have been observed, "." means that semi-conserved substitutions are observed.

The 3D structure of CYP26A1 model was similar to those of other CYPs reported so far. The model is mainly alpha helical with some beta sheet mostly on one side of the molecule (**Figure 3.7**). As expected, the I-helix lies just above the haem and is connected to the J-helix through a loop. This is a counterpart with the possible role of the I-helix in the active site. B-sheets are located at the far side of the protein except those which are involved closely in the active site.

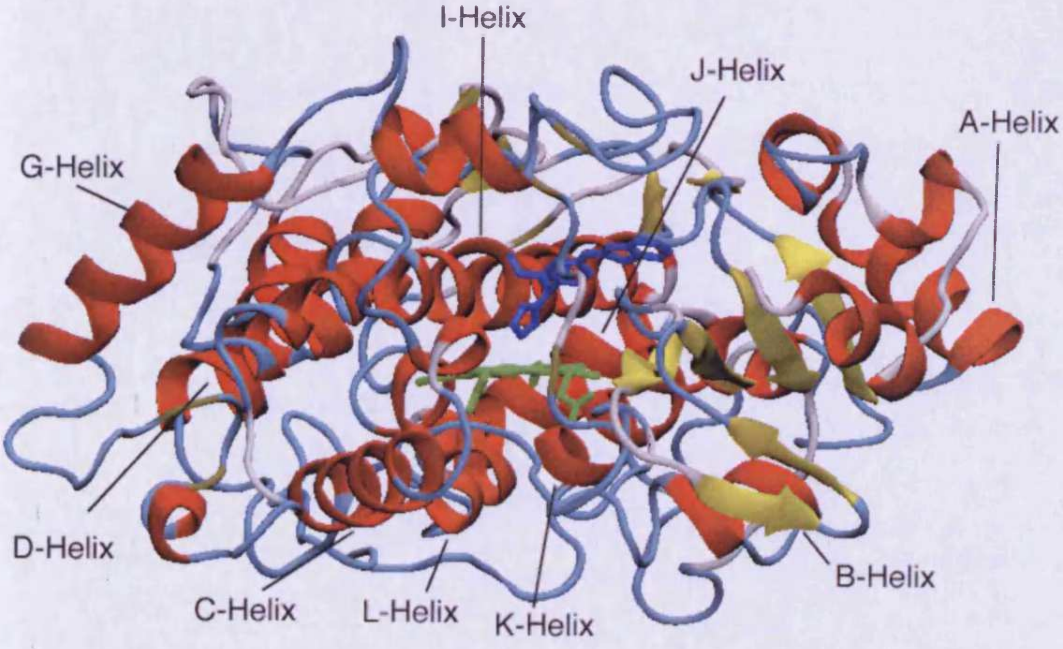

Figure 3.7: 3D Structure of the CYP26A1 model. α-Helices are in red, β-sheets are in yellow, loops are cyan and coils are grey.

The secondary structure is derived from the template structure CYP3A4 therefore further comparison with the template secondary structure was performed (**Table 3.4**). A good overlap between the model and template secondary structure do exist especially the position of the A-, E-, J-, J'-, K-, L- and the G-helices which is broken in the model and the template. The I-helix which is well conserved among P450s shows a high degree of conservation in the model and template. The glycine residue that is usually very well conserved across the P450s in the I-helix matches up. The model differs from the template in that the B'-, F- and H-helices are not identified in the model.

Table 3.4: Comparison between the model of CYP26A1 based on CYP3A4 and the template secondary structure.

Model		template	
Residues	Secondary structure	Residues	Secondary structure
LEU58-MET60	Helix	LEU32-LEU36	Helix
ARG64-TYR75	A-helix	PHE57-TYR68	A-helix
TYR79-LEU83	B-sheet	LYS70-GLY77	B-sheet
ARG86-VAL91	B-sheet	GLN79-THR85	B-sheet
ALA94-LEU101	B-helix	PRO87-LEU94	B-helix
ASP105-LEU107		MET114-LYS115	B'-helix
SER132-ARG142	C-helix	GLU124-ARG128	C-helix
ARG146-SER169	D-helix	LEU132-PRO135	
ARG173-VAL177	D'-helix	SER139-GLU165	D-helix
PHE186-GLY195	E-helix	LYS173-SER186	E-helix
ASP227-VAL228	F'-helix	PRO202-LYS208	F-helix
GLY232-ALA239	G-helix	PRO218-THR224	F'-helix
GLU248-GLU262		PHE228-LEU236	G-helix
GLN288-GLY317	I-helix	ARG243-LYS257	
HIS321-LYS331	J-helix	PHE271-GLN279	H-helix
ASP346-ILE349	J'-helix	ASP292-LEU321	I-helix
VAL359-LEU366	K-helix	PRO325-VAL338	J-helix
GLY373-ALA377	B-sheet	TYR347-LEU351	J'-helix
TRP392-SER397	B-sheet	TYR355-LEU366	K-helix
CYS399-HIS402	K'-helix	MET371-CYS377	B-sheet

PRO422-GLU425	Helix	VAL381-ILE383	B-sheet
GLU446-ARG461	L-helix	MET386-ILE388	B-sheet
ASP464-GLN466	B-sheet	VAL392-SER398	B-sheet
THR473-LYS475	B-sheet	TYR399-LEU401	K'-helix
TYR481-VAL483	B-sheet	GLU417-ARG418	Helix
ARG489-THR491	B-sheet	MET445-LEU460	L-helix
		ASN462-LYS466	B-sheet
		LYS476-SER478	B-sheet
		GLN484-GLU486	B-sheet
		VAL489-ARG496	B-sheet

To find likely residues involved in the active site, residues within a 7Å radius of the haem were selected. The residues above the haem molecule are of main interest since they are the residues expected to be involved in the ligand interaction. The main residues involved in the active site belong to the I-helix including THR295, GLU296, LEU297, GLY300, GLY301, THR304, THR305, SER307 and ALA308. The remainder of the residues are as follows: HIS111, TRP112, PRO113, CYS124, LEU125, SER126, ASP127 in the loop between the B-helix and C-helix, CYS192, LEU193 in the E-helix, PRO368, PRO369, VAL370 in the loop between the K-helix and the D-sheet and the two last residues GLY373, PHE374 in the C-sheet. The active site cysteine 442 lies below the haem within a coil. There is a large pocket just above the haem molecule surrounded by the previously mentioned residues which is believed to accommodate all-*trans* retinoic acid and relatively large substrates. There are also many oxygen and nitrogen atoms toward the active site that could provide sites for hydrogen bonding. It is also worth noting that all the residues involved in the binding of ATRA and (*S*)-R115688, are located in the substrate recognition sites (SRSs) (**Figure 3.6**).

Chapter 4

Design of CYP26A1 inhibitors

4 Design of CYP26A1 inhibitors

4.1 Design of CYP26A1 inhibitors through docking studies of some CYP26 inhibitors with known IC_{50}

In this section, different CYP26 inhibitors with known IC_{50} synthesised and tested by our group at the Welsh School of Pharmacy, (Yee *et al.*, 2005) were docked in our active site.

The aim of this docking study was to use the different docking scoring functions to find any correlation between the chemical structure and the inhibition constant of the docked compounds, which might be helpful in the rational design of seletive inhibitors. The docked compounds are chemically different comprising benzofuran, benzofuran-2-carboxamide, benzyl tetralone and benzylidene tetralone derivatives (**Figure 4.1**), which might give insight to how different compounds could interact with the active site and if there are specific moieties needed for tight binding with the active site. FlexX was used for the docking due to its rapidity and to benefit from its various scoring functions in the analysis of the results.

Docking interactions at the enzyme active site were shown to be comparable with ATRA. All the compounds were present in the active site and positioned in a hydrophobic tunnel. However, no evidence emerged that could correlate the enzyme inhibition of these compounds and any of the studied scoring function with any of the different groups and obviously, no specific chemical moieties or features have been found to be correlated to the inhibition activity in this study.

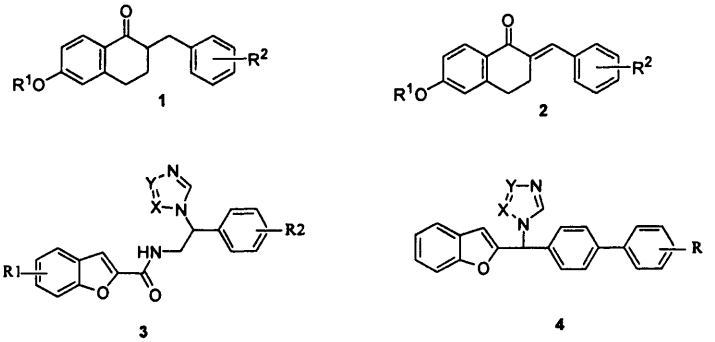

Figure 4.1: Chemical structure of compounds used in the docking studies including derivatives of 1) benzyl tetralone 2)benzylidene tetralone, 3) benzofuran-2-carboxamide 4) benzofuran

4.2 Design of CYP26A1 inhibitors through virtual screening

4.2.1 Introduction

In molecular modelling, virtual screening is a technology that is gaining increasing use in drug design and discovery (Walters *et al.*, 1998; Ostrov *et al.*, 2007). There are many tools available for performing these computational analyses and they can be grouped as being either ligand-based or receptor-based. For ligand-based methods, the strategy is to use information provided by a compound or set of compounds that are known to bind to the desired target and to use this to identify other compounds in corporate databases or external databases with similar properties. This can be performed by a variety of methods including similarity and substructure searching (Mestres and Knegtel, 2000), pharmacophore matching (Mason *et al.*, 2001) or 3D shape matching (Srinivasan *et al.*, 2002). When the structure of the target protein is known, receptor-based computational methods can be employed. These involve explicit molecular docking of each ligand into the binding site of the target, producing a predicted binding mode for each database compound, together with a measure of the quality of the fit of the compound in the target binding site. This information is then used to rank the compounds with a view to selecting and experimentally testing a small subset for biological activity.

Virtual screening covers a variety of sequential computational phases, including the preparation of a library of molecules using combinatorial chemistry, the docking of the later into the target active site and the post-docking analysis leading to a selection of compounds for synthesising and testing

4.2.2 Preparation of a library of compounds

In order to design new inhibitors, our objective was to create a new library of compounds and to dock them in our active site. MOE QuaSAR-CombiGen (MOE, 2004; Abdel-Hamid *et al.*, 2007) was used to generate a fully-enumerated combinatorial library from a scaffold database and a set of substituent R-group databases. MOE QuaSAR-CombiGen enumerates a virtual library of all possible products that are combinatorially generated from a set of fragment molecules. The virtual library is constructed by functionalising central molecular fragments

(scaffolds) by attaching R-groups at marked attachment points called ports. The entire combinatorial library is enumerated by exhaustively cycling through all combinations of R-groups at every attachment point on every scaffold. The virtual library is then written to an output database.

The intuition of the researcher, the knowledge of the interactions involved in the ligand-receptor binding and the use of comparative computational methods can successfully guide the choice of the suitable scaffold and either the location of the ports on the scaffold or the selection of the more reasonable fragments to be inserted onto the scaffold for a stable and efficient binding of the designed final compounds to the active site.

Our library was designed by taking the best known inhibitor of CYP26, R115866, and simplifying its structure to a scaffold that contains only the main part supposed to be crucial for enzyme inhibition. The library of compounds was then built up as follows. The profile of the compounds was divided in three parts.

The scaffold was chosen to be the 4-(1,2,4)triazol or imidazol-1-ylmethyl-phenylamine moiety. This moiety contains two essential components for the active binding of the molecule. The triazole or imidazole is essential for metal-ligand interaction with the haem part of the enzyme. For simplification, only the triazole will be included in the library. The phenylamino group holds the inhibitor tightly in the active site with the phenyl ring forming hydrophobic bonds mainly with the haem, TRP112, PHE374 and the amino group forming hydrogen bonding with PRO113. It also plays a role in positioning the triazole in an optimal position from the haem.

The A substituent is designed to be a heteroaryl or aryl analogues. This part seems to be very important because it affects the dimensions, the stereochemistry and the hydrophobicity of the molecule. It is therefore important in placing the triazole ring in the right position just above the haem portion of the enzyme. It is also crucial in determining the overall binding pattern of the inhibitor to the enzyme and holding the inhibitor tightly in the active site through hydrophobic bond formation mainly with PHE374, PRO113 ,SER115 and PHE84 and hydrogen bond formation with different hydrogen donors or acceptors at the active site as SER115 and ALA114 thereby affecting the selectivity and efficacy of the molecule. In total 23 different structures were considered including, phenyl, naphthyl, benzimidazole, benzothiazole, benzoxazole, benzofuran, furan and thiophene analogues (**Table 4.1**).

The B substituent, which was chosen to be a methyl, phenyl or mainly an acid substituent, including amino acids, since, it was reported that the introduction of a carboxylic group to the structure of certain members of a group of CYP26 inhibitors was found to greatly increase the biological activity of the synthesised compounds (Mulvihill *et al.*, 2005). Another reason is to mimic the natural substrate, retinoic acid, which contains a carboxylic group. In case of amino acids, they are also available in their chemically pure enantiomeric forms which will ease the production and eliminate the need for expensive and time consuming enantiomeric separation in case of discovery of highly active drug. This part is very important in determining the physicochemical properties, the stereochemistry as well as the dimensions of the molecule. The carboxylic moiety affects the binding of the molecule to the active site through hydrogen bonds it might form with different residues at the active site such as GLY300, GLU303 and THR304. It may also affect the movement and penetration of the molecule through biological membranes. In total, 33 side chains were designed (**Table 4.1**).

Finally, a library of 690 molecules was created by combination of the three parts and was written to an output database.

Table 4.1: Scaffold and substituent A and B used for building of the combinatorial library.

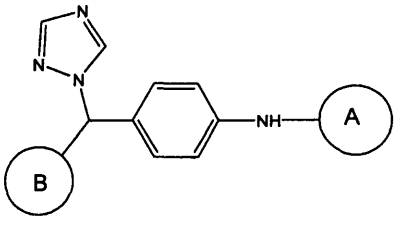

	A		B
1	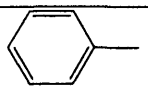	1	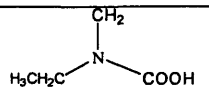
2	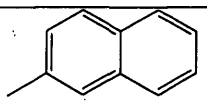	2	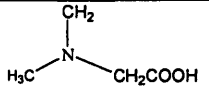
3	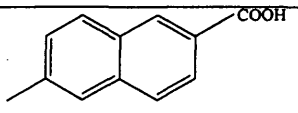	3	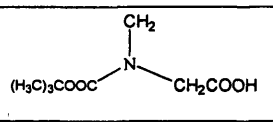
4	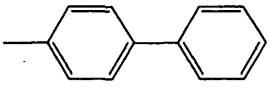	4	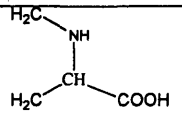

5	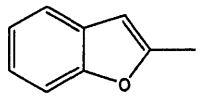	5	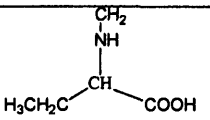
6	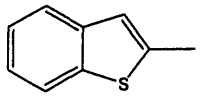	6	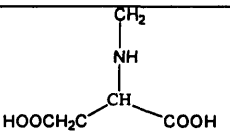
7	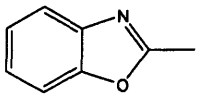	7	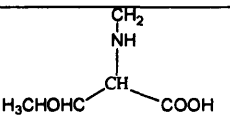
8	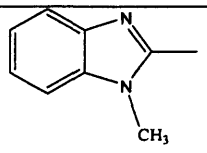	8	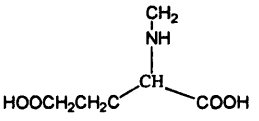
9	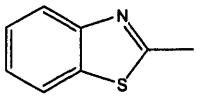	9	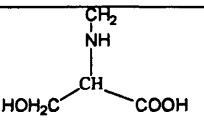
10	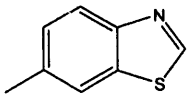	10	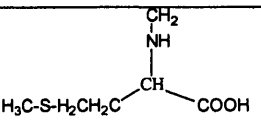
11	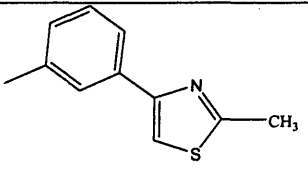	11	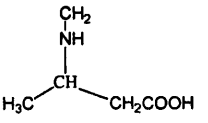
12	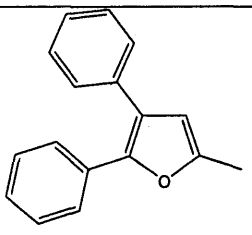	12	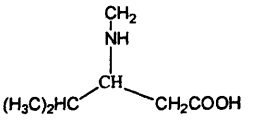
13	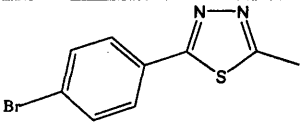	13	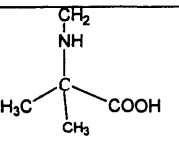
14	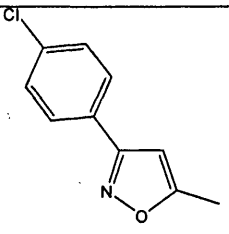	14	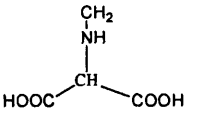
15	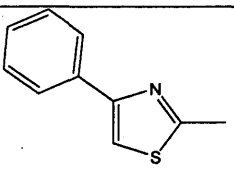	15	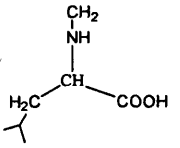

16	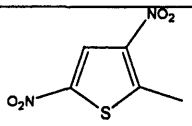	16	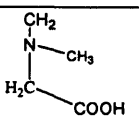
17	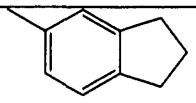	17	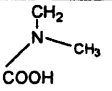
18	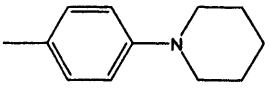	18	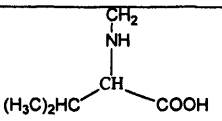
19	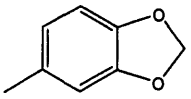	19	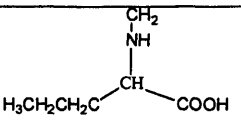
20	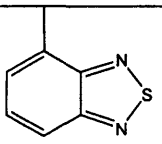	20	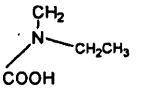
21	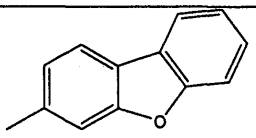	21	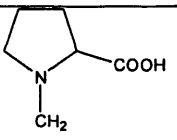
22	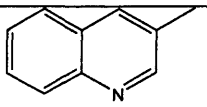	22	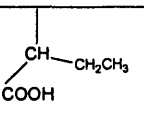
23	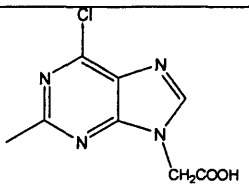	23	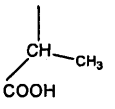
		24	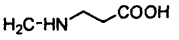
		25	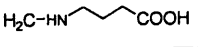
		26	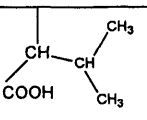
		27	
		28	CH_3
		29	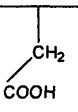
		30	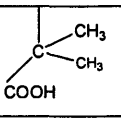

4.2.3. Docking of the molecules and analysis of the results

The FlexX programme was chosen as it is one of the most suitable software to perform a virtual screening. Indeed, it can screen a large number of molecules on a workstation computer within a few days. Other docking programmes such as those using a genetic algorithm or a Monte Carlo approach can screen a smaller number of molecules under the same conditions or require a more powerful computer to be applied to a large number of molecules (Lyne, 2002).

In the database, the formal charges of all the constructed compounds in the library were first computed and their conformation energy minimised using MMFF94X as force field. The database was then exported in Mol2 format to SYBYL databases and docked as multiple ligands in the active site using the same parameters applied in the docking of retinoic acid, R115866 and liarozole.

The results of the docking were only analysed visually due to the lack of correlation between the FlexX scoring functions and the visual compound-active site interaction. The position of the triazole ring from the haem was first evaluated. In the well docked compounds, the distance between the triazole N4 and the iron of the haem should be 3 Å or less thereby allowing the coordination bond to be formed. Secondly, the side chain A was assessed for its ability to form hydrophobic bonds with different residues at the active site especially TRP112 and PHE374. This part together with the position of side chain B is crucial in driving the triazole ring in a conformation that allows good interaction with the haem. Finally, side chain B was evaluated for its capacity to offer the maximal hydrogen bonding and lipohilic interaction with the active site especially GLY300, thereby, holding the inhibitor tightly in the active site.

In general, compounds having bicyclic heterocyclic side chain A had the highest number of well docked conformations especially the benzoxazolyl moiety A7 which gave well docked compounds with side chain B1, B4, B9,B16, B17, B20, B21, B22, B23, B27, B29 and B30. With the 2-benzofuranyl moiety A5, compounds A5_B2, A5_B4, A5_B9, A5_B10, A5_B11, A5_B13, A5_21, A5_B22, A5_B23 and A5-24 showed good interaction with the active site while, in case of the 2-benzimidazolyl moiety A8 and the 2-benzothiazolyl moiety A9, side chains B1, B4, B9, B10, B20, B21, B22, B23, B27, B29 and B30 were the most promising. In case of the 2-naphthyl moiety A2, compounds A2_B1,A2_B4, A2_B9, A2-B10, A2-B16, A2-

B17, A2-B20, A2-B21, A2-B22, A2-B23, A2-B27, A2-B29 and A2-B30 were docked well in the active site while with the 6-benzothiazolyl moiety A10, only compounds having side chain B2, B5, B9, B10, B21 and B24 showed good interaction.

In case of the phenyl moiety, compounds containing side chain B1, B4, B5, B9, B10, B21 and B24 were docked well within the haem pocket with the triazole ring above the haem at a distance that would allow coordinate bond formation.

Compounds having substituent A11 together with side chain B1, B4, B9, B10, B14, B21 and B24 showed good interaction while in the case of compounds having sustituent A17 only those with side chain B2, B4, B5, B9, B10, B22, B24, B27, B29 and B30 showed good docking.

Compounds containing a monocyclic heterocycle did not show good docking. In case of those with phenyl substituent such as A12, A13, A14 and A15, the compounds became too large to be docked in the active site, while with the small substituents A16, they have been found to move freely within the active site and the triazole ring was not in the right position above the haem.

Compounds containing A4, A18 and A21 have been found to be too large to fit into the active site and all the conformations obtained were away from the haem pocket or with the triazole ring too far from the haem.

In conclusion, the analysis of the docking of all the compounds of the combinatorial library revealed that compounds having substituents A2, A5, A7, A8 and A9 are the most promising compounds. While, for side chain B, moieties giving well docked compounds have been found to be mainly B1, B4, B9, B16, B17, B20, B21, B22, B23, B27, B29 and B30.

Therefore, it would be interesting to synthesise and test a series of these compounds for CYP26 inhibitory activity.

Chapter 5

Chemical synthesis of CYP26A1 inhibitors

5 Chemical synthesis of CYP26A1 inhibitors

5.1 Synthesis of α substituted 4-(1,2,4)triazol- and imidazol-1-ylmethylphenylaryl and heteroarylamine derivatives

5.1.1 Synthesis of α substituted 4-(1,2,4)triazol- and imidazol-1-ylmethylphenylarylamine derivatives

5.1.1.1 General chemistry

The synthesis of substituted 4-(1,2,4)triazol and imidazol-1-ylmethylphenylarylamines were carried out according to a sequence of 3 steps (**Scheme 5.1**):

- The preparation of the 4-aminophenyl ketone using the Suzuki reaction
- The reduction of the ketone to alcohol
- The addition of the aza ring (triazole or imidazole)

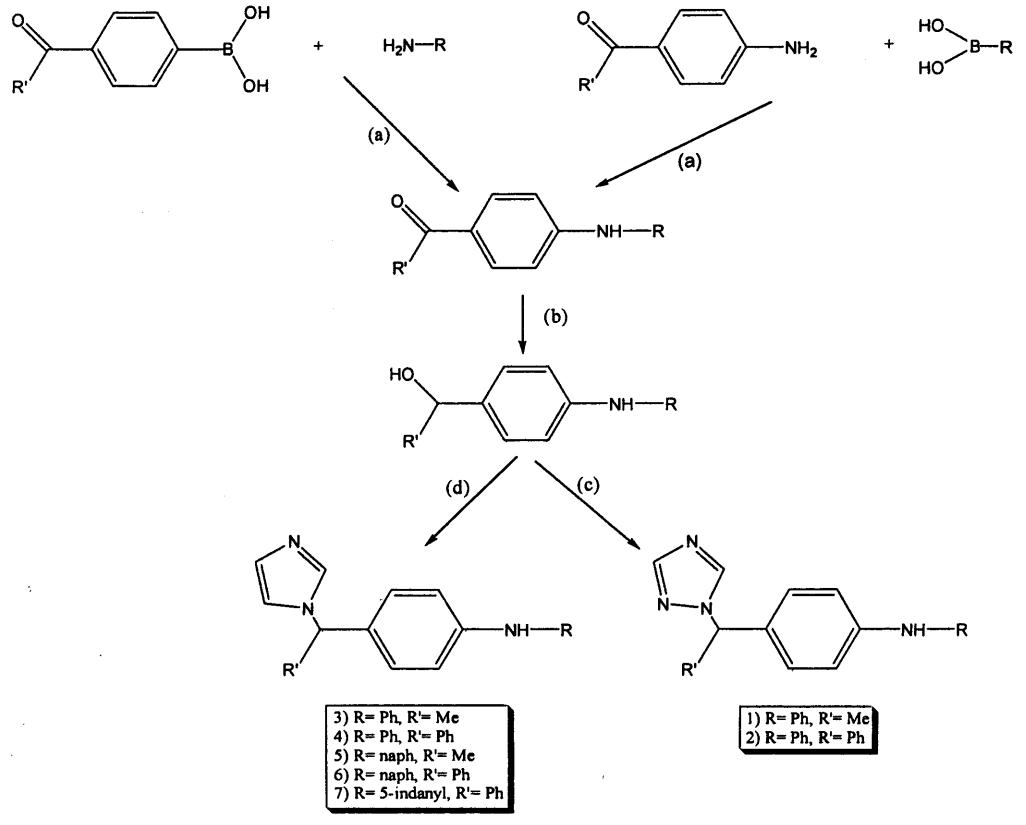

Scheme 5.1: General reaction scheme for the synthesis of α substituted 4-(1,2,4)triazol- and imidazol-1-yl-methyl-phenyl-arylamine. Reagents and conditions: (a) $CuII(OAc)_2$, pyridine, CH_2Cl_2, r.t., 3 days (b) $NaBH_4$, MeOH, r.t., 2-3 h (c) (i) 1,2,4-triazole, $SOCl_2$, CH_3CN, 10 ^{O}C, 1 h,

(ii) K_2CO_3, r.t., 4 – 6 days (d) imidazole, 1,1'-carbonyldiimidazole, CH_3CN, reflux, 1h.

5.1.1.1.1 Synthesis of α substituted 4-arylaminoketone

This synthesis involves the formation of an aromatic C-N bond. Despite the importance of aromatic amines and their use in pharmaceutical and agrochemical industries, few methods have been found in the literature for C-N coupling.

The classic technique has been the venerable Ullmann condensation (Lindley, 1985) which involves the condensation of an aromatic amine and an unactivated aryl halide with catalysis by some form of copper in the presence of added base. The reaction is noted for its capricious nature and sensitivity to catalyst type. Strongly aggressive conditions involving high temperature and extended reaction times are generally needed to secure at best moderate yields.

The most successful C-N coupling methods in the literature have utilised the palladium- or nickel-catalysed coupling of amines with aryl halides in the presence of a hydroxide base (Yang and Buchwald, 1999, Hartwig, 1996; Wolfe and Buchwald, 1997; Hartwig *et al.*, 1999; Yamamoto *et al.*, 1998). The major drawback of this reaction is its incompatibility with base sensitive functional groups as esters and ketones. Recently, the use of alkali metal hydroxide bases in the presence of a phase-transfer agent has been reported instead of the commonly used sodium tertiary butoxide base, which was better tolerated by some functional groups such as ketones and esters (Kuwano *et al.*, 2002). As our compounds contain a ketone group, this reaction was tried, however no satisfactory results were obtained.

Recently, the arylation of NH containing arenes and heteroarenes has been performed with arylboronic acids in a Suzuki type coupling reaction (Chan *et al.*, 1998; Lam *et al.*, 1998). This reaction has been found to be successful in the synthesis of our compounds. This reaction is performed in the presence of a stoichiometric amount of copper and a tertiary amine base such as triethylamine or pyridine. However, Quach and Batey, used a catalytic amount of $CuII(OAc)_2$ for the cross-coupling of arylboronic acids with aliphatic amines and anilines (Quach and Batey, 2003). It should be noted that the yield of the reaction is quite dependent on the nature of the substrate, the substitution on the boronic acid and the choice of the tertiary amine base. The reaction is performed in air allowing oxygen uptake and therefore more efficient oxidation of a reduced copper intermediate (Evans *et al.*, 1998). This

can be done by using vigorous stirring in flasks with a large volume relative to that of the solvent volume. This is more important during the first few hours of the reaction since it was found that the reaction proceeded smoothly to 35-45% conversion in the first 4-5 h, and catalytic activity rapidly diminished over the next 20 h (Antilla and Buchwald, 2001). The use of molecular sieves has been found important to obtain the best yield (Chan *et al.*, 1998).

The general conditions for this coupling reaction involve the addition of 2 equivalents of arylboronic acid and 2 equivalents of base (pyridine) to 1 equivalent of amine in CH_2Cl_2 (8 mL/0.5g of the substrate) followed by (1-2) equivalent of anhydrous $CuII(OAc)_2$ and 4Å molecular sieves. The mixture is stirred under air atmosphere at room temperature for 3 days, chromatographed on silica gel to give the desired *N*-arylated amine.

The mechanism of the reaction (**Figure 5.1**) is believed to be analogous to that of the bismuth arylation proposed by Barton, with the arylboronic acid playing a role similar to the triarylbismuth (Barton *et al.*, 1987). It involves $CuII(OAc)_2$ forming a complex with the amine and transmetallating with arylboronic acid. Reductive elimination of the resulting amine/copper/aryl complex (Barton *et al.*, 1987; Wipf, 1993; Evans *et al.*, 1998) affords the *N*-arylated amine. The role of the base in the catalytic cycle is to increase the carbanion character of the phenyl groups in organoboranes by their coordination with the boron atoms. This will then facilitate the transfer of phenyl groups from the boron to the copper complexes in the transmetallation step to form Ar-NH-Cu-Ar'.

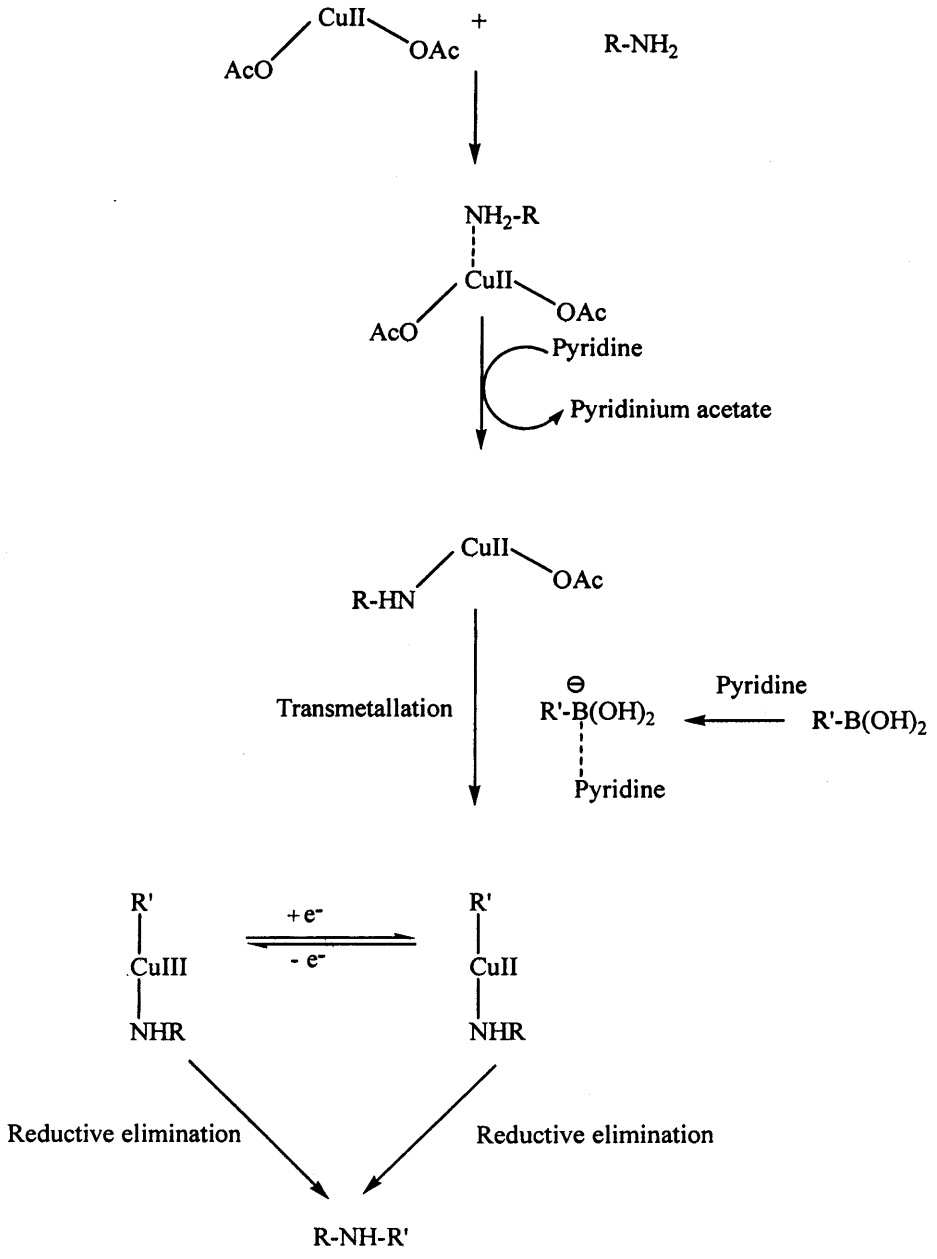

Figure 5.1: Proposed mechanism of action of the Suzuki coupling reaction of aryl boronic acids with amines (Evans *et al.*, `1998; Barton *et al.*, 1987).

Synthesis of (**3**), (**5**), (**7**) and (**8**) were carried out by the Suzuki reaction. In the reaction, phenylboronic acid (**1**) and naphthylboronic acid (**6**) were reacted with 4-aminoacetophenone (**2**) to give (**3**) and (**7**) respectively, while 4-amino benzophenone (**4**) was reacted with phenylboronic acid (**1**) and naphthylboronic acid (**6**) to form (**5**) and (**8**) respectively (**Scheme 5.2**)

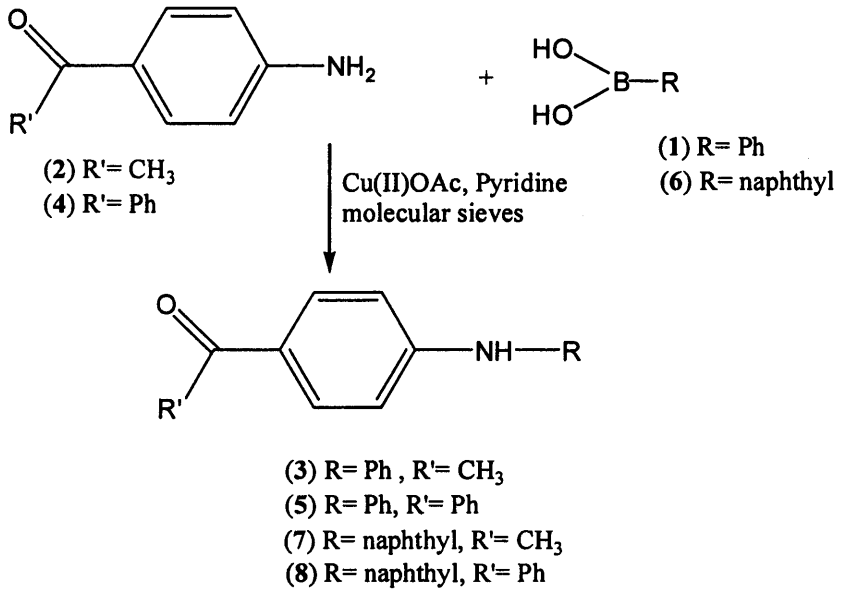

Scheme 5.2: The synthesis of (**3**), (**5**), (**7**) and (**8**) using Suzuki reaction. Reaction conditions: $CuII(OAc)_2$, pyridine, 4Å molecular sieves, CH_2Cl_2, r.t., vigorous stirring, 3 days.

Synthesis of (**12**) and (**13**) were carried out by the reaction of 5-aminoindane (**9**) with 4-acetyl-phenylboronic acid (**10**) and 4-benzoyl-phenylboronic acid (**11**) respectively while (**15**) was synthesized by reaction of 6-aminobenzothiazole (**14**) with 4-benzoyl-phenylboronic acid (**11**) (**Scheme 5.3**)

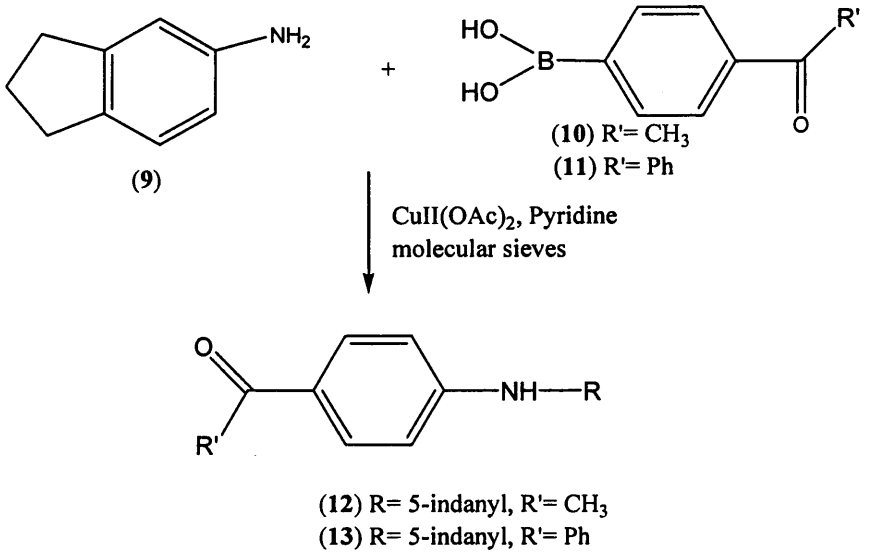

Scheme 5.3: The synthesis of (**12**), (**13**) and using Suzuki reaction. Reagents and conditions: $CuII(OAc)_2$, pyridine, 4Å molecular sieves, CH_2Cl_2, r.t., vigourous stirring, 3 days.

The Suzuki reaction gives good yield of products (**3**), (**5**), (**7**), (**8**), (**12**), and (**13**). The summary of the results of the synthesis are given in **Table 5.1**. The coupled

products were confirmed by the presence of NH singlet peak at approximately 5.5 ppm in ^{1}H NMR.

Table 5.1: Summary of the synthesis of compounds (**3**), (**5**), (**7**), (**8**), (**12**) and (**13**).

Product	Yield (%)	Melting point (^{0}C)
3	64	118-120
5	65	140-142
7	63	154-156
8	61	140-142
12	71	126-128
13	67	96-98

However, the coupling of the heteroaryl boronic acids, benzofuran boronic acid and benzothiophene boronic acid with 4-aminoacetophenone or 4-amino benzophenone under these conditions was unsatisfactory and no product was observed.

On the other hand, the coupling of the electron deficient heterocylic amine, 5-chloro-2-aminobenzoxazole (**14**) with 4-acetylphenylboronic acid or 4-benzoyl phenylboronic acid did not proceed toward the formation of the coupled aromatic amine. Alternatively, the aryl boronic acid is oxidised with $CuII(OAc)_2$ to the corresponding alcohol followed by subsequent arylation of the later (Lam *et al.*, 1998) to give the aromatic ether (**15**) and (**16**) for 4-acetyl phenylboronic acid and 4-benzoyl phenylboronic acid respectively (**Scheme 5.4**).

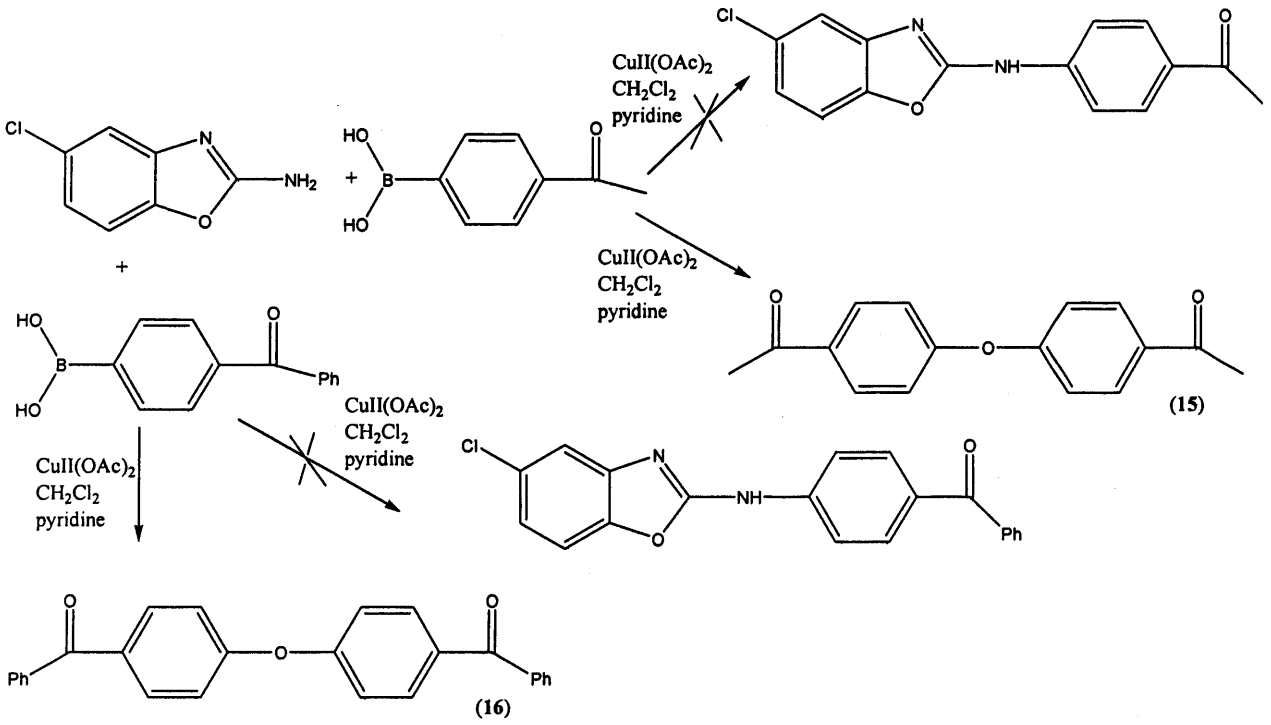

Scheme 5.4: Reaction of 5-chloro-2-aminobenzoxazole with 4-acetyl phenylboronic acid and 4-benzoyl phenylboronic acid.

The same has been found in the reaction of 4-aminomethyl benzoate with 4-benzoyl phenylboronic acid with the aromatic ether (**16**) and the starting material 4-aminobenzoate was the main products.

5.1.1.1.2 Synthesis of α substituted 4-arylamino-phenyl-methanol

The reduction of the ketones to the corresponding alcohols was achieved in mild conditions using the reducing agent $NaBH_4$. The reduction was unsuccesful with dioxane as solvent, however in MeOH the corresponding alcohols were obtained in very high yield (**Scheme 5.5**).

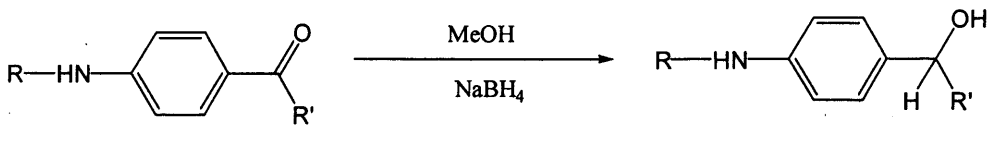

(3) R= Ph , R'= CH_3
(5) R= Ph, R'= Ph
(7) R= naphthyl, R'= CH_3
(8) R= naphthyl, R'= Ph
(13) R= 5-indanyl, R'= Ph

(17) R= Ph , R'= CH_3
(18) R= Ph, R'= Ph
(19) R= naphthyl, R'= CH_3
(20) R= naphthyl, R'= Ph
(21) R= 5-indanyl, R'= Ph

Scheme 5.5: Reduction of the ketones to the corresponding alcohols.

The summary of the synthesis of the alcohols are represented in **Table 5.2**. The secondary alcohols were confirmed by ^{1}H NMR by the presence of the OH group at approximately 1.5 – 2.0 ppm and the H atom at C-1 at approximately 5.0 – 6.0 ppm. ^{13}C NMR confirmed the disappearance of the C=O group.

Table 5.2: Summary of the synthesis of compounds (**17**) - (**21**).

Product	Reaction time	Yield (%)	Melting point (^{0}C)
17	2 h	88	66-68
18	3 h	86	-
19	3 h	89	98-100
20	1 h	92	-
21	7 h	91	-

5.1.1.1.3 Synthesis of α substituted 4-(1,2,4)triazol-1-yl-methyl-phenyl-arylamine

Drabel and Regel in 1975 patented a superior method (Draber and Regel, 1975) by reacting thionyl-imidazole with a substituted carbinol (**Scheme 5.6**) to form *N*-(1,1,1-trisubstituted)-methylazoles. The thionyl-1,2,4-triazole was obtained in an analogous way. This involved the *in situ* preparation of the reactive species *N*-*N*'-di(1*H*-1,2,4-triazol-1-yl)sulphoxide by coupling the triazole-ring and thionyl chloride during 1 h at 10 ^{0}C with anhydrous CH_3CN as solvent.

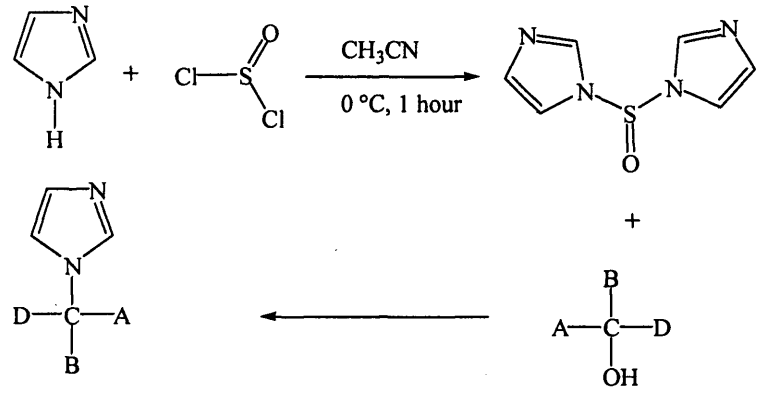

N-(1,1,1-trisubstituted)-methylazoles

Scheme 5.6: Synthesis of *N*-(1,1,1-trisubstituted)-methylazoles by reacting thionyl-imidazole with substituted carbinol.(Draber and Regel, 1975).

The synthesis of the triazole compounds (**22** – **23**) involved the reaction of the carbinol compounds (**17** – **18**) with the *in situ* prepared di(1*H*-1,2,4-triazole-1-

yl)sulphoxide. This was done by adding a solution of the alcohol in dry acetonitrile to the above mixture, followed by activated K_2CO_3. Then, the suspension was stirred under nitrogen at room temperature for 4 to 6 days. The reaction was then purified by flash column chromatography to give the pure products in moderate yield.

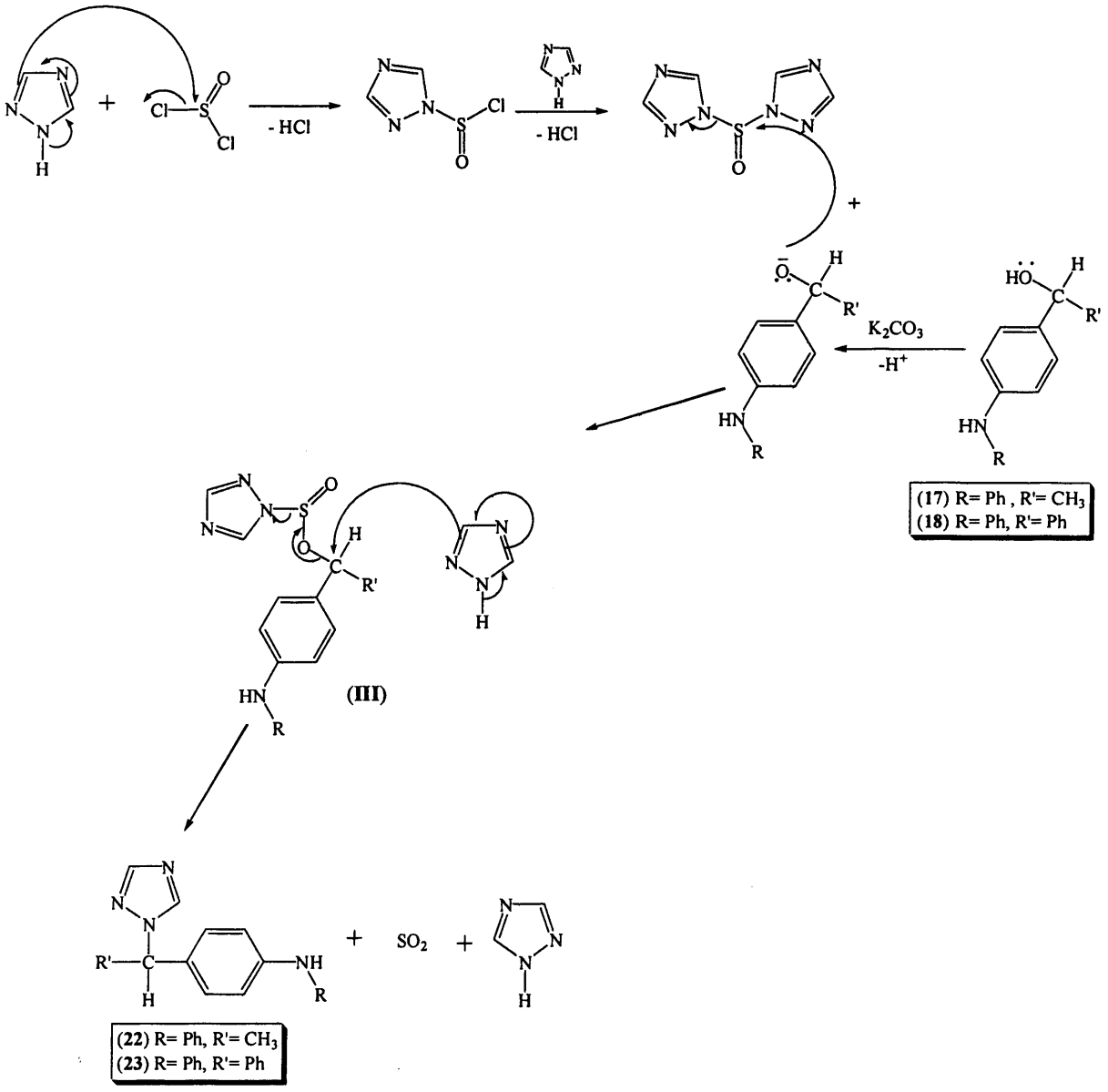

Scheme 5.7: The mechanism of the synthesis of compounds (**22**) and (**23**). Reagents and conditions: 1,2,4-triazole, $SOCl_2$, CH_3CN, 10 °C, 1 h then add K_2CO_3, carbinol compound (**6** or **7**), r.t., 4 – 6 days.

The mechanism of the reaction is shown in **Scheme 5.7** and the synthesis of compounds **22** and **23** are summarised in **Table 5.3**.

The products were confirmed by ^1H NMR after purification by flash column chromatography. The ^1H NMR showed the disappearance of the OH group at

approximately 1.5 – 2.0 ppm and the presence of the two protons of the triazoles for compounds (**8**) and (**9**) at approximately 8.1 and 8.2 ppm.

Table 5.3: Summary of the synthesis of compounds (**22**) and (**23**).

Product	Yield (%)	Melting point (^{0}C)
22	72	108-110
23	69	138-140

5.1.1.1.4 Synthesis of α substituted 4-imidazol-1-ylmethylphenylarylamine

In this case, the synthesis of the imidazole compounds was carried out through the direct reaction of the carbinol compounds with 1,1'-carbonyldiimidazole in the presence of exess imidazole as previously reported (Mulvihill *et al.*, 2005; Aelterman *et al.*, 2001). Therefore, the need for the *in situ* preparation of the reactive species *N-N'*-di(1*H*-imidazol-1-yl)sulphoxide was eliminated. The reaction was heated at reflux for one hour. The mechanism of the reaction is almost the same as that described for the triazole derivatives, involving two nucleophilic substitution reactions. The carbinol compounds reacted with 1,1'-carbonyldiimidazole to produce the intermediate (**III**) which undergoes a second nucleophilic substitution by imidazole to give the products (**Scheme 5.8**).

The yield of this reaction is higher than the triazole reaction (**Table 5.4**).The products were confirmed by ^{1}H NMR after purification by flash column chromatography. The ^{1}H NMR showed the disappearance of the OH group at approximately 1.5 – 2.0 ppm and the presence of additional signals from the imidazole ring, most notably a singlet (^{1}H) at approximately 7.5-8.0 ppm.

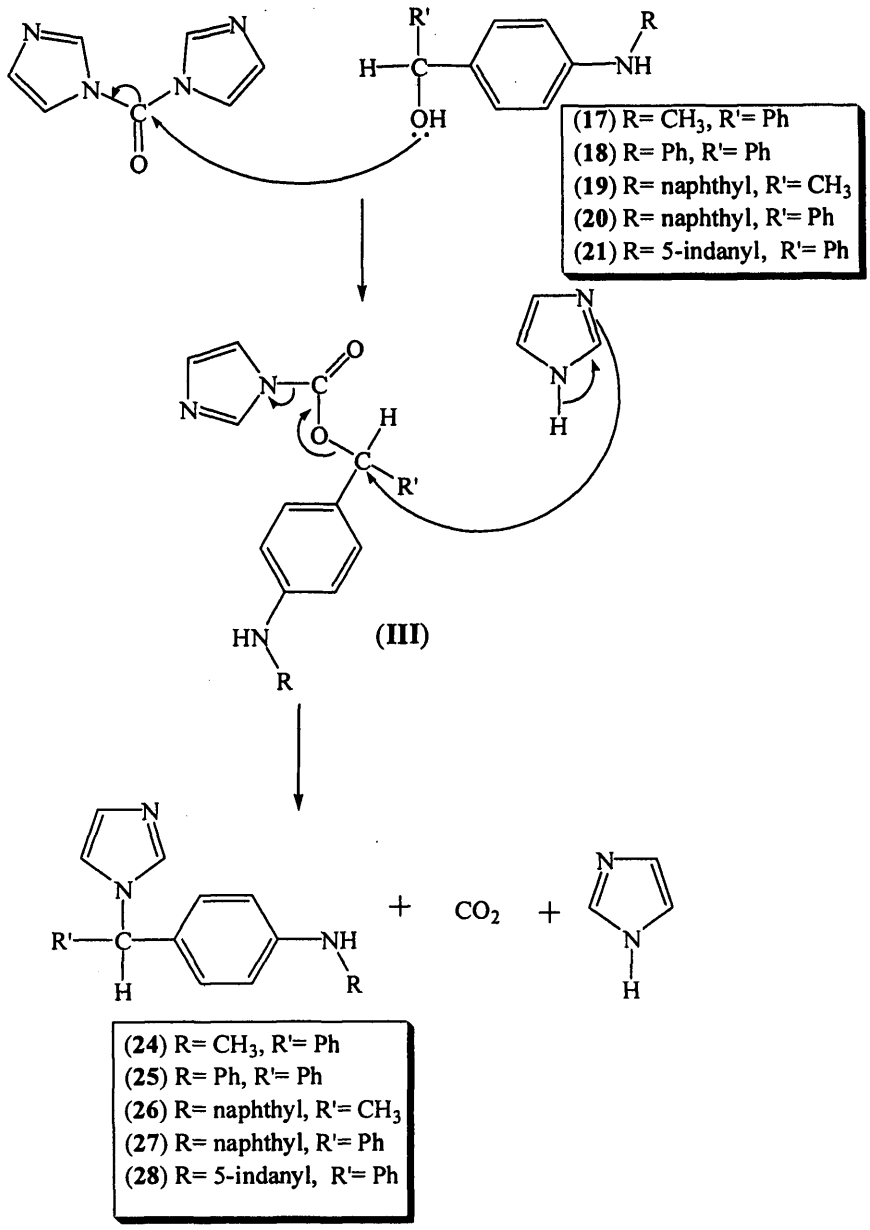

Scheme 5.8: The mechanism of the synthesis of compounds (**24**), (**25**), (**26**), (**27**) and (**28**). Reagents and conditions: imidazole, 1,1'-carbonyldiimidazole, CH_3CN, reflux, 1 h, carbinol compound (**17, 18, 19, 20** or **21**).

Table 5.4: Summary of the synthesis of compounds (**24**) - (**28**).

Product	Reaction time	Yield (%)	Melting point (^{0}C)
24	1 h	84	110-112
25	1 h	89	208-210
26	3 h	80	170-172
27	1 h	88	94-96
28	1 h	83	88-90

5.1.1.2 Experimental

5.1.1.2.1 General considerations

All reactions were carried out under an atmosphere of nitrogen when necessary. All reagents and solvents employed were of general purpose or analytical grade and purchased from Sigma-Aldrich Chemical Company, Fluka and Acros Chemicals. Then solvents were appropriately dried over molecular sieves (3Å) or when necessary by distillation.

^{1}H and ^{13}C NMR spectra were recorded on a Bruker Avance DP500 spectrometer at 500 MHz and 125 MHz respectively. Each resonance signal was reported according to the following convention:

- chemical shifts are given in parts per million (ppm) relative to the internal standard tetramethyl silane (Me_4Si).
- coupling constants [J in hertz (Hz)].
- multiplicity are denoted as s (singlet), d (doublet), t (triplet), m (multiplet) or combinations thereof.

Low resolution mass spectra ES (Electrospray) were recorded on Fisions VG Platform Electrospray Mass Spectrometer. Mass spectra were determined under EI (Electron Impact) or CI (Chemical Ionisation) conditions at the EPSRC National Mass Spectrometry Service Centre, University of Wales, Swansea. Accurate mass measurements were also performed at the EPSRC National Mass Spectrometry Service Centre. Microanalysis data were performed by Medac Ltd., Brunel Science Centre, Surrey.

For column chromatography, a glass column was slurry packed in the appropriate eluent with silica gel (Fluka Kieselgel 60). Flash column chromatography was performed with the aid of a pump. Analytical thin layer chromatography (t.l.c.) was carried out on pre-coated silica plates (Merck Kieselgel 60 F_{254}) with visualisation *via* UV light (254 nm) and/or vanillin stain.

Melting points were determined using a Gallenkamp melting point apparatus and were uncorrected.

All NMR characterisations were made by comparison with previous NMR spectra of the appropriate structure class and/ or predictions from ACD/HNMR and ACD/CNMR (Advanced Chemistry Development Inc., Version 2.51, 1997) and ChemDraw Ultra™ 7.0 (CambridgeSoft).

5.1.1.2.2 Results

1-(4-Phenylaminophenyl)-ethanone (3) (Antilla and Buchwald, 2001)

($C_{14}H_{13}NO$, M.W. 211.257)

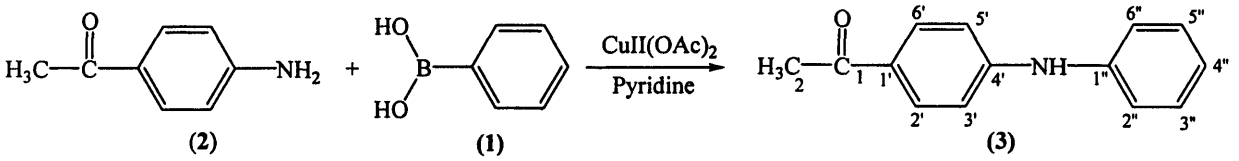

(2) (1) (3)

To phenylboronic acid (**1**) (2.44 g, 20 mmol), 4-aminoacetophenone (**2**) (1.35 g, 10 mmol), anhydrous $CuII(OAc)_2$ (3.63 g, 20 mmol), pyridine (1.58 g, 20 mmol) and 250 mg activated 4Å molecular sieves under an atmosphere of air was added CH_2Cl_2 (25 mL) and the reaction stirred under air atmosphere at ambient temperature for 3 days. The product was isolated by flash column chromatography of the crude reaction mixture (petroleum ether - EtOAc 100:0 v/v increasing to 80:20 v/v) to give 1-(4-phenylaminophenyl)-ethanone (**3**) as a pale yellow crystalline solid. Yield: 1.35 g (64 %), t. l. c. system: petroleum ether – EtOAc 4:1 v/v, R_F: 0.57, stain positive.

^{1}H NMR: δ ($CDCl_3$): 2.57 (s, 3H, H-2), 6.58 (s, 1H, NH), 7.03 (d, J= 8.7 Hz, 2H, Ar), 7.10 (t, J= 7.3 Hz, 1H, H-4''), 7.21 (d, J= 7.7 Hz, 2H, Ar), 7.36 (m, 2H, Ar), 7.89 (d, J= 8.7 Hz, 2H, Ar).

^{13}C NMR: δ ($CDCl_3$): 26.14 (CH_3, C-2), 114.46 (CH, C-3', C-5'), 120.73 (CH, C-2'', C-6''), 123.40 (CH, C-4''), 129.15 (C, C-1'), 129.55 (CH, C-3'', C-5''), 130.62 (CH, C-2', C-6'), 140.64 (C, C-1''), 148.36 (C, C-4'), 196.31 (C, C-1).

Melting point: 118-120 ^{0}C

Phenyl-(4-phenylaminophenyl)-methanone (5)

($C_{19}H_{15}NO$, M.W. 273.33)

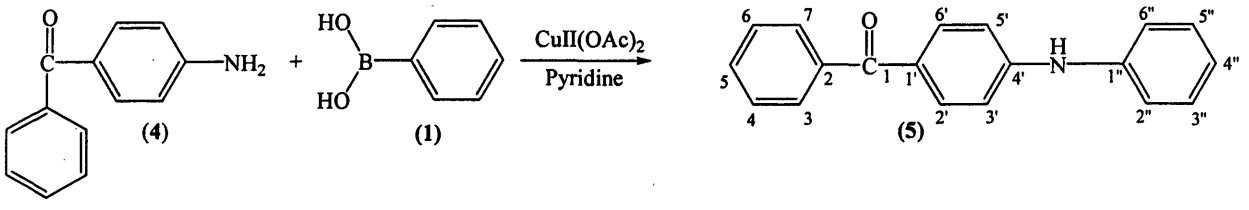

(4) (1) (5)

To phenylboronic acid (**1**) (2.44 g, 20 mmol), 4-aminobenzophenone (**4**) (1.97 g, 10 mmol), anhydrous $CuII(OAc)_2$ (3.63 g, 20 mmol), pyridine (1.58 g, 20 mmol) and 250 mg activated 4Å molecular sieves under an atmosphere of air was added CH_2Cl_2 (25 mL) and the reaction stirred under air atmosphere at ambient temperature for 3 days. The product was isolated by direct flash column chromatography of the

crude reaction mixture (petroleum ether - EtOAc 100:0 v/v increasing to 80:20 v/v) to give phenyl-(4-phenylaminophenyl)-methanone (**5**) as a shiny yellow crystalline solid. Yield: 1.79 g (65 %), t. l. c. system: petroleum ether – EtOAc 4:1 v/v, R_F: 0.67, stain positive.

^{1}H NMR: δ ($CDCl_3$): 6.12 (s, 1H, NH), 6.93 (d, J= 8.5 Hz, 2H, Ar), 7.00 (t, J= 7.3 Hz, 1H, Ar), 7.12 (d, J= 8.0, 2H, Ar), 7.26 (t, J= 7.8 Hz, 2H, Ar), 7.38 (t, J= 7.6 Hz, 2H, Ar), 7.46 (t, J= 7.3 Hz, 1H, Ar), 7.67 (d, J= 7.4 Hz, 2H, Ar), 7.69 (d, J= 8.6 Hz, 2H, Ar).

^{13}C NMR: δ ($CDCl_3$): 114.36 (CH, C-3', C-5'), 120.72 (CH, C-2'', C-6''), 123.37 (CH, C-4''), 128.15 (CH, C-4, C-6), 128.68 (C, C-1'), 129.56 (CH, C-3', C-5'), 129.62 (CH, C-3, C-7), 131.59 (CH, C-5), 132.76 (CH, C-2', C-6'), 138.72 (C, C-2), 140.66 (C, C-1''), 148.24 (C, C-4'), 195.21 (C, C-1).

Microanalysis: Calculated for $C_{19}H_{15}NO$; Theoretical: %C= 83.49, %H= 5.53, %N= 5.12; Found: %C= 83.26, %H= 5.61, %N= 5.04.

Melting point: 140-142 ^{0}C

1-[4-(Naphthalen-2-ylamino)-phenyl]-ethanone (7)

($C_{18}H_{15}NO$, M.W. 261.318)

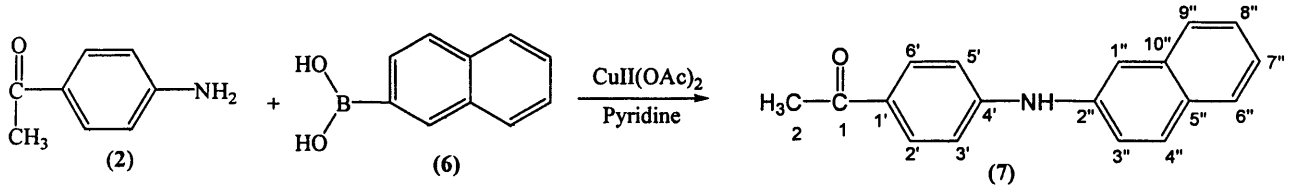

To naphthylboronic acid (**6**) (5.16 g, 30 mmol), 4-aminoacetophenone (**2**) (1.35 g, 10 mmol), anhydrous CuII(OAc)$_2$ (3.63 g, 20 mmol), pyridine (2.37 g (2.4 mL), 30 mmol) and 250 mg activated 4Å molecular sieves under an atmosphere of air was added CH_2Cl_2 (25 mL) and the reaction stirred under air atmosphere at ambient temperature for 3 days. The product was isolated by direct flash column chromatography of the crude reaction mixture (petroleum ether - EtOAc 100:0 v/v increasing to 80:20 v/v) to give 1-[4-(naphthalen-2-ylamino)-phenyl]-ethanone (**7**) as a yellowish brown crystalline solid. Yield: 1.65 g (63 %), t. l. c. system: petroleum ether – EtOAc 4:1 v/v, R_F: 0.61, stain positive.

^{1}H NMR: δ ($CDCl_3$): 2.57 (s, 3H, H-2), 6.37 (s, 1H, NH), 6.98 (d, J= 8.8 Hz, 2H, H-3', H-5'), 7.22 (dd, J_1= 2.2 Hz, J_2= 8.5 Hz, 1H, H-3''), 7.3 (m, 1H, H-7''), 7.37

(m, 1H, H-8''), 7.49 (d, J= 2.1 Hz, 1H, H-1''), 7.62 (d, J= 8.4 Hz, 1H, 4''), 7.72 (t, J= 8.7 Hz, 2H, H-6'', H-9''), 7.81 (d, J= 8.8 Hz, 2H, H-2', H-6').

^{13}C NMR: δ ($CDCl_3$): 26.20 (CH, C-2), 114.82 (CH, C-3', C-5'), 115.97 (CH, C-1''), 121.37 (CH, C-3''), 124.67 (CH, C-7''), 126.72 (CH, C-9''), 126.91 (CH, C-8''), 127.75 (CH, C-6''), 129.36 (C, C-5''), 129.46 (CH, C-4''), 130.26 (C, C-1'), 130.68 (CH, C-2', C-6'), 134.30 (C, C-10''), 138.30 (C, C-2''), 148.25 (C, C-4'), 196.44 (C, C-1).

Microanalysis: Calculated for $C_{18}H_{15}NO.\ 0.1H_2O$ (279.33); Theoretical: %C= 82.17, %H= 5.75, %N= 5.32; Found: %C= 82.25, %H= 5.78, %N= 5.17.

Melting point: 154-156 ^{0}C

[4-(Naphthalen-2-ylamino)-phenyl]-phenylmethanone (8)

($C_{23}H_{17}NO$, M.W. 323.39)

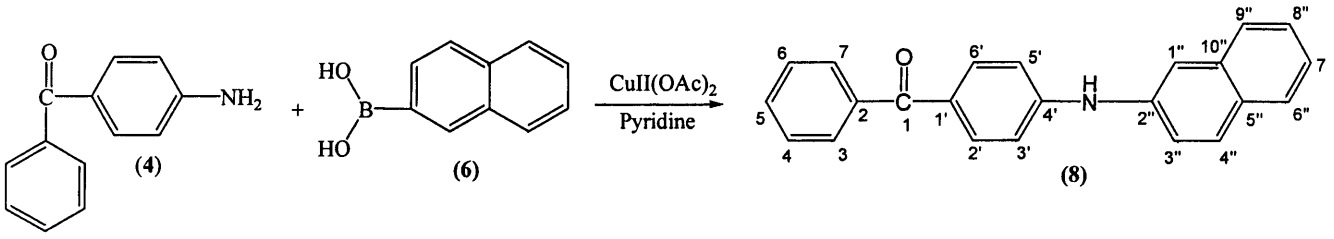

To naphthylboronic acid (**6**) (5.16 g, 30 mmol), 4-aminobenzophenone (**4**) (1.97 g, 10 mmol), anhydrous $CuII(OAc)_2$ (3.63 g, 20 mmol), pyridine (2.4 mL, 30 mmol) and 250 mg activated 4Å molecular sieves under an atmosphere of air was added CH_2Cl_2 (25 mL) and the reaction stirred under air atmosphere at ambient temperature for 3 days. The product was isolated by direct flash column chromatography of the crude reaction mixture (petroleum ether - EtOAc 100:0 v/v increasing to 80:20 v/v) to give [4-(naphthalen-2-ylamino)-phenyl]-phenylmethanone (**8**) as a yellowish brown crystalline solid. Yield: 1.98 g (61 %), t. l. c. system: petroleum ether – EtOAc 4:1 v/v, R_F: 0.69, stain positive.

^{1}H NMR: δ ($CDCl_3$): 6.31 (s, 1H, NH), 7.0 (d, J= 8.7 Hz, 2H, H-3', H-5'), 7.22 (dd, J_1= 2.2 Hz, J_2= 8.5 Hz, 1H, H-3''), 7.3 (m, 1H, H-7''), 7.37 (m, 3H, H-4, H-6, H-8''), 7.45 (m, 1H, H-2'), 7.49 (d, J= 2.2 Hz, 1H, H-1''), 7.62 (d, J= 7.9 Hz, 1H, H-4''), 7.70 (m, 6H, H-3, H-5, H-7, H-6', H-6'', H-9'').

^{13}C NMR: δ ($CDCl_3$): 114.75 (CH, C-3', C-5'), 115.95 (CH, C-1''), 123.39 (CH, C-3''), 124.65 (CH, C-7''), 126.71 (CH, C-9''), 126.93 (CH, C-8''), 127.75

(CH, C-6''), 128.18 (CH, C-4, C-6), 128.98 (C, C-5''), 129.45 (CH, C-4''), 129.65 (CH, C-3, C-7), 130.26 (C, C-1'), 131.66 (CH, C-5), 132.79 (CH, C-2', C-6'), 134.32 (C, C-10''), 138.33 (C, C-2), 138.69 (C, C-2''), 148.10 (C, C-4'), 195.29 (C, C-1).

Microanalysis: Calculated for $C_{23}H_{17}NO.\ 0.2H_2O$ (326.99); Theoretical: %C= 84.48, %H= 5.24, %N= 4.28; Found: %C= 84.54, %H= 5.26, %N= 4.04.

Melting point: 140-142 ^{0}C

1-[4-(Indan-5-ylamino)-phenyl]-ethanone (12)

($C_{17}H_{17}NO$, M.W. 251.32)

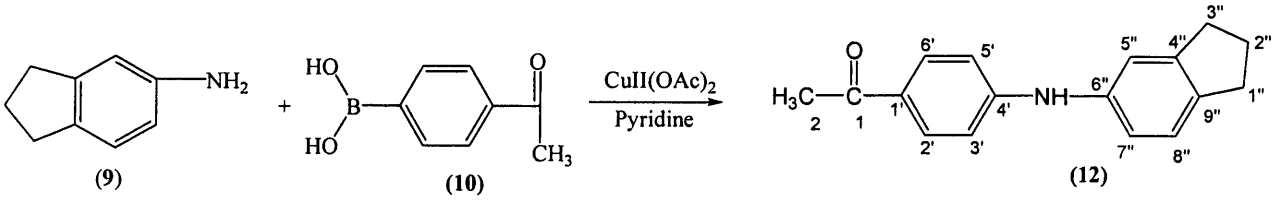

(9) (10) (12)

To 4-acetylphenylboronic acid (**10**) (4.92 g, 30 mmol), 5-aminoindane (**9**) (1.33 g, 10 mmol), anhydrous CuII(OAc)$_2$ (3.63 g, 20 mmol), pyridine (2.4 mL, 30 mmol) and 250 mg activated 4 Å molecular sieves under an atmosphere of air was added CH_2Cl_2 (25 mL) and the reaction stirred under air atmosphere at ambient temperature for 3 days. The product was isolated by direct flash column chromatography of the crude reaction mixture (petroleum ether - EtOAc 100:0 v/v increasing to 80:20 v/v) to give 1-[4-(indan-5-ylamino)-phenyl]-ethanone (**12**) as an off white crystalline solid. Yield: 1.79 g (71 %), t. l. c. system: petroleum ether – EtOAc 4:1 v/v, R_F: 0.66, stain positive.

^{1}H NMR: δ ($CDCl_3$): 2.03 (m, 2H, H-2''), 2.44 (s, 3H, H-2), 2.82 (m, 4H, H-1'', H-3''), 6.00 (s, 1H, NH), 6.84 (d, J= 8.8, 2H, H-3', H-5'), 6.88 (dd, J_1= 1.9 Hz, J_2= 7.7 Hz, 1H, H-7''), 6.99 (s, 1H, H-5''), 7.12 (d, J= 8.0 Hz, 1H, H-8''), 7.76 (d, J= 8.8 Hz, 2H, H-2', H-6').

^{13}C NMR: δ ($CDCl_3$): 25.68 (C, C-2''), 26.11 (CH, C-2), 32.36 (C, C-1''), 33.02 (C, C-3''), 113.82 (CH, C-3', C-6'), 117.93 (CH, C-7''), 119.86 (CH, C-5''), 125.06 (CH, C-8''), 128.45 (C, C-1'), 130.66 (CH, C-2', C-6'), 138.60 (C, C-9''), 139.95 (C, C-4''), 145.82 (C, C-6''), 149.38 (C, C-4'), 196.33 (C, C-1).

Microanalysis: Calculated for $C_{17}H_{17}NO$; Theoretical: %C= 81.24, %H= 6.82, %N= 5.57; Found: %C= 80.97, %H= 6.81, %N= 5.51.

Melting point: 126-128 ^{0}C

[4-(Indan-5-ylamino)-phenyl]-phenylmethanone (13)

($C_{22}H_{19}NO$, M.W. 313.39)

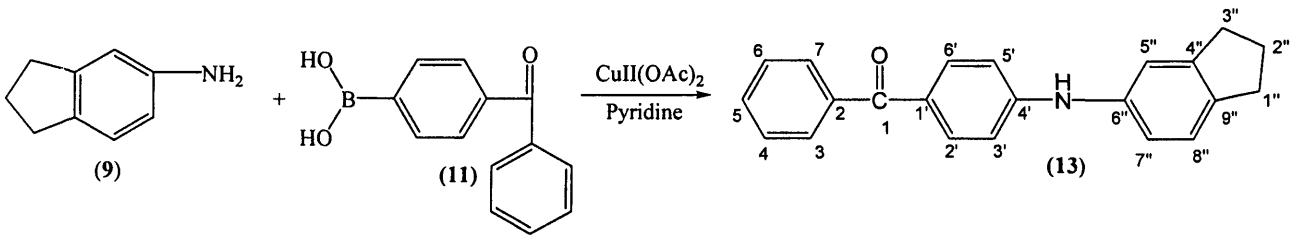

To 4-benzoylphenylboronic acid (**11**) (6.78 g, 30 mmol), 5-aminoindane (**9**) (1.33 g, 10 mmol), anhydrous $CuII(OAc)_2$ (3.63 g, 20 mmol), pyridine (2.4 mL, 30 mmol) and 250 mg activated 4Å molecular sieves under an atmosphere of air was added CH_2Cl_2 (25 mL) and the reaction stirred under air atmosphere at ambient temperature for 3 days. The product was isolated by direct flash column chromatography of the crude reaction mixture (petroleum ether - EtOAc 100:0 v/v increasing to 80:20 v/v) to give [4-(indan-5-ylamino)-phenyl]-phenylmethanone (**13**) as a shiny yellow crystalline solid. Yield: 2.1 g (67 %), t. l. c. system: petroleum ether – EtOAc 4:1 v/v, R_F: 0.73, stain positive.

^{1}H NMR: δ ($CDCl_3$): 2.0 (m, 2H, H-2''), 2.82 (m, 4H, H-1'', H-3''), 6.00 (s, 1H, NH), 6.86 (d, J= 8.8, 2H, H-3', H-5'), 6.90 (m, 1H, Ar), 7.00 (s, 1H, H-5''), 7.10 (d, J= 8.0 Hz, 1H, H-8''), 7.37 (m, 2H, H-4, H-6), 7.44 (m, 1H, H-5), 7.67 (m, 4H, Ar).

^{13}C NMR: δ ($CDCl_3$): 25.69 (C, C-2''), 32.36 (C, C-1''), 33.03 (C, C-3''), 113.75 (CH, C-3', C-5'), 117.93 (CH, C-7''), 119.86 (CH, C-5''), 125.07 (CH, C-8''), 128.01 (CH, C-4, C-6), 128.01 (C, C-1'), 129.56 (CH, C-3, C-7), 131.44 (CH, C-5), 132.81 (CH, C-2', C-6'), 138.60 (C, C-9''), 138.90 (C, C-2), 139.95 (C, C-4''), 145.82 (C, C-6''), 149.23 (C, C-4'), 195.13 (C, C-1).

Microanalysis: Calculated for $C_{22}H_{19}NO$; Theoretical: %C= 84.32, %H= 6.11, %N= 4.47; Found: %C= 84.12, %H= 6.08, %N= 4.33.

Melting point: 96-98 ^{0}C

1-[4-(4-Acetylphenoxy)-phenyl]-ethanone (15)

($C_{16}H_{14}O_3$, M.W. 254.27)

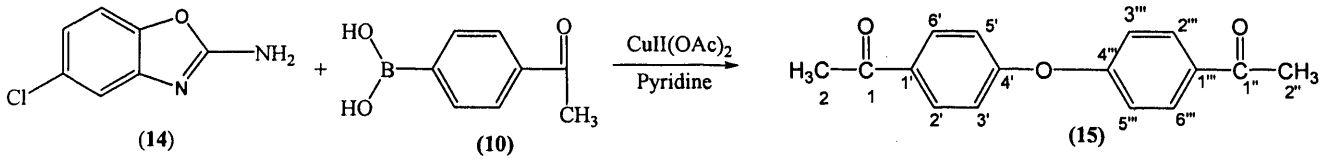

To 4-acetylphenylboronic acid (**10**) (4.92 g, 30 mmol), 5-chloro-2-aminobenzoxazole (**14**) (1.69 g, 10 mmol), anhydrous $CuII(OAc)_2$ (3.63 g, 20 mmol), pyridine (2.37 g (2.4 mL), 30 mmol) and 250 mg activated 4 Å molecular sieves under an atmosphere of air was added CH_2Cl_2 (25 mL).and the reaction stirred under air atmosphere at ambient temperature for 3 days. The product was isolated by direct flash column chromatography of the crude reaction mixture (petroleum ether - EtOAc 100:0 v/v increasing to 70:30 v/v) to give 1-[4-(4-acetylphenoxy)-phenyl]-ethanone (**15**) as a white solid. Yield: 1.27 g (50 %), t. l. c. system: petroleum ether – EtOAc 2:1 v/v, R_F: 0.62, stain positive.

^{1}H NMR: δ ($CDCl_3$): 2.64 (s, 6H, H-2, H-2''), 7.05 (d, J= 8.5 Hz, 4H, H-3', H-5', H3'', H5''), 8.00 (d, J= 8.5 Hz, 4H, H-2', H-6', H-2'', H-6'').

^{13}C NMR: δ ($CDCl_3$): 26.50 (CH, C-1, C-2, C-1'', C-2''), 118.77 (CH, C-3', C-5, C-3''', C-5'''), 130.74 (CH, C-2', C-6', C-2''', C-6'''), 133.09 (C, C-1', C-1'''), 160.21 (C, C-4', C-4'''), 196.71 (C, C-1, C-1'').

[4-(4-Benzoylphenoxy)-phenyl]-phenylmethanone (16)

($C_{26}H_{18}O_3$, M.W. 349)

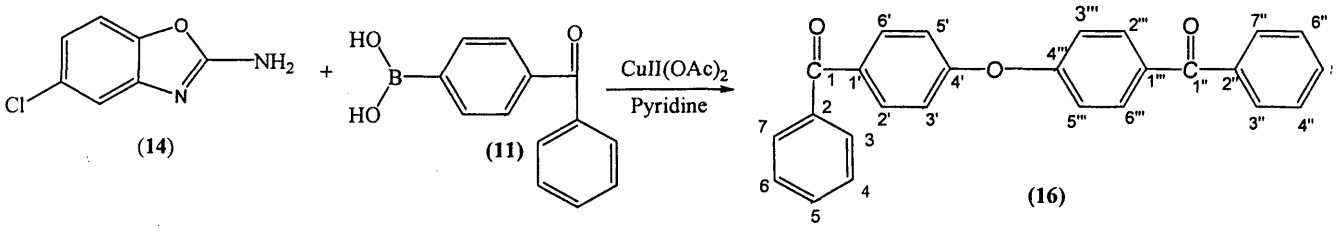

To 4-benzoylphenylboronic acid (**11**) (6.78 g, 30 mmol), 5-chloro-2-aminobenzoxazole (**14**) (1.69 g, 10 mmol), anhydrous $CuII(OAc)_2$ (3.63 g, 20 mmol), pyridine (2.4 mL, 30 mmol) and 250 mg activated 4Å molecular sieves under an atmosphere of air was added CH_2Cl_2 (25 mL) and the reaction stirred under air atmosphere at ambient temperature for 3 days. The product was isolated by direct flash column chromatography of the crude reaction mixture (petroleum ether - EtOAc 100:0 v/v increasing to 70:30 v/v) to give [4-(4-benzoylphenoxy)-phenyl]-

phenylmethanone (**16**) as a white solid. Yield: 1.75 g (50 %), t. l. c. system: petroleum ether – EtOAc 2:1 v/v, R_F: 0.68, stain positive.

^{1}H NMR: δ ($CDCl_3$): 7.05 (d, J= 8.7 Hz, 4H, H-3', H-5', H-3''', H-5'''), 7.43 (m, 4H, H-4, H-6, H-4'', H-6''), 7.5 (m, 2H, H-5, H5''), 7.72 (d, J= 8.5 Hz, 4H, H-2', H-6', H-2''', H-6'''), 7.82 (d, J= 8.5 Hz, 4H, H-3, H-7, H-3'', H-7'').

^{13}C NMR: δ ($CDCl_3$): 118.62 (CH, C-3', C-5', C-3''', C-5'''), 129.87 (CH, C-4, C-6, C-4'', C-6''), 131.54 (CH, C-2', C-6', C-2''', C-6'''), 132.81 (CH, C-5, C-5''), 132.89 (CH, C-3, C-7, C-3'', C-7''), 133.25 (C, C-1', C-1'''), 137.71 (C, C-2, C-2''), 168.89 (C, C-4', C-4'''), 195.50 (C, C-1, C-1'').

1-(4-Phenylaminophenyl)-ethanol (17)

($C_{14}H_{15}NO$, M.W. 213.273)

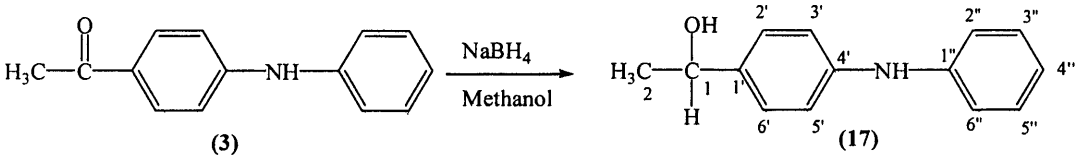

(3) (17)

To a cooled solution of 1-(4-phenylamino-phenyl)-ethanone (**3**) (1.2 g, 5.68 mmol) in anhydrous MeOH (20 mL) was added $NaBH_4$ (0.43 g, 11.36 mmol) and the mixture stirred under N_2 at room temperature for 2 h. The solvent was evaporated *in vacuo* and acetone (1 mL) was added to the residue in order to quench any excess reducing agent. The oil that separated was extracted with Et_2O (2 x 150 mL), washed with H_2O (3 x 100 mL), then the organic layer was dried with $MgSO_4$, filtered and reduced *in vacuo*. The residue was then purified by flash column chromatography (petroleum ether – EtOAc 95:5 v/v increasing to 50:50 v/v) to give 1-(4-phenylaminophenyl)-ethanol (**17**) as a white solid. Yield: 1.07 g (88 %), t. l. c. system: petroleum ether – EtOAc 1:1 v/v, R_F: 0.51, stain positive.

^{1}H NMR: δ ($CDCl_3$): 1.41 (d, J= 6.4 Hz, 3H, H-2), 1.73 (s, 1H, OH), 4.76 (q, J= 6.3 Hz, 1H, H-CH), 5.63 (s, 1H, NH), 6.84 (t, J= 7.3 Hz, 1H, H-4''), 6.97 (m, 4H, Ar), 7.18 (m, 4H, Ar).

^{13}C NMR: δ ($CDCl_3$): 24.94 (CH_3, C-2), 70.12 (CH, C-1), 117.79 (CH, C-2'', C-6''), 117.84 (CH, C-3', C-5'), 121.04 (CH, C-4''), 126.62 (CH, C-2', C-6'), 129.38 (CH, C-3'', C-5''), 138.37 (C, C-1'), 142.55 (C, C-4'), 143.15 (C, C-1'').

Microanalysis: Calculated for $C_{14}H_{15}NO$. $0.1H_2O$ (215.08); Theoretical: %C= 78.18, %H= 7.12, %N= 6.51; Found: %C= 78.19, %H= 7.16, %N= 6.46.

Melting point: 66-68 ^{0}C

Phenyl-(4-phenylaminophenyl)-methanol (18)

($C_{19}H_{17}NO$, M.W. 275.346)

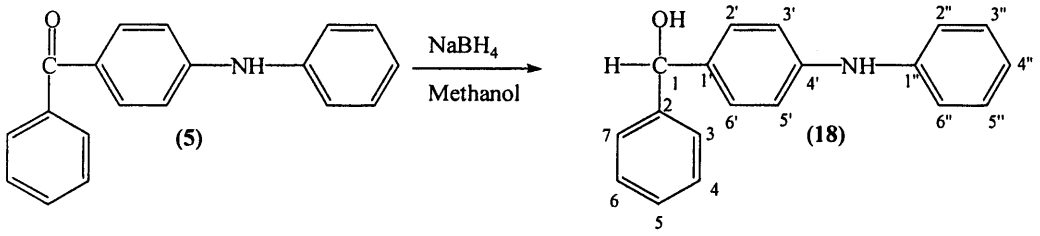

To a cooled solution of phenyl-(4-phenylamino-phenyl)-methanone (**5**) (1.1 g, 4.00 mmol) in anhydrous MeOH (10 mL) and anhydrous dioxane (10 mL) was added $NaBH_4$ (0.30 g, 8.00 mmol) and the mixture stirred under N_2 at room temperature for 3 h. The solvent was evaporated *in vacuo* and acetone (1 mL) was added to the residue in order to quench any excess reducing agent. The oil that separated was extracted with Et_2O (2 x 150 mL), washed with H_2O (3 x 100 mL), then the organic layer was dried with $MgSO_4$, filtered and reduced *in vacuo*. The residue was then purified by flash column chromatography (petroleum ether – EtOAc 95:5 v/v increasing to 50:50 v/v) to give phenyl-(4-phenylaminophenyl)-methanol (**18**) as a brown oil. Yield: 0.95 g (86 %), t. l. c. system: petroleum ether – EtOAc 1:1 v/v, R_F: 0.58, stain positive.

^{1}H NMR: δ ($CDCl_3$): 2.94 (s, 1H, OH), 5.81 (s, 1H, H-1), 5.87 (s, 1H, NH), 7.04 (t, J= 7.3 Hz, 1H, Ar), 7.08 (d, J= 8.5 Hz, 2H, Ar), 7.13 (d, J= 7.6 Hz, 2H, Ar), 7.31 (d, J= 8.4 Hz, 2H, Ar), 7.36 (m, 3H, Ar), 7.44 (t, J= 7.3 Hz, 2H, Ar), 7.49 (d, J= 7.3 Hz, 2H, Ar).

^{13}C NMR: δ ($CDCl_3$): 75.76 (CH, C-1), 117.44 (CH, C-2'', C-6''), 117.70 (CH, C-3', C-5'), 121.34 (CH, C-4''), 126.37 (CH, C-3, C-7), 127.48 (CH, C-5), 128.16 (CH, C-4, C-6), 128.87 (CH, C-2', C-6'), 129.82 (CH, C-3'', C-5''), 136.51 (C, C-1'), 142.69 (C, C-4'), 143.15 (C, C-2), 144.24 (C, C-1'').

HRMS (EI): Calculated mass: 275.1305$(M)^+$, Measured mass : 275.1309$(M)^+$.

1-[4-(Naphthalen-2-ylamino)-phenyl]-ethanol (19)

($C_{18}H_{17}NO$, M.W. 263.33)

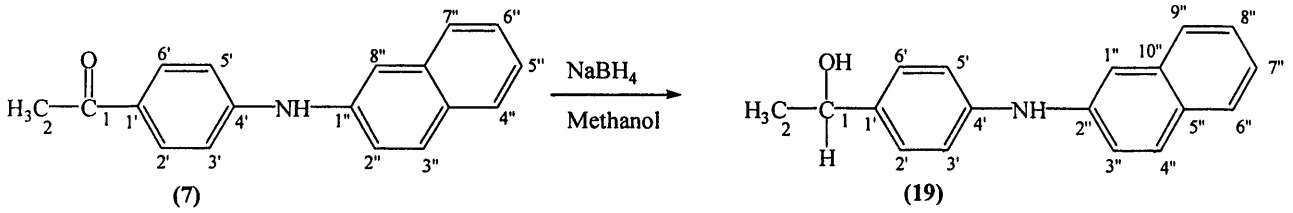

(7) (19)

To a cooled solution of 1-[4-(naphthalen-2-ylamino)-phenyl]-ethanone (**7**) (1.5 g, 5.74 mmol) in anhydrous MeOH (10 mL) and anhydrous dioxane (10 mL) was added $NaBH_4$ (0.43 g, 11.48 mmol) and the mixture stirred under N_2 at room temperature for 3 h. The solvent was evaporated *in vacuo* and acetone (1 mL) was added to the residue in order to quench any excess reducing agent. The oil that separated was extracted with CH_2Cl_2 (2 x 150 mL), washed with H_2O (3 x 100 mL), then the organic layer was dried with $MgSO_4$, filtered and reduced *in vacuo*. The product was then purified by flash column chromatography (petroleum ether – EtOAc 95:5 v/v increasing to 50:50 v/v) to give 1-[4-(naphthalen-2-ylamino)-phenyl]-ethanol (**19**) as a brown solid. Yield: 1.34 g (89 %), t. l. c. system: petroleum ether – EtOAc 2:1 v/v, R_F: 0.57, stain positive.

^{1}H NMR: δ ($CDCl_3$): 1.42 (d, J= 6.5 Hz, 1H, H-2), 1.76 (s, 1H, OH), 4.78 (q, J= 6.5 Hz, 1H, H-1), 5.81 (s, 1H, NH), 7.04 (d, J= 8.5 Hz, 2H, H-3', H5'), 7.11 (dd, J_1= 2.3 Hz, J_2= 8.7 Hz, 1H, H-3''), 7.2 (d, J= 1.2 Hz, 1H, H-1''), 7.22 (d, J= 8.3 Hz, 2H, H-2', H-6'), 7.31 (m, 2H, H-7'', H-8''), 7.54 (d, J= 8.2 Hz, 1H, H-4''), 7.64 (d, J= 8.8 Hz, 2H, H-6'', H-9'').

^{13}C NMR: δ ($CDCl_3$): 24.98 (CH, C-2), 70.13 (CH, C-1), 111.57 (CH, C-1''), 118.32 (CH, C-3', C-5'), 120.02 (CH, C-3''), 123.54 (CH, C-7''), 126.50 (CH, C-6'', C-9''), 126.70 (CH, C-2', C-6'), 127.03 (C, C-5''), 127.68 (CH, C-8''), 129.23 (CH, C-4''), 134.66 (C, C-1'), 138.79 (C, C-10''), 140.90 (C, C-4'), 142.35 (C, C-2'').

Microanalysis: Calculated for $C_{18}H_{17}NO$. $0.3H_2O$ (268.73); Theoretical: %C= 80.45, %H= 6.38, %N= 5.21; Found: %C= 80.80, %H= 6.44, %N= 5.13.

Melting point: 98-100 ^{0}C

[4-(Naphthalen-2-ylamino)-phenyl]-phenylmethanol (20)

($C_{23}H_{19}NO$, M.W. 325.41)

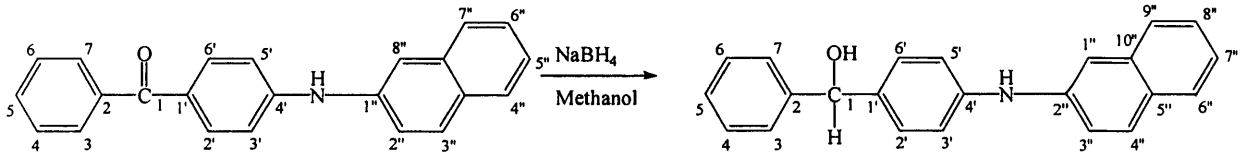

(8) (20)

To a cooled solution of [4-(naphthalen-2-ylamino)-phenyl]-phenyl-methanone (**8**) (1.5 g, 4.6 mmol) in anhydrous MeOH (10 mL) and anhydrous dioxane (10 mL) was added $NaBH_4$ (0.35 g, 9.2 mmol) and the mixture stirred under N_2 at room temperature for 1 h. The solvent was evaporated *in vacuo* and acetone (1 mL) was added to the residue in order to quench any excess reducing agent. The oil that separated was extracted with CH_2Cl_2 (2 x 150 mL), washed with H_2O (3 x 100 mL), then the organic layer was dried with $MgSO_4$, filtered and reduced *in vacuo*. The product was then purified by flash column chromatography (petroleum ether – EtOAc 95:5 v/v increasing to 50:50 v/v) to give [4-(naphthalen-2-ylamino)-phenyl]-phenylmethanol (**20**) as a reddish brown oil. Yield: 1.38 g (92 %), t. l. c. system: petroleum ether – EtOAc 2:1 v/v, R_F: 0.69, stain positive.

^{1}H NMR: δ ($CDCl_3$): 3.24 (s, 1H, OH), 5.81 (s, 1H, H-1), 6.01 (s, 1H, NH), 7.15 (d, J= 8.6 Hz, 2H, H-3', H-5'), 7.23 (dd, J_1= 2.2 Hz, J_2= 8.7 Hz, 1H, H-3''), 7.35 (d, J= 8.7 Hz, 2H, H-2', H-6'), 7.39 (m, 1H, H-7''), 7.41 (d, J= 2.2 Hz, 1H, H-1''), 7.47 (m, 6H, H-3, H-4, H-5, H-6, H-7, H-8''), 7.70 (d, J= 8.2 Hz, 1H, H-4''), 7.78 (d, J= 8.8 Hz, 1H, H-9''), 7.82 (d, J= 8.1 Hz, 1H, H-6'').

^{13}C NMR: δ ($CDCl_3$): 76.26 (CH, C-1), 117.84 (CH, C-1''), 118.43 (CH, C-3', C-5'), 120.50 (CH, C-3''), 123.37 (CH, C-7''), 126.95 (CH, C-9''), 127.19 (CH, C-3, C-7), 127.79 (CH, C-8''), 128.00 (CH, C-6''), 128.33 (CH, C-4, C-6), 128.78 (CH, C-2', C-6'), 128.88 (CH, C-5), 129.25 (CH, C-4''), 129.28 (C, C-5''), 134.75 (C, C-1'), 136.99 (C, C-10''), 140.92 (C, C-4'), 142.46 (C, C-2''), 144.37 (C, C-2).

HRMS (EI): Calculated mass: 326.1539 $(M+H)^+$, Measured mass : 326.1538 $(M+H)^+$.

[4-(Indan-5-ylamino)-phenyl]-phenylmethanol (21)

($C_{22}H_{21}NO$, M.W. 315.40)

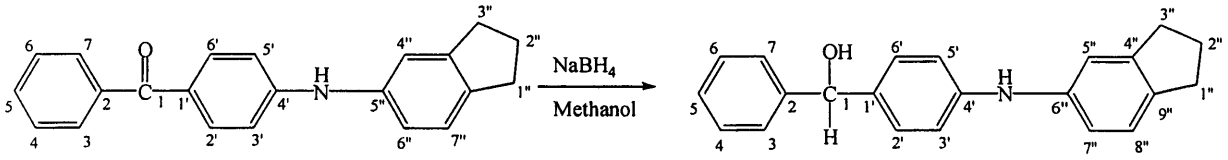

(13) (21)

To a cooled solution of [4-(indan-5-ylamino)-phenyl]-phenylmethanone (**13**) (1.5 g, 4.75 mmol) in anhydrous MeOH (10 mL) and anhydrous dioxane (10 mL) was added $NaBH_4$ (0.36 g, 9.5 mmol) and the mixture stirred under N_2 at room temperature for 7 h. The solvent was evaporated *in vacuo* and acetone (1 mL) was added to the residue in order to quench any excess reducing agent. The oil that separated was extracted with CH_2Cl_2 (2 x 150 mL), washed with H_2O (3 x 100 mL), then the organic layer was dried with $MgSO_4$, filtered and reduced *in vacuo*. The product was then purified by flash column chromatography (petroleum ether – EtOAc 95:5 v/v increasing to 50:50 v/v) to give [4-(indan-5-ylamino)-phenyl]-phenyl-MeOH (**21**) as a brown oil Yield: 1.36 g (91 %), t. l. c. system: petroleum ether – EtOAc 2:1 v/v, R_F: 0.71, stain positive.

^{1}H NMR: δ ($CDCl_3$): 1.98 (m, 2H, H-2''), 2.12 (s, 1H, OH), 2.77 (t, J= 7.4Hz, 4H, H-1'', H-3''), 5.51 (s, 1H, NH), 5.21 (s, 1H, H-1), 6.76 (dd, J_1= 2.0 Hz, J_2= 8.5 Hz, 1H, H-7''), 6.87 (m, 3H, H-3, H-7, H-5''), 7.02 (d, J= 8.0 Hz, 1H, H-8''), 7.11 (d, J= 8.5 Hz, 2H, H-2', H-6'), 7.17 (m, 1H, H-5), 7.25 (m, 2H, H-4, H-6), 7.30 (d, J= 7.5 Hz, 2H, H-3', H-5').

^{13}C NMR: δ ($CDCl_3$): 25.71 (C, C-2''), 32.38 (C, C-1''), 33.08 (C, C-3''), 76.00 (CH, C-1), 115.28 (CH, C-7''), 116.70 (CH, C-3', C-5'), 117.35 (CH, C-5''), 124.89 (CH, C-5), 126.60 (CH, C-3, C-7), 127.86 (CH, C-8''), 128.11 (CH, C-4, C-6), 128.42 (CH, C-2', C-6'), 135.62 (C, C-9''), 137.64 (C, C-1'), 140.99 (C, C-4''), 143.78 (C, C-6''), 144.12 (C, C-4'), 145.59 (C, C-2).

HRMS (EI): Calculated mass: 316.1696 $(M+H)^+$, Measured mass : 316.1695 $(M+H)^+$.

Phenyl-[4-(1-[1,2,4]triazol-1-ylethyl)-phenyl]-amine (22)

($C_{16}H_{16}N_4$, M.W. 264.329)

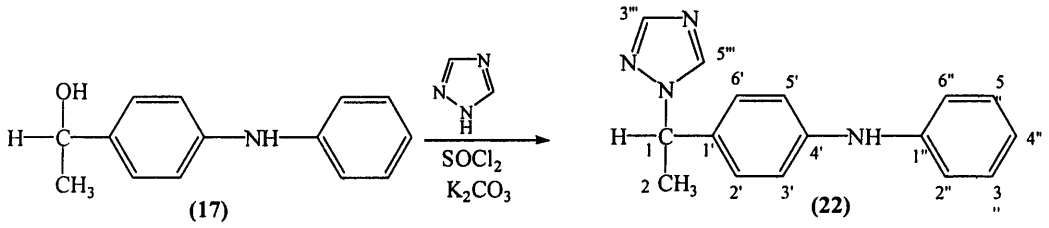

(17) (22)

Thionyl chloride (0.24 g, 2 mmol) in anhydrous CH_3CN (10 mL) was added dropwise to a stirred solution of 1,2,4-triazole (0.28 g, 4 mmol) in anhydrous CH_3CN (10 mL) at a temperature of 10 °C. The white suspension formed was stirred for 1 h at 10 °C. A solution of 1-(4-phenylamino-phenyl)-ethanol (**17**) (0.21 g, 1 mmol) in anhydrous CH_3CN (10 mL) was added to the mixture followed by activated K_2CO_3 (0.28 g, 2 mmol). The suspension was stirred under N_2 at room temperature for 4 days. The resulting suspension was filtered and the filtrate was evaporated *in vacuo* to yield a light brown oil. The oil was extracted with CH_2Cl_2 (150 mL) and H_2O (3 x 100 mL). The organic layer was dried with $MgSO_4$, filtered and reduced *in vacuo*. The product was then purified by flash column chromatography (petroleum ether – EtOAc 90:10 v/v increasing to 10:90 v/v) to give phenyl-[4-(1-[1,2,4]triazol-1-ylethyl)-phenyl]-amine (**22**) as a light brown solid. Yield 0.19 g (72 %), t. l. c. system: petroleum ether – EtOAc 1:1 v/v, R_F: 0.32, stain positive.

^{1}H NMR: δ ($CDCl_3$): 1.93 (d, J= 7.0 Hz, 3H, H-2), 5.50 (q, J= 7.0 Hz, 1H, H-1), 5.89 (s, 1H, NH), 6.98 (t, J= 7.3 Hz, 1H, Ar), 7.05 (d, J= 8.5 Hz, 2H, Ar), 7.10 (d, J= 7.9 Hz, 2H, Ar), 7.19 (d, J= 8.5 Hz, 2H, Ar), 7.30 (t, J= 7.6 Hz, 2H, Ar), 7.98 (s, 1H, H-3'''), 8.03 (s, 1H, H-5''').

^{13}C NMR: δ ($CDCl_3$): 21.26 (CH_3, C-2), 59.32 (CH, C-1), 117.26 (CH, C-3', C-5'), 118.58 (CH, C-2'', C-6''), 121.70 (CH, C-4''), 127.87 (CH, C-2', C-6'), 129.42 (CH, C-3'', C-5''), 131.45 (C, C-1'), 141.83 (CH, C-3'''), 142.39 (C, C-4'), 143.75 (C, C-1''), 151.81 (C, C-5''').

Microanalysis: Calculated for $C_{16}H_{16}N_4$. $0.3H_2O$ (269.734); Theoretical: %C= 71.24, %H= 5.97, %N= 20.77; Found: %C= 71.44, %H= 6.03, %N= 20.37.

Melting point: 108-110 ^{0}C

Phenyl-[4-(phenyl-[1,2,4]triazol-1-ylmethyl)-phenyl]-amine (23)

($C_{21}H_{18}N_4$, M.W. 326.40)

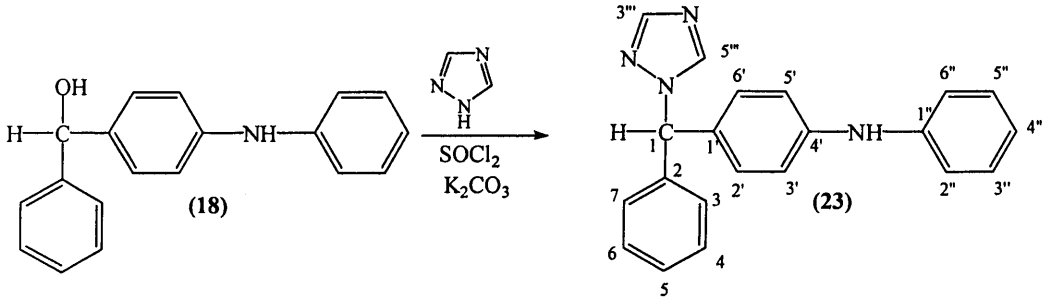

Thionyl chloride (0.44 g, 3.64 mmol) in anhydrous CH_3CN (10 mL) was added dropwise to a stirred solution of 1,2,4-triazole (0.5 g, 7.28 mmol) in anhydrous CH_3CN (10 mL) at a temperature of 10 °C. The white suspension formed was stirred for 1 h at 10 °C. A solution of phenyl-(4-phenylaminophenyl)-methanol (**18**) (0.5 g, 1.82 mmol) in anhydrous CH_3CN (10 mL) was added to the mixture followed by activated K_2CO_3 (0.5 g, 3.64 mmol). The suspension was stirred under N_2 at room temperature for 4 days. The resulting suspension was filtered and the filtrate was evaporated *in vacuo* to yield a light brown oil. The oil was extracted with CH_2Cl_2 (150 mL) and H_2O (3 x 100 mL). The organic layer was dried with $MgSO_4$, filtered and reduced *in vacuo*. The product was then purified by flash column chromatography (petroleum ether – EtOAc 90:10 v/v increasing to 10:90 v/v) to give phenyl-[4-(phenyl-[1,2,4]triazol-1-ylmethyl)-phenyl]-amine (**23**) as a light brown solid. Yield 0.41 g (69 %), t. l. c. system: petroleum ether – EtOAc 1:1 v/v, R_F: 0.42, stain positive.

^{1}H NMR: δ ($CDCl_3$): 5.91 (s, 1H, NH), 6.72 (s, 1H, H-1), 7.04 (m, 4H, Ar), 7.13 (m, 4H, Ar), 7.31 (m, 3H, Ar), 7.39 (m, 3H, Ar), 7.97 (s, 1H, H-3'''), 8.06 (s, 1H, H-5''').

^{13}C NMR: δ ($CDCl_3$): 67.56 (CH, C-1), 116.95 (CH, C-2'', C-6''), 118.83 (CH, C-3', C-5'), 121.90 (CH, C-4''), 127.77 (CH, C-3, C-7), 128.39 (CH, C-5), 128.89 (CH, C-4, C-6), 129.40 (C, C-1'), 129.43 (CH, C-2', C-6'), 129.57 (CH, C-3'', C-5''), 138.52 (C, C-4'), 142.16 (C, C-2), 143.51 (CH, C-3'''), 143.93 (C, C-1''), 152.27 (CH, C-5''').

Microanalysis: Calculated for $C_{21}H_{18}N_4$; Theoretical: %C= 77.28, %H= 5.56, %N= 17.16; Found: %C= 76.90, %H= 5.54, %N= 17.04.

Melting point: 138-140 ^{0}C

Phenyl-[4-(1-imidazol-1-ylethyl)-phenyl]-amine (24)

($C_{17}H_{17}N_3$, M.W. 263.34)

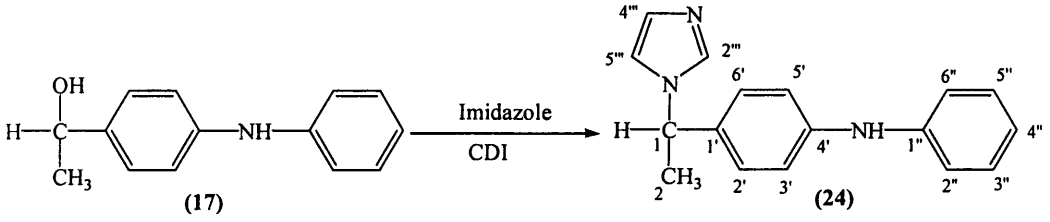

(17) (24)

To a solution of 1-(4-phenylamino-phenyl)-ethanol (**17**) (0.5 g, 2.35 mmol) in anhydrous CH_3CN (20 mL) was added imidazole (0.48 g, 7.05 mmmol) and CDI (0.57 g, 3.5 mmol). The mixture was then heated under reflux at 85 ^{0}C for 1 h. The reaction mixture was allowed to cool and then extracted with CH_2Cl_2 (150 mL) and H_2O (3 x 100 mL). The organic layer was dried with $MgSO_4$, filtered and reduced *in vacuo*. The product was then purified by flash column chromatography (CH_2Cl_2 – MeOH 99:1 v/v increasing to 90:10 v/v) to give phenyl-[4-(phenyl-imidazol-1-ylmethyl)-phenyl]-amine (**24**) as a light brown solid. Yield 0.52 g (84 %), t. l. c. system: CH_2Cl_2 – MeOH 90:10 v/v, R_F: 0.37, stain positive.

^{1}H NMR: δ ($CDCl_3$): 1.85 (d, J= 7.0 Hz, 3H, H-2), 5.30 (q, J= 7.0 Hz, 1H, H-1), 6.02 (s, 1H, NH), 6.97 (m, 2H, Ar), 7.07 (m, 7H, Ar), 7.29 (m, 2H, Ar), 7.60 (s, 1H, H-2'''').

^{13}C NMR: δ ($CDCl_3$): 22.07 (CH_3, C-2), 56.15 (CH, C-1), 117.35 (CH, C-3', C-5'), 117.89 (CH, C-4'''), 118.35 (CH, C-2'', C-6''), 121.47 (CH, C-4'', C-5'''), 127.24 (CH, C-2', C-6'), 129.40 (CH, C-3'', C-5''), 133.28 (C, C-1'), 136.05 (CH, C-2'''), 142.63 (C, C-4'), 143.35 (C, C-1'').

Microanalysis: Calculated for $C_{17}H_{17}N_3$. $0.1H_2O$ (265.141); Theoretical: %C= 77.01, %H= 6.46, %N= 15.85; Found: %C= 76.89, %H= 6.46, %N= 15.87.

Melting point: 110-112 ^{0}C

Phenyl-[4-(phenylimidazol-1-ylmethyl)-phenyl]-amine (25)

($C_{22}H_{19}N_3$, M.W. 325.412)

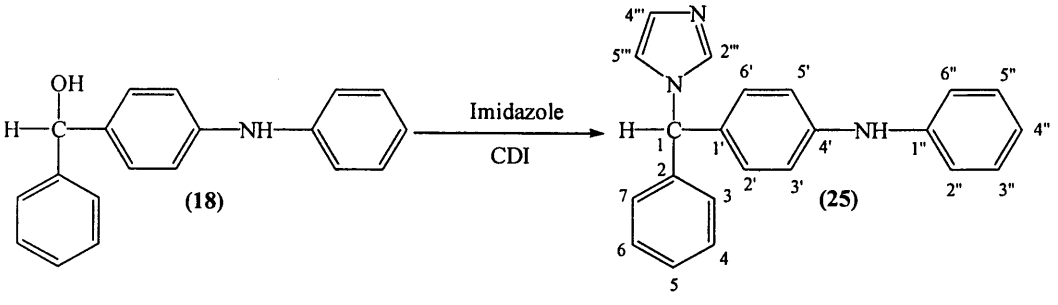

(18) (25)

To a solution of phenyl-(4-phenylaminophenyl)-methanol (**18**) (0.5 g, 1.82 mmol) in anhydrous CH_3CN (20 mL) was added imidazole (0.37 g, 5.5 mmmol) and CDI (0.57 g, 3.5 mmol). The mixture was then heated under reflux at 85 ^{0}C for 1 h. The reaction mixture was allowed to cool and then extracted with CH_2Cl_2 (150 mL) and H_2O (3 x 100 mL). The organic layer was dried with $MgSO_4$, filtered and reduced *in vacuo*. The product was then purified by flash column chromatography (CH_2Cl_2 – MeOH 99:1 v/v increasing to 90:10 v/v) to give phenyl-[4-(phenylimidazol-1-ylmethyl)-phenyl]-amine (**25**) as a white solid. Yield 0.53 g (89 %), t. l. c. system: CH_2Cl_2 – MeOH 90:10 v/v, R_F: 0.41, stain positive.

^{1}H NMR: δ ($CDCl_3$): 5.80 (s, 1H, NH), 6.48 (s, 1H, H-1), 7.01 (m, 4H, Ar), 7.17 (m, 4H, Ar), 7.30 (m, 4H, Ar), 7.38 (m, 3H, Ar), 7.46 (s, 1H, H-2'''').

^{13}C NMR: δ ($CDCl_3$): 64.83 (CH, C-1), 116.79 (CH, C-2'', C-6''), 117.06 (CH, C-4''), 118.42 (CH, C-3', C-5'), 121.92 (CH, C-4'''), 126.93 (CH, C-5, C-5'''), 128.27 (CH, C-3, C-7), 128.87 (CH, C-4, C-6), 129.30 (CH, C-2', C-6'), 129.40 (CH, C-3'', C-5''), 129.75 (C, C-1'), 132.54 (CH, C-2'''), 139.55 (C, C-4'), 143.06 (C, C-2), 143.91 (C, C-1'').

Microanalysis: Calculated for $C_{22}H_{19}N_3$. $0.3H_2O$ (330.815); Theoretical: %C= 79.87, %H= 5.78, %N= 12.70; Found: %C= 79.72, %H= 5.86, %N= 12.56.

Melting point: 208-210 ^{0}C

[4-(1-Imidazol-1-ylethyl)-phenyl]-naphthalen-2-ylamine (26)

($C_{21}H_{19}N_3$, M.W. 313.40)

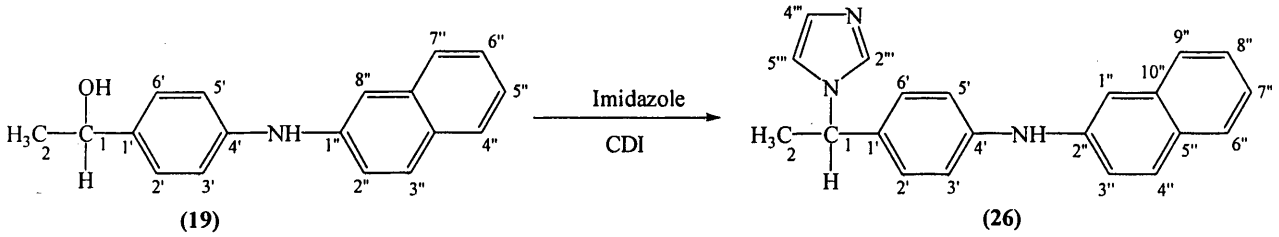

(19) (26)

To a solution of 1-[4-(naphthalen-2-ylamino)-phenyl]-ethanol (**19**) (0.5 g, 1.9 mmol) in anhydrous CH_3CN (20 mL) was added imidazole (0.38 g, 5.7 mmmol) and CDI (0.46 g, 2.85 mmol). The mixture was then heated at 85 ^{0}C for 1 h. The reaction mixture was allowed to cool and then extracted with CH_2Cl_2 (150 mL) and H_2O (3 x 100 mL). The organic layer was dried with $MgSO_4$, filtered and reduced *in vacuo*. The product was then purified by flash column chromatography (CH_2Cl_2 – MeOH 99:1

v/v increasing to 95:5 v/v) to give [4-(1-imidazol-1-ylethyl)-phenyl]-naphthalen-2-ylamine (**26**) as a white solid. Yield 0.5 g (84 %), t. l. c. system: CH_2Cl_2 – MeOH 90:10 v/v, R_F: 0.33, stain positive.

^{1}H NMR: δ ($CDCl_3$): 1.78 (d, J= 6.4Hz, 1H, H-2), 5.19 (q, J= 6.4 Hz, 1H, H-1), 5.87 (s, 1H, NH), 6.91 (d, J= 1.7 Hz, 1H, H-1''), 7.05 (d, J= 8.5 Hz, 4H, H-2', H-3', H-5', H-6'), 7.15 (dd, J_1= 2.1 Hz, J_2= 8.6 Hz, 1H, H-3''), 7.19 (m, 1H, H-7''), 7.32 (m, 1H, H-8''), 7.38 (d, J= 7.7 Hz, 2H, H-4''', H-5'''), 7.51 (s, 1H, H-2'''), 7.59 (d, J= 8.4 Hz, 1H, H-4''), 7.71 (d, J= 8.8 Hz, 2H, H-6'', H-9'').

^{13}C NMR: δ ($CDCl_3$): 21.05 (CH, C-1), 52.40 (CH, C-2), 111.45 (CH, C-1''), 116.79 (CH, C-3', C-5'), 119.22 (CH, C-3''), 122.78 (CH, C-4''', C-7''), 125.53 (CH, C-8'', C-9''), 126.31 (CH, C-5''', C-6''), 126.65 (C, C-5''), 128.30 (CH, C-2', C-6'), 128.42 (C, C-4''), 132.75 (C, C-1'), 133.52 (C, C-10''), 135.03 (CH, C-2'''), 139.18 (C, C-4'), 142.06 (C, C-2'').

HRMS (EI): Calculated mass: 314.1652 $(M+H)^+$, Measured mass : 314.1654 $(M+H)^+$.

Melting point: 170-172 ^{0}C

[4-(Imidazol-1-ylphenylmethyl)-phenyl]-naphthalen-2-ylamine (27)

($C_{26}H_{21}N_3$, M.W. 375.47)

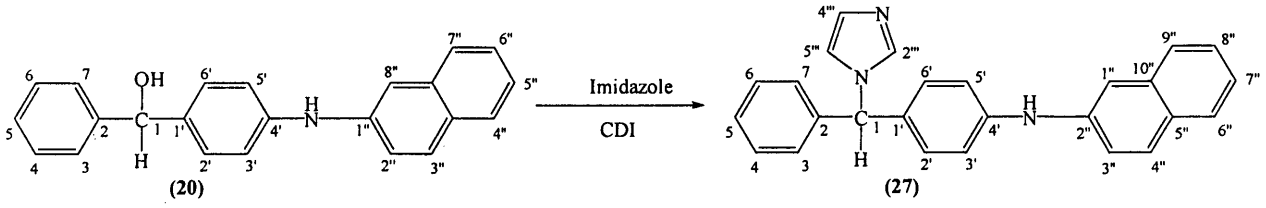

To a solution of [4-(naphthalen-2-ylamino)-phenyl]-phenyl-methanol (**20**) (0.5 g, 1.54 mmol) in anhydrous CH_3CN (20 mL) was added imidazole (0.31 g, 4.62 mmmol) and CDI (0.38 g, 2.31 mmol). The mixture was then heated at 85 ^{0}C for 1 h. The reaction mixture was allowed to cool and then extracted with CH_2Cl_2 (150 mL) and H_2O (3 x 100 mL). The organic layer was dried with $MgSO_4$, filtered and reduced *in vacuo*. The product was then purified by flash column chromatography (CH_2Cl_2 – MeOH 99:1 v/v increasing to 95:5 v/v) to give [4-(imidazol-1-ylphenylmethyl)-phenyl]-naphthalen-2-ylamine (**27**) as a pink solid. Yield 0.51 g (88 %), t. l. c. system: CH_2Cl_2 – MeOH 90:10 v/v, R_F: 0.40, stain positive.

^{1}H NMR: δ ($CDCl_3$): 6.06 (s, 1H, NH), 6.38 (s, 1H, H-1), 6.81 (s, 1H, H-1''), 6.94 (d, J= 8.6 Hz, 2H, H-3', H-5'), 7.03 (m, 5H, Ar), 7.15 (dd, J_1= 2.3 Hz, J_2= 8.5 Hz, 1H, H-3''), 7.23 (m, 4H, Ar), 7.32 (m, 1H, Ar), 7.38 (m, 2H, Ar), 7.57 (d, J= 8.2 Hz, 1H, H-4''), 7.66 (d, J= 8.8 Hz, 2H, H-6'', H-9'').

^{13}C NMR: δ ($CDCl_3$): 64.73 (CH, C-1), 112.80 (CH, C-1''), 117.36 (CH, C-3', C-5'), 120.40 (CH, C-3''), 123.87 (CH, C-7''), 126.56 (CH, C-9''), 126.60 (CH, C-8'', C-4'''), 127.69 (CH, C-5, C-5'''), 127.80 (CH, C-3', C-7), 128.23 (CH, C-6''), 128.85 (C, C-2', C-6'), 129.29 (CH, C-2'''), 129.45 (C, C-4''), 129.51 (CH, C-4, C-6), 129.51 (C, C-5''), 131.10 (C, C-1'), 134.53 (C, C-10''), 139.67 (C, C-4'), 140.00 (C, C-2''), 143.45 (C, C-2).

Microanalysis: Calculated for $C_{26}H_{21}N_3$. $0.3H_2O$ (380.87); Theoretical: %C= 81.99, %H= 5.56, %N= 11.03; Found: %C= 81.86, %H= 5.59, %N= 10.82.

Melting point: 94-96 ^{0}C

[4-(Imidazol-1-ylphenylmethyl)-phenyl]-indan-5-ylamine (28)

($C_{25}H_{23}N_3$, M.W. 365.48)

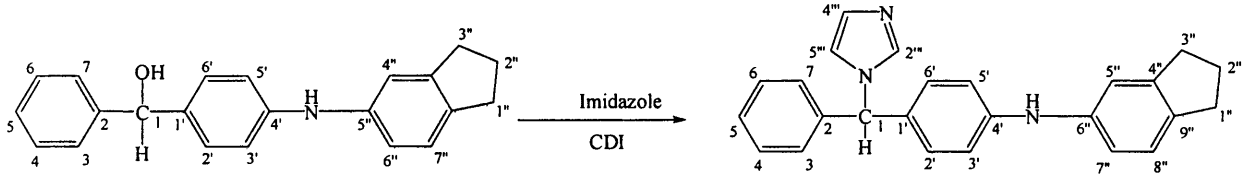

(21) **(28)**

To a solution of [4-(indan-5-ylamino)-phenyl]-phenyl-methanol (**21**) (0.5 g, 1.59 mmol) in anhydrous CH_3CN (20 mL) was added imidazole (0.32 g, 4.77 mmmol) and CDI (0.25 g, 2.39 mmol). The mixture was then heated at 85 ^{0}C for 1 h. The reaction mixture was allowed to cool and then extracted with CH_2Cl_2 (150 mL) and water (3 x 100 mL). The organic layer was dried with $MgSO_4$, filtered and reduced *in vacuo*. The product was then purified by flash column chromatography (CH_2Cl_2 – MeOH 99:1 v/v increasing to 95:5 v/v) to give [4-(imidazol-1-ylphenylmethyl)-phenyl]-indan-5-ylamine (**28**) as a white solid. Yield 0.48 g (83 %), t. l. c. system: CH_2Cl_2 – MeOH 90:10 v/v, R_F: 0.43, stain positive.

^{1}H NMR: δ ($CDCl_3$): 1.98 (m, 2H, H-2''), 2.76 (m, 4H, H-1'', H-3''), 5.78 (s, 1H, NH), 6.35 (s, 1H, H-1), 6.79 (m, 2H, Ar), 6.87 (m, 4H, Ar), 6.92 (d, J= 1.5 Hz,

1H, H-5''), 7.01 (m, 3H, Ar), 7.04 (d, J= 8.0 Hz, 1H, H-8''), 7.25 (m, 3H, Ar), 7.34 (s, 1H, H-2''').

^{13}C NMR: δ ($CDCl_3$): 25.69 (C, C-2''), 32.31 (C, C-1''), 33.05 (C, C-3''), 64.73 (CH, C-1), 115.98 (CH, C-7''), 116.09 (CH, C-3', C-5'), 118.02 (CH, C-5''), 124.57 (CH, C-4'''), 127.63 (CH, C-5, C-5'''), 127.97 (CH, C-8''), 128.67 (CH, C-3, C-7), 129.02 (CH, C-4, C-6), 129.19 (CH, C-2', C-6'), 129.38 (C, C-9''), 132.81 (CH, C-2'''), 138.25 (C, C-1'), 139.83 (C, C-4''), 140.30 (C, C-6''), 145.19 (C, C-4'), 145.64 (C, C-2).

Microanalysis: Calculated for $C_{25}H_{23}N_3$. $0.7H_2O$ (378.08); Theoretical: %C= 79.42, %H= 6.13, %N= 11.11; Found: %C= 79.37, %H= 6.48, %N= 11.32.

Melting point: 88-90 ^{0}C

5.1.2 Synthesis of 4-imidazol-1-yl-(phenyl)-methylphenylheteroarylamine

5.1.2.1 General chemistry

The synthesis of 4-imidazol-1-yl-(phenyl)-methylphenylheteroarylamine was carried out according to a sequence of 4 steps (**Scheme 5.9**):

- The reduction of 4-aminobenzophenone to the corresponding carbinol
- The formation of the isothiocyanate derivative through the reaction with thiophosgene
- The formation of the heteroaryl amine derivative through reaction with the appropriate *o*-substituted aniline followed by cyclisation using HgO
- The addition of the imidazole ring

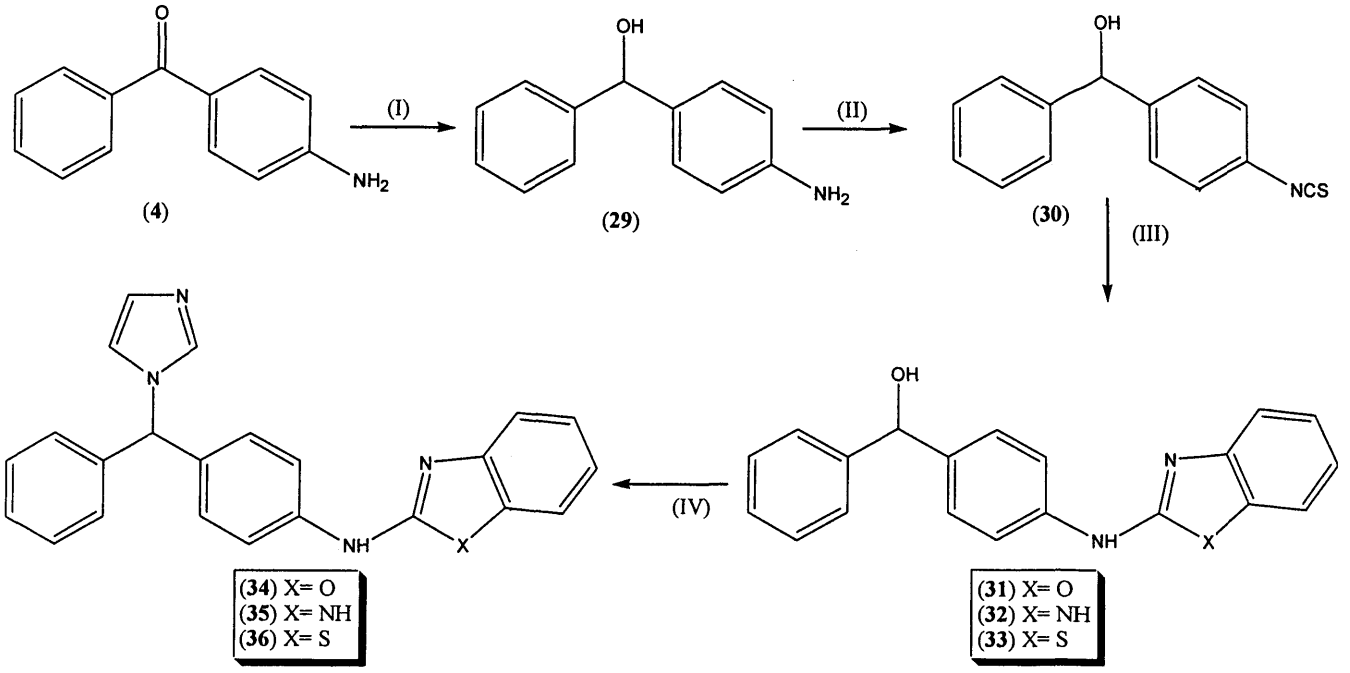

Scheme 5.9: General reaction scheme for the synthesis of 4-imidazol-1-yl-(phenyl)-methyl-phenyl-heteroaryl amine. Reagents and conditions: (I) $NaBH_4$, MeOH, 1 h (b) thiophosgene, ice, H_2O, CH_2Cl_2, r.t., overnight (c) (i) 2-aminophenol, 1,2-phenylenediamine, 2-aminothiophenol for X= O and NH and S respectively, EtOH, r.t., 24 h (ii) HgO, S, EtOH, reflux at 85°C, 2 h (d) imidazole, 1,1'carbonyldiimidazole, acetonitrile, reflux, 1h.

5.1.2.1.1 Synthesis of (4-amino-phenyl)-phenyl-methanol

The reduction of 4-aminobenzophenone to the corresponding alcohol was performed in MeOH using the reducing agent $NaBH_4$. The reaction was complete after 1 h at room temperature and the product was obtained in a 93% yield without purification by column chromatography. The secondary alcohol was confirmed by ^1H NMR by the presence of the OH group at 3.25 ppm and the H atom at C-1 at 5.6 ppm. ^{13}C NMR confirmed the disappearance of the C=O group.

5.1.2.1.2 Synthesis of the isothiocyanate

This was performed using thiophosgene as described in the literature (Bertha *et al.*, 1983). Thiophosgene was added to a mixture of (4-amino-phenyl)-phenyl-methanol, CH_2Cl_2, ice and H_2O. The reaction was then complete after overnight stirring at 0 ^0C. The thiophosgene residue and the HCl formed during the reaction were removed by washing the organic layer thoroughly with H_2O and $NaHCO_3$. The product was then obtained with 91 % yield after purification by flash column

chromatography. The same reaction performed with 4-aminobenzophenone gave the product in much lower yield (45%). Therefore, the reduction of 4-aminobenzophenone was performed before formation of the isothiocyanate.

The mechanism of the reaction (**Figure 5.2**) involves the attack of the nitrogen on the thiophosgene thiocarbonyl.

The result was confirmed by the disappearance of the 2 proton peaks from the amino group at 4.8 ppm in ^{1}H NMR and the characteristic isothiocyanate peak at 143.25 ppm in ^{13}C NMR.

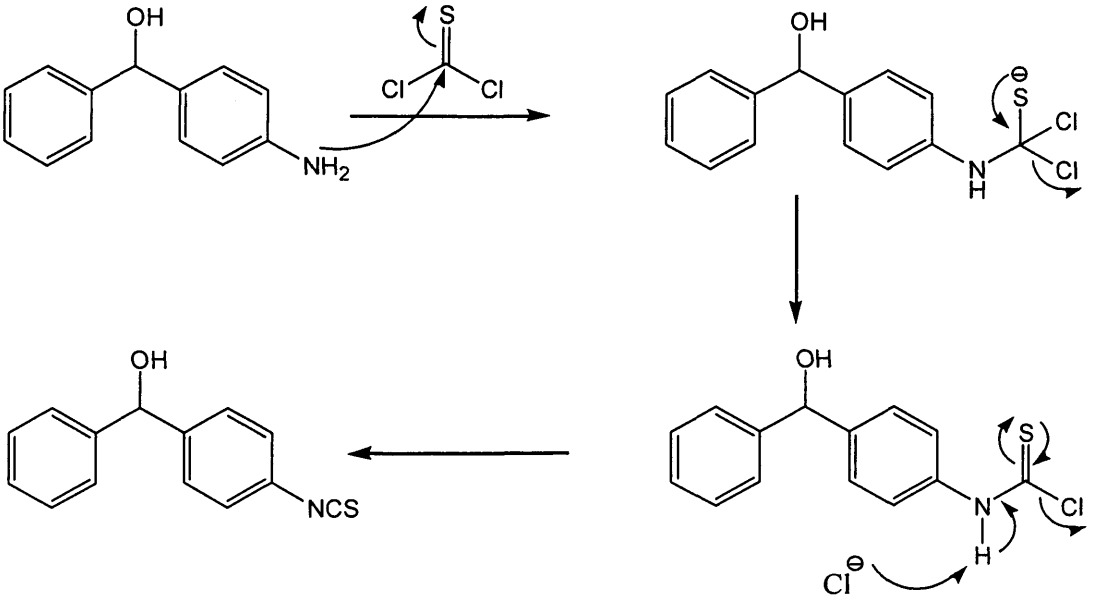

Figure 5.2: Mechanism of the thiophosgene reaction.

5.1.2.1.3 Synthesis of the 2-substituted amino benzoheterocycle

There is considerable synthetic methodology reported for the synthesis of unsubstituted 2-aminobenzoheterocycles, but the pathways described for the preparation of 2-substituted derivatives are limited. The three methods that can be applied for the synthesis of 2-substituted-amino-benzoxazole or benzimidazole or benzothiazole were path A, path B and path C described below.

Path A:

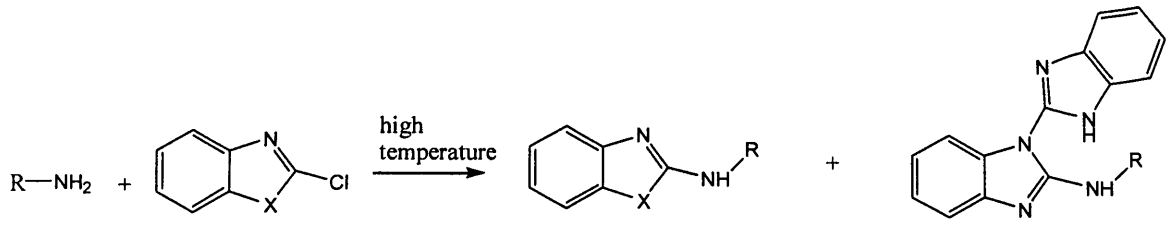

Path A (Janssens *et al.*, 1985) required the amination of 2-chlorobenzoheterocycle with an amine at elevated temperatures. However, this reaction usually has poor yields and major by-products in case of benzimidazole including amino-bis(benzimidazoles).

Path B:

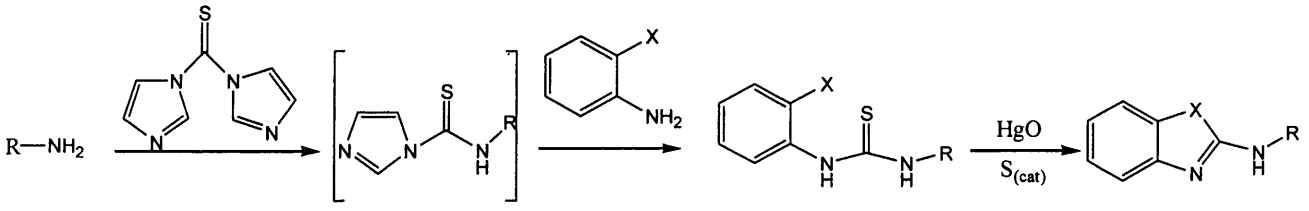

Path B (Perkins *et al.*, 1999) involved the acylation of the amine with thiocarbonyldiimidazole followed by the addition of an excess of the required o-substituted aniline, promoting formation of the unsymmetric thiourea. Cyclodesulfurisation can then be affected by treatment with HgO in refluxing EtOH (Janssens *et al.*, 1985). However, this method when applied to 4-aminobenzophenone gave a very poor yield of the thiourea (11%) and it could not be applied to the corresponding alcohol due to interference of the OH.

Path C:

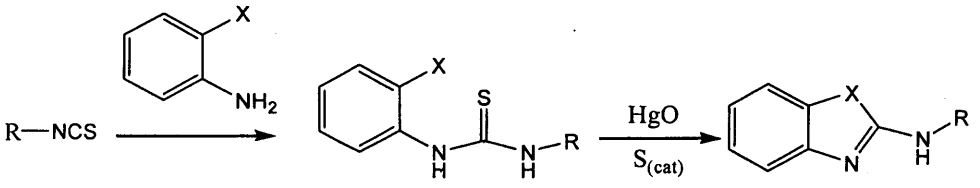

Path C involved the reaction of the required *o*-substituted aniline with an isothiocyanate (Ogura *et al.*, 1981) leading to the formation of a thiourea derivative

which was then cyclised using HgO in the presence of a catalytic amount of S (Perkins *et al.*, 1999; Janssens *et al.*, 1985).

The last method has been used successfully in the preparation of the 2-substituted amino-benzoxazole, benzimidazole and benzothiazole (**Scheme 5.10**). This involved stirring the isothiocyanate with the appropriate *o*-substituted aniline in EtOH at room temperature for 24 h. This was followed by the addition of HgO and catalytic amount of S and the reaction mixture was then refluxed at 85°C for 2 h. The products were obtained in good yield after filtration and purification by flash column chromatography. The summary of the results is shown in **Table 5.5**.

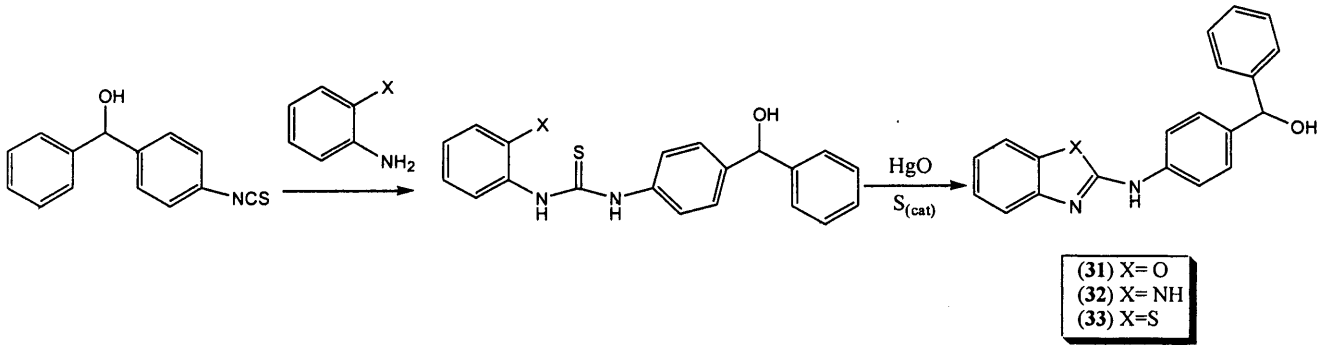

Scheme 5.10: Scheme for the synthesis of the 2-substituted amino benzoheterocycle.

The products were confirmed by the appearance of the NH peak at approximately 10.5 ppm and the OH peak that has been shifted to 5.7 ppm approximately in ^{1}H NMR. The ^{13}C NMR confirmed the presence of the characteristic benzoheterocycle quaternary carbon at about 157 ppm. A summary of the results is presented in **Table 5.5**.

Table 5.5: Summary of the synthesis of compounds (**31**) - (**33**).

Product	Yield (%)	Melting point (^{0}C)
31	77	160-162
32	81	190-192
33	82	138-140

5.1.2.1.4 Addition of the imidazole ring

The same method previously described (5.1.1.1.4) was applied to the *N*-heteroaryl substituted derivatives. The products have been obtained in good yield after

refluxing for 1 h and purification by flash column chromatography (**Scheme 5.11**). The summary of the results is presented in **Table 5.6**.

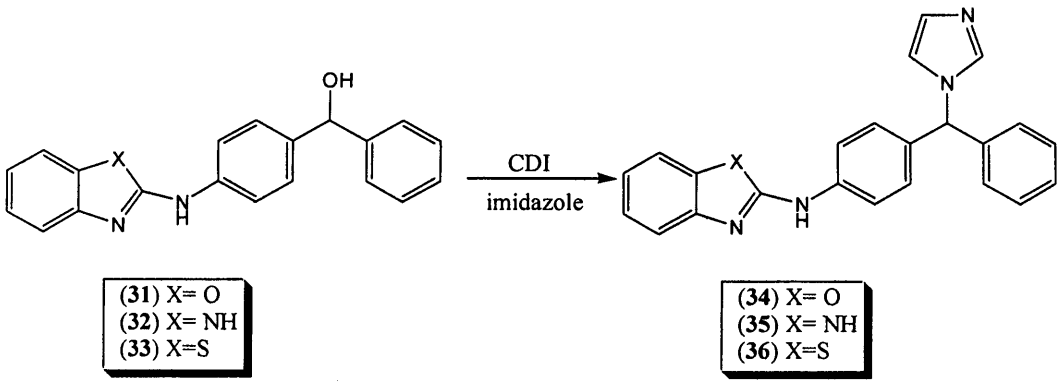

Scheme 5.11: synthesis of compounds (**34**), (**35**) and (**36**).

Table 5.6: Summary of the synthesis of compounds (**35**) - (**36**).

Product	Yield (%)	Melting point (^{0}C)
34	71	214-216
35	76	274-276
36	73	258-260

5.1.2.2 Experimental

(4-Aminophenyl)-phenylmethanol (29)

($C_{13}H_{13}NO$, M.W. 199.25)

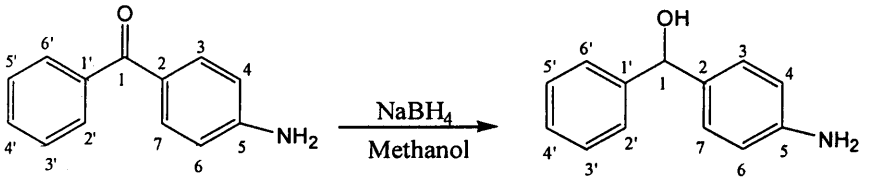

(**4**) (**29**)

To a cooled solution of 4-aminobenzophenone (**4**) (2 g, 10.14 mmol) in anhydrous MeOH (20 mL) was added $NaBH_4$ (0.76 g, 20.28 mmol) and the mixture stirred under N_2 at room temperature for 1 h. The solvent was evaporated *in vacuo* and acetone (1 mL) was added to the residue in order to quench any excess reducing agent. The oil that separated was extracted with CH_2Cl_2 (2 x 150 mL), washed with H_2O (3 x 100 mL), then the organic layer was dried with $MgSO_4$, filtered and reduced

in vacuo. The product was then obtained without further purification to give (4-aminophenyl)-phenylmethanol (**29**) as a white solid. Yield: 1.92 g (95 %), t. l. c. system: petroleum ether – EtOAc 2:1 v/v, R_F: 0.39, stain positive.

^{1}H NMR: δ ($CDCl_3$): 3.21 (s, 1H, OH), 4.83 (s, 2H, NH), 5.62 (s, 1H, H-1), 6.59 (dd, J_1= 1.7 Hz, J_2= 7.6 Hz, 2H, H-4, H-6), 7.00 (dd, J_1= 1.6 Hz, J_2= 7.8 Hz, 2H, H-3, H-7), 7.12 (m, 2H, H-3', H-5'), 7.20 (m, 1H, H-4'), 7.25 (m, 2H, H-2', H-6').

^{13}C NMR: δ ($CDCl_3$): 76.86 (CH, C-1), 116.42 (CH, C-4, C-6), 127.58 (CH, C-2', C-6'), 127.94 (CH, C-4'), 128.93 (CH, C-3', C-5'), 129.13 (CH, C-3, C-7), 135.63 (C, C-2), 146.36 (C, C-1'), 147.88 (C, C-5).

Microanalysis: Calculated for $C_{13}H_{13}NO.\ 0.3H_2O$ (204.653); Theoretical: %C= 76.30, %H= 6.40, %N= 6.84; Found: %C= 76.36, %H= 6.43, %N= 6.80.

Melting point: 116-118 ^{0}C

(4-Isothiocyanatophenyl)-phenylmethanol (30)

($C_{14}H_{11}NOS$, M.W. 241.24)

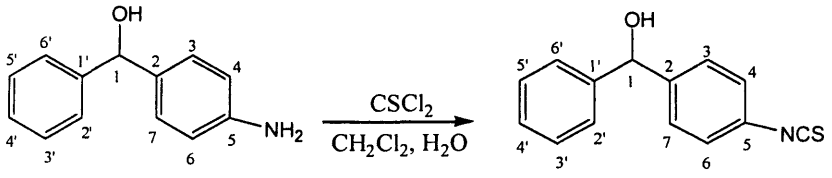

(29) **(30)**

To a solution of **29** (1.4 g, 7.03 mmol) in CH_2Cl_2 (20 mL) was added a mixture of ice (2 g) and H_2O (1 mL) and subsequently dropwise with vigorous stirring thiophosgene (0.64 mL, 8.4 mmol). The mixture was stirred 2 h at 0 °C and kept overnight in a refrigerator. The organic layer was separated and extracted successively with water (2 × 50 mL), 10 % $NaHCO_3$ aq. (50 mL) and H_2O again (50 mL), dried ($MgSO_4$) and evaporated to dryness to obtain the pure product as a yellow oil. Yield: 1.34 g, (79 %). t.l.c system: petroleum ether - EtOAc 1:1 v/v, R_F = 0.73.

^{1}H NMR: δ ($CDCl_3$): 2.69 (s, 1H, OH), 5.59 (s, 1H, H-1), 7.00 (d, J= 8.3 Hz, 2H, H-4, H-6), 7.18 (m, 7H, H-3, H-7, H-2', H-3', H-4', H-5', H-6').

^{13}C NMR: δ ($CDCl_3$): 75.58 (CH, C-1), 125.50 (CH, C-4, C-6), 126.08 (CH, C-2', C-6'), 127.46 (CH, C-4'), 127.89 (CH, C-3', C-5'), 129.02 (CH, C-3, C-7), 130.29 (C, C-5), 135.45 (C, C-2), 143.06 (C, C-1'), 143.25 (C, C-NCS).

HRMS (EI): Calculated mass: 241.0556 $(M)^+$, Measured mass : 241.0557 $(M)^+$.

[4-(Benzooxazol-2-ylamino)-phenyl]-phenylmethanol (31)

($C_{20}H_{16}N_2O_2$, M.W. 316.348)

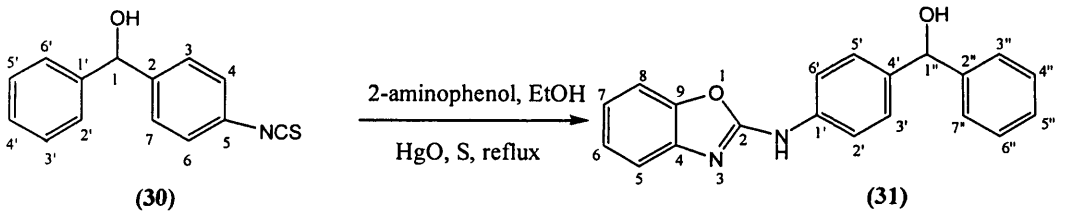

(30) **(31)**

2-Aminophenol (0.18 g, 1.66 mmol) was added to a solution of (**30**) (0.4 g, 1.66 mmol) in absolute EtOH (10 mL). The mixture was then stirred overnight at room temperature. To the same flask HgO (0.7 g, 3.3 mmol) and S (10 mg, 0.33 mmol) was added and the reaction mixture was refluxed at 85 ^{0}C for 2 h then filtered through Celite. The solvent was evaporated in *vacuo* to give an oil which was purified by column chromatography (petroleum ether - EtOAc 100:0 v/v increasing to 75:25 v/v) to give the product as a yellow solid. Yield: 0.4 g (77 %). t.l.c system: petroleum ether - EtOAc 2:1 v/ v R_F = 0.57.

^{1}H NMR: δ (DMSO-d_6): 5.71 (s, 1H, H-1''), 5.85 (s, 1H, OH), 7.15 (m, 1H, H-5''), 7.25 (m, 2H, H-2', H-6'), 7.34 (m, 2H, Ar), 7.41 (m, 4H, Ar), 7.49 (dd, J_1= 1.9 Hz, J_2= 7.8 Hz, 2H, H-3', C-5'), 7.72 (d, J= 8.4 Hz, 2H, H-5, C-8), 10.59 (s, 1H, NH).

^{13}C NMR: δ (DMSO-d_6): 73.92 (CH, C-1''), 108.87 (CH, C-5), 116.51 (CH, C-8), 117.39 (CH, C-2', C-6'), 121.54 (CH, C-6), 123.94 (CH, C-7), 126.17 (CH, C-3'', C-7''), 126.58 (CH, C-5''), 126.87 (CH, C-4'', C-6''), 127.99 (CH, C-3', C-5'), 137.31 (C, C-4'), 139.59 (C, C-9), 142.44 (C, C-2''), 145.84 (C, C-1'), 147.00 (C, C-4), 158.04 (C, C-2).

Microanalysis: Calculated for $C_{20}H_{16}N_2O_2$. 1.6H_2O (345.166); Theoretical: %C= 69.59, %H= 4.67, %N= 8.12; Found: %C= 69.83, %H= 4.86, %N= 8.07.

HRMS (EI): Calculated mass: 317.1285 $(M+H)^+$, Measured mass : 317.1287 $(M+H)^+$.

Melting point: 160-162^{0}C

[4-(1*H*-Benzoimidazol-2-ylamino)-phenyl]-phenylmethanol (32)

($C_{20}H_{16}N_3O$, M.W. 314.366)

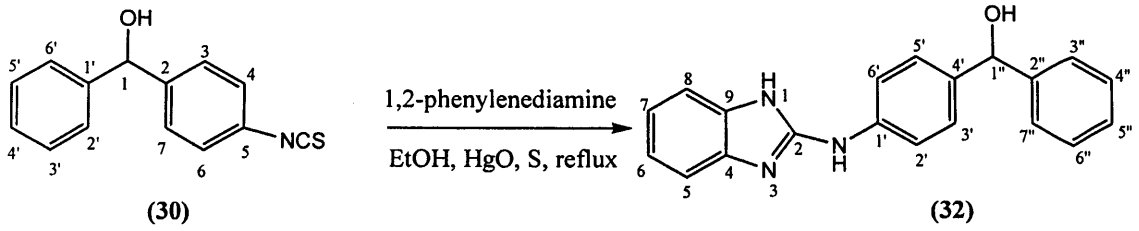

(30) (32)

1,2-phenylenediamine (0.18 g, 1.66 mmol) was added to a solution of (**30**) (0.4 g, 1.66 mmol) in absolute EtOH (10 mL). The mixture was then stirred overnight at room temperature. To the same flask HgO (0.7 g, 3.3 mmol) and S (10 mg, 0.33 mmol) was added and the reaction mixture was refluxed at 85 ^{0}C for 2 h then filtered through Celite. The solvent was evaporated in *vacuo* to give an oil which was purified by column chromatography (CH_2Cl_2 - MeOH 100:0 v/v increasing to 95:5 v/v) to give the product as a yellowish white solid. Yield: 0.42 g (81 %). t.l.c system: CH_2Cl_2 - MeOH 95:5 v/v, R_F = 0.54.

^{1}H NMR: δ (DMSO-d_6): 5.67 (s, 1H, H-1''), 5.78 (s, 1H, OH), 6.98 (s, 2H, Ar), 7.18 (m, 1H, H-5''), 7.29 (m, 6H, Ar), 7.38 (d, J= 7.4 Hz, 2H, H-3', H-5'), 7.66 (d, J= 8.3 Hz, 2H, H-5, C-8), 9.41 (s, 1H, NH), 10.87 (s, 1H, NH).

^{13}C NMR: δ (DMSO-d_6): 76.73 (CH, C-1''), 113.65 (CH, C-5''), 119.54 (CH, C-5, C-8), 122.05 (CH, C-2', C-6'), 127.71 (CH, C-6, C-7), 128.20 (CH, C-3'', C-7''), 129.08 (CH, C-4'', C-6''), 129.54 (CH, C-3', C-5'), 138.78 (C, C-4'), 139.97 (C, C-4, C-9), 140.66 (C, C-2), 146.06 (C, C-1'), 152.81 (C, C-2'').

Microanalysis: Calculated for $C_{20}H_{16}N_3O$. $0.7H_2O$ (326.973); Theoretical: %C= 73.47, %H= 5.36, %N= 12.85; Found: %C= 73.36, %H= 5.35, %N= 12.63.

Melting point: 190-192 ^{0}C

[4-(Benzothiazol-2-ylamino)-phenyl]-phenylmethanol (33)

($C_{20}H_{16}N_2OS$, M.W. 332.414)

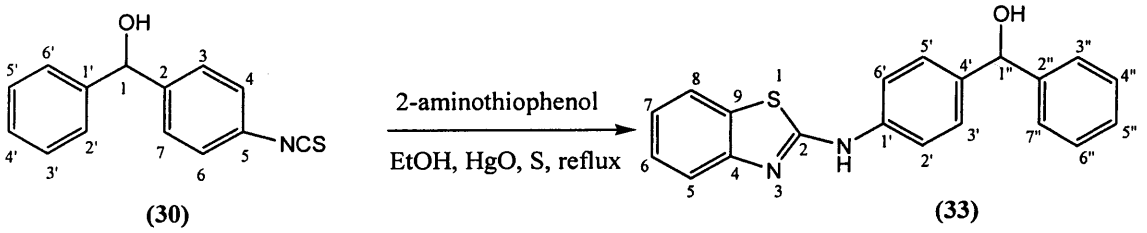

(30) (33)

2-aminothiophenol (0.18 mL, 1.66 mmol) was added to a solution of (**30**) (0.4 g, 1.66 mmol) in absolute EtOH (10 mL). The mixture was then stirred overnight at

room temperature. To the same flask HgO (0.7 g, 3.3 mmol) and S (10 mg, 0.33 mmol) was added and the reaction mixture was refluxed at 85 ^{0}C for 2 h then filtered through Celite. The solvent was evaporated in *vacuo* to give an oil which was purified by column chromatography (CH_2Cl_2 - MeOH 100:0 v/v increasing to 95:5 v/v) to give the product as a greyish white solid. Yield: 0.45 g (82 %). t.l.c system: CH_2Cl_2 - MeOH 95:5 v/v, R_F = 0.54.

^{1}H NMR: δ (DMSO-d_6): 5.68 (s, 1H, H-1''), 5.81 (s, 1H, OH), 7.15 (m, 1H, Ar), 7.21 (m, 1H, Ar), 7.35 (m, 7H, Ar), 7.58 (d, J= 7.9 Hz, 1H, Ar), 7.70 (d, J= 8.3 Hz, 2H, H-3', C-5'), 7.79 (d, J= 7.7 Hz, 2H, H-5, C-8), 10.51 (s, 1H, NH).

^{13}C NMR: δ (DMSO-d_6): 73.94 (CH, C-1''), 117.65 (CH, C-2', C-6'), 119.10 (CH, C-5), 120.98 (CH, C-8), 122.14 (CH, C-6), 125.80 (CH, C-7), 126.16 (CH, C-3'', C-7''), 126.57 (CH, C-5''), 126.88 (CH, C-4'', C-6''), 127.99 (CH, C-3', C-5'), 129.96 (C, C-9), 139.25 (C, C-4'), 139.54 (C, C-1'), 145.85 (C, C-2''), 152.10 (C, C-4), 161.64 (C, C-2).

Microanalysis: Calculated for $C_{20}H_{16}N_2OS$. $0.4H_2O$ (339.618); Theoretical: %C= 70.73, %H= 4.99, %N= 8.24; Found: %C= 70.87, %H= 5.08, %N= 7.84.

Melting point: 138-140 ^{0}C

Benzooxazol-2-yl-{4-[(5*H*-imidazol-1-yl)-phenylmethyl]-phenyl}-amine (34)

($C_{23}H_{18}N_4O$, M.W. 366.417)

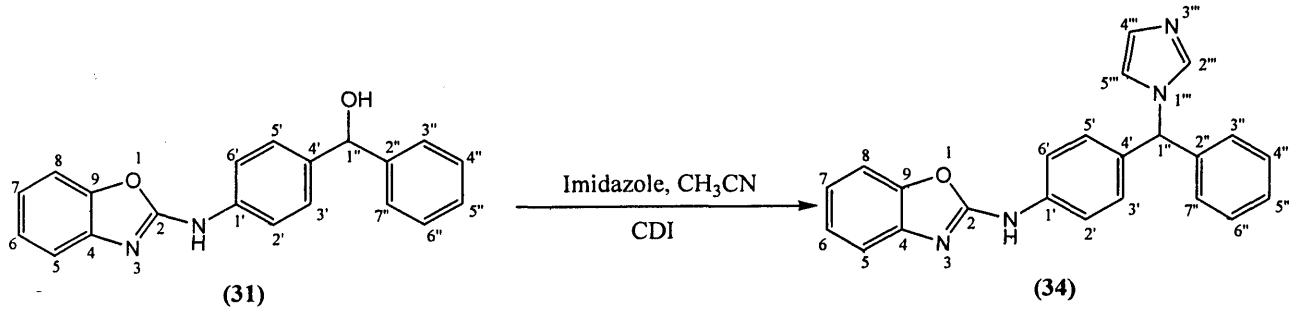

(31) (34)

To a solution of (**31**) (0.23 g, 0.73 mmol) in anhydrous CH_3CN (20 mL) was added imidazole (0.15 g, 2.19 mmmol) and CDI (0.18 g, 1.1 mmol). The mixture was then heated at 85 ^{0}C for 1 h. The reaction mixture was allowed to cool and then extracted with EtOAc (150 mL) and H_2O (3 x 100 mL). The organic layer was dried with $MgSO_4$, filtered and reduced *in vacuo*. The product was then purified by flash column chromatography (petroleum ether – EtOAc 80:20 v/v increasing to 0:100 v/v)

to give benzooxazol-2-yl-{4-[(5*H*-imidazol-1-yl)-phenylmethyl]-phenyl}-amine (**34**) as a yellow solid. Yield 0.19 g (71 %), t. l. c. system: EtOAc 100%, R_F: 0.37, stain positive.

^{1}H NMR: δ (DMSO-d_6): 6.84 (s, 1H, H-1''), 6.98 (s, 1H, Ar), 7.14 (m, 4H, Ar), 7.21 (m, 3H, Ar), 7.35 (m, 1H, H-5''), 7.39 (m, 3H, Ar), 7.49 (d, J= 7.9 Hz, 1H, H-4'''), 7.66 (s, 1H, H-2'''), 7.77 (d, J= 8.0 Hz, 2H, H-5, H-8), 10.78 (s, 1H, NH).

^{13}C NMR: δ (DMSO-d_6): 62.99 (CH, C-1''), 108.97 (CH, C-8), 116.64 (CH, C-5), 117.75 (CH, C-2', C-6'), 119.15 (CH, C-6), 121.74 (CH, C-7), 124.01 (CH, C-5''), 127.54 (CH, C-3'', C-7''), 127.81 (CH, C-5'''), 128.65 (CH, C-4'', C-6'', C-3', C-5'), 128.74 (CH, C-2'', C-4''), 133.39 (C, C-4'), 138.44 (C, C-4), 140.27 (C, C-2''), 142.29 (C, C-1'), 147.00 (C, C-9), 157.86 (C, C-2).

Microanalysis: Calculated for $C_{23}H_{18}N_4O$. $0.4H_2O$ (373.621); Theoretical: %C= 74.00, %H= 5.07, %N= 14.99; Found: %C= 74.03, %H= 5.11, %N= 14.54.

HRMS (EI): Calculated mass: 367.1553 $(M+H)^+$, Measured mass : 367.1555 $(M+H)^+$.

Melting point: 214-216 ^{0}C

(1*H*-benzoimidazol-2-yl)-{4-[(5H-imidazol-1-yl)-phenylmethyl]-phenyl}-amine (35)

($C_{23}H_{19}N_5$, M.W. 365.438)

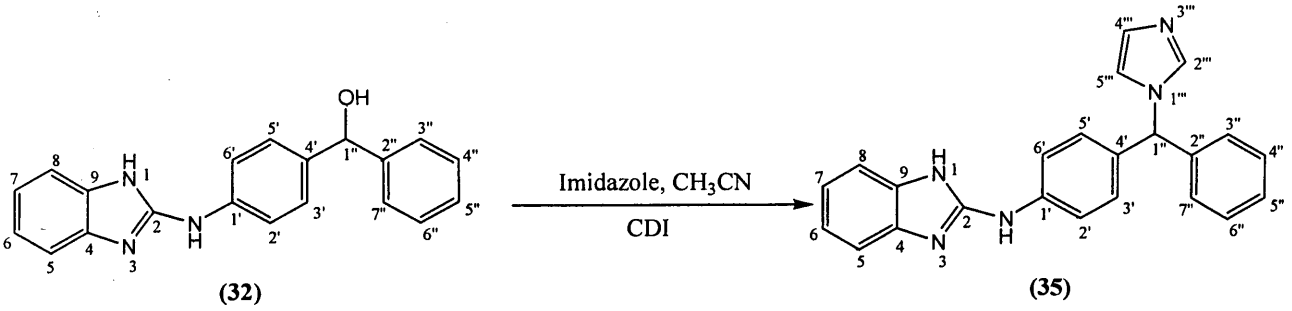

(**32**) (**35**)

To a solution of (**32**) (0.32 g, 1.02 mmol) in anhydrous CH_3CN (20 mL) was added imidazole (0.21 g, 3.06 mmmol) and CDI (0.25 g, 1.53 mmol). The mixture was then heated at 85 ^{0}C for 1 h. The reaction mixture was allowed to cool and then extracted with EtOAc (150 mL) and H_2O (3 x 100 mL). The organic layer was dried with $MgSO_4$, filtered and reduced *in vacuo*. The product was then purified by flash

column chromatography (CH_2Cl_2 – MeOH 100:0 v/v increasing to 95:5 v/v) to give (**35**) as a yellowish white solid. Yield 0.28 g (76 %), t. l. c. system: CH_2Cl_2 - MeOH 95:5 v/v, R_F: 0.17, stain positive.

^{1}H NMR: δ (DMSO-d_6): 6.80 (s, 1H, H-1''), 6.99 (m, 3H, Ar), 7.13 (m, 5H, Ar), 7.35 (m, 5H, Ar), 7.6 (s, 1H, H-2'''), 7.78 (d, J= 7.4 Hz, 2H, H-5, H-8), 9.54 (s, 1H, NH), 10.68 (s, 1H, NH).

^{13}C NMR: δ (DMSO-d_6): 63.13 (CH, C-1''), 117.14 (CH, C-5, C-8), 119.18 (CH, C-5''), 120.08 (CH, C-6, C-7), 127.48 (CH, C-3'', C-7''), 127.73 (CH, C-5'''), 128.51 (CH, C-3', C-5', C-4'', C-6''), 128.78 (CH, C-2''', C-4'''), 131.58 (C, C-4'), 140.48 (C, C-4, C-9), 140.66 (C, C-2), 150.35 (C, C-1', C-2'').

HRMS (EI): Calculated mass: 366.1713 $(M+H)^+$, Measured mass : 366.1715 $(M+H)^+$.

Melting point: 274-276 ^{0}C

Benzothiazol-2-yl-{4-[(5*H*-imidazol-1-yl)-phenylmethyl]-phenyl}-amine (36)

($C_{23}H_{18}N_4S$, M.W. 382.483)

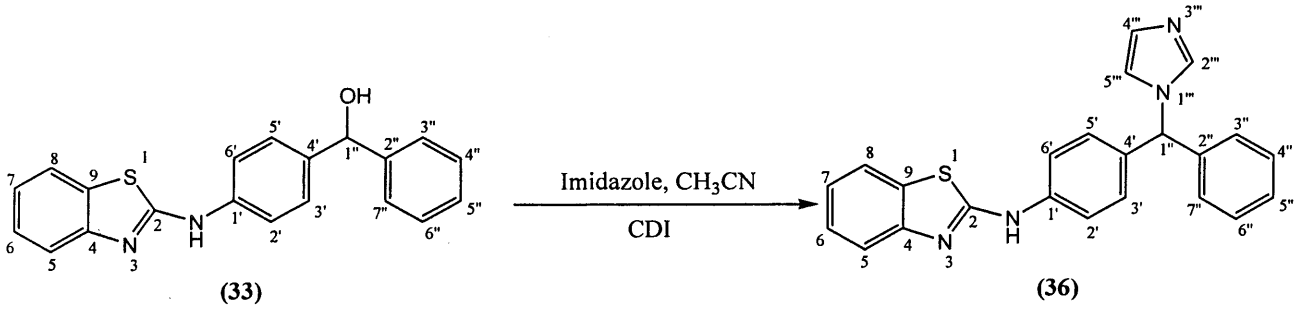

(**33**) (**36**)

To a solution of (**33**) (0.35 g, 1.05 mmol) in anhydrous CH_3CN (20 mL) was added imidazole (0.22 g, 3.16 mmmol) and CDI (0.26 g, 1.58 mmol). The mixture was then heated at 85 ^{0}C for 1 h. The reaction mixture was allowed to cool and the precipitate that formed was filtered washed with hot CH_3CN (2 x 5 mL) and dried to give (**36**) as a yellowish white solid. Yield 0.29 g (73 %), t. l. c. system: EtOAc 100%, R_F: 0.26, stain positive.

^{1}H NMR: δ (DMSO-d_6): 6.83 (s, 1H, H-1''), 6.97 (s, 1H, Ar), 7.15 (m, 6H, Ar), 7.34 (m, 2H, Ar), 7.40 (m, 2H, Ar), 7.59 (d, J= 7.9 Hz, 1H, H-4'''), 7.65 (s, 1H, H-2'''), 7.80 (m, 3H, Ar), 10.59 (s, 1H, NH).

^{13}C NMR: δ (DMSO-d_6): 63.01 (CH, C-1''), 117.88 (CH, C-2', C-6'), 119.15 (CH, C-5), 119.25 (CH, C-8), 121.05 (CH, C-6), 122.34 (CH, C-7), 125.86 (CH, C-5''), 127.56 (CH, C-3'', C-7''), 127.81 (CH, C-5'''), 127.99 (CH, C-4'', C-6''), 128.62 (CH, C-3', C-5'), 128.71 (CH, C-2''', C-5'''), 130.02 (C, C-9), 133.21 (C, C-4'), 137.14 (C, C-2''), 140.29 (C, C-1'), 151.96 (C, C-4), 161.43 (C, C-2).

Microanalysis: Calculated for $C_{23}H_{18}N_4S$. $0.3H_2O$ (387.886); Theoretical: %C= 71.22, %H= 4.68, %N= 14.44; Found: %C= 71.01, %H= 4.73, %N= 14.18.

Melting point: 258-260 ^{0}C

5.2 Synthesis of *N*-aryl and heteroaryl substituted 3-(4-aminophenyl)-3-imidazol-1-yl-2,2-dimethylpropionic acid methyl ester

5.2.1 General chemistry

The synthesis of *N*-aryl and heteroaryl substituted 3-(4-aminophenyl)-3-imidazol-1-yl-2,2-dimethylpropionic acid methyl ester was carried out according to a sequence of 4 steps (**Scheme 5.12**):

- Synthesis of 3-hydroxy-2,2-dimethyl-3-(4-nitrophenyl)-propionic acid methyl ester
- The reduction of the nitro group
- The formation of the aryl and heteroaryl amine derivatives
- The addition of the imidazole ring

5.2.1.1 Synthesis of 3-hydroxy-2,2-dimethyl-3-(4-nitrophenyl)-propionic acid methyl ester

The synthesis of 3-hydroxy-2,2-dimethyl-3-(4-nitrophenyl)-propionic acid methyl ester was performed using a Mukaiyama aldol type reaction (Hagiwara *et al.*, 2005). This reaction invented by Mukaiyama is an aldol reaction that utilises a stable metal enolate such as trimethyl silyl enolate and a Lewis acid such as titanium

chloride to activate the carbonyl compound (Sato *et al.*, 1989). This reaction overcame the drawbacks of the classical aldol reaction including reversibility and difficulty in generating an enol or enolate quantitatively to react with the keto component. However there are several limitations in choosing substrates due to presence of a strong Lewis acid such as titanium chloride. Subsequently, Denmark *et al.* used another concept which is activation of the silicon atom of the trimethyl silyl enolate by using a Lewis base to form a hypervalent silicate intermediate (Denmark *et al.*, 1996; Hagiwara *et al.*, 2005; Hagiwara *et al.*, 2006). The synthesis of 3-hydroxy-2,2-dimethyl-3-(4-nitro-phenyl)-propionic acid methyl ester involved the reaction of trimethylsilyl ketene acetal with 4-nitrobenzaldehyde in the presence of a catalytic amount of pyridine *N*-oxide and LiCl. This reaction used trimethylsilyl enolate in which the trimethylsilyl group is thought to activate the enol and trap the aldol hydroxyl. In this reaction, pyridine *N*-oxide acts as the Lewis base that activates the silyl enolate while LiCl and pyridine *N*-oxide might operate synergistically to drive the catalytic cycle (Hagiwara *et al.*, 2005). The mechanism of the reaction involved coordination of the Lewis base pyridine *N*-oxide to the silicon atom of the silylketene acetal to form a penta-coordinated hypervalent silicate intermediate, addition of the aldehyde proceeded to provide a hypervalent alkoxysilicate intermediate, from which pyridine *N*-oxide was pushed out by LiCl and re-used in the catalytic cycle (Hagiwara *et al.*, 2005; Nakagawa *et al.*, 2003; Denmark *et al.*, 1996; Sato *et al.*, 1989) (**Figure 5.3**).

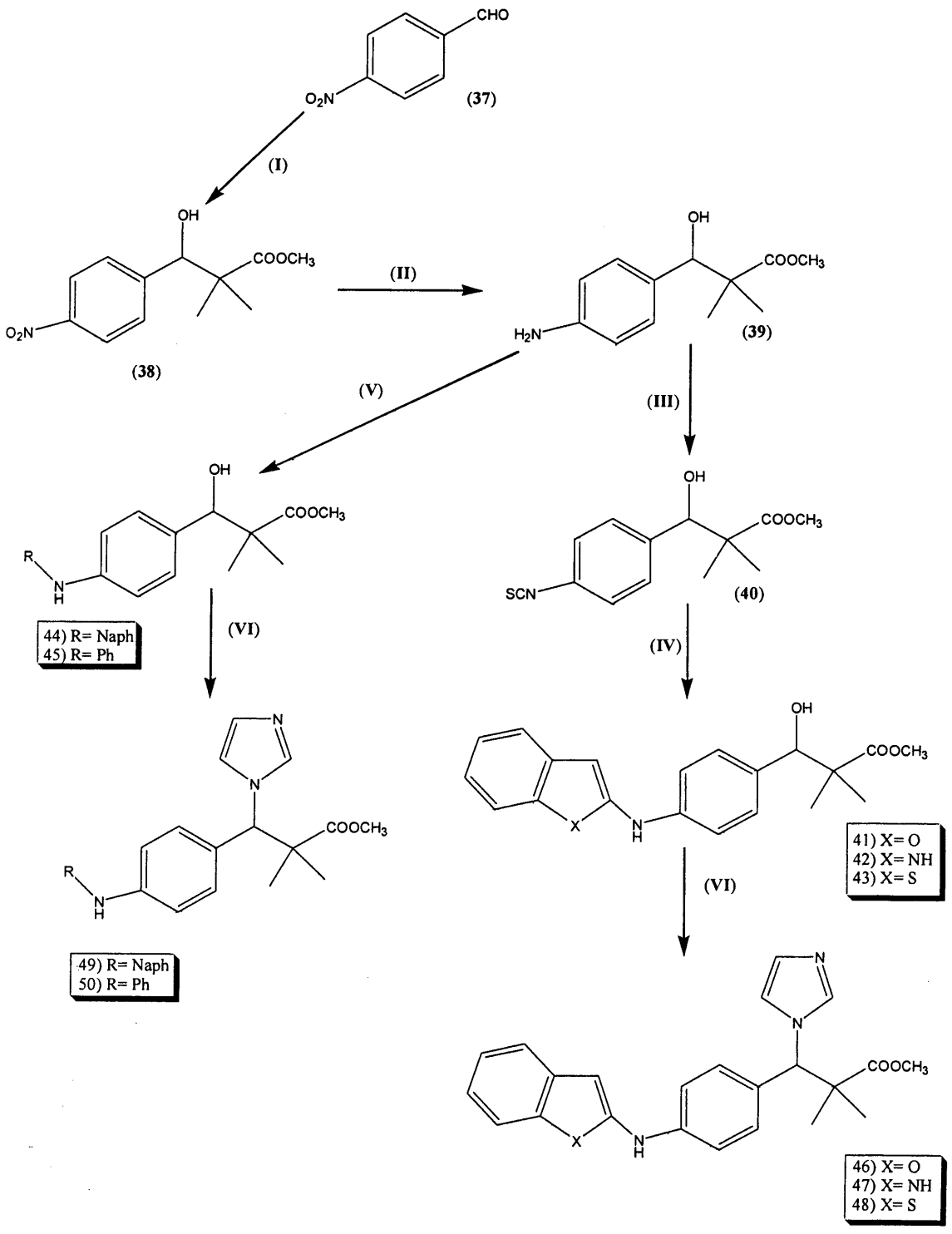

Scheme 5.12: General reaction scheme for the synthesis of *N*-substituted 3-(4-amino-phenyl)-3-imidazol-1-yl-2,2-dimethyl-propionic acid methyl ester Reagents and conditions: (I) trimethylsilyl ketene acetal, LiCl, pyridine *N*-oxide, r.t., 24 h (II) H_2, 1 psi, EtOH. (III) thiophosgene, ice, H_2O, CH_2Cl_2, r.t., overnight (IV) (i) 2-aminophenol, 1,2-phenylenediamine, 2-aminothiophenol for X= O and NH and S respectively, EtOH, r.t., 24 h (ii) HgO, S, EtOH, reflux at 85°C, 2 h (V) naphthyl boronic acid or phenyl boronic acid, $CuII(OAc)_2$, CH_2Cl_2, pyridine, r.t.,

2

days (VI) imidazole, CDI, CH_3CN, reflux.

The reaction was performed in DMF and after stirring overnight at room temperature, the pure product was separated in 69 % yield after purification by flash column chromatography.

Other aldol type reactions (Xu and Yuan, 2005) have been found unsatisfactory in the preparation of 3-hydroxy-2,2-dimethyl-3-(4-nitro-phenyl)-propionic acid methyl ester including classical Reformatsky reaction that used zinc catalyst (Overberger and Bonsignore, 1958) and other methods that utilise highly activated metals such as $CrCl_2$ (Wessjohann and Gabriel, 1997).

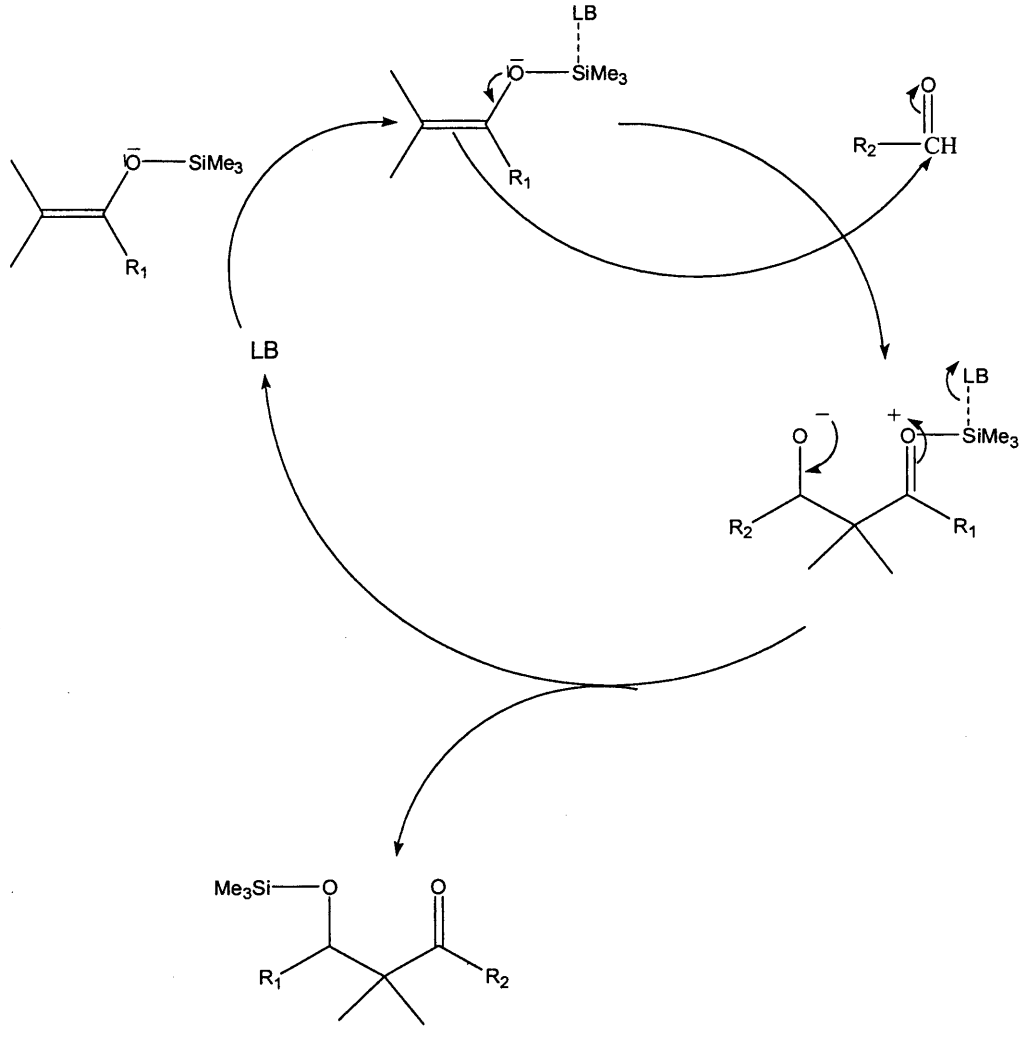

Figure 5.3: Proposed mechanism of the aldol type reaction, LB is Lewis base (pyridine *N*-oxide), R_1 is OCH_3, R_2 is 4-nitrophenyl.

5.2.1.2 Selective reduction of the nitro group

The selective reduction of the nitro group into amino was carried out using a mild hydrogenation method (Mateus *et al.*, 2000). The reduction was performed in a fume cupboard and using a H_2 balloon rather than a hydrogenator. The pressure is reduced thereby from 20-30 psi to 1-3 psi. A complete and selective reduction of the nitro group was observed after 30 min stirring in EtOH at room temperature. The product was obtained in 87% yield without the need for purification by column chromatography.

5.2.1.3 Synthesis of *N*-aryl and heteroaryl substituted derivatives

5.2.1.3.1 Synthesis of *N*-heteroaryl substituted derivatives

5.2.1.3.1.1 Synthesis of the isothiocyanate

This was performed using thiophosgene as previously described in section 4.1.2.1.2. Thiophosgene was added to a mixture of 3-(4-amino-phenyl)-3-hydroxy-2-methyl-propionic acid methyl ester, CH_2Cl_2, ice and H_2O. The reaction was complete after stirring overnight at 0 ^{0}C. The product was obtained with 71 % yield without the need for purification by flash column chromatography.

5.2.1.3.1.2 Synthesis of the *N*-2-benzoheterocycle substituted derivatives

The method previously described in section 4.1.2.1.3 was used in the preparation of the 2-substituted aminobenoxazole (**41**), benzimidazole (**42**) and benzothiazole (**43**) (**Scheme 5.13**). The products were obtained in good yield after purification by flash column chromatography.

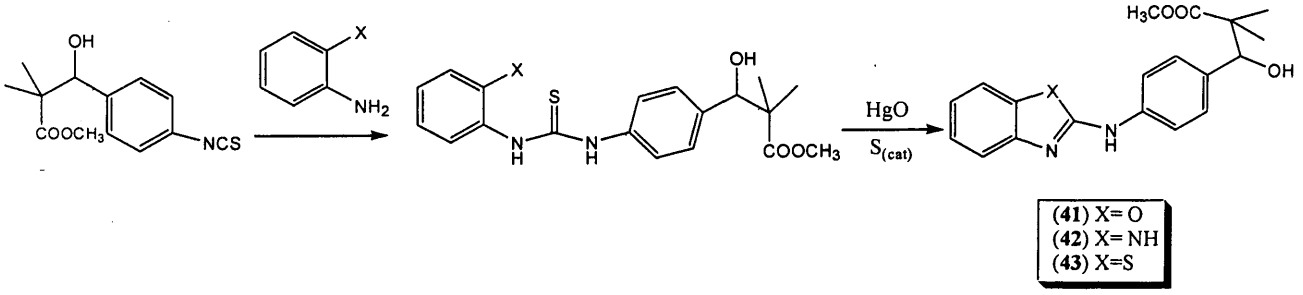

Scheme 5.13: Scheme for synthesis of the *N*-2-benzoheterocycle substituted derivatives.

The products were confirmed by the appearence of the NH peak at approximately 10.5 ppm and the OH peak that has been shifted to approximately 5.7

ppm in ^{1}H NMR. The ^{13}C NMR confirmed the presence of the characteristic benzoheterocycle quaternary carbon at about 157 ppm. A summary of the results is presented in **Table 5.7**.

Table 5.7: Summary of the synthesis of compounds (**41**) - (**43**).

Product	Yield (%)	Melting point (^{0}C)
41	87	164-166
42	83	210-212
43	84	156-158

5.2.1.3.2 Synthesis of *N*-aryl substituted derivatives

The synthesis of *N*-substituted aryl derivatives was carried out using a Suzuki coupling reaction as previously described in section 4.1.1.1.1 (**Scheme 5.12**). The products (**44**) and (**45**) were obtained in a good yield of 82 % and 79 % for naphthyl and phenyl respectively after purification by flash column chromatography.

5.2.1.4 Addition of the imidazole ring

The same method described earlier in section (5.1.1.1.4) was applied to the *N*-heteroaryl and aryl substituted derivatives (**Scheme 5.12**). The products (**46-50**) have been obtained in moderate yield after refluxing and purification by flash column chromatography. The summary of the results is presented in **Table 5.8**.

Table 5.8: Summary of the synthesis of compounds (**46**) - (**50**).

Product	Yield (%)	Time (h)	Melting point (^{0}C)
46	47	2	158-160
47	56	1	-
48	44	2	-
49	54	24	190-192
50	44	2	-

5.2.2 Experimental

3-Hydroxy-2,2-dimethyl-3-(4-nitrophenyl)-propionic acid methyl ester (38)

($C_{12}H_{15}NO_5$, M.W. 253.228)

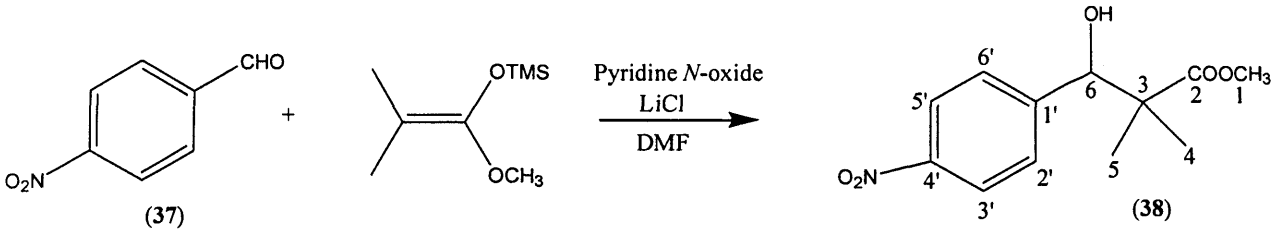

(37) (38)

To an anhydrous stirred solution of pyridine *N*-oxide (0.19 g, 0.2 mmol) and LiCl (0.17 g, 0.4 mmol) in DMF (20 mL) were added 4-nitrobenzaldehyde (**37**) (3 g, 19.85 mmol) and trimethylsilyl ketene acetal (5.25 mL, 25.9 mmol) at r.t. under a N_2 atmosphere. After stirring overnight, the reaction was quenched by the addition of 1 N aq HCl (5 mL). The product was extracted with EtOAc (2 x 50 mL). The combined organic layer was washed with H_2O (50 mL), brine (50 mL) and evaporated to dryness. The product was then purified by flash column chromatography (petroleum ether - EtOAc 100:0 v/v increasing to 80:20 v/v) to give 3-hydroxy-2,2-dimethyl-3-(4-nitrophenyl)-propionic acid methyl ester (**38**) as a creamy white solid. Yield: 3.47 g (69 %), t. l. c. system: petroleum ether – EtOAc 3:1 v/v, R_F: 0.33.

^{1}H NMR: δ ($CDCl_3$): 1.15 (s, 3H, H-4), 1.16 (s, 3H, H-5), 3.42 (s, 1H, OH), 3.78 (s, 3H, H-1), 5.04 (s, 1H, H-6), 7.51 (d, J= 8.4 Hz, 2H, H-2', H-6'), 8.20 (d, J= 8.3 Hz, 2H, H-3', H-5').

^{13}C NMR: δ ($CDCl_3$): 19.23 (CH, C-4), 22.75 (CH, C-5), 47.67 (C, C-3), 52.36 (CH, C-1), 77.76 (CH, C-6), 122.93 (CH, C-3', C-5'), 128.59 (CH, C-2', C-6'), 147.30 (C, C-4'), 147.54 (C, C-1'), 177.73 (C, C-2).

Melting point: 188-192 ^{0}C

3-(4-aminophenyl)-3-hydroxy-2,2-dimethylpropionic acid methyl ester (39)

($C_{12}H_{17}NO_3$, M.W. 223.255)

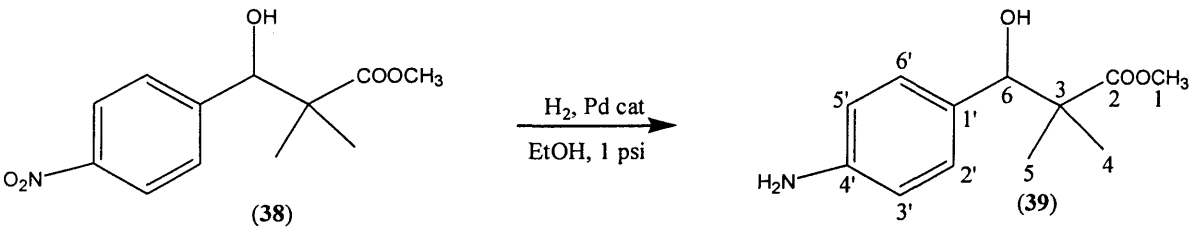

(38) (39)

Pd/C catalyst (100 mg) was added to a solution of (**38**) (1 g, 3.95 mmol) dissolved in EtOH (20 mL) and then the reaction was stirred under a H_2 atmosphere. After 30 min the hydrogen balloon was removed and the mixture was filtered through Celite. The solvent was then removed under reduced pressure and the oil formed was extracted with CH_2Cl_2 (100 mL), washed with H_2O (2 × 50 mL) and dried ($MgSO_4$), filtered and evaporated in *vacuo*. The product was then obtained without further purification to give 3-(4-aminophenyl)-3-hydroxy-2,2-dimethylpropionic acid methyl ester (**39**) as a yellow solid . Yield: 0.87 g (87 %). t.l.c system: petroleum ether - EtOAc 2:1 v/v, R_F = 0.31, stain positive.

^{1}H NMR: δ (DMSO-d_6): 0.90 (s, 3H, H-4), 1.02 (s, 3H, H-5), 3.58 (s, 3H, H-1), 4.65 (s, 1H, OH), 4.93 (s, 2H, NH_2), 5.17 (s, 1H, H-6), 6.50 (d, J= 7.9 Hz, 2H, H-3', H-5'), 6.92 (d, J= 7.8 Hz, 2H, H-2', H-6').

^{13}C NMR: δ (DMSO-d_6): 18.52 (CH, C-4), 19.41 (CH, C-5), 47.88 (C, C-3), 51.30 (CH, C-1), 76.82 (CH, C-6), 112.84 (CH, C-3', C-5'), 128.01 (CH, C-2', C-6'), 128.67 (C, C-1'), 147.61 (C, C-4'), 176.76 (C, C-2).

Microanalysis: Calculated for $C_{12}H_{17}NO_3$. $0.2H_2O$ (226.857); Theoretical: %C= 63.53, %H= 7.55, %N= 6.17; Found: %C= 63.38, %H= 7.75, %N= 5.97.

Melting point: 130-132^{0}C

3-Hydroxy-3-(4-isothiocyanatophenyl)-2,2-dimethylpropionic acid methyl ester (40)

($C_{13}H_{15}NO_3S$, M.W. 265.321)

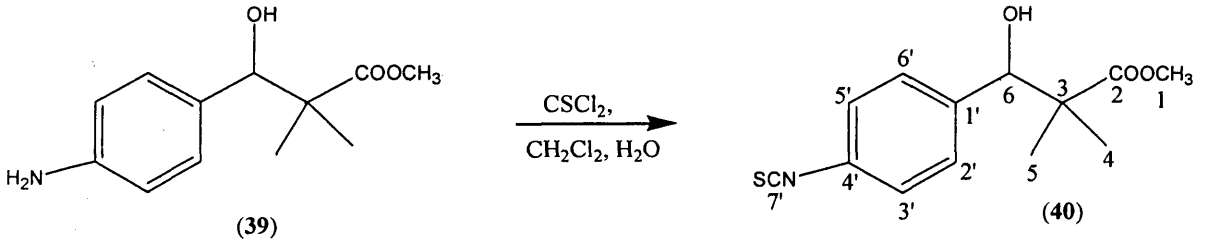

(**39**) (**40**)

To a solution of (**39**) (2.3 g, 10.3 mmol) in CH_2Cl_2 (20 mL) was added a mixture of ice (2 g) and H_2O (1 mL) and subsequently dropwise with vigorous stirring thiophosgene (0.92 mL, 12.07 mmol). The mixture was stirred for 2 h at 0 ^{0}C and kept overnight in a refrigerator. The organic layer was separated and extracted successively with H_2O (2 × 50 mL), 10 % $NaHCO_3$ aq. (50 mL) and H_2O again (50 mL), dried ($MgSO_4$) and evaporated to dryness to obtain the pure product 3-hydroxy-3-(4-

isothiocyanatophenyl)-2,2-dimethylpropionic acid methyl ester (**40**) as a yellow oil. Yield: 1.94 g, (71 %). t.l.c system: petroleum ether - EtOAc 2:1 v/v, R_F = 0.57.

^{1}H NMR: δ ($CDCl_3$): 1.01 (s, 1H, H-4), 1.04 (s, 1H, H-5), 3.21 (s, 1H, OH), 3.67 (s, 3H, H-1), 4.81 (s, 1H, H-6), 7.10 (d, J= 7.2 Hz, 2H, H-3', H-5'), 7.21 (d, J= 7.4 Hz, 2H, H-2', H-6').

^{13}C NMR: δ ($CDCl_3$): 19.15 (CH, C-4), 22.79 (CH, C-5), 47.71 (C, C-3), 52.22 (CH, C-6), 77.95 (CH, C-1), 125.07 (CH, C-3', C-5'), 128.84 (CH, C-2', C-6'), 130.63 (C, C-4'), 135.61 (C, C-1'), 139.38 (C, C-7'), 177.93 (C, C-2).

HRMS (EI): Calculated mass: 265.0767$(M)^+$, Measured mass : 265.0768$(M)^+$.

3-[4-(Benzooxazol-2-ylamino)-phenyl]-3-hydroxy-2,2-dimethylpropionic acid methyl ester (41)

($C_{19}H_{20}N_2O_4$, M.W. 340.357)

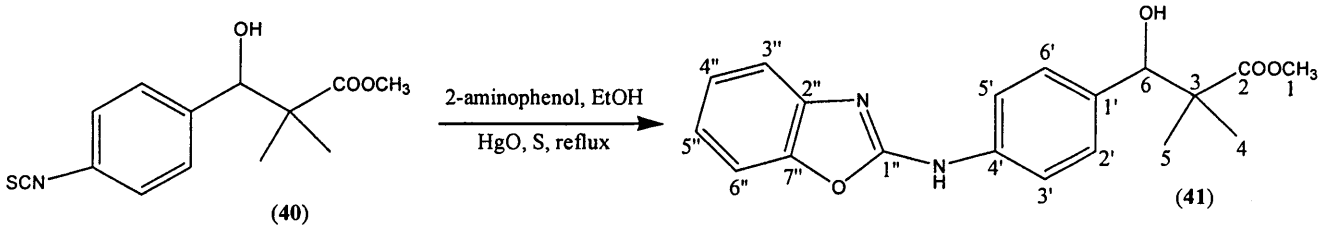

(40) (41)

2-Aminophenol (0.33 g, 3.02 mmol) was added to a solution of (**40**) (0.8 g, 3.02 mmol) in absolute EtOH (10 mL). The mixture was then stirred overnight at room temperature. To the same flask HgO (1.3 g, 6.0 mmol) and S (20 mg, 0.62 mmol) was added and the reaction mixture was refluxed at 85 ^{0}C for 2 h then filtered through Celite. The solvent was evaporated in *vacuo* to give an oil which was purified by column chromatography (petroleum ether - EtOAc 100:0 v/v increasing to 70:30 v/v) to give 3-[4-(benzooxazol-2-ylamino)-phenyl]-3-hydroxy-2,2-dimethylpropionic acid methyl ester (**41**) as a yellow solid. Yield: 0.89 g (87 %). t.l.c system: petroleum ether - EtOAc 1:1 v/v, R_F = 0.59, stain positive.

^{1}H NMR: δ (DMSO-d_6): 0.95 (s, 3H, H-4), 1.07 (s, 3H, H-5), 3.62 (s, 3H, H-1), 4.81 (s, 1H, H-6), 5.49 (s, 1H, OH), 7.13 (t, J= 7.7 Hz, 1H, H-3'), 7.22 (t, J= 7.6 Hz, 1H, H-5'), 7.28 (d, J= 8.2 Hz, 2H, H-2', H-6'), 7.47 (m, 2H, H-4", H-5"), 7.70 (d, J= 8.2 Hz, 2H, H-3", H-6"), 10.59 (s, 1H, NH).

^{13}C NMR: δ (DMSO-d_6): 19.59 (CH, C-4), 21.38 (CH, C-5), 47.84 (C, C-3), 51.44 (CH, C-1), 76.46 (CH, C-6), 108.89 (CH, C-6"), 116.53 (CH, C-3', C-5'), 121.57 (CH, C-3"), 123.95 (CH, C-4", C-5"), 127.99 (CH, C-2', C-6'), 135.46 (C, C-

1'), 137.64 (C, C-2"), 142.43 (C, C-4'), 146.99 (C, C-7"), 157.99 (C, C-1"), 176.49 (C, C-2).

Microanalysis: Calculated for $C_{19}H_{20}N_2O_4$. $0.2H_2O$ (343.959); Theoretical: %C= 66.35, %H= 5.86, %N= 8.14; Found: %C= 66.50, %H= 5.99, %N= 8.05.

Melting point: 164-166 ^{0}C

3-[4-(1*H*-Benzoimidazol-2-ylamino)-phenyl]-2,2-dimethylpropionic acid methyl ester (42)

($C_{19}H_{21}N_3O_3$, M.W. 339.378)

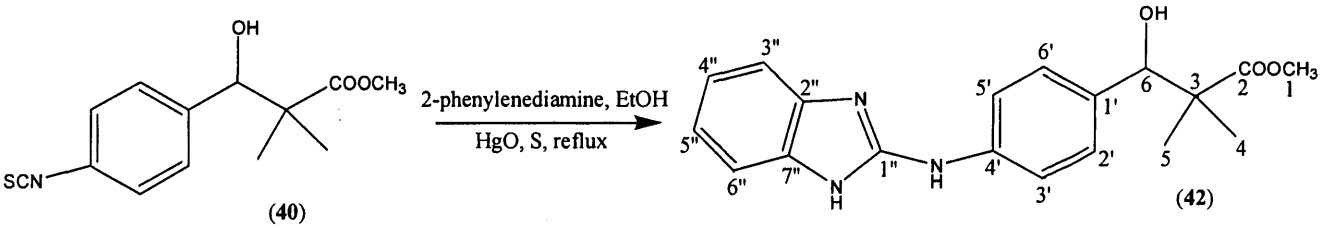

1,2-Phenylenediamine (0.32 g, 2.96 mmol) was added to a solution of (**40**) (0.8 g, 3.02 mmol) in absolute EtOH (10 mL). The mixture was then stirred overnight at room temperature. To the same flask HgO (1.3 g, 6.0 mmol) and S (20 mg, 0.62 mmol) was added and the reaction mixture was refluxed at 85 ^{0}C for 2 h then filtered through Celite. The solvent was evaporated in *vacuo* to give an oil which was purified by column chromatography (CH_2Cl_2 - MeOH 100:0 v/v increasing to 95:5 v/v) to give 3-[4-(1*H*-benzoimidazol-2-yl-amino)-phenyl]-2,2-dimethyl-propionic acid methyl ester (**42**) as a white solid. Yield: 0.85 g (83 %). t.l.c system: CH_2Cl_2 - MeOH 95:5 v/v, R_F = 0.47, stain positive.

^{1}H NMR: δ (DMSO-d_6): 0.97 (s, 3H, H-4), 1.08 (s, 3H, H-5), 3.67 (s, 3H, H-1), 4.79 (s, 1H, H-6), 5.48 (s, 1H, OH), 6.99 (m, 2H, H-3', H-5'), 7.22 (d, J= 8.1 Hz, 2H, H-2', C-6'), 7.31 (m, 2H, H-4", H-5"), 7.69 (d, J= 8.1 Hz, 2H, H-3", H-6"), 9.39 (s, 1H, NH-benzim), 10.59 (s, 1H, NH).

^{13}C NMR: δ (DMSO-d_6): 19.54 (CH, C-4), 21.48 (CH, C-5), 47.87 (C, C-3), 51.42 (CH, C-1), 76.59 (CH, C-6), 116.03 (CH, C-6", C-3', C-5'), 119.99 (CH, C-3"), 127.85 (CH, C-4", C-5", C-2', C-6'), 133.76 (C, C-1', C-2"), 139.82 (C, C-4', C-7"), 150.56 (C, C-1"), 176.60 (C, C-2).

Microanalysis: Calculated for $C_{19}H_{21}N_3O_3$. $0.3H_2O$ (344.781); Theoretical: %C= 66.19, %H= 6.14, %N= 12.19; Found: %C= 66.26, %H= 6.16, %N= 12.12.

Melting point: 210-212 ^{0}C

3-[4-(Benzothiazol-2-ylamino)-phenyl]-3-hydroxy-2,2-dimethylpropionic acid methyl ester (43)

($C_{19}H_{20}N_2O_3S$, M.W. 356.423)

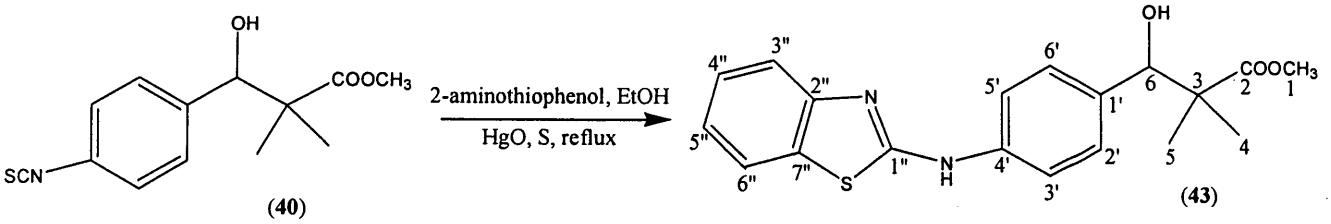

(40) (43)

2-Aminothiophenol (0.32 mL, 2.99 mmol) was added to a solution of (**40**) (0.8 g, 3.02 mmol) in absolute EtOH (10 mL). The mixture was then stirred overnight at room temperature. To the same flask HgO (1.3 g, 6.0 mmol) and S (20 mg, 0.62 mmol) was added and the reaction mixture was refluxed at 85 ^{0}C for 2 h then filtered through Celite. The solvent was evaporated in *vacuo* to give an oil which was purified by column chromatography (petroleum ether - EtOAc 100:0 v/v increasing to 70:30 v/v) to give **3-**[4-(benzothiazol-2-ylamino)-phenyl]-3-hydroxy-2,2-dimethyl-propionic acid methyl ester (**43**) as a yellow solid. Yield: 0.9 g (84 %). t.l.c system: petroleum ether - EtOAc 1:1 v/v, R_F = 0.51, stain positive.

^{1}H NMR: δ (DMSO-d_6): 0.95 (s, 3H, H-4), 1.07 (s, 3H, H-5), 3.63 (s, 3H, H-1), 4.82 (s, 1H, H-6), 5.51 (s, 1H, OH), 7.16 (t, J= 7.4 Hz, 1H, Ar), 7.27 (d, J= 8.0 Hz, 2H, H-2', H-6'), 7.33 (t, J= 7.5 Hz, 1H, Ar), 7.60 (d, J= 7.9 Hz, 1H, C-6"), 7.73 (d, J= 8.0 Hz, 2H, H-4", H-5"), 7.80 (d, J= 7.7 Hz, 1H, C-3"), 10.48 (s, 1H, NH).

^{13}C NMR: δ (DMSO-d_6): 19.52 (CH, C-4), 21.48 (CH, C-5), 47.84 (C, C-3), 51.45 (CH, C-1), 76.50 (CH, C-6), 116.78 (CH, C-3', C-5'), 119.13 (CH, C-3"), 120.99 (CH, C-6"), 122.18 (CH, C-4"), 125.82 (CH, C-5"), 128.02 (CH, C-2', C-6'), 129.96 (C, C-7"), 135.36 (C, C-1'), 139.59 (C, C-4'), 152.11 (C, C-2"), 161.55 (C, C-1"), 176.51 (C, C-2).

Microanalysis: Calculated for $C_{19}H_{20}N_2O_3S$. $0.1H_2O$ (358.224); Theoretical: %C= 63.71, %H= 5.63, %N= 7.82; Found: %C= 63.61, %H= 5.74, %N= 7.57.

Melting point: 156-158 ^{0}C

3-Hydroxy-2,2-dimethyl-3-[4-(naphthalen-2-ylamino)-phenyl]-propionic acid methyl ester (44)

($C_{22}H_{23}NO_3$, M.W. 349.413)

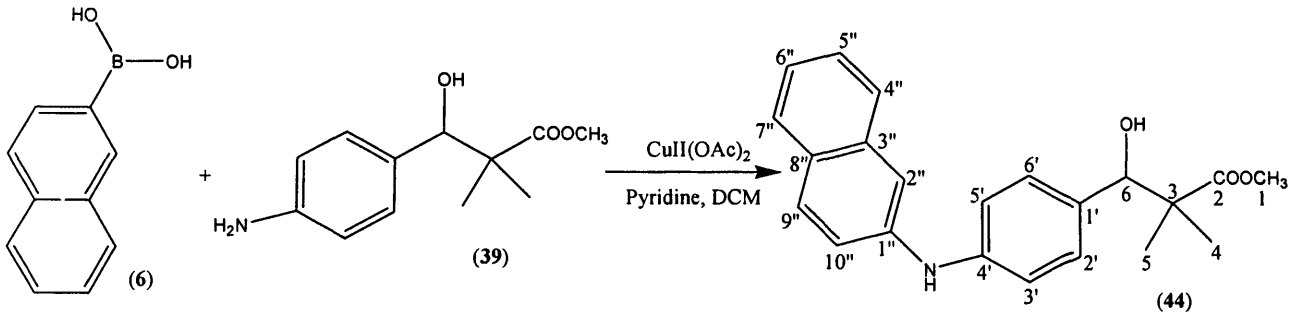

To naphthylboronic acid (**6**) (0.69 g, 4.01 mmol), (**39**) (0.5 g, 2.24 mmol), anhydrous $CuII(OAc)_2$ (0.54 g, 2.97 mmol), pyridine (0.32 mL, 3.96 mmol) and 250 mg activated 4 Å molecular sieves under an atmosphere of air was added CH_2Cl_2 (15 mL) and the reaction stirred under air atmosphere at ambient temperature for 2 days. The product was isolated by direct flash column chromatography of the crude reaction mixture (petroleum ether - EtOAc 70:30 v/v) to give 3-hydroxy-2,2-dimethyl-3-[4-(naphthalen-2-ylamino)-phenyl]-propionic acid methyl ester (**44**) as a yellowish brown oil. Yield: 0.64 g (82%), t. l. c. system: petroleum ether – EtOAc 2:1 v/v, R_F: 0.59, stain positive.

^{1}H NMR: δ ($CDCl_3$): 1.18 (s, 3H, H-4), 1.22 (s, 3H, H-5), 3.15 (s, 1H, OH), 3.76 (s, 3H, H-1), 4.90 (s, 1H, H-6), 5.98 (s, 1H, NH), 7.13 (d, J= 7.5 Hz, 2H, H-3', H-5'), 7.23 (s, 1H, H-2"), 7.26 (d, J= 8.5 Hz, 2H, H-2', H-6'), 7.33 (t, J= 7.2 Hz, 1H, H-6"), 7.44 (m, 2H, H-5", H-10"), 7.67 (d, J= 8.2 Hz, 1H, H-4"), 7.77 (d, J= 8.3 Hz, 2H, H-7", H-9").

^{13}C NMR: δ ($CDCl_3$): 19.18 (CH, C-4), 23.05 (CH, C-5), 47.91 (C, C-3), 52.10 (CH, C-1), 78.52 (CH, C-6), 111.80 (CH, C-2"), 117.27 (CH, C-3', C-5', C-10"), 120.11 (CH, C-6"), 123.56 (CH, C-4"), 12.51 (CH, C-5"), 127.75 (CH, C-7"), 128.73 (CH, C-9"), 129.19 (CH, C-2', C-6'), 129.25 (C, C-8"), 132.79 (C, C-1'), 134.63 (C, C-3"), 140.71 (C, C-4'), 142.60 (C, C-1"), 178.30 (C, C-2).

HRMS (EI): Calculated mass: 372.1570 $(M+Na)^+$, Measured mass : 372.1568 $(M+Na)^+$.

3-Hydroxy-2,2-dimethyl-3-(4-phenylaminophenyl)-propionic acid methyl ester (45)

($C_{18}H_{21}NO_3$, M.W. 299.353)

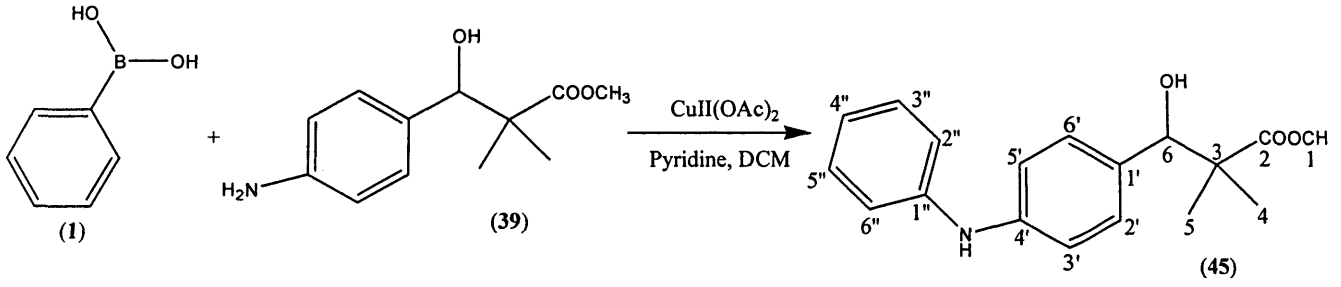

To phenylboronic acid (**1**) (0.55 g, 4.51 mmol), (**39**) (0.5 g, 2.24 mmol), anhydrous $CuII(OAc)_2$ (0.61 g, 3.36 mmol), pyridine (0.36 mL, 4.45 mmol) and 250 mg activated 4Å molecular sieves under an atmosphere of air was added CH_2Cl_2 (15 mL) and the reaction stirred under air atmosphere at ambient temperature for 2 days. The product was isolated by direct flash column chromatography of the crude reaction mixture (petroleum ether - EtOAc 70:30 v/v) to give 3-hydroxy-2,2-dimethyl-3-(4-phenylaminophenyl)-propionic acid methyl ester (**45**) as a light brown oil. Yield: 0.53 g (79 %), t. l. c. system: petroleum ether – EtOAc 2:1 v/v, R_F: 0.53, stain positive.

^{1}H NMR: δ ($CDCl_3$): 1.17 (s, 3H, H-4), 1.22 (s, 3H, H-5), 3.21 (s, 1H, OH), 3.75 (s, 3H, H-1), 4.86 (s, 1H, H-6), 5.91 (s, 1H, NH), 6.96 (t, J= 7.2 Hz, 1H, H-4"), 7.03 (d, J= 7.8 Hz, 2H, H-3', H-5'), 7.09 (d, J= 7.9 Hz, 2H, H-2", H-6"), 7.21 (d, J= 7.8 Hz, 2H, H-2', H-6'), 7.29 (t, J= 7.4 Hz, 2H, H-3", H-5").

^{13}C NMR: δ ($CDCl_3$): 19.19 (CH, C-4), 22.95 (CH, C-5), 47.96 (C, C-3), 52.08 (CH, C-1), 78.48 (CH, C-6), 116.56 (CH, C-3', C-5'), 117.95 (CH, C-2", C-6"), 121.04 (CH, C-4"), 128.84 (CH, C-3", C-5"), 129.56 (CH, C-2', C-6'), 132.39 (C, C-1'), 143.06 (C, C-4'), 143.25 (C, C-1"), 178.29 (C, C-2).

HRMS (EI): Calculated mass: 299.1516 $(M)^+$, Measured mass : 299.1521 $(M)^+$.

3-[4-(Benzooxazol-2-ylamino)-phenyl]-3-imidazol-1-yl-2,2-dimethylpropionic acid methyl ester (46)

($C_{22}H_{22}N_4O_3$, M.W. 390.426)

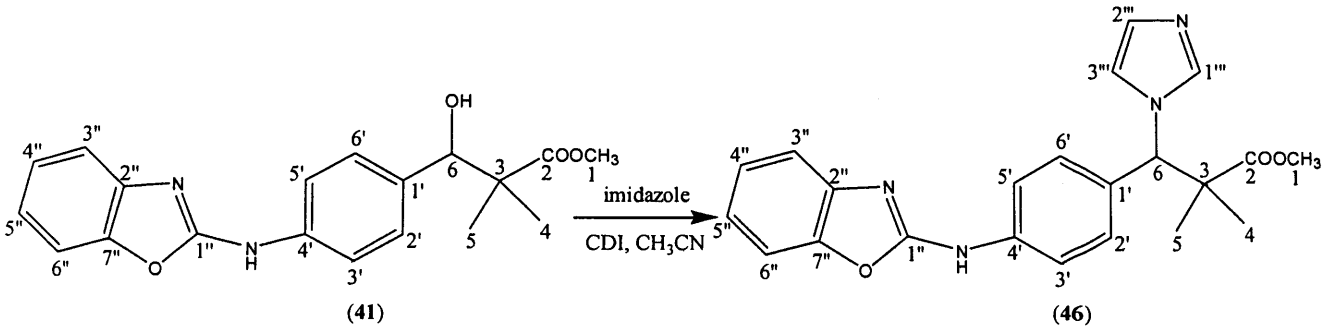

(41) (46)

To a solution of (**41**) (0.35 g, 1.03 mmol) in anhydrous CH_3CN (20 mL) was added imidazole (0.21 g, 3.09 mmol) and CDI (0.25 g, 1.55 mmol). The mixture was then heated under reflux for 2 h. The reaction mixture was allowed to cool and then extracted with EtOAc (150 mL) and H_2O (3 x 100 mL). The organic layer was dried with $MgSO_4$, filtered and reduced *in vacuo*. The product was purified by flash column chromatography (EtOAc) to give 3-[4-(benzooxazol-2-ylamino)-phenyl]-3-imidazol-1-yl-2,2-dimethylpropionic acid methyl ester (**46**) as a white solid. Yield 0.19 g (47 %), t. l. c. system: EtOAc, R_F: 0.28, stain positive.

^{1}H NMR: δ (DMSO-d_6): 1.21 (s, 6H, H-4, H-5), 3.57 (s, 3H, H-1), 5.62 (s, 1H, H-6), 6.91 (s, 1H, H-3'''), 7.14 (t, = 7.7 Hz, 1H, H-4''), 7.23 (t, J= 7.6 Hz, 1H, H-5''), 7.48 (m, 5H, H-3', H-5', H-3'', H-6'', H-2'''), 7.75 (d, J= 8.1 Hz, 2H, H-2', H-6'), 7.84 (s, 1H, H-1'''), 10.71 (s, 1H, NH).

^{13}C NMR: δ (DMSO-d_6): 22.78 (CH, C-4, C-5), 47.30 (C, C-3), 51.97 (CH, C-1), 66.62 (CH, C-6), 108.99 (CH, C-6''), 116.64 (CH, C-2'''), 117.20 (CH, C-3', C-5', -3''), 121.77 (CH, C-3'''), 124.03 (CH, C-4'', C-5''), 128.15 (CH, C-1'''), 129.55 (CH, C-2', C-6'), 130.34 (C, C-1'), 138.47 (C, C-2''), 142.26 (C, C-4'), 146.97 (C, C-7''), 157.79 (C, C-1''), 175.20 (C, C-2).

HRMS (EI): Calculated mass: 391.1765 $(M+H)^+$, Measured mass : 391.1761 $(M+H)^+$.

Melting point: 158-160 ^{0}C

3-[4-(1*H*-Benzoimidazol-2-ylamino)-phenyl]-3-imidazol-1-yl-2,2-dimethylpropionic acid methyl ester (47)

($C_{22}H_{23}N_5O_2$, M.W. 389.447)

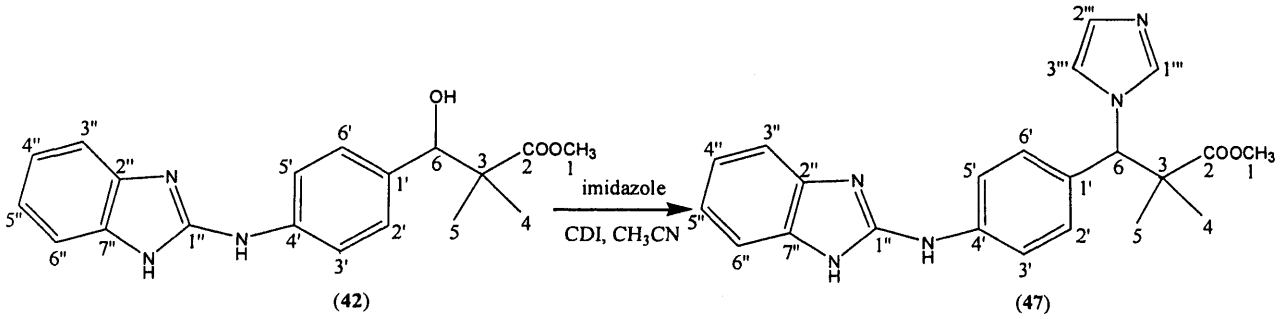

(42) (47)

To a solution of (**42**) (0.65 g, 1.92 mmol) in anhydrous CH_3CN (20 mL) was added imidazole (0.39 g, 5.76 mmol) and CDI (0.47 g, 2.88 mmol). The mixture was then heated under reflux for one hour. The reaction mixture was allowed to cool and then extracted with EtOAc (150 mL) and H_2O (3 x 100 mL). The organic layer was dried with $MgSO_4$, filtered and reduced *in vacuo*. The product was purified by flash column chromatography (EtOAc - MeOH 100:0 v/v increasing to 95:5 v/v) to give 3-[4-(1*H*-benzoimidazol-2-ylamino)-phenyl]-3-imidazol-1-yl-2,2-dimethylpropionic acid methyl ester (**47**) as a yellow oil. Yield 0.42 g (56 %), t. l. c. system: EtOAc-MeOH 95:5 v/v, R_F: 0.31, stain positive.

^{1}H NMR: δ (DMSO-d_6): 1.22 (s, 6H, H-4, H-5), 3.59 (s, 3H, H-1), 5.62 (s, 1H, H-6), 6.90 (s, 1H, H-3'''), 7.0 (m, 2H, Ar), 7.31 (m, 2H, Ar), 7.40 (d, J= 7.7 Hz, 2H, H-2', H-6'), 7.45 (s, 1H, H-2'''), 7.74 (d, J= 7.5 Hz, 2H, H-3", H-6"), 7.83 (s, 1H, H-1'''), 9.50 (s, 1H, NH-benzim), 10.91 (s, 1H, NH).

^{13}C NMR: δ (DMSO-d_6): 22.83 (CH, C-4, C-5), 47.35 (C, C-3), 51.94 (CH, C-1), 66.74 (CH, C-6), 109.48 (CH, C-6"), 116.59 (CH, C-3', C-5', C-3"), 117.20 (CH, C-2'''), 119.76 (CH, C-4", C-5"), 120.44 (CH, C-3'''), 128.10 (CH, C-1'''), 128.60 (C, C-1'), 129.36 (CH, C-2', C-6'), 140.66 (C, C-2", C-7"), 142.95 (C, C-1"), 150.28 (C, C-4'), 175.27 (C, C-2).

HRMS (EI): Calculated mass: 390.1925 $(M+H)^+$, Measured mass : 390.1925 $(M+H)^+$.

3-[4-(Benzothiazol-2-ylamino)-phenyl]-3-imidazol-1-yl-2,2-dimethylpropionic acid methyl ester (48)

($C_{22}H_{22}N_4O_2S$, M.W. 406.492)

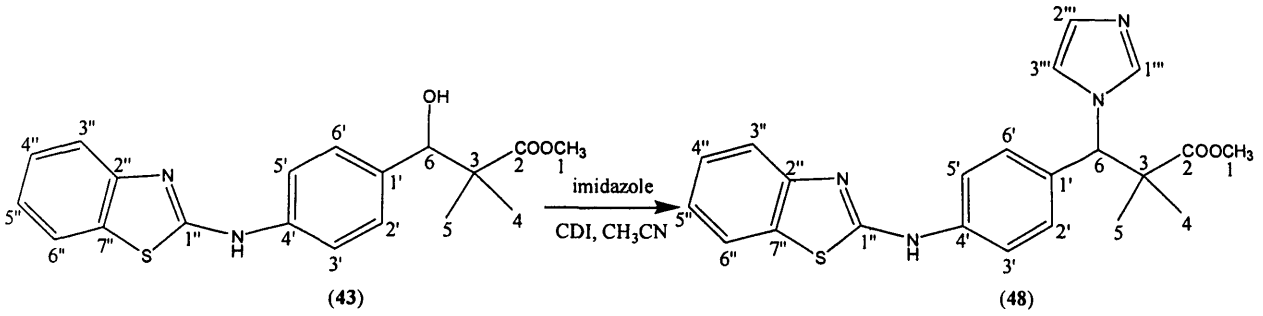

(43) (48)

To a solution of (**43**) (0.3 g, 0.84 mmol) in anhydrous CH_3CN (20 mL) was added imidazole (0.17 g, 2.52 mmol) and CDI (0.2 g, 1.26 mmol). The mixture was then heated under reflux for 2 h. The reaction mixture was allowed to cool and then extracted with EtOAc (150 mL) and H_2O (3 x 100 mL). The organic layer was dried with $MgSO_4$, filtered and reduced *in vacuo*. The product was purified by flash column chromatography (CH_2Cl_2 - MeOH 100:0 v/v increasing to 95:5 v/v) to give 3-[4-(benzothiazol-2-ylamino)-phenyl]-3-imidazol-1-yl-2,2-dimethylpropionic acid methyl ester (**48**) as a yellow oil. Yield 0.15 g (44 %), t. l. c. system: CH_2Cl_2 - MeOH 95:5 v/v, R_F: 0.46, stain positive.

^{1}H NMR: δ (DMSO-d_6): 1.22 (s, 6H, H-4, H-5), 3.61 (s, 3H, H-1), 5.62 (s, 1H, H-6), 6.85 (s, 1H, H-3'''), 7.09 (m, 3H, H-4", H-6", H-2'''), 7.34 (t, J= 7.6 Hz, 1H, H-5"), 7.46 (d, J= 8.2 Hz, 2H, H-3', H-5'), 7.61 (d, J= 7.9 Hz, 1H, H-3"), 7.78 (d, J= 8.1 Hz, 1H, H-2'), 7.81 (d, J= 7.9 Hz, 1H, H-6'), 7.85 (s, 1H, H-1'''), 10.59 (s, 1H, NH).

^{13}C NMR: δ (DMSO-d_6): 22.91 (CH, C-4), 23.53 (CH, C-5), 47.56 (C, C-3), 52.50 (CH, C-1), 67.63 (CH, C-6), 118.49 (CH, C-3', C-5'), 119.76 (CH, C-3"), 120.73 (CH, C-6", C-2'''), 122.66 (CH, C-4"), 126.08 (CH, C-5", C-3'''), 128.66 (CH, C-1'''), 129.35 (CH, C-2', C-6'), 130.25 (C, C-7"), 130.58 (C, C-1'), 140.54 (C, C-4'), 151.71 (C, C-2"), 162.54 (C, C-1"), 176.15 (C, C-2).

HRMS (EI): Calculated mass: 407.1536 $(M+H)^+$, Measured mass : 407.1535 $(M+H)^+$.

3-Imidazol-1-yl-2-methyl-3-[4-(naphthalen-2-ylamino)-phenyl]-propionic acid methyl ester (49)

($C_{25}H_{25}N_3O_2$, M.W. 399.482)

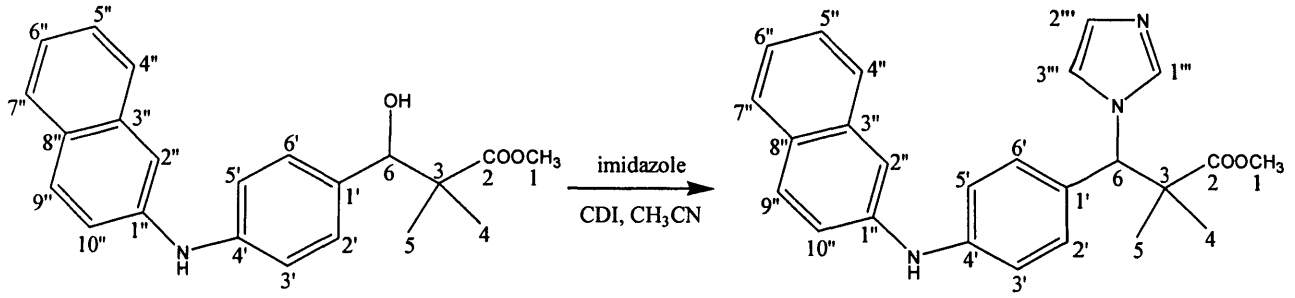

(44) (49)

To a solution of (**44**) (0.4 g, 1.15 mmol) in anhydrous CH_3CN (20 mL) was added imidazole (0.24 g, 3.45 mmol) and CDI (0.28 g, 1.73 mmol). The mixture was then heated under reflux overnight. The reaction mixture was allowed to cool and then extracted with EtOAc (150 mL) and H_2O (3 x 100 mL). The organic layer was dried with $MgSO_4$, filtered and reduced *in vacuo*. The product was purified by flash column chromatography (CH_2Cl_2 - MeOH 100:0 v/v increasing to 97:3 v/v) to give 3-imidazol-1-yl-2-methyl-3-[4-(naphthalen-2-ylamino)-phenyl]-propionic acid methyl ester (**49**) as a light brown solid. Yield 0.25 (54), t. l. c. system: CH_2Cl_2 - MeOH 97:3 v/v, R_F: 0.61, stain positive.

^{1}H NMR: δ (DMSO-d_6): 1.21 (s, 6H, H-4, H-5), 3.55 (s, 3H, H-1), 5.58 (s, 1H, H-6), 6.91 (s, 1H, H-2"), 7.17 (d, J= 8.0 Hz, 2H, H-3', H-5'), 7.28 (m, 2H, H-6", H-10"), 7.38 (m, 3H, H-2', H-6', H-5"), 7.44 (s, 1H, H-3'"), 7.50 (s, 1H, H-2'"), 7.71 (d, J= 8.2 Hz, 1H, H-4"), 7.77 (m, 2H, H-7", H-9"), 7.83 (s, 1H, H-1'"), 8.51 (s, 1H, NH).

^{13}C NMR: δ (DMSO-d_6): 22.70 (CH, C-4), 22.90 (CH, C-5), 47.34 (C, C-3), 51.92 (CH, C-1), 66.73 (CH, C-6), 109.84 (CH, C-2"), 112.84 (CH, C-10"), 116.20 (CH, C-3', C-5'), 120.10 (CH, C-6". C-2'"), 122.98 (CH, C-4"), 126.23 (CH, C-5", C-7"), 127.37 (CH, C-9"), 127.96 (C, C-8"), 128.00 (CH, C-3'"), 128.10 (C, C-1'), 128.82 (CH, C-1'"), 129.79 (CH, C-2', C-6'), 134.29 (C, C-3"), 140.68 (C, C-4'), 142.99 (C, C-1"), 175.31 (C, C-2).

Microanalysis: Calculated for $C_{25}H_{25}N_3O_2$. $0.3H_2O$ (404.885); Theoretical: %C= 74.16, %H= 6.22, %N= 10.38; Found: %C= 74.09, %H= 6.26, %N= 10.11.

Melting point: 190-192 ^{0}C

3-Imidazol-1-yl-2,2-dimethyl-3-(4-phenylaminophenyl)-propionic acid methyl ester (50)

($C_{21}H_{23}N_3O_2$, M.W. 349.422)

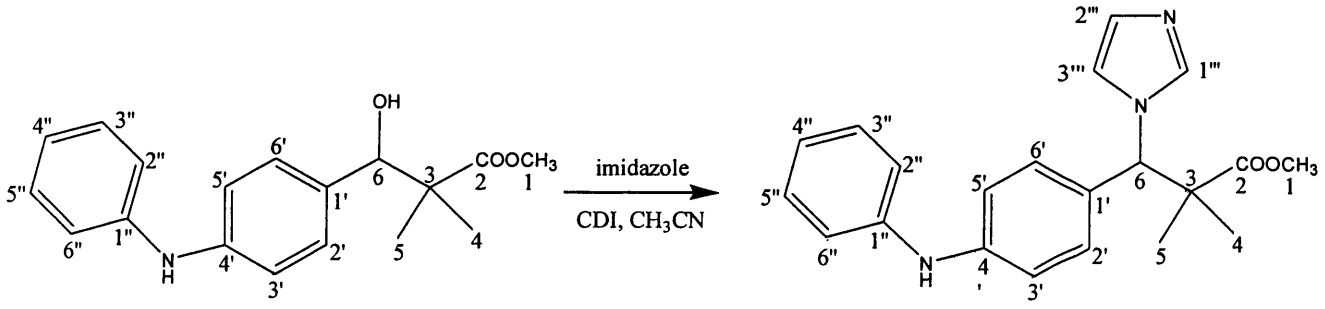

(45) (50)

To a solution of (**45**) (0.4 g, 1.49 mmol) in anhydrous CH_3CN (20 mL) was added imidazole (0.31 g, 4.47 mmol) and CDI (0.36 g, 2.24 mmol). The mixture was then heated under reflux for 2 h. The reaction mixture was allowed to cool and then extracted with EtOAc (150 mL) and H_2O (3 x 100 mL). The organic layer was dried with $MgSO_4$, filtered and reduced *in vacuo*. The product was purified by flash column chromatography (EtOAc 100 %) to give 3-imidazol-1-yl-2,2-dimethyl-3-(4-phenylaminophenyl)-propionic acid methyl ester (**50**) as a colourless oil. Yield 0.23 g (44 %), t. l. c. system: EtOAc 100 %, R_F: 0.38, stain positive.

^{1}H NMR: δ ($CDCl_3$): 1.30 (s, 3H, H-4), 1.31 (s, 3H, H-5), 3.63 (s, 3H, H-1), 5.52 (s, 1H, NH), 6.37 (s, 1H, H-6), 6.97 (m, 4H, H-3', H-5', H-4", H-3'"), 7.05 (s, 1H, H-2'"), 7.09 (d, J= 6.8 Hz, 2H, H-2", H-6"), 7.14 (d, J= 7.9 Hz, 2H, H-2', H-6'), 7.27 (t, J= 6.9 Hz, 2H, H-3", H-5"), 7.61 (s, 1H, H-1'").

^{13}C NMR: δ ($CDCl_3$): 22.90 (CH, C-4), 23.45 (CH, C-5), 47.68 (C, C-3), 52.38 (CH, C-1), 67.55 (CH, C-6), 116.78 (CH, C-3', C-5'), 118.66 (CH, C-2", C-6"), 119.57 (CH, C-4"), 121.61 (CH, C-2'"), 127.86 (C, C-1'), 128.85 (CH, C-3'"), 129.56 (CH, C-3", C-5"), 129.89 (CH, C-2', C-6'), 137.97 (CH, C-1'"), 142.36 (C, C-4'), 143.75 (C, C-1"), 176.27 (C, C-2).

HRM-S (EI): Calculated mass: 350.1863 $(M+H)^+$, Measured mass : 350.1862 $(M+H)^+$.

Chapter 6

Biological evaluation of CYP26A1 inhibitors

6 Biological evaluation of CYP26A1 inhibitors

The assay was performed using all-*trans* retinoic acid as substrate and using method previously developed by our group.

6.1 Materials and equipment

Material/Chemical	**Source**
ATRA	Sigma Chemicals (Dorset, UK)
[^{3}H-11,12] ATRA (9.25 MBq, 250 μCi)	Perkin Elmer Life Science Ltd. (Massachussets, USA)
HPLC grade solvents (acetonitrile, MeOH)	Fisher Scientific (Leicestershire, UK)
Buffer (see preparation below)	Aldrich Chemicals, UK
EtOAc, EtOH, ammonium acetate	Sigma Chemicals, UK
OptiFlow Safe 1 liquid scintillation cocktail	Fisions Chemicals, UK
Borosilicate tubes (12 × 75 mm and 13 × 100 mm)	Corning (New York, USA)
Equipment	**Source**
Centrifuge	MSE Harrier 18/80, Santo, Japan
Pump	Milton-Roy
Water bath with shaker	Grant, UK
Rotating evaporator	Christ Alpha RVC (Germany)
10 μm C_{18} μBondapak® 309 × 300 mm column	Waters, UK
Beta-RAM online scintillation detector	LKB Wallace 1217 Rackbeta
Computer	Compaq ™
Laura data acquisition and analysis software	Lablogic Ltd.

➢ *Preparation of [^{3}H] ATRA stock solution*

100 μL of 1.2 mM all-*trans* retinoic acid in EtOH was diluted with 900 μL of of ^{i}PrOH:EtOH 1:1 v/v. To this was added 10 μL of [^{3}H] ATRA (9.25 MBq, 250 μCi).

- 1 mL of the above stock solution contains 10/250 x 9.25 MBq = 0.37 MBq.
- 10 μL of the stock solution contains 0.01 μCi x 0.37 MBq/0.037 MBq = 0.10 μCi.

- *Preparation of phosphate buffer (50 mM, pH 7.4)*

To prepare 1000 mL of phosphate buffer (50 mM, pH 7.4), 6.68 g of disodium hydrogen orthophosphate dehydrate was dissolved in 750 mL of water and 1.95 g of monosodium dihydrogen orthophosphate dihydrate was dissolved in 250 mL of water. This mixture was then titrated to pH 7.4 with aqueous NaOH (5 M).

6.2 Cell-line used

Retinoids have been known to have anti-proliferative effects on the growth of breast carcinoma cells (MCF-7, ZR-75.1) (VanHeusden *et al.*, 1998; Toma *et al.*, 1997). The cell line used in this assay is the oestrogen responsive MCF-7 human mammary-carcinoma cell line which is oestrogen receptor-positive. This cell line is also known as the wild-type MCF-7 cell line. This cell was routinely grown in RPMI medium, supplemented with 5 % (v/v) foetal calf serum (FCS), antibiotics (streptomycin and penicillin) and fungizone at the same concentration of 10 iU/mL. This is the basal medium for MCF-7. This cell line was chosen because it is available at the Welsh School of Pharmacy from the Tenovus group.

6.3 General method for the MCF-7 wild type ATRA assay

The method described below were based on a modification of the method of Jarno (Jarno, 2003) and Farhan *et al.* (Farhan *et al.*, 2002; Yee *et al*, 2005).

1. The wild-type MCF-7 cell lines supplied by Tenovus were seeded at 3 x 10^{6} cells per well (12 wells) and left to settle for 24 h.
2. After 24 h, the experimental medium of the wild-type MCF-7 cells were removed and then 1 mL of PBS was added to each well then removed and replaced by fresh experimental medium plus various treatments.

3. These treatments were prepared as follows: each treatment was performed in duplicate (one tube for 2 wells) therefore, 6 well dried and sterile glass tubes were prepared. To the first one was added 20 µl of EtOH as control and to the other five tubes was added separately 20 µl of five different concentrations of the inhibitor ranging from 50-1 µmol, one concentration for each tube. 2 mL of the experimental media supplied by Tenovus was added to each tube (1 mL per well). 20 µl of [^{3}H] ATRA was then added quickly to avoid exposure to air to each of the six tube (10 µl per well). The tubes were placed in the water bath and were shacked gently for 10-15 minutes.
4. The corresponding experimental media containing the substrate and inhibitor or control is transferred by the aid of micropipettes to the corresponding well (each glass tube into 2 wells).
5. Tissue culture plates were then wrapped in aluminum foil and incubated for 9 hours.
6. The incubation with the respective substrate was stopped by the addition of 2 % v/v acetic acid (100 µL/well).
7. The medium and acetic acid from each well was then removed and transferred to borosilicate glass tubes (13 x 100 mm) which contained 2 mL solution of EtOAc with 0.05 % (w/v) butylated-hydroxyanisole.
8. 0.5 mL of distilled water was subsequently added to each well plate and the cells were scrapped off using the rubber end of a 1 mL syringe.
9. The cell suspension from each tube was transferred to the respective glass tubes.
10. Finally, each well was rinsed with 0.5 mL of distilled water and then transferred to the respective glass tubes.
11. The glass tubes were centrifuged (6000 rpm for 15 min at room temperature).
12. The top organic layer containing the substrate and metabolites was transferred into respective borosilicate glass tubes (12 x 75 mm).
13. The tubes were placed in a rotating evaporator for 35 min.
14. The residues in each tube were redissolved in MeOH, then analysed using an on-line radioactive detector connected to a HPLC.

The HPLC system was equipped with a high pressure pump (Milton-Roy pump), injector with a 50 µL loop connected to a beta-RAM radioactivity detector, connected

to a Compaq™ computer running Laura® data acquisition and analysis software. This enabled on-line detection and quantification of radioactive peaks. The 5 μm ODS EXSIL® 4.6 x 200 mm column (for vitamin D_3 assay) or 10 μm C_{18} μBondapak® 3.9 x 300 mm column (for ATRA assay) operating at ambient temperature was used to separate the metabolites which were eluted with 750 mL acetonitrile/250 mL 1 % ammonium acetate in water/1 mL acetic acid at a flow rate of 1.9 mL/min.

The experimental medium used (obtained from Tenovus) was as follows:
RPMI phenol red-free, supplemented with 5 % (v/v) stripped foetal calf serum (S-FCS), antibiotics (streptomycin and penicillin) and fungizone at the same concentration of 10 iU/mL and 2 % v/v L-glutamine (200 mM).

6.4 Experimental results

The IC_{50} of our final compounds can be measured using the HPLC and the Laura software. Two major peaks can be observed on the HPLC. The first peak (retention time 1.5-2.5 min) corresponds to the metabolites of ATRA (4-oxo-ATRA, 4-hydroxy-ATRA and other polar metabolites) which are metabolised by the action of CYP26 on ATRA and the second peak (retention time 5-6.5 min) correspond to the ATRA itself.

Consequently, a disappearance of the first peak would be observed if we add an inhibitor to the media. The separated metabolites were quantitatively calculated from the area under the curves and the percentage inhibition was calculated from:
100[(%metabolites (control) – %metabolites (inhibitors) / %(metabolites control)].
The results of the assay are summarised in **Table 6.1**.

Table 6.1: IC_{50} of the tested α substituted 4-(1,2,4)triazol- and imidazol-1-yl-methyl-phenyl-aryl and heteroaryl amine derivatives.

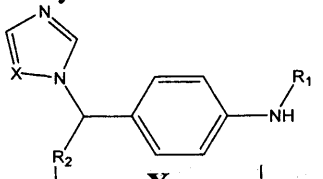

R1	R2	X	IC_{50}	CMPD
Ph	CH_3	N	>50 μM	**22**
Ph	Ph	N	5 μM	**23**
Ph	CH_3	CH	35 μM	**24**

Ph	Ph	CH	5 μM	**25**
Naphthyl	CH_3	CH	15 μM	**26**
Naphthyl	Ph	CH	0.5 μM	**27**
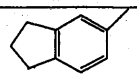	Ph	CH	1 μM	**28**
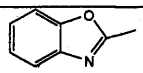	Ph	CH	0.9 μM	**34**
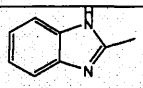	Ph	CH	3.5 μM	**35**
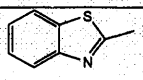	Ph	CH	2.5 μM	**36**
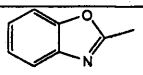	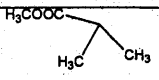	CH	190 nM	**46**
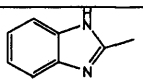	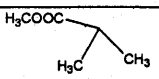	CH	1.5 μM	**47**
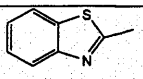	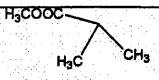	CH	230 nM	**48**
Naphthyl	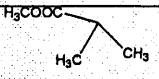	CH	20 nM	**49**
Ph	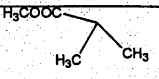	CH	0.5 μM	**50**

These results showed that compounds **27, 28** and **34** are good CYP26 inhibitors being about 10 times more active than the well-known CYP26 inhibitor liarazole. However, they were still less active than R115866. Compounds **23, 25, 35** and **36** are not as active as but still equipotent to liarozole, which was used as the standard inhibitor in this assay (IC_{50}= 7 μM). The results also showed that compounds **22, 24** and **26** are not good inhibitors. This is consistent with the results of the virtual screening study as compounds having R_2= CH_3 being relatively small, have been found to move freely in the active site and are not selective inhibitors while, compounds **27, 28** and **34** fitted well into the active site establishing multiple hydrophobic interactions that hold the inhibitors tightly in the active site.

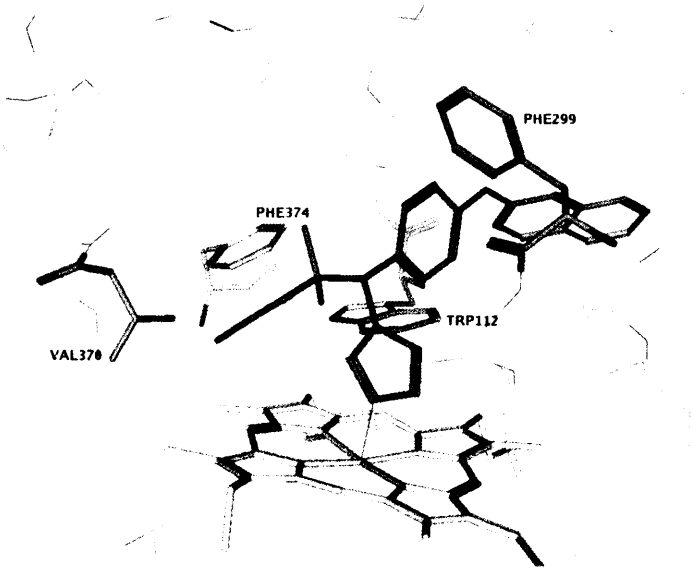

Figure 6.1: Interactions between compound **49** and the CYP26A1 active site.

Compounds having isobutyric acid methyl ester side chain showed enhanced CYP26 inhibitory activity with compound (**49**) being the most active having IC_{50} of 20 nM. Compounds (**46**) and (**47**) are less active but they still have IC_{50} in the low nanomolar range. Compound (**49**) docked well in the active site establishing multiple hydrophobic interactions with residues at the active site including TRP112, PHE299, PHE374, VAL370, ALA114, SER115, VAL116 and THR304. The dimethyl side chain is interacting well with PHE299, PHE374 and VAL370. The imidazole is residing directly above the haem with its nitrogen at a distance of 2.16 Å from the haem iron allowing the transition metal interaction (**Figure 6.1**). Unfortunately, it was not possible to explain the difference in activity between compounds having R_2= Ph and compounds having R_2= isobutyric acid methyl ester based only on the docking studies. It could be there are other factors affecting the activity of the last series like penetration through biological membranes, cellular uptake, solubility that could interfere with the procedure of the biological assay.

It is worth noting that only the (*S*)-conformation of these compounds docked in the active site while the (*R*)- did not dock favourably suggesting that the pure (*S*)-enantiomer may be more active than the racemic compound.

Chapter 7

Homology modelling of CYP24A1

7 Homology modelling of CYP24A1

7.1 Homology searching

The human CYP24 in Swiss-Prot database, code (Q07973), (synonyms vitamin D_3 24-hydroxylase, 1,25-dihydroxyvitamin D_3 24-hydroxylase, 24-OHase) has a molecular weight of 58875 Daltons and a chain length of 514 amino acid with the iron of the haem directly attached to the cysteine 462 (Deloukas *et al.*, 2001; Expasy server, 2004e; Chen and DeLuca, 1995).

An advanced WU-BLAST2 search at the EMBL (EMBL, 2004) was performed for the query protein against the PDB database

The BLAST search returned the amino acid sequence of different P450s isolated from different species including the three human P450s recently deposited in the PDB database with % identity of 36%-22%, scores of 345-79 and E values of $4.6e^{-31}$ - 0.47 (**Table 7.1**).

The fourth column in the table lists the percentage of sequence identities of the structure to the target. They all have a sequence identity of about 25%.

In this respect, CYP3A4 (1TQN), CYP2C9 (1R90) and CYP2C8 (1PQ2) were identified as the best templates as they are all human P450s, have good BLAST score, % sequence identity and E-value (**Table 7.1**). They also have chain length similar to that of CYP24 and they are all crystal structures determined by X-ray crystallography to a high resolution.

Table 7.1: The P450 structures recovered by a WU-BLAST search at the EMBL server using the sequence of P45024.

Protein[(a)]	WU BLAST score[(b)]	Sequence identity[(c)]	% sequence identity	Chain length	E-Value
1TQN-A	**345**	**126/467**	**26**	**486**	**$4.9e^{-31}$**
1PO5-A	310	121/454	26	476	$1.6e^{-26}$
1R90-A	**289**	**116/446**	**26**	**477**	**$5.3e^{-24}$**
1PQ2-A	**275**	**113/446**	**25**	**476**	**$2.3e^{-22}$**
1DT6-A	262	111/452	24	473	$6.8e^{-21}$
1JPZ-A	260	109/437	24	473	$1.2e^{-20}$

[a] The PDB code of the cytochrome P450

[b] The PSI-BLAST score for an alignment is calculated by summing the score for each

aligned position and the scores for gaps

[c] (The number of identical residues) / (the length of sequence fragment identified by PSI-BLAST).

7.2 Building the homology model

The query protein sequence was aligned to the template sequence with an alignment constraint between the active site cysteine residue of CYP24A1 (Deloukas *et al.*, 2001; Expasy server, 2004e; Chen and DeLuca, 1995) and the corresponding active site cysteine residue of CYP3A4, CYP2C9 and CYP2C8 then the model was built as described for CYP26A1 (**Section 2.5**)

7.3 Model validation

The models obtained showed that the distance between the thiolate of the cysteine at the model active site and the iron of the haem was 2.57Å in the model based on CYP3A4, 2.84Å in the model based on CYP2C9 and 2.77Å in the model based on CYP2C8.

As for CYP26 models, it is concluded from the validation results obtained for the CYP24 models that CHARMM22 was the best force field to give models having good stereochemical quality together with good sidechain envioronment.

The results of the validation checks performed on the final lowest energy model for each template are listed in **Table 7.2**. These results were compared with those of the template crystal structures (**Table 3.3**)

From **Table 7.2** it is apparent that our models have about 85% of their residues in the most favoured region of the Ramachnadran plot. These scores are highly approaching those of the template crystal structures (**Table 3.3**) which indicate high stereochemical quality of the models. The Errat and Verify3D scores are also acceptable indicating that most of the residues are in normal sidechain environment.

Table 7.2: Results of validation studies performed on the CYP24 models produced from the homology modelling with the three templates.

Model	Ramachandran plot[a] (%)	Errat[b] (%)	Verify3D[c] (total score)
Based on 3A4 as template	84.8	79.0	133
Based on 2C9 as template	83.9	78.8	123
Based on 2C8 as template	87.3	77.6	141

[a] percentage of residues with Phi and Psi conformation in the most favoured regions of the Ramachandran plot.

[b] the percentage of residues in normal non-bonded environment.

[c] The total Verify3D score summed overall residues.

7.4 Docking studies

Although, most of the residues constituting the active-site in the three models are nearly the same including: LEU148, Glu322, ALA326, THR330 and VAL391, only the CYP24A1 model built using the CYP3A4 template was able to accommodate the natural substrate calcitriol in the right position with C24 atom positioned in proximity of the haem iron at a distance of 6.1 Å, this distance would accommodate a water molecule between the 24-position of calcitriol and the haem iron (**Figure 7.1**). On the other hand, the potent and selective inhibitor (*R*)-VID400 (Schuster *et al.*, 2001) was also docked on the model. However, the orientation of the inhibitor would not allow perfect coordination between the nitrogen of the imidazole heterocycle and the haem iron transition metal (**Figure 7.2a**). It is worth noting that the (*S*)-conformation of the inhibitor didn't dock in the active site with the imidazole ring pointing toward the haem. Docking studies do not take into account protein flexibility therefore molecular dynamics were performed on the active site containing (*R*)-VID400 resulting in optimised active site architecture. This resulted in the imidazole

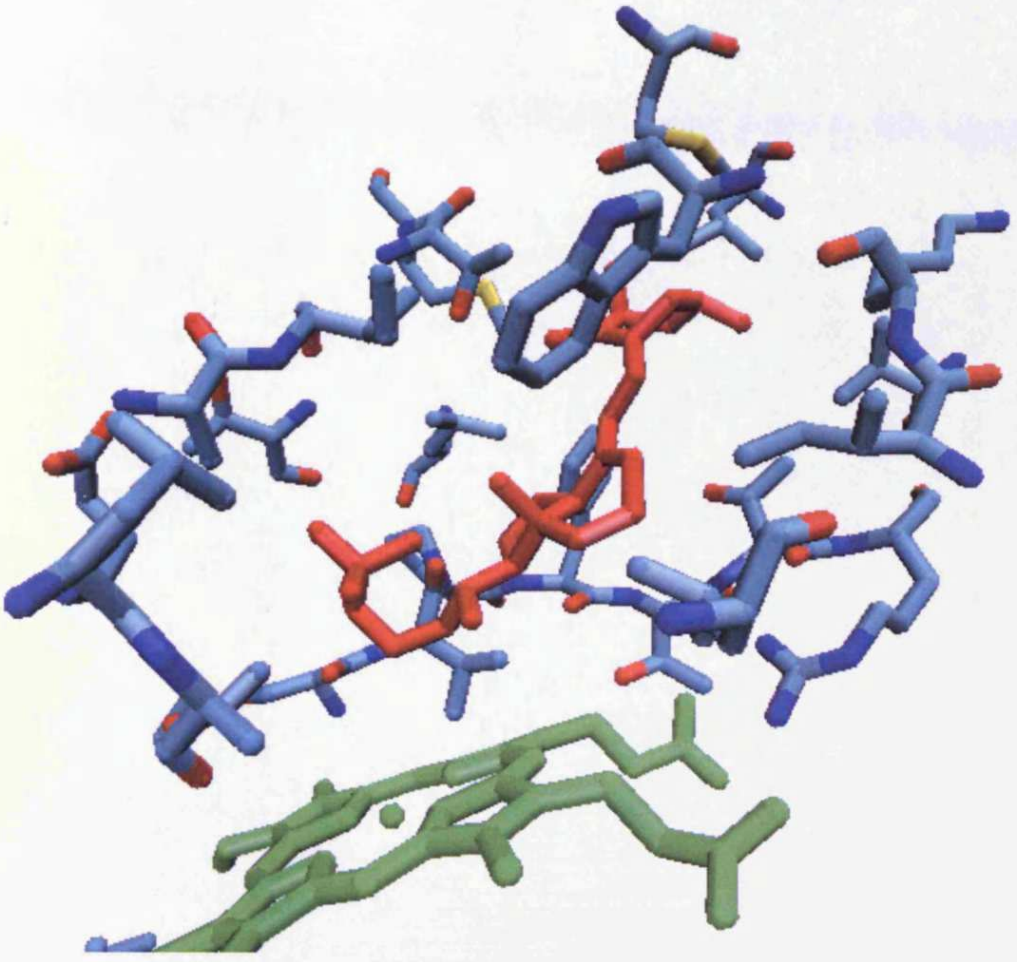

Figure 7.1: Calcitriol docked in CYP24A1 active site.

ring positioned in a more favourable conformation with respect to receptor binding (**Figure 7.2b**) with the imidazole nitrogen perpendicular to the haem iron at a distance of 2.73 Å. Furthermore, (*R*)-VID400 forms hydrophobic interaction with ALA326, an I-helix residue, that has been proven to be crucial in substrate side chain contact (Masuda *et al.*, 2007). (*R*)-VID400 occupies the same hydrophobic tunnel as the natural substrate and accesses the active site through the same channel with establishing several hydrophobic interactions with the side chains of LEU101, PHE104, TRP134, LEU148, ILE149, ILE242, THR244, MET245, GLU322, ALA326, THR330, SER390, VAL391, PRO392, PHE393, THR394, THR395 and MET416 (**Figure 7.3**).

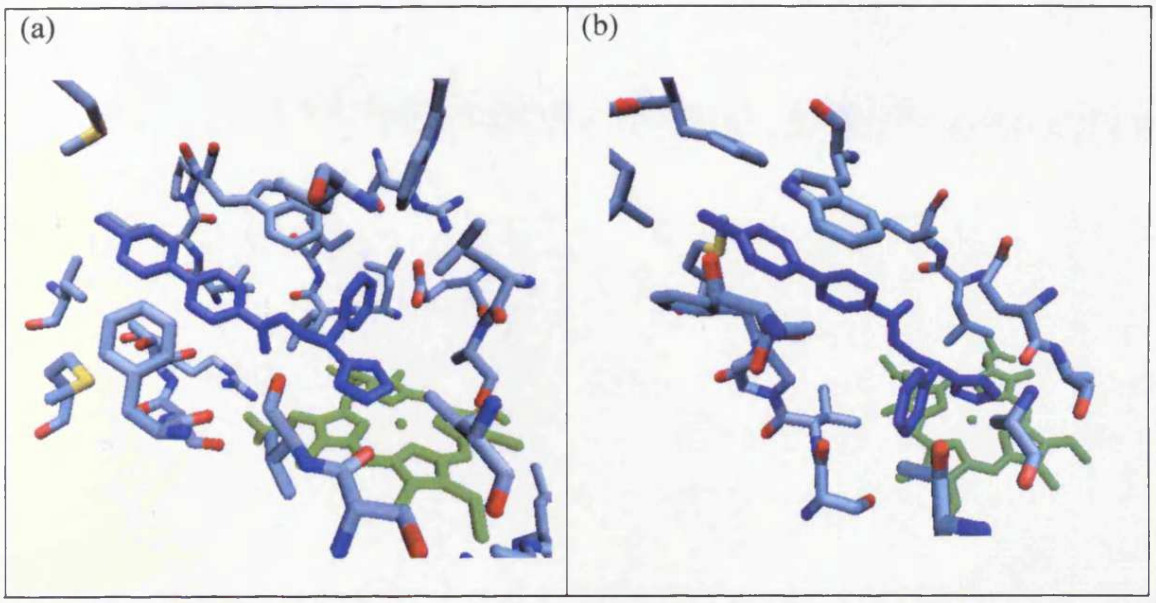

Figure 7.2: CYP24A1 model active site (a) before and (b) after active site optimisation with the (*R*)-VID400 bound inhibitor.

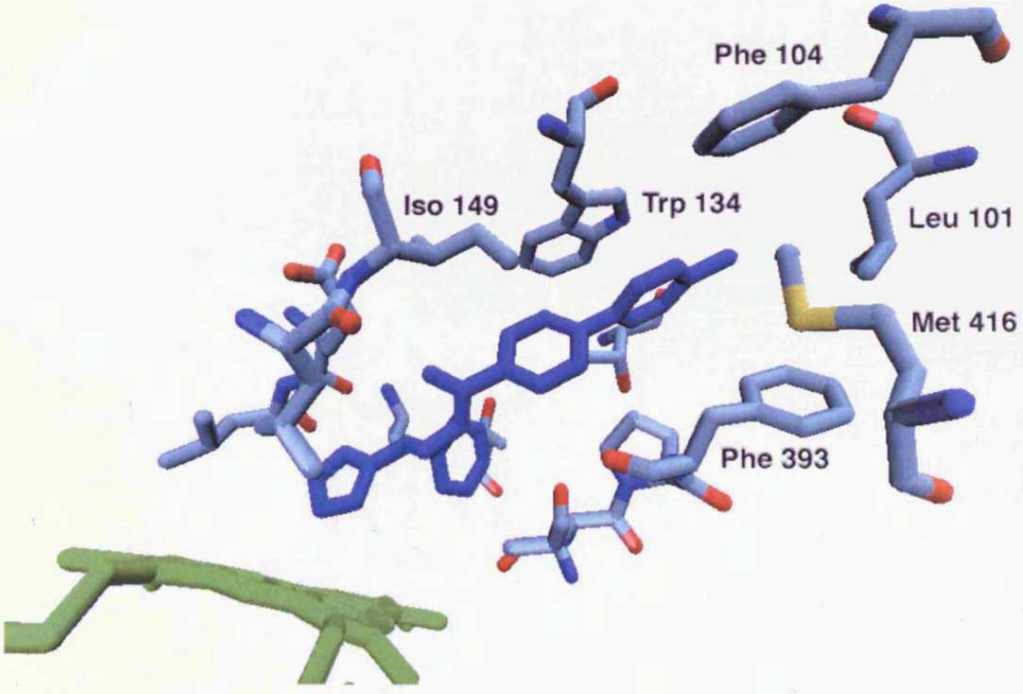

Figure 7.3: Interactions between (*R*)-VID400 and the CYP24A1 active site.

The optimised active site also accommodated the natural substrate with the C-24 in a better position from the haem iron at a distance of 4.93 Å. ALA326 is forming hydrophobic interaction with the branched side chain of calcitriol thereby holding C24 above the haem iron in a perpendicular position that would allow C24 oxidation. It is worth noting that a mutagenesis study carried out on this amino acid showed that replacing this amino acid with GLY leaded to the the transformation of human CYP24A1 from a 24-hydroxylase into a 23-hydroxylase (Prosser, *et al.*, 2007; Masuda *et al.*, 2007). The substrate is forming multiple hydrophobic interactions with residues TYR119, LEU129, LEU148, ILE149, LEU150, ILE215, ILE242, GLU322, LEU323, ALA326, ALA327, THR 331, SER390, VAL391, THR394 and THR395. The 1α OH is establishing hydrogen bonding with TYR119, THR395 and ARG396 while the OH at position 3 is forming hydrogen bonds with the backbone of LEU148 and LEU150. (**Figure 7.4**).

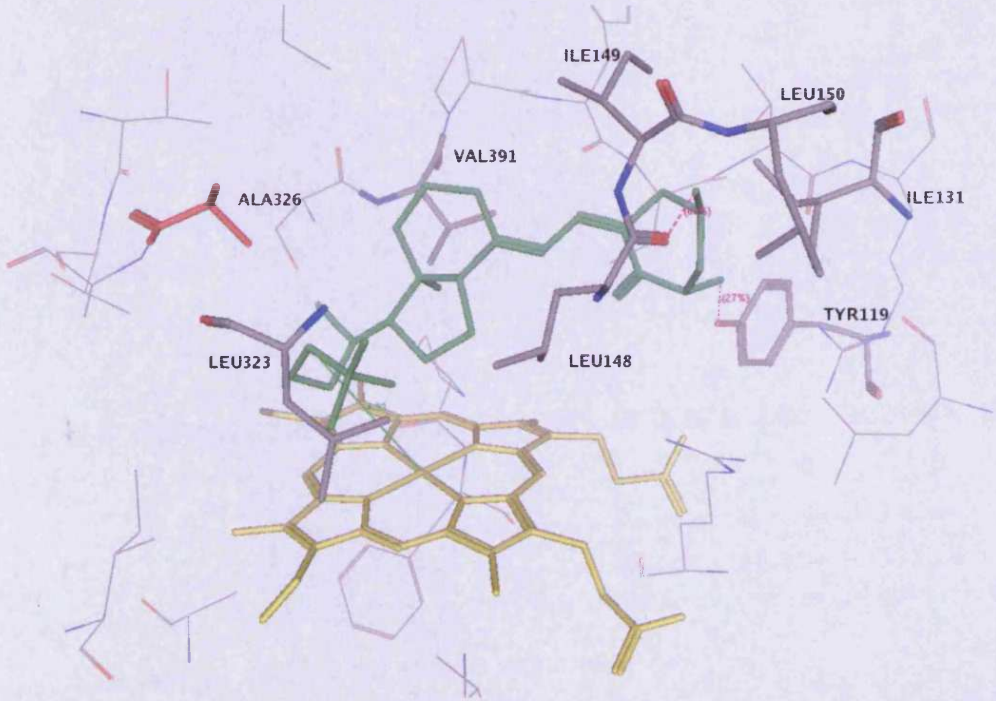

Figure 7.4: Interactions between calcitriol and the optimized CYP24A1 active site.

The 24-sulfone analogue selective inhibitor also docked well in the optimised active site. It occupies the same channel as the natural substrate with establishing multiple hydrophobic interactions with LEU148, ILE 149, ILE215,

LEU323, ALA326 and VAL391. The OH at position 3 is also forming hydrogen bond with SER 390. The sulfonyl oxygen is residing just above the haem at a distance of 4.19 Å (**Figure 7.5**).

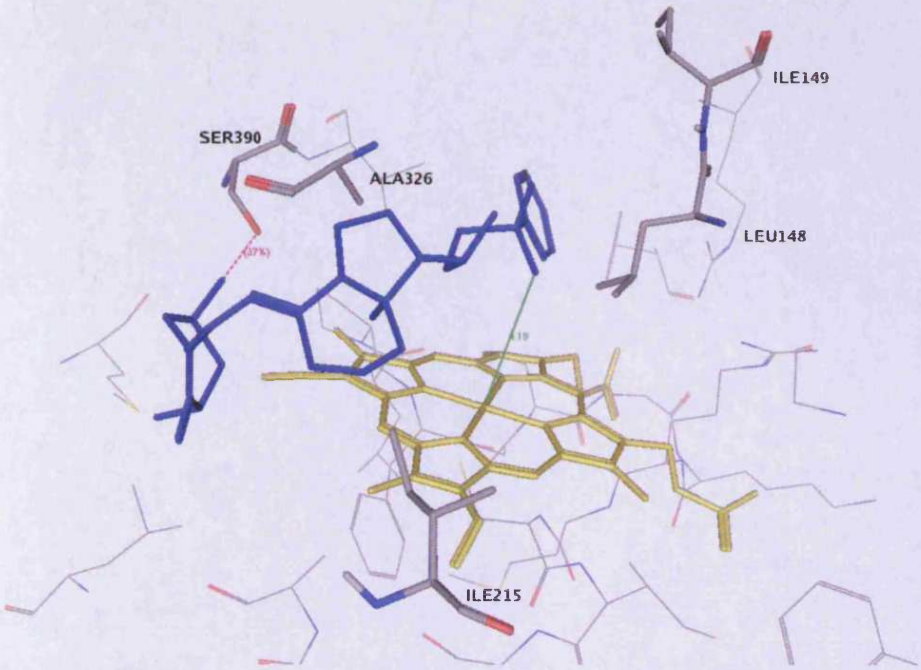

Figure 7.5: Interactions between the 24-sulfone analogue inhibitor and the CYP24A1 active site.

7.5 Model explanation and discussion

The secondary structure of the final CYP24A1 model was determined using Swiss-PdbViewer 3.7 (Guex and Peitsch, 1997) with identification of α–helices, β-sheets, coils and loops as shown in **Table 7.3**. Structural alignment of the CYP24A1 with the most homologus human P450s allowed the assignment of substrate recognition sites and P450 binding motifs (ETLR, PERF and haem binding domains) and identification of specific α–helices, β-sheets, coils and loops (**Figure 7.6**). The alignment was performed using ClustalW (Thomson *et al.*, 1994) on the EBI server (Clustal W).

```
                                  Membrane anchor region
sp|P11712|CPC9_HUMAN    -------MDSLVVLVLCLSCLLLLS--------LWRQSSGRGKLP--------------- 30
sp|P10632|CPC8_HUMAN    -------MEPFVVLVLCLSFMLLFS--------LWRQSCRRRKLP--------------- 30
sp|P00179|CPC5_RABIT    -------MDPVVVLVLGLCCLLLLS--------IWKQNSGRGKLP--------------- 30
sp|Q07973|CP24_HUMAN    -------MSSPISKSRSLAAFLQQLRSPRQPPRLVTSTAYTSPQPREVPVCPLTAGGETQ 53
sp|P08684|CP34_HUMAN    ALIPDLAMETWLLLAVSLVLLYLYG---------THSHGLFKKLG--------------- 36
```

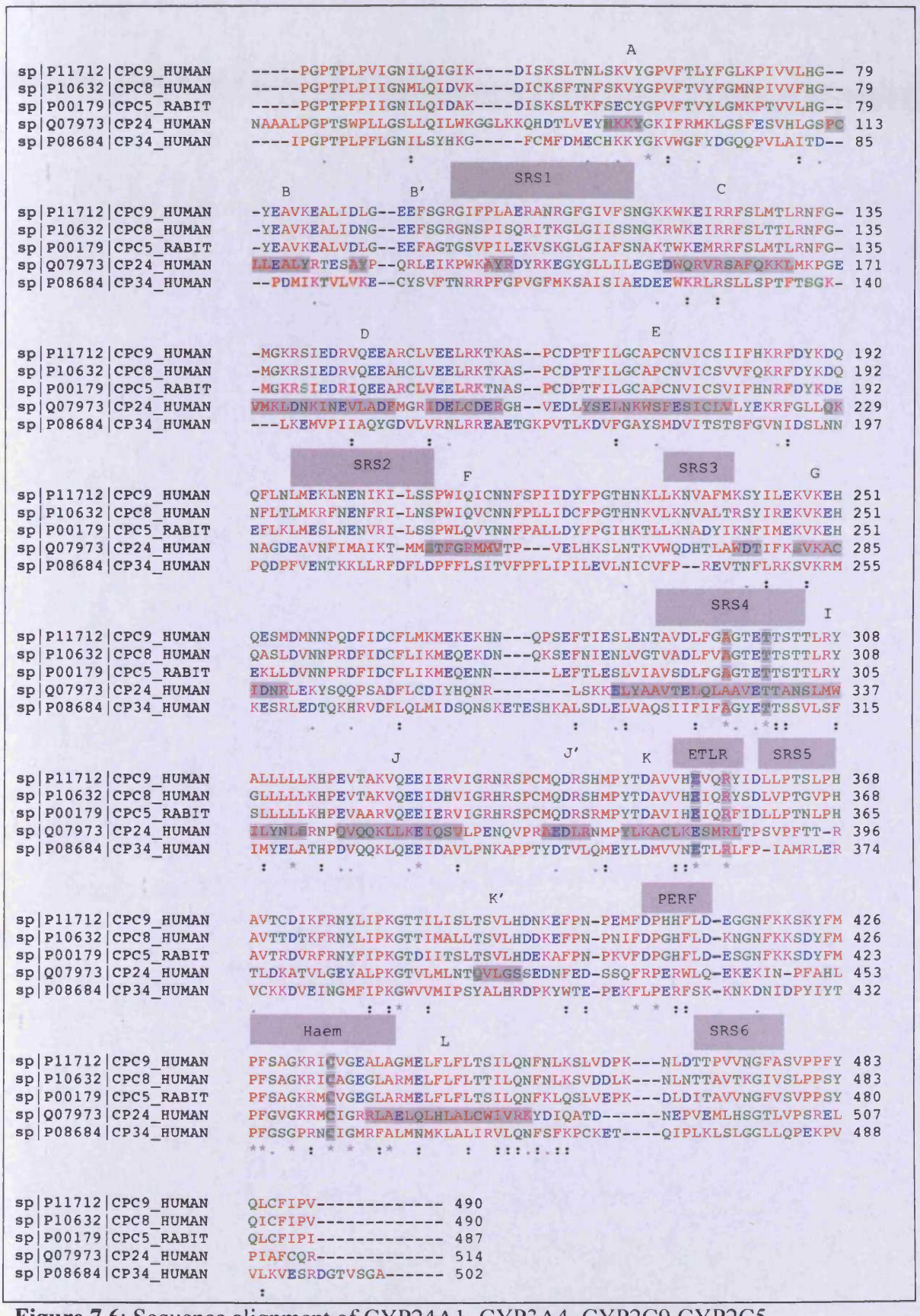

Figure 7.6: Sequence alignment of CYP24A1, CYP3A4, CYP2C9,CYP2C5, CYP2C8, using Clustal W in which star= identical residues, colon= closely similar residues and dot= moderately similar residues. The

residues are coloued according to their chemical properties where red, small hydrophobic (AVFPMILWY); blue, acidic (DE); magenta, basic (RHK); green, hydroxyl + amine + basic (STYHCNGQ).

The resultant alignment was subsequently checked to ensure that highly conserved and functionally important residues in the CYP superfamily are correctly aligned with each other including: 1) three absolutely conserved residues, EXXR in the K helix (E386, R389 in CYP24A1) and C just before the L-helix (C462 in CYP24A1); 2) the consensus sequence A(G/A)XET in the middle of the I helix; 3) the consensus sequence F(G/S)XGX(H/R)XCXGXX(I/L/F)A containing the Cys (C462 in CYP24A1) responsible for haem binding.

The 3D structure of CYP24A1 model was similar to those of other CYPs reported so far. The model is mainly alpha helical with some beta sheet mostly on one side of the molecule (Figure 6.5). As expected, the I-helix lies just above the haem and is connected to the J-helix through a small loop. This is a counterpart with the possible role of the I-helix in the active site. ALA326 and THR330 in the I-helix are highly conserved. THR330, located near the haem, is thought to be involved in the oxygen activation mechanism. B-sheets are located at the far side of the protein except those which are involved closely in the active site. There is a large pocket just above the haem molecule which is believed to accommodate vitamin D_3 and relatively large substrates. Residues whose side-chain faces the substrate-binding pocket are ALA319, GLU322, LEU323, GLN324, ALA326, ALA327, VAL328, GLU329, THR330, THR331 SER334 in the I helix, LEU101 in the B-sheet, PHE104 in the C-sheet, TRP134 in the loop between the B-helix and the B'-helix, GLY146, LEU147, LEU148, ILE149 in the loop between the B'-helix and C-helix, ILE215 in the E-helix, ILE 242, THR244, THR245 in the loop joining the broken F-helix, MET385 in the K-helix, PRO389, SER390, VAL391, PRO392, PHE393, in the loop between the K-helix and the E-sheet, THR394 and THR395 in the E-sheet and MET416 in the H-sheet. It is also worth noting that all the residues involved in the binding of calcitriol and (*R*)-VID400, are located in the substrate recognition sites (SRSs) proposed by Gotoh (Gotoh, 1992) (**Figure 7.6**).

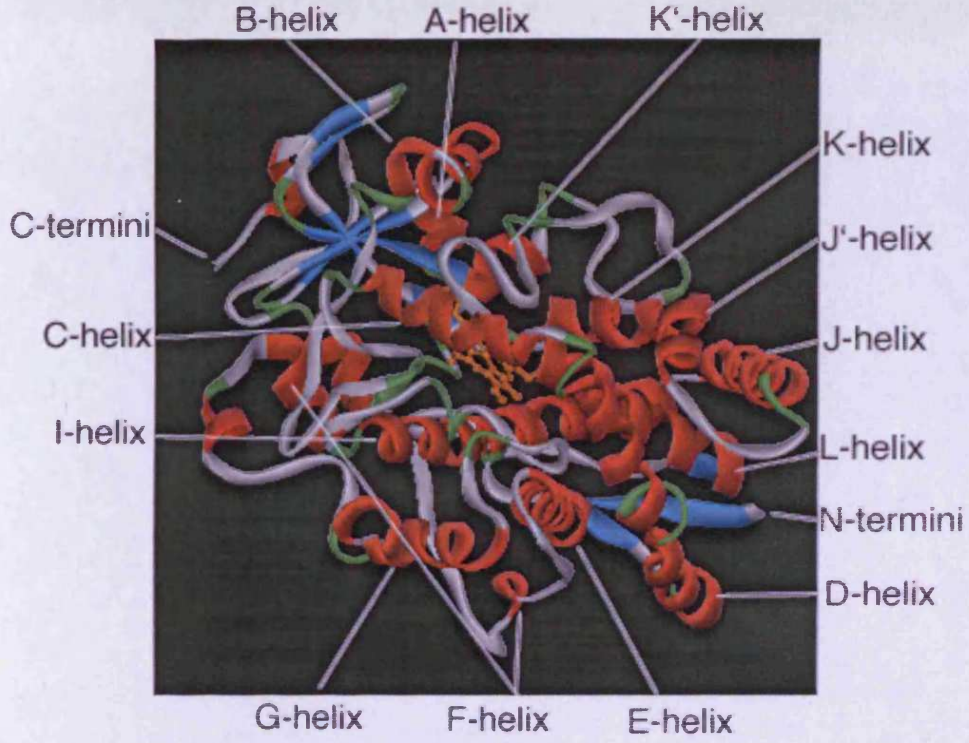

Figure 7.7: 3D Structure of the CYP24A1 model. α-Helices are in red, β-sheets are in yellow, loops are cyan and coils are grey.

The secondary structure is derived from the template structure CYP3A4 therefore further comparison with the template secondary structure was performed (**Table 7.3**).

A good overlap between the model and template secondary structure do exist especially the position of the A-helix, B'-helix, E-helix, H-helix, I-helix, J-helix, J'-helix, K-helix, K'-helix, L-helix and the G-helix which is broken in the model and the template (**Figure 7.7**). The model differs from the template in that the B-helix, D-helix, and F-helix are broken in the model but not in the template while the C-helix is broken in the template but not in the model. At the same time, the F'- and H-helices identified in the template are not present in the model and the A-helix in the model is short compared to that of the template.

Table 7.3: Comparison between the model of CYP24A1 based on CYP3A4 and the template secondary structure.

Model		template	
Residues	Secondary structure	Residues	Secondary structure
GLU51-ASN54	Helix	LEU32-LEU36	Helix
LEU67-SER69	B-sheet	PHE57-TYR68	A-helix
LEU71-LYS76	Helix	LYS70-GLY77	B-sheet
HIS90-TYR93	A-helix	GLN79-THR85	B-sheet
PHE97-GLY102	B-sheet	PRO87-LEU94	B-helix
PHE104-HIS108	B-sheet	MET114-LYS115	B'-helix
PRO112-TYR119	B-helix	GLU124-ARG128	C-helix
ALA124-TYR125		LEU132-PRO135	
ALA136-ARG138	B'-helix	SER139-GLU165	D-helix
ASP154-LEU166	C-helix	LYS173-SER186	E-helix
VAL172-PHE186	D-helix	PRO202-LYS208	F-helix
ILE190-ARG197		PRO218-THR224	F'-helix
TYR204-VAL218	E-helix	PHE228-LEU236	G-helix
GLN228-LYS229	F-helix	ARG243-LYS257	
SER247-VAL254		PHE271-GLN279	H-helix
LEU259-SER262	Helix	ASP292-LEU321	I-helix
THR265-VAL267	B-sheet	PRO325-VAL338	J-helix
TRP275-THR277	G-helix	TYR347-LEU351	J'-helix
SER281-ARG289		TYR355-LEU366	K-helix
GLU315-SER343	I-helix	MET371-CYS377	B-sheet
GLN347-VAL359	J-helix	VAL381-ILE383	B-sheet
ALA368-ARG372	J'-helix	MET386-ILE388	B-sheet
TYR376-LEU387	K-helix	VAL392-SER398	B-sheet
THR394-ASP399	B-sheet	TYR399-LEU401	K'-helix
THR402-LEU404	B-sheet	GLU417-ARG418	Helix
TYR407-LEU409	B-sheet	MET445-LEU460	L-helix
GLY412-LEU417	B-sheet	ASN462-LYS466	B-sheet
GLN420-SER424	K'-helix	LYS476-SER478	B-sheet
ARG466-LYS482	L-helix	GLN484-GLU486	B-sheet

ASP484-GLN486	B-sheet	VAL489-ARG496	B-sheet
ALA510-CYS512	B-sheet		

Chapter 8

Design of CYP24A1 inhibitors

8. Design of CYP24A1 inhibitors through virtual screening

8.1 Preparation of a library of compounds

Our aim was to design highly selective inhibitors of CYP24A1 compared with CYP27B1, a related member of the CYP superfamily, in order to inhibit the catabolism of calcitriol while avoiding impairment of its synthesis. The designed compounds should be easily synthesised under usual laboratory facilities.

In order to design new selective CYP24A1 inhibitors, our objective was to create a new library of compounds and to dock them in the modeled CYP24A1 active site. MOE QuaSAR-CombiGen (MOE, 2004; Abdel-Hamid *et al.*, 2007) was used to generate a fully-enumerated combinatorial library from a scaffold database and a set of substituent R-group databases.

The library was designed based on the structure of the best known selective inhibitors of CYP24A1, (*R*)-VID 400 and the 24-sulfone or sulfoximine analogues of calcitriol and intuition. The profile of the compounds was divided into three parts.

The scaffold was chosen to be 4- or 5- substituted indole. The indole moiety was chosen over a phenyl or a naphthyl moiety as it resembles more the skeleton of the natural substrate and the 24-sulfone or sulfoximine calcitriol analogue inhibitors. This moiety holds the inhibitor tightly in the active site forming hydrophobic bonds possibly with the haem, LEU148, ILE149, ILE242, GLU322, ALA326, SER390 and VAL391. It also plays a role in positioning the side chain haem-binding group in an optimal position with respect to the haem.

R_1 was chosen to be an alkyl, alkenyl or an aryl substituent including or not including heteroatoms such as tertiary nitrogen to increase the number of hydrogen acceptors or secondary nitrogen or hydroxyl to increase the number of hydrogen donors. In the case of an alkenyl side chain the *E* configuration was chosen over the *Z* configuration to further simulate the natural substrate and selective 24-sulfone or sulfoximine analogue inhibitors. This part is important in determining the overall binding pattern of the inhibitor to the enzyme and holding the inhibitor tightly in the active site through hydrophobic bond formation possibly with TYR119, LEU129, LEU148, ILE149, LEU150, THR394 and THR350 and hydrogen bond formation with different hydrogen donors or acceptors at the active site such as TYR119, ARG396,

THR349 and SER390 thereby affecting the selectivity and efficacy of the molecule. It is also important in placing the haem-binding moeity in the correct position relative to the haem portion of the enzyme. In total 14 different structures were considered (**Table 8.1**).

The linker was designed to be an alkyl chain ranging from 1-4 atoms with or without heteroatom to further explore the side chain conformation which could affect the docking pattern. This part seems to be very important because it affects the dimensions, and the hydrophobicity of the molecule. It is also important in positioning the haem binding moiety in an optimal position from the haem iron. It also helps in holding the inhibitor tightly in the active site through hydrophobic bond formation possibly with Haem, ILE215, LEU323, ALA326, ALA327, and THR331. In total 7 different structures were considered

R_2, which contains the haem-binding domain, was chosen to be a heteroatom substituted or unsubstituted aryl sulfonyl alkyl sulfonyl, cyclic or acyclic basic nitrogen containing moiety such as imidazole, triazole, or other imidazole or triazole containing groups. This part is very crucial for the inhibitory activity as it contains the moiety responsible for the haem binding. In total 12 different structures were considered. (**Table 8.1**).

Finally, a library of 1176 molecules for each of the 4-substituted and the 5-substituted indoles was created by combination of the three parts and was written to an output database.

Table 8.1: Scaffold and substituents R_1, L and R_2 used for building of the combinatorial library.

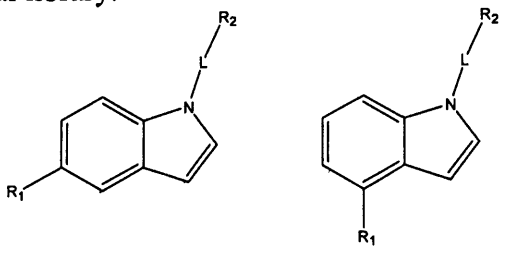

	R_1	L	R_2
1	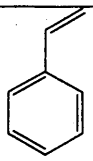	CH_2	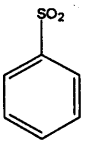

2	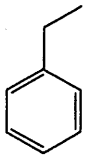		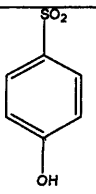
3	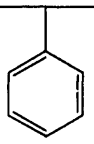		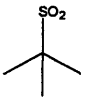
4	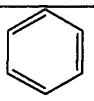		
5	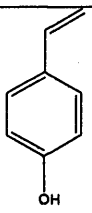	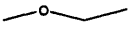	
6	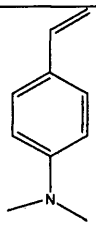		
7	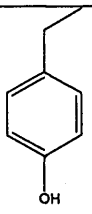		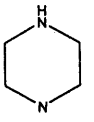
8	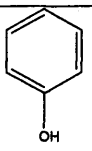		
9	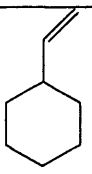		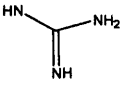
10	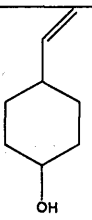		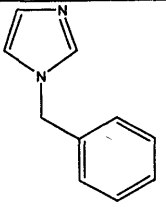

11	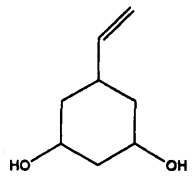		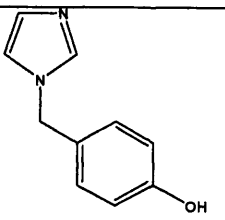
12			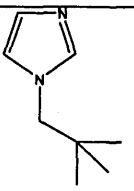
13	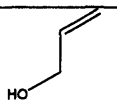		
14	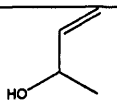		

8.2 Docking of the molecules and analysis of the results

The FlexX programme was chosen as it is one of the most suitable software to perform a virtual screening.

In the database, the formal charges of all the constructed compounds in the library were first computed and their conformation energy minimised using MMFF94X as force field. The database was then exported in Mol2 format to SYBYL databases and docked as multiple ligands in the active site using the same parameters applied in the docking of calcitriol, 24-sulfone analogue inhibitor and (*R*)-VID 400.

The results of the docking were only analysed visually due to the lack of correlation between the FlexX scoring functions and the visual compound-active site interaction. The position of the haem binding domain including the basic nitrogen or the sulfonyl group from the haem was first evaluated. In the well docked compounds, the distance between the nitrogen or the sulfonyl oxygen and the iron of the haem should be 3 Å or less thereby allowing the coordination bond to be formed. Secondly, the side chain R_1 was assessed for its ability to form hydrophobic bonds and hydrogen bonding with different residues at the active site especially TYR119, LEU129, LEU148, ILE149, LEU150, THR394 and THR350. This part together with the position and the number of atom of the alkyl side chain is crucial in driving the haem binding moiety in a conformation that allows good interaction with the haem through their hydrophobic interaction especially with ALA326, ALA327, and THR331.

Finally, side chain R_2 was evaluated for its capacity to offer the maximal lipohilic interaction and hydrogen bonding with the active site, thereby, holding the inhibitor tightly in the active site.

Compounds substituted at the 4-position showed better docking pattern then compounds substituted in the 5-position.

In general, compounds having R_1 styryl, phenylethyl, cyclohexylethenyl showed good interaction with the active site in the case where L is 2 or 3 atoms containing (or not) a heteroatom. In these compounds the haem binding moiety is interacting well with the iron of the haem especially in the case of sulphonylphenyl, imidazole and triazole. Extra hydrogen bondings were also noticed in some compounds where R_1 is substituted with hydrogen donors or acceptors. Some of the compounds that showed good docking are compounds $R_1$1-L3-$R_2$2, $R_1$1-L3-$R_2$4, $R_1$1-L3-$R_2$5, $R_1$5-L6-$R_2$4, $R_1$10-L6-$R_2$4, $R_1$2-L2-$R_2$4, $R_1$2-L3-$R_2$1.

R_1-4 and R_1-12, 13 and 14, compounds having L 4 atoms including or not heteroatom, showed good docking with extra hydrogen bonding noticed for R_1-13 and 14 *e.g.* $R_1$4-L4-$R_2$5, $R_1$12-L4-$R_2$1, $R_1$14-L5-$R_2$4.

R_2-10 interacted well with the haem in several compounds with L 1 or 2 atoms *eg.* $R_1$1-L1-$R_2$10, $R_1$7-L1-$R_2$10, $R_1$4-L2-$R_2$10, $R_1$13-L2-$R_2$10.

Therefore, it would be interesting to synthesise and test a series of these compounds for CYP24 inhibitory activity.

Chapter 9

Chemical synthesis of CYP24A1 inhibitors

9 Synthesis of 4 or 5 substituted 1-(3-benzenesulfonylpropyl)-1*H*-indole for CYP24A1 inhibition

9.1 General chemistry

The synthesis of 4 or 5 substituted 1-(3-benzenesulfonylpropyl)-1*H*-indole was carried out according to a sequence of 4 steps (**Scheme 9.1**):

- Synthesis of the 4 or 5 substituted 2-styryl 1*H*-indole
- Synthesis of 4 or 5 substituted 1-(3-bromopropyl)-1*H*-indole
- Attachment of the benzene sulfonyl moiety
- Reduction of the styryl group

9.1.1 Synthesis of *E*-4 or 5 styryl 1*H*-indole

The synthesis of *E*-4 or 5 styryl 1*H*-indole was performed by the Suzuki-Miyaura coupling reaction of 4 or 5-bromo-1*H*-indole with *trans*-phenylvinyl boronic acid. The Suzuki-Miyaura coupling reaction is a palladium-catalysed cross coupling between organoboronic acid and halides (Miyaura *et al.*, 1979; Miyaura *et al.*, 1981). This reaction is now arguably the most important and useful transformation for construction of carbon-carbon bonds in modern day organic chemistry. Recent catalyst and methods developments have broadened the possible applications enormously, so that the scope of the reaction partners is not restricted to aryls, but includes heteroaryls (Laufer *et al.*, 2005; Qing *et al.*, 2003; Azzam *et al.*, 2005; Barder *et al.*, 2005), alkyls (Kirchhoff *et al.*, 2002), alkenyls and alkynyls (Molander and Bernardi, 2002; Laufer *et al.*, 2005). Potassium trifluoroborates and organoboranes (Molander and Bernardi, 2002) or boronate esters (Barder *et al.*, 2005) may be used in place of boronic acids. Some pseudohalides (for example triflates) were also used as coupling partners (Molander and Bernardi, 2002). *Trans*-phenylvinyl boronic acid is a highly common substrate for the Suzuki cross coupling reaction (Barder *et al.*, 2005; Azzam *et al.*, 2005; Laufer *et al.*, 2005; Molander and Bernardi, 2002). On the other hand it has been reported that the best results for the Suzuki coupling of heteroaryl halides were obtained using tetrakis (triphenyl-phosphine)palladium(0) ($Pd(PPh_3)_4$) as a catalyst, aqueous Na_2CO_3 as a base and toluene as solvent (Azzam *et al.*, 2005). It was also reported that using 10 mol % of the catalyst rather than 2.5 mol % together with saturated aqueous Na_2CO_3 rather than

10 % aqueous solution increased the yield of the reaction (Zandt *et al.*, 2005). These optimised Suzuki coupling conditions were used in the coupling of 4 or 5-bromo-1*H*-indole with *trans*-phenylvinyl boronic acid. The reaction was complete after refluxing for 20 h in toluene.

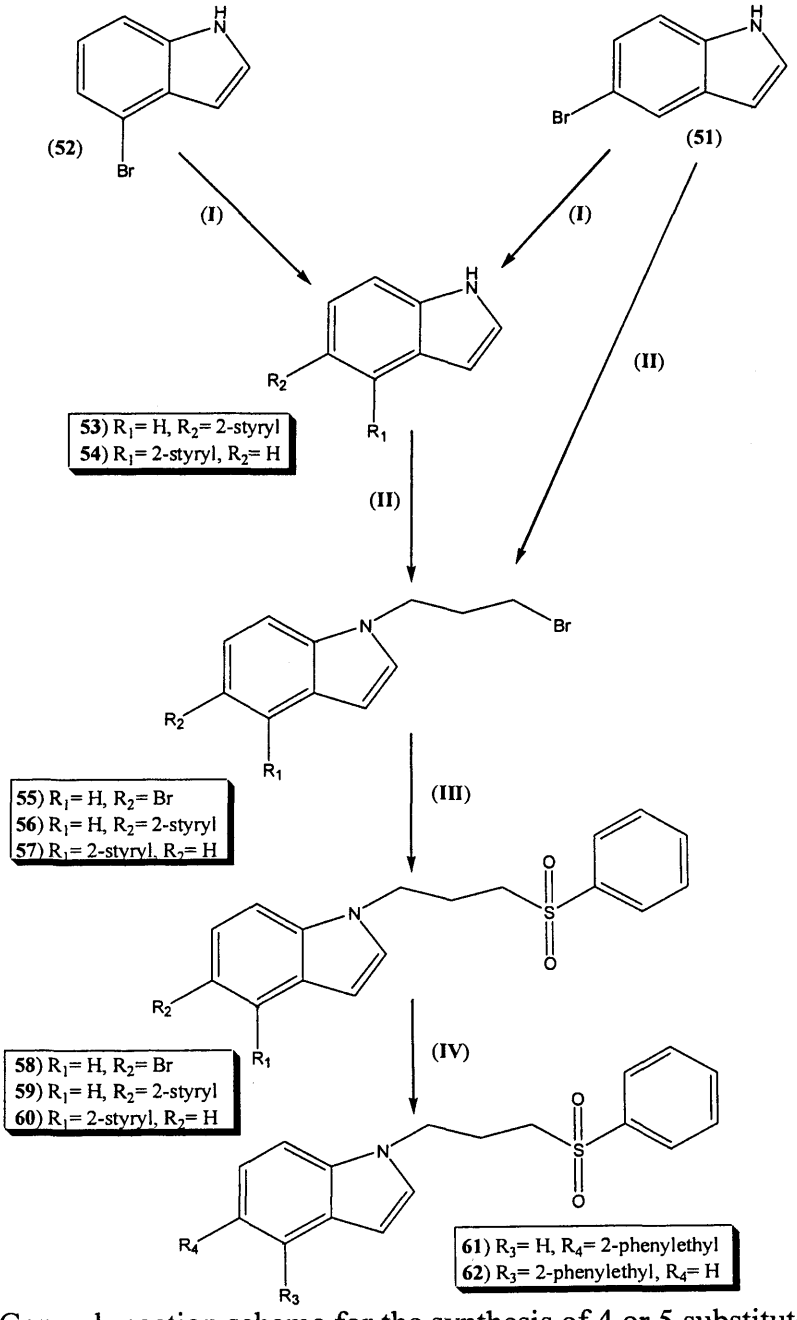

Scheme 9.1: General reaction scheme for the synthesis of 4 or 5 substituted 1-(3-benzenesulfonyl-propyl)-1*H*-indole. Reagents and conditions: (I) *trans*-phenylvinyl boronic acid, $Pd(PPh_3)_4$, aq. Na_2CO_3, toluene, reflux, 20h (II) dibromopropane, NaH, DMF, r.t. (III) $C_6H_5SO_2Na$, DMF, r.t., 24 h (IV) H_2, Pd, EtOH, r.t., 20 h.

The mechanism for the cross-coupling reaction involves (a) oxidative addition, (b) transmetallation, and (c) reductive elimination (Miyaura *et al.*, 1981; Suzuki, 1999) (**Figure 9.1**). Miyaura and co-workers (Miyaura *et al.*, 1985) suggested that the role of the base in the initial stage of the catalytic cycle (**Figure 9.1**) is to increase the carbanion character of the phenyl groups in organoboranes by their coordination with the boron atoms (by formation of an organoborate (**I**) with a tetravalent boron atom). This will then facilitate the transfer of phenyl groups from the boron to the palladium complexes in the transmetallation step to form Ar-Pd-Ar' (**II**) (**Figure 9.1**).

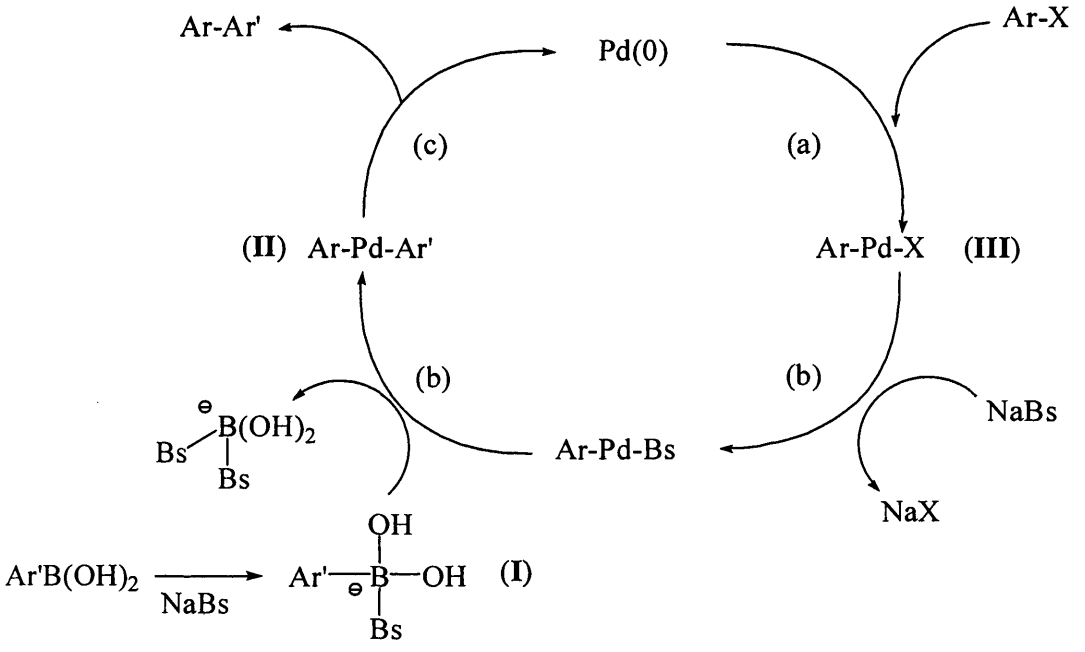

Figure 9.1: The catalytic cycle for the cross-coupling of arylboronic acid ($Ar'B(OH)_2$) with organic halide (Ar-X) catalysed by transition metal $Pd(PPh_3)_4$. Note: (a) Oxidative addition; (b) transmetallation; (c) reductive elimination; Pd(0) = $Pd(PPh_3)_4$; X = halides; Ar and Ar'= Phenyl group; Bs = base. (Suzuki, 1999).

The Suzuki reaction gave reasonably good yields of *E*-5-styryl-1*H*-indole (**53**) (71 %) and *E*-4-styryl-1*H*-indole (**54**) (87 %). The *E* configuration of the styryl side chain double bond was determined from the ^{1}H NMR coupling constant (J= 16.5 Hz).

Other palladium-catalysed coupling reactions such as Heck reaction (Schmidt and Smirnov, 2003) and Sonogoshira reaction (Henon *et al.*, 2006) have been tried and have been found much less satisfactory than the Suzuki reaction in the preparation of *E*-4 or 5-styryl-1*H*-indole.

9.1.2 Synthesis of *E*-4 or 5 substituted 1-(3-bromopropyl)-1*H*-indole

The synthesis of *N*-substituted indoles has been widely described in the literature. This involved the nucleophilic substitution of indoles with alkyl halides in basic media. Different bases have been used for this purpose including K_2CO_3 (Jorapur *et al.*, 2006), Cs_2CO_3 (Kumaraswamy *et al.*, 2006), KOH (Evans *et al.*, 2003), KO*t*Bu (Elokhdah *et al.*, 2004; Evans *et al.*, 2003) and NaH (Leze *et al.*, 2004; Evans *et al.*, 2005; Lane *et al.*, 2005). This reaction has been used successfully in the preparation of *N*-alkyl indoles (Lane *et al.*, 2005) and *N*-(aryl substituted)alkyl indoles (Evans *et al.*, 2005). In our case, the synthesis of 4 or 5 substituted 1-(3-bromo - propyl)-1*H*-indole was carried out through the reaction of dibromopropane with the corresponding indole in DMF in the presence of NaH as base (**Scheme 9.2**). The reaction was performed at 0 ^{O}C and in the presence of excess dibromopropane in order to decrease the formation of side-products such as the di-substituted propane. The reaction was complete after 5 min and the products were separated in good yield and purity after purification by flash column chromatography. The product was confirmed by the appearance of the three CH_2 peaks at approximately 2.1, 3.1 and 4.1 ppm in ^{1}H NMR. A summary of the results is presented in **Table 9.1**.

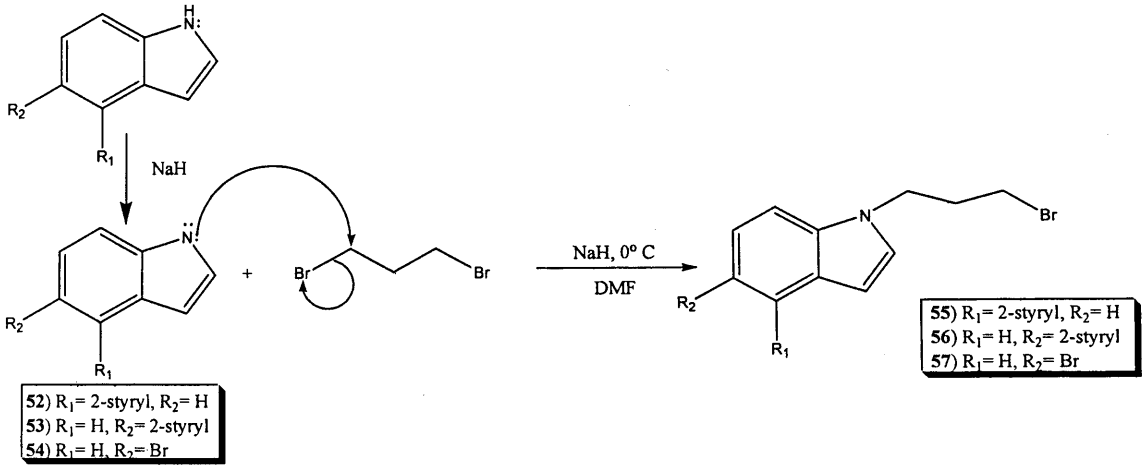

Scheme 9.2: Reaction of *E*-4 or 5-styryl-1*H*-indole with 1,3-dibromopropane.

Table 9.1: Summary of the synthesis of compounds (**55**) - (**57**).

Product	Yield (%)	Melting point (^{0}C)
55	74	70-72
56	71	78-80
57	78	-

9.1.3 Attachment of the benzenesulfonyl moiety

This was performed through the direct reaction of 4 or 5 substituted 1-(3-bromopropyl)-1*H*-indole with benzene sulfinic acid Na salt ($C_6H_5SO_2Na$) (**Scheme 9.3**) as previously described in the literature for the reaction of alkyl bromide with benzene sulfinic acid Na salt (Munz-Seeref *et al.*, 2005; Billaud *et al.*, 2003). The reaction was done in DMF with overnight stirring at room temperature. The products were obtained in good yield after purification by flash column chromatography. A summary of the results is presented in **Table 9.2**.

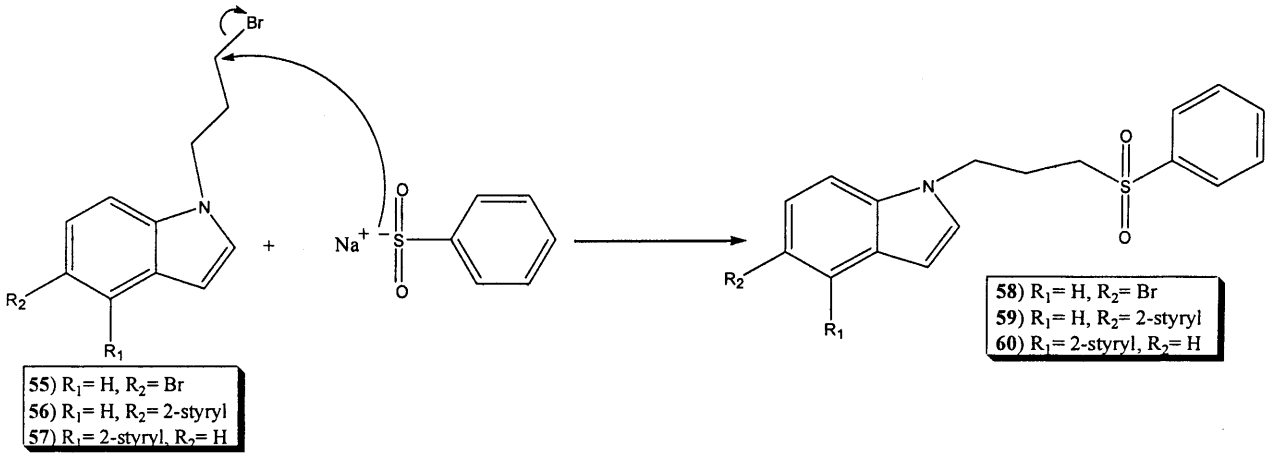

Scheme 9.3: Reaction of *E*-4 or 5 substituted 1-(3-bromo -propyl)-1*H*-indole with benzene sulphinic acid Na salt.

Table 9.2: Summary of the synthesis of compounds (**58**) - (**60**).

Product	Yield (%)
58	70
59	66
60	68

9.1.4 Reduction of the styryl side chain

The reduction was performed in a fume cupboard and using a hydrogen balloon as previously described in section **5.2.1.2** (Mateus *et al.*, 2000). The reaction was complete after 20 h stirring in EtOH at room temperature. The product was obtained in 82 % and 87 % yield for 5-styryl substituted indole (**59**) and 4-styryl substituted indole (**60**) respectively after purification by column chromatography. The

product was confirmed by the appearance of the two CH_2 peaks at approximately 2.9 ppm in ^1H NMR.

9.2 Experimental

<u>*E*-5-Styryl-1-*H*-indole (53)</u>

($C_{16}H_{13}N$, M.W. 219.286)

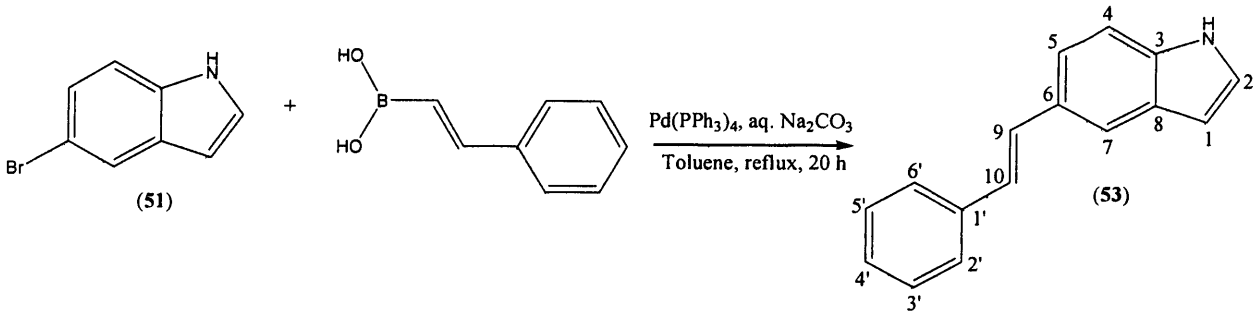

A solution of 5-bromoindole (2.0 g, 10.2 mmol) in anhydrous toluene (20 mL) was treated with $Pd(PPh_3)_4$ (1.18 g, 1.02 mmol). The mixture was then purged with N_2 and stirred for 30 minutes. *Trans*-2-phenylvinyl boronic acid (2.5 g, 16.9 mmol) was then added followed by sat. aq. Na_2CO_3 (8 mL) and the reaction mixture purged again with N_2 and refluxed for 20 h. The solvent was then evaporated in *vacuo* and the residue was dissolved in CH_2Cl_2 (100 mL), extracted with H_2O (2 x 50 mL) and dried ($MgSO_4$). The organic layer was evaporated to dryness under reduced pressure and the residue was purified by flash column chromatography (petroleum ether - EtOAc 100:0 v/v increasing to 70:30 v/v) to give *E*-5-styryl-1-*H*-indole (**53**) as a light brown solid. Yield: 1.59 g (71 %), t. l. c. system: petroleum ether – EtOAc 3:1 v/v, R_F: 0.27.

<u>^1H NMR:</u> δ ($CDCl_3$): 6.49 (s, 1H, H-1), 7.00 (d, J= 16.3 Hz, 1H, H-9), 7.11 (m, 1H, H-4'), 7.16 (s, 1H, Ar), 7.17 (d, J= 16.3 Hz, 1H, H-10), 7.28 (m, 3H, Ar), 7.37 (dd, J_1= 1.6 Hz, J_2= 7.8 Hz, 1H, Ar), 7.45 (d, J= 7.4 Hz, 2H, H-2', H-6'), 7.69 (s, 1H, H-7), 8.05 (s, 1H, NH).

<u>^{13}C NMR:</u> δ ($CDCl_3$): 103.07 (CH, C-1), 111.28 (CH, C-4), 119.51 (CH, C-5), 120.75 (CH, C-7), 124.75 (CH, C-2), 126.14 (CH, C-9), 126.23 (CH, C-10), 126.98 (CH, C-2', C-6'), 128.29 (C, C-8), 128.64 (CH, C-3', C-5'), 129.60 (C, C-6), 130.09 (CH, C-4'), 135.63 (C, C-3), 138.06 (C, C-1').

<u>Microanalysis:</u> Calculated for $C_{16}H_{13}N$. $0.3H_2O$ (224.689); Theoretical: %C= 85.53, %H= 5.83, %N= 6.23; Found: %C= 85.83, %H= 6.10, %N= 5.83.

Melting point: 146-148 ^{0}C

***E*-4-Styryl-1-*H*-indole (54)**

($C_{16}H_{13}N$, M.W. 219.286)

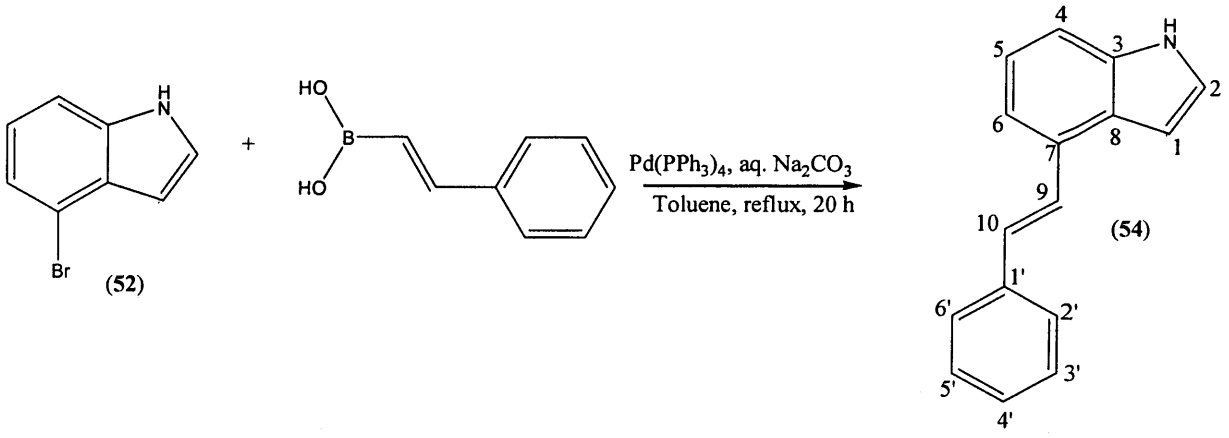

A solution of 4-bromoindole (2.0 g, 10.2 mmol) in anhydrous toluene (20 mL) was treated with $Pd(PPh_3)_4$ (1.18 g, 1.02 mmol). The mixture was then purged with N_2 and stirred for 30 minutes. *Trans*-phenylvinyl boronic acid (2.5 g, 16.9 mmol) was then added followed by sat. aq. Na_2CO_3 (8 mL) and the reaction mixture purged again with N_2 and refluxed for 20 h. The solvent was then evaporated in *vacuo* and the residue was dissolved in CH_2Cl_2 (100 mL), extracted with H_2O (2 x 50 mL) and dried ($MgSO_4$). The organic layer was evaporated to dryness under reduced pressure and the residue was purified by flash column chromatography (petroleum ether - EtOAc 100:0 v/v increasing to 70:30 v/v) to give *E*-4-styryl-1-*H*-indole (**54**) as a brownish green solid. Yield: 1.95 g (87 %), t. l. c. system: petroleum ether – EtOAc 3:1 v/v, R_F: 0.27.

^{1}H NMR: δ ($CDCl_3$): 6.72 (s, 1H, H-1), 7.03 (m, 1H, H-4'), 7.15 (m, 4H, H-2, H-4, H-5, H-6), 7.24 (d, J= 16.1 Hz, 1H, H-9), 7.28 (d, J= 7.4 Hz, 2H, H-3', H-5'), 7.45 (d, J= 16.3 Hz, 1H, H-10), 7.48 (d, J= 7.6 Hz, 2H, H-2', H-6'), 7.89 (s, 1H, NH).

^{13}C NMR: δ ($CDCl_3$): 100.07 (CH, C-1), 109.51 (CH, C-4), 113.60 (CH, C-5), 119.33 (CH, C-6), 121.62 (CH, C-2), 125.11 (C, C-8), 125.44 (CH, C-3', C-5'), 126.27 (CH, C-9), 126.36 (CH, C-10), 127.53 (CH, C-2', C-6'), 128.28 (CH, C-4'), 128.62 (C, C-7), 135.14 (C, C-1'), 136.87 (C, C-3).

Microanalysis: Calculated for $C_{16}H_{13}N$. $0.1H_2O$ (221.087); Theoretical: %C= 86.92, %H= 5.93, %N= 6.34; Found: %C= 87.10, %H= 5.86, %N= 6.40.

Melting point: 126-128 ^{0}C

***E*-5-Bromo-1-(3-bromopropyl)-1*H*-indole (55)**

($C_{11}H_{11}Br_2N$, M.W. 316.126)

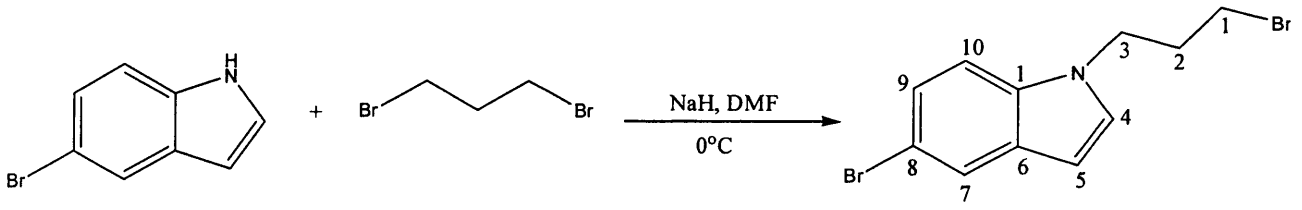

(51) (55)

To 5-bromoindole (1.0 g, 5.1 mmol) was added NaH (0.37 g, 15.3 mmol) and the mixture was cooled to 0 ^{0}C using an ice bath. Dry DMF (10 mL) was then added followed by dibromopropane (5.1 mL, 50.5 mmol) and the reaction mixture was stirred for 5 min. The solvent was evaporated under reduced pressure and the residue was dissolved in CH_2Cl_2 (100 mL), extracted with H_2O (2 x 50 mL) and dried ($MgSO_4$). The organic layer was then evaporated to dryness and the residue was purified by flash column chromatography (petroleum ether - EtOAc 100:0 v/v increasing to 95:5 v/v) to obtain the pure product 5-bromo-1-(3-bromopropyl)-1*H*-indole (**55**) as a white solid. Yield: 1.19 g, (74 %). t.l.c system: petroleum ether - EtOAc 3:1 v/v, R_F = 0.52.

^{1}H NMR: δ ($CDCl_3$): 2.18 (m, 2H, H-2), 3.12 (t, J= 6.1 Hz, 2H, H-1), 4.14 (t, J= 6.4 Hz, 2H, H-3), 6.32 (d, J= 3.1 Hz, 1H, H-5), 6.99 (d, J= 3.1 Hz, 1H, H-4), 7.10 (dd, J_1= 1.9 Hz, J_2= 7.9 Hz, 1H, H-9), 7.63 (d, J= 1.8 Hz, 1H, H-7).

^{13}C NMR: δ ($CDCl_3$): 29.79 (C, C-1), 32.73 (C, C-2), 44.18 (C, C-3), 101.62 (CH, C-5), 110.84 (CH, C-10), 112.91 (C, C-8), 123.58 (CH, C-9), 124.55 (CH, C-7), 129.20 (CH, C-4), 130.44 (C, C-6), 134.63 (C, C-11).

Microanalysis: Calculated for $C_{11}H_{11}Br_2N$ (316.126); Theoretical: %C= 41.68, %H= 3.50, %N= 4.42; Found: %C= 41.84, %H= 3.40, %N= 4.30.

Melting point: 70-72 ^{0}C

***E*-1-(3-Bromopropyl)-5-styryl-1*H*-indole (56)**

($C_{19}H_{18}BrN$, M.W. 340.262)

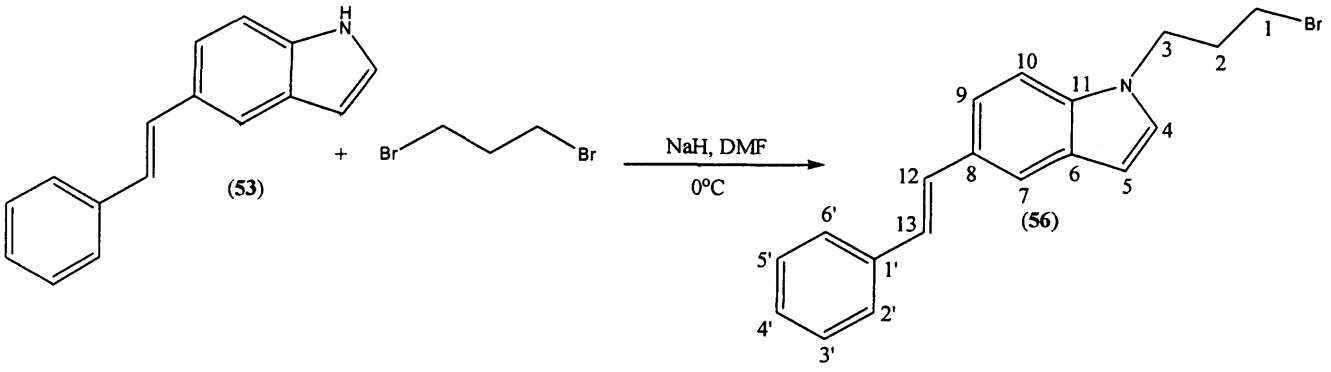

To (**53**) (1.0 g, 4.56 mmol) was added NaH (0.33 g, 13.68 mmol) and the mixture was cooled to 0 ^{0}C using an ice bath. Dry DMF (10 mL) was then added followed by dibromopropane (4.7 mL, 45.6 mmol) and the reaction mixture was stirred for 5 min. The solvent was evaporated under reduced pressure and the residue was dissolved in CH_2Cl_2 (100 mL), extracted with H_2O (2 x 50 mL) and dried ($MgSO_4$). The organic layer was then evaporated to dryness and the residue was purified by flash column chromatography (petroleum ether - EtOAc 100:0 v/v increasing to 90:10 v/v) to obtain the pure product *E*-1-(3-bromopropyl)-5-styryl-1*H*-indole (**56**) as a white solid. Yield: 1.1 g, (71 %). t.l.c system: petroleum ether - EtOAc 3:1 v/v, R_F = 0.43.

^{1}H NMR: δ ($CDCl_3$): 2.15 (m, 2H, H-2), 3.16 (t, J= 6.1 Hz, 2H, H-1), 4.11 (t, J= 6.4 Hz, 2H, H-3), 6.38 (d, J= 2.9 Hz, 1H, H-5), 6.96 (m, 2H, Ar), 7.13 (m, 2H, Ar), 7.21 (m, 3H, Ar), 7.33 (dd, J_1= 1.4 Hz, J_2= 7.6 Hz, 1H, H-9), 7.40 (d, J= 7.4 Hz, 2H, H-2', H-6'), 7.61 (s, 1H, H-7).

^{13}C NMR: δ ($CDCl_3$): 30.70 (C, C-1), 32.87 (C, C-2), 44.15 (C, C-3), 102.13 (CH, C-5), 109.43 (CH, C-10), 119.85 (CH, C-9), 120.49 (CH, C-7), 126.05 (CH, C-12), 126.22 (CH, C-13), 127.10 (CH, C-2', C-6'), 127.46 (CH, C-4, C-4'), 128.08 (C, C-6), 128.28 (C, C-8), 129.57 (CH, C-3', C-5'), 135.82 (C, C-1'), 138.13 (C, C-11).

Microanalysis: Calculated for $C_{19}H_{18}BrN$ (340.262); Theoretical: %C= 67.07, %H= 5.33, %N= 4.11; Found: %C= 67.61, %H= 5.39, %N= 4.02.

Subsequent product (**59**), (**61**) passed MS analysis.

Melting point: 78-80 ^{0}C

_E_-1-(3-Bromopropyl)-4-styryl-1*H*-indole (57)

($C_{19}H_{18}BrN$, M.W. 340.262)

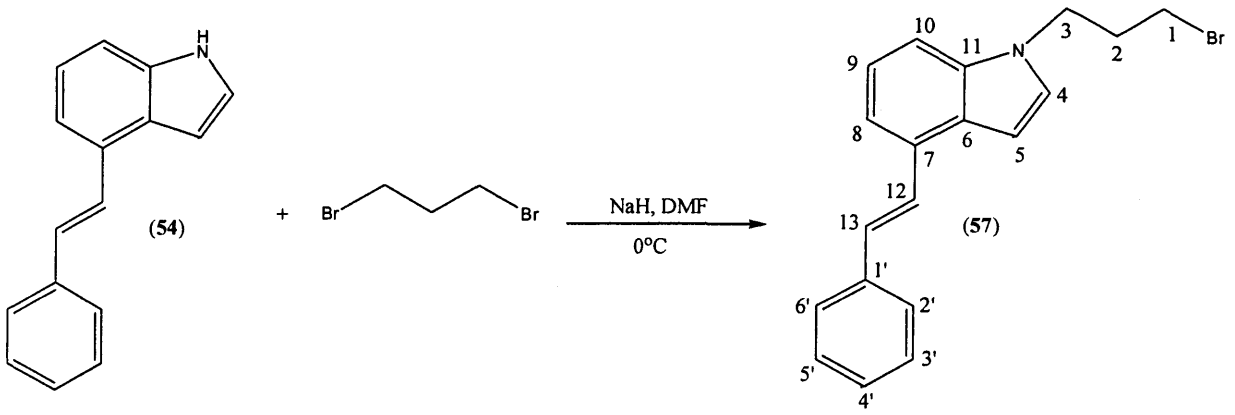

To (**54**) (1.0 g, 4.56 mmol) was added NaH (0.33 g, 13.68 mmol) and the mixture was cooled to 0 ^{0}C using an ice bath. Dry DMF (10 mL) was then added followed by dibromopropane (4.7 mL, 45.6 mmol) and the reaction mixture was stirred for 5 min. The solvent was evaporated under reduced pressure and the residue was dissolved in CH_2Cl_2 (100 mL), extracted with H_2O (2 x 50 mL) and dried ($MgSO_4$). The organic layer was then evaporated to dryness and the residue was purified by flash column chromatography (petroleum ether - EtOAc 100:0 v/v increasing to 90:10 v/v) to obtain the pure product *E*-1-(3-bromopropyl)-4-styryl-1*H*-indole (**57**) as a yellow oil. Yield: 1.21 g, (78 %). t.l.c system: petroleum ether-EtOAc 3:1 v/v, R_F = 0.45.

^{1}H NMR: δ ($CDCl_3$): 2.25 (m, 2H, H-2), 3.20 (t, J= 6.1 Hz, 2H, H-1), 4.25 (t, J= 6.7 Hz, 2H, H-3), 1.24 (t, J= 6.4 Hz, 2H, H-3), 6.71 (d, J= 2.6 Hz, 1H, H-5), 7.17 (m, 5H, Ar), 7.29 (m, 3H, Ar), 7.43 (d, J= 16.4 Hz, 1H, H-12), 7.50 (d, J= 7.3 Hz, 2H, H-2', H-6').

^{13}C NMR: δ ($CDCl_3$): 30.48 (C, C-1), 32.77 (C, C-2), 44.17 (C, C-3), 100.20 (CH, C-5), 108.77 (CH, C-10), 117.30 (CH, C-8), 121.99 (CH, C-9), 126.54 (CH, C-2', C-6'), 127.16 (CH, C-12), 127.46 (CH, C-13), 128.17 (CH, C-4'), 128.56 (CH, C-3', C-5'), 129.34 (C, C-4), 130.13 (C, C-6, C-7), 136.37 (C, C-1'), 137.98 (C, C-11).

LRMS indicated a mixture although NMR was clear and subsequent products (**60**), (**62**) passed MS analysis.

***E*-1-(3-Benzenesulfonylpropyl)-5-bromo-1*H*-indole (58)**

($C_{17}H_{16}NSO_2Br$, M.W. 377.271)

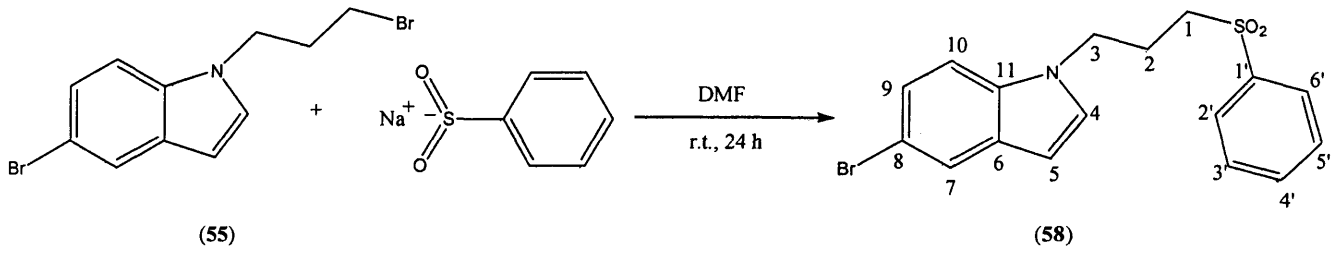

(55) (58)

To a solution of (**55**) (0.5 g, 1.58 mmol) in DMF (10 mL) was added $C_6H_5SO_2Na$ (0.26 g, 1.58 mmol) and the reaction stirred at room temperature for 24 h. The reaction mixture was then evaporated in *vacuo* and the residue was dissolved in CH_2Cl_2 (100 mL), extracted with H_2O (2 x 50 mL) and dried ($MgSO_4$). The organic layer was reduced in *vacuo* to give an oil which was purified by column chromatography (petroleum ether - EtOAc 70:30 v/v) to give 1-(3-benzenesulfonylpropyl)-5-bromo-1*H*-indole (**58**) as a brown oil. Yield: 0.42 g (70 %). t.l.c system: petroleum ether - EtOAc 2:1 v/v, R_F = 0.46, stain positive.

^{1}H NMR: δ ($CDCl_3$): 2.13 (m, 2H, H-2), 2.85 (t, J= 7.1 Hz, 2H, H-1), 4.13 (m, 2H, H-3), 6.30 (s, 1H, H-5), 6.94 (s, 1H, H-4), 7.02 (d, J= 8.7 Hz, 1H, H-10), 7.12 (d, J= 8.6 Hz, 1H, H-9), 7.40 (m, 2H, H-3', H-5'), 7.51 (m, 1H, C-4'), 7.61 (s, 1H, H-7), 7.71 (d, J= 7.7 Hz, 2H, C-2', C-6').

^{13}C NMR: δ ($CDCl_3$): 23.52 (C, C-2), 44.42 (C, C-1), 53.16 (C, C-3), 101.85 (CH, C-5), 110.70 (CH, C-10), 112.92 (C, C-8), 123.56 (CH, C-9), 124.63 (CH, C-7), 127.87 (CH, C-2', C-6'), 128.90 (CH, C-4), 129.45 (CH, C-3', C-5'), 130.38 (C, C-6), 133.97 (CH, C-4'), 134.50 (C, C-11), 138.78 (C, C-1').

HRMS (EI): Calculated mass: 378.0158 $(M+H)^+$, Measured mass : 378.0160 $(M+H)^+$.

E-1-(3-Benzenesulfonylpropyl)-5-styryl-1*H*-indole (59)

($C_{25}H_{23}NSO_2$, M.W. 401.518)

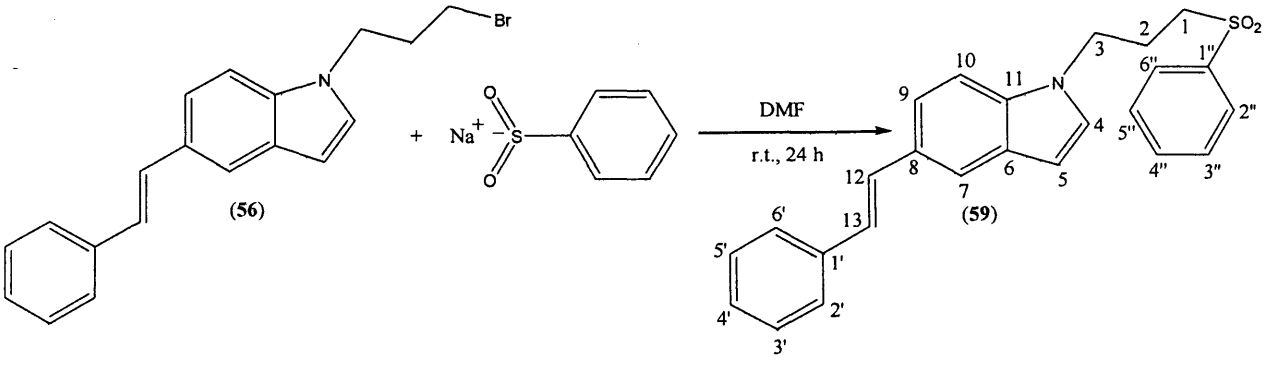

To a solution of (**56**) (0.5 g, 1.47 mmol) in DMF (10 mL) was added $C_6H_5SO_2Na$ (0.24 g, 1.47 mmol) and the reaction stirred at room temperature for 24 h. The reaction mixture was then evaporated in *vacuo* and the residue was dissolved in CH_2Cl_2 (100 mL), extracted with H_2O (2 x 50 mL) and dried ($MgSO_4$). The organic layer was reduced in *vacuo* and the crude product was recrystallised from EtOH to give *E*-1-(3-benzenesulfonylpropyl)-5-styryl-1*H*-indole (**59**) as white solid. Yield: 0.39 g (66 %). t.l.c system: petroleum ether - EtOAc 2:1 v/v, R_F = 0.37, stain positive.

^{1}H NMR: δ ($CDCl_3$): 2.23 (m, 2H, H-2), 2.92 (t, J= 7.1 Hz, 2H, H-1), 4.23 (t, J= 6.7 Hz, 2H, H-3), 6.43 (d, J= 3.1 Hz, 1H, H-5), 6.98 (d, J= 3.2, 1H, H-4), 7.00 (d, J= 16.2 Hz, 1H, H-12), 7.17 (m, 3H, H-10, H-13, H-4'), 7.28 (t, J= 7.7 Hz, 2H, H-3', H-5'), 7.35 (dd, J_1= 1.6 Hz, J_2= 7.8 Hz, 1H, H-7), 7.46 (m, 4H, H-2', H-6', H-3", H-5"), 7.55 (m, 1H, H-4"), 7.64 (s, 1H, H-9), 7.78 (m, 2H, H-2", H-6").

^{13}C NMR: δ ($CDCl_3$): 23.58 (C, C-2), 44.42 (C, C-1), 52.95 (C, C-3), 102.39 (CH, C-5), 109.40 (CH, C-10), 119.85 (CH, C-9), 120.58 (CH, C-7), 126.22 (CH, C-2', C-6'), 126.26 (CH, C-12), 127.03 (CH, C-13), 127.92 (CH, C-2", C-6"), 128.24 (CH, C-4), 128.64 (CH, C-3', C-5'), 129.08 (C, C-6'), 129.37 (C, C-8), 129.42 (CH, C-3", C-5"), 129.84 (CH, C-4'), 133.89 (CH, C-4"), 135.65 (C, C-1'), 137.97 (C, C-11), 138.69 (C, C-1").

HRMS (EI): Calculated mass: 402.1522 $(M+H)^+$, Measured mass : 402.1520 $(M+H)^+$.

_E_-1-(3-Benzenesulfonylpropyl)-4-styryl-1*H*-indole (60)

($C_{25}H_{23}NSO_2$, M.W. 401.518)

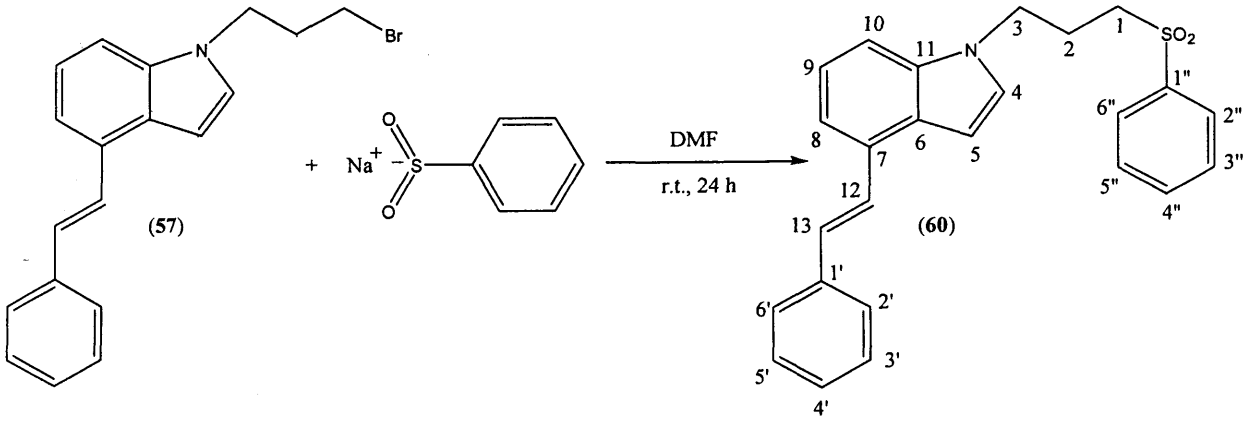

To a solution of (**57**) (0.5 g, 1.47 mmol) in DMF (10 mL) was added $C_6H_5SO_2Na$ (0.24 g, 1.47 mmol) and the reaction stirred at room temperature for 24 h.

The reaction mixture was then evaporated in *vacuo* and the residue was dissolved in CH_2Cl_2 (100 mL), extracted with H_2O (2 x 50 mL) and dried ($MgSO_4$). The organic layer was reduced in *vacuo* to give an oil which was purified by column chromatography (petroleum ether - EtOAc 100:0 v/v increasing to 70:30 v/v) to give *E*-1-(3-benzenesulfonylpropyl)-4-styryl-1*H*-indole (**60**) as a yellow oil. Yield: 0.4 g (68 %). t.l.c system: petroleum ether - EtOAc 2:1 v/v, R_F = 0.38, stain positive.

^{1}H NMR: δ ($CDCl_3$): 2.24 (m, 2H, H-2), 2.92 (t, J= 7.1 Hz, 2H, H-1), 4.25 (t, J= 6.7 Hz, 2H, H-3), 6.71 (d, J= 3.2 Hz, 1H, H-5), 7.07 (d, J= 3.2, 1H, H-4), 7.13 (d, J= 2.0 Hz, 1H, H-10), 7.16 (d, J= 18.3 Hz, 1H, H-12), 7.21 (m, 2H, H-9, H-4'), 7.30 (m, 3H, H-8, H-3', H-5'), 7.42 (d, J= 16.7 Hz, 1H, H-13), 7.45 (t, J= 7.9 Hz, 2H, H-3", H-5"), 7.50 (d, J= 7.3 Hz, 2H, H-2', H-6'), 7.56 (m, 1H, H-4"), 7.78 (m, 2H, H-2", H-6").

^{13}C NMR: δ ($CDCl_3$): 23.54 (C, C-2), 44.46 (C, C-1), 52.99 (C, C-3), 100.54 (CH, C-5), 108.55 (CH, C-10), 117.39 (CH, C-8), 122.15 (CH, C-9), 126.51 (CH, C-2', C-6'), 126.98 (C, C-6), 127.10 (CH, C-12), 127.48 (CH, C-13), 127.93 (CH, C-2" C-6"), 128.69 (CH, C-3', C-5'), 129.41 (C, C-3", C-5"), 129.59 (CH, C-4, C-4'), 130.16 (C, C-7), 133.94 (CH, C-4"), 136.30 (C, C-1'), 137.88 (C, C-1"), 138.93 (C, C-11).

HRMS (EI): Calculated mass: 402.1522 $(M+H)^+$, Measured mass : 402.1523 $(M+H)^+$.

1-(3-Benzenesulfonylpropyl)-5-phenethyl-1*H*-indole (61)

($C_{25}H_{25}NSO_2$, M.W. 403.534)

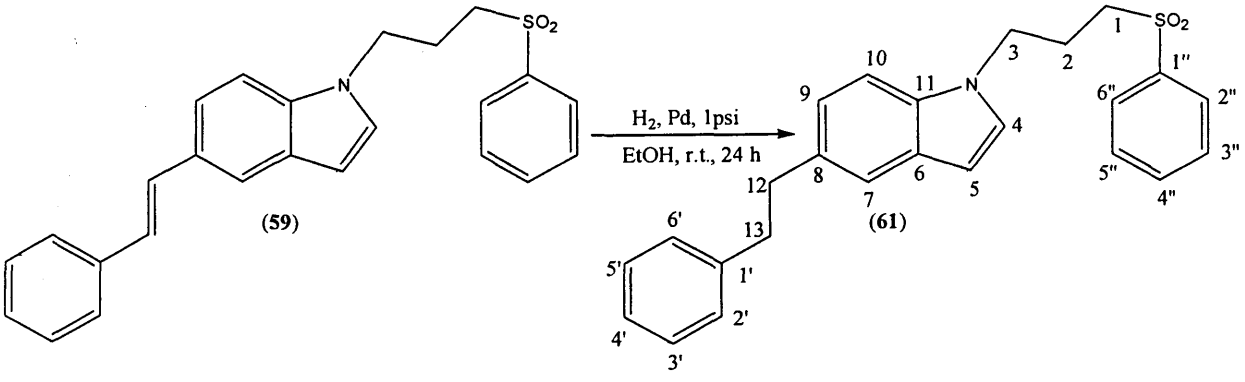

Pd/C catalyst (100 mg) was added to a solution of (**59**) (0.4 g, 1.0 mmol) in EtOH (20 mL) and the reaction was stirred under a H_2 atmosphere. After 30 min the H_2 balloon was removed and the mixture was filtered through Celite. The solvent was

removed under reduced pressure and the oil formed was extracted with CH_2Cl_2 (100 mL), washed with water (2 × 50 mL) and dried ($MgSO_4$). The organic layer was filtered and evaporated in *vacuo* and the product was then purified by column chromatography (petroleum ether - EtOAc 100:0 v/v increasing to 75:25 v/v) to give *E*-1-(3-benzenesulfonylpropyl)-5-phenethyl-1*H*-indole (**61**) as yellow oil. Yield: 0.33 g (82 %). t.l.c system: petroleum ether-EtOAc 3:1 v/v, R_F = 0.39, stain positive.

^{1}H NMR: δ ($CDCl_3$): 2.22 (m, 2H, H-2), 2.92 (m, 6H, H-1, H-12, H-13), 4.20 (t, J= 6.7 Hz, 2H, H-3), 6.35 (d, J= 3.1 Hz, 1H, H-5), 6.96 (d, J= 3.2, 1H, H-4), 6.98 (d, J= 1.6 Hz, 1H, H-9), 7.14 (m, 4H, Ar), 7.21 (m, 2H, Ar), 7.36 (s, 1H, Ar), 7.46 (m, 2H, H-3", H-5"), 7.56 (m, 1H, H-4"), 7.78 (m, 2H, H-2", H-6").

^{13}C NMR: δ ($CDCl_3$): 23.57 (C, C-2), 38.03 (C, C-13), 38.79 (C, C-12), 44.37 (C, C-1), 53.07 (C, C-3), 101.60 (CH, C-5), 108.92 (CH, C-10), 120.31 (CH, C-9), 122.88 (CH, C-7), 125.81 (CH, C-4'), 127.73 (CH, C-4), 127.95 (CH, C-2", C-6"), 128.32 (CH, C-2', C-6'), 128.46 (CH, C-3', C-5'), 128.93 (C, C-6), 129.40 (CH, C-3", C-5"), 133.19 (C, C-8), 133.86 (CH, C-4"), 134.54 (C, C-11), 140.71 (C, C-1"), 142.24 (C, C-1').

HRMS (EI): Calculated mass: 404.1679 $(M+H)^+$, Measured mass : 404.1678 $(M+H)^+$.

1-(3-Benzenesulfonylpropyl)-4-phenethyl-1*H*-indole (62)

($C_{25}H_{25}NSO_2$, M.W. 403.534)

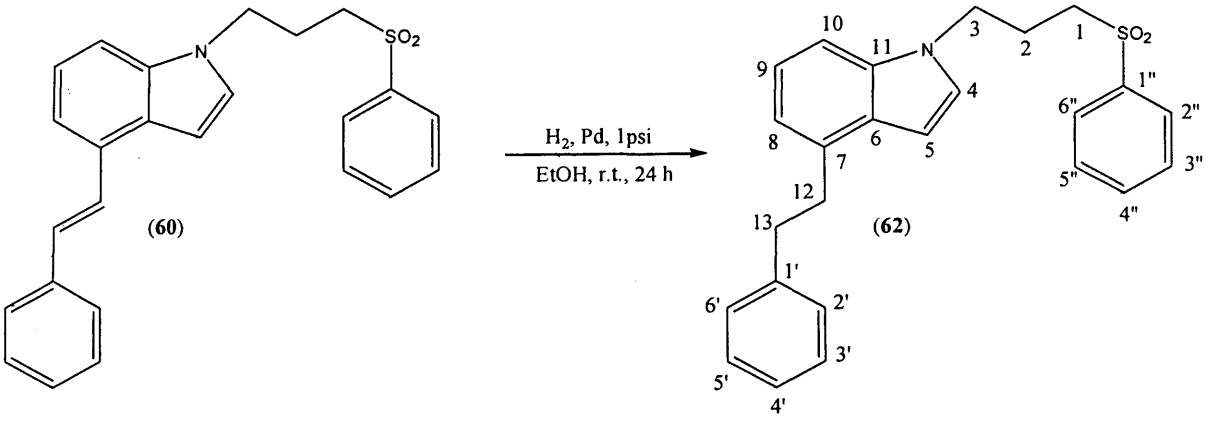

Pd/C catalyst (100 mg) was added to a solution of (**60**) (0.4 g, 1.0 mmol) in EtOH (20 mL) and then the reaction was stirred under a H_2 atmosphere. After 30 min the H_2 balloon was removed and the mixture was filtered through Celite. The solvent

was removed under reduced pressure and the oil formed was extracted with CH_2Cl_2 (100 mL), washed with water (2 × 50 mL) and dried ($MgSO_4$). The organic layer was filtered and evaporated in *vacuo* and the product was then purified by column chromatography (petroleum ether - EtOAc 100:0 v/v increasing to 75:25 v/v) to give *E*-1-(3-benzenesulfonylpropyl)-4-phenethyl-1*H*-indole (**62**) as colourless oil. Yield: 0.35 g (87 %). t.l.c system: petroleum ether - EtOAc 3:1 v/v, R_F = 0.39, stain positive.

^{1}H NMR: δ ($CDCl_3$): 2.22 (m, 2H, H-2), 2.94 (m, 4H, H-12, H-13), 3.10 (m, 2H, H-1), 4.21 (t, J= 6.7 Hz, 2H, H-3), 6.46 (d, J= 3.2 Hz, 1H, H-5), 6.90 (d, J= 6.5, 1H, H-4), 6.98 (d, J= 3.2 Hz, 1H, H-10), 7.05 (m, 3H, H-8, H-9, H-4'), 7.17 (d, J= 7.9 Hz, 2H, H-2', H-6'), 7.21 (m, 2H, H-3', H-5'), 7.45 (m, 2H, H-3", H-5"), 7.55 (m, 1H, 4"), 7.78 (m, 2H, H-2", H-6").

^{13}C NMR: δ ($CDCl_3$): 23.59 (C, C-2), 35.49 (C, C-12), 36.93 (C, C-13), 44.45 (C, C-1), 53.08 (C, C-3), 100.18 (CH, C-5), 107.20 (CH, C-10), 118.98 (CH, C-9), 122.07 (CH, C-8), 125.89 (CH, C-4'), 127.18 (CH, C-4), 127.60 (C, C-6), 127.96 (CH, C-2", C-6"), 128.38 (CH, C-2' C-6'), 128.43 (CH, C-3', C-5'), 129.42 (CH, C-3", C-5"), 133.89 (CH, C-4"), 134.51 (C, C-7), 135.84 (C, C-1"), 138.97 (C, C-11), 142.36 (C, C-1').

HRMS (EI): Calculated mass: 404.1679 $(M+H)^+$, Measured mass : 404.1677 $(M+H)^+$.

Chapter 10

Biological evaluation of CYP24A1 inhibitors

10 Biological evaluation of CYP24A1 inhibitors

The inhibitory activity of the novel compounds versus CYP24A1 was performed by Professor Glen Jones, Queen's University Kingston, Ontario, Canada. This involved an *in vitro* assay using recombinant cell lines expressing human CYP24 enzyme (V79-CYP24) (Prosser *et al.*, 2007; Masuda and Jones, 2006; Posner *et al.*, 2004). V79-CYP24 cells were cultured in DMEM media supplemented with 100 μg/mL hygromycin and 10% fetal bovine serum at 37 ^{O}C humidified atmosphere plus 5% CO_2. On the day of the assay, V79-CYP24 cells were collected by washing with 1 X PBS buffer, trypsinization and centrifugation. The cell pellet was resuspended in DMEM +1% BSA media and 250,000 cells in 150 μL were added to wells of a 48-well plate. After the cells were left for a preincubation period of 30 min at 37 °C in a humidified atmosphere containing 5% CO_2, 25 μL of inhibitor was added to each well. After 10 min, 25 μL of substrate [^{3}H-1β]-1α,25(OH)$_2$D$_3$ (20 nM) was added and the plate incubated for 2 h at 37 ^{O}C in a humidified atmosphere containing 5% CO_2. Both inhibitors and radiolabeled substrate were prepared in DMEM with 1% BSA media in the absence and presence of 100 μM 1,2 dianilinoethane, respectively. The reaction was terminated by the addition of 500 μL of methanol and transferred to glass tube. The aqueous phase was extracted and samples were then spun at 4000 rpm for 5 min. Triplicate 100 μL aliquots of aqueous fraction containing water-soluble CYP24 products were mixed with 600 μL of scintillation fluid and the radioactivity was measured using a scintillation counter.

The results of the assay are presented in **Table 10.1**. A good preliminary structure activity relationship was found with compounds having a styryl side chain in the 4-position (compounds **60**, **62**) being more active than those having styryl side chain in the 5-position (compounds **59**, **61**). On the other hand compounds having styryl side chain are more active then those having 2-phenylethyl-side chain, compounds **59**, **60** compared with compounds **61**, **62**. It is also noticeable that although compounds with benzenesulphonyl group are not very active they are still more active than those having a bromo group instead, compounds **59**, **60** compared with compounds **56**, **57**. Therefore, it is worth trying substituting the benzenesulphonyl group with a more basic group such as an imidazole or a triazole ring, such as compounds **4**, **5** in the library that showed good docking in the CYP24 active site and are expected to have better interaction with the haem.

Table 10.1: Results of the CYP 24 inhibitory assay.

Compound	Structure	IC_{50} (nM)
58	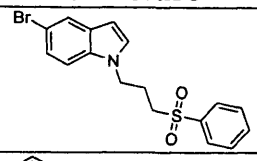	194.5
56	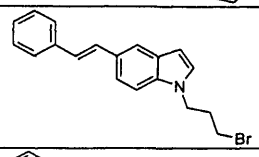	1503
59	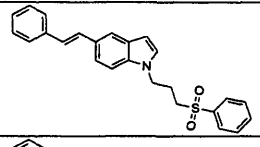	569
61	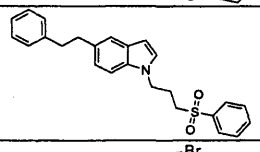	989
57	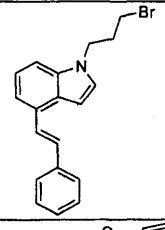	1200
60	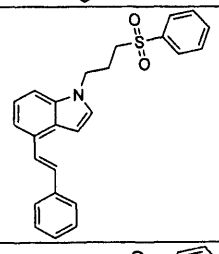	204
62	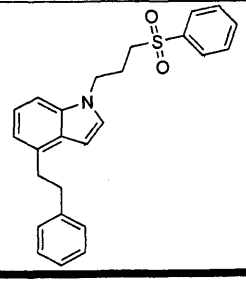	536

Ketoconazole 0.86 nM.

Chapter 11

Conclusions

11 Conclusions

This project was divided into two main parts; development of potential inhibitors firstly for CYP26 and secondly for CYP24 that could be used in differentiation therapy for prostate and breast cancer. The project involved the construction of 2 homology models for CYP26A1 and CYP24A1 that was used in the rational design of potential inhibitors. This was followed by chemical synthesis and biological evaluation of some of the promising compounds.

Homology models of cytochrome P450 RA1 (CYP26A1) and cytochrome P450 24 (CYP24A1) were constructed using MOE software. The lowest energy CYP26A1 and CYP24A1 models were then assessed and showed good stereochemical quality and side chain environment comparable with the templates. Further active site optimisation of the CYP26A1 and CYP24A1 models built using the CYP3A4 template was performed by molecular dynamics using Gromax software to generate final CYP26A1 and CYP24A1 models. The docking studies carried out on the final models showed that the models accommodated the natural substrate ATRA and vitamin D_3 as well as the potent inhibitors R115866 and VID-400 for CYP26A1 and CYP24A1 respectively. The constructed models were used to design potent inhibitors for CYP26A1 and CYP24A1 using virtual screening (Gomaa *et al.*, 2006; Gomaa *et al.*, 2007 – see appendix). A library of compounds based on the structure of potent inhibitors, natural sustrate and intuition was constructed using MOE QuaSAR-CombiGen and docked in the enzyme active site using FlexX program for CYP26A1 and CYP24A1 separately. The results revealed good interaction with the active site of several compounds and therefore potentially good CYP26A1 and CYP24A1 inhibition activity.

Two series were synthesised for CYP26A1 inhibition and were biologically evaluated using a MCF-7 breast cancer cell assay previously described by our group. Series 1 componds were designed to be α substituted 4-(1,2,4)triazol- and imidazol-1-ylmethylphenylaryl and heteroarylamine. This series showed moderate to good inhibitory activity with some compounds having IC_{50} of 0.5 μM (Gomaa *et al.*, 2008 – see appendix). Series 2 compounds were designed to contain an ester group that could be hydrolysed *in vivo* to a carboxylate group to further mimic the natural substrate and they were aryl and heteroaryl substituted 3-(4-aminophenyl)-3-imidazol-1-yl-2,2-dimethylpropionic acid methyl ester derivatives. These compounds showed enhanced

CYP26 inhibitory activity from which some have shown potent inhibitory activity, with IC_{50} in the low nanomolar range (20 nm), and others less active but still much more active then the well known inhibitor liarozole (patent in progress).

A series of 4 or 5 substituted 1-(3-benzenesulfonylpropyl)-1*H*-indole was synthesized and biologically tested for CYP24A1 inhibition. The series showed moderate inhibition activity with a good preliminary structure-activity relationship, suggesting SAR.

Chapter 12

References

12 References

Aapro, M.S. Adjuvant therapy of primary breast cancer: an overview of key findings from 7th international conference, St Gallen. *The Oncologist*, **2001** (6), 376-385.

Abbas, F. and Scardino, P.T. The natural history of clinical prostate carcinoma. *Cancer*, **1997** (80), 827-833.

Abdel-Hamid, M.K.; Abdel-Hafez, A.A.; El-Koussi, N.A.; Mahfouz, N.M.; Innocenti, A. and Supuran, C.T. Design, synthesis and docking studies of new 1,3,4-thiadiazole-2-thione derivatives with carbonic anhydrase inhibitory activity. *Bioorganic and Medicinal Chemistry*, **2007** (15), 6975-6984.

Abrahamsson, P.A.. Treatment of locally advanced prostate cancer: a new role for antiandrogen monotherapy. *European Urology*, **2001** (39), 22-28.

Abu-Abed, S.S.; Beckett, B.R.; Chiba, H.; Chithalen, J.V.; Jones, G.; Metzger, D.; Chambon, P. and Petkovich, M. Mouse P450RAI (CYP26) expression and retinoic acid-inducible retinoic acid metabolism in F9 cells are regulated by retinoic acid receptor gamma and retinoid X receptor alpha. *Journal of Biological Chemistry*, **1998** (273), 2409-2415.

Accelrys, **2004**, http://www.accelrys.com/

Adlercreutz, H. Phyto-oestrogens and cancer. *Lancet Oncology*, **2002** (3), 364-373.

Aelterman, W.; Lang, Y.; Willemsens, B.; Vervest, I; Leurs, S. and De Knaep, F. *Organic Process Research and Development*, **2001** (5), 467-471.

Ahmad, M.; Ahmadi, M.; Nicholls, P.J. and Smith, H.J. In-vitro metabolism of retinoic acid by different tissues from male rats. *Journal of Pharmacy and Pharmacology*, **2000** (52), 511-515.

Akiyoshi-Shibata, M.; Sakaki, T.; Ohyama, Y.; Noshiro, M.; Okuda, K. and Yabusaki, Y. Further oxidation of hydrocalcidiol by calcidiol-24-hydroxylase: A study with the mature enzyme expressed in *Escherichia Coli. European Journal of Biochemistry.*, **1994** (224), 335-343.

American cancer society, updated Sep **2007**, http://www.sciencedaily.com/releases/2007/09/070925130014.htm

Anonymous, *British National Formulary,* 47 March **2004**, British medical association and royal pharmaceutical society of Great Britain, London.

Anonymous,http://training.seer.cancer.gov/ss_module01_breast/until02_sec02_breast _ Anatomy.htmL, accessed: 15 July 2005.

Anonymous, dailymail breast cancer special report, http://www.dailymail.co.uk/pages/live/articles/health/healthmain.html?in_article_id=364338&in_page_id=1774, accessed: 11 December 2007.

Anonymous, Breast radiotherapy after breast-conserving surgery. The steering committee on clinical practice guidelines for the care and treatment of breast cancer. Canadian association of radiation oncologists, *Canadian Medical Association Journal,* **1998** (158 Suppl 3), S35-42.

Antilla, J.C. and Buchwald, S.L. Copper-catalysed coupling of arylboronic acids and amines. *Organic Letters*, **2001** (3), 2077-2079.

Armstrong, J.L.; Ruiz, M.; Boddy, A.V.; Redfern, C.P.F.; Pearson, A.D.J. and Veal, G.J. Increasing the intracellular availability of all-trans retinoic acid in neuroblastoma cells. *British Journal of Cancer*, **2005** (92), 696-704.

Assikis, V. J. and Buzdar, A. Recent advances in aromatase inhibitor therapy for breast cancer. *Seminars in Oncology,* **2002** (29), 120-128.

Altschul, S.F.; Madden, T.L.; Schaffer, A.A.; Zhang, G.; Zhang, Z.; Miller, W. and Lipman, D.J. Gapped BLAST and PSI-BLAST: a new generation of protein database search programs. *Nucleic. Acids Research.*, **1997** (25), 3389-3402.

Azzam, R.; Borggraeve, W.M.D.; Compernolle, F. and Hoornaert, G.J. Expanding the substitution pattern of 2(1*H*)-pyrazinones via Suzuki and Heck reactions. *Tetrahedron*, **2005** (61), 3953-3962.

Baker, A.R.; McDonnell, D.P.; Hughes, M.; Crisp, T.M.; Mangelsdorf, D.J.; Haussler, M.R.; Pike, J.W.; Shine, J. and Omalley, B.W. cloning and expression of full-length cDNA-encoding human vitamin-D receptor. *Proceedings of the National Academy of Sciences of the United States of America*, **1988** (85), 3294-3298.

Barder, T.E.; Walker, S.D.; Martinelli, J.R. and Buchwald, S.L. Catalysis for Suzuki-Miyaura coupling processes: Scope and studies of the effect of ligand structure. *Journal of the American Chemical Society*, **2005** (127), 4685-4696.

Barton, D.H.R.; Finet, J.P. and Khamsi, J. Copper-salts catalysis of *N*-phenylation of amines by trivalent organobismuth compounds. *Tetrahedron Letters*, **1987** (28), 887-890.

Barton, G.J. In protein structure prediction: A practical approach, *ed. M. J. E. Sternberg, IRL press at Oxford university press, Oxford*, **1996**, 31-64.

Beer, T.M.; Park, B.; Morie, M.; Sauer, D. and Eilers, K. Effect of calcitriol on prostate-specific antigen *in vitro* and in humans. *Clinical Cancer Research*, **2006** (12), 2812-2816.

Bentrem, D. J. and Craig Jordan, V. Tamoxifen, raloxifene and the prevention of breast cancer. *Minerva Endocrinology,* **2002** (27), 127-139.

Berendsen, H.J.C.; vander Spoel, D.; van Drunen, R. GROMACS: A message-passing parallel molecular dynamics implementation. *Computer Physics Communications*, **1995** (91), 43-56.

Bergfeldt, K.; Rydh, B.; Granath, F.; Gronberg, H.; Thalib, L.; Adami, H. O. and Hall, P. Risk of ovarian cancer in breast-cancer patients with a family history of breast or ovarian cancer: A population-based cohort study. *Lancet,* **2002** (360), 891-894.

Berman, H.M.; Westbrook, J.; Feng, Z.; Gilliland, G.; Bhat, T.N.; Weissig, H.; Shindyalov, P.E. and Bourne, P.E. the protein Data Bank. *Nucleic Acids Research*, **2000** (28), 235-242.

Bertha F., Hornyak G., Lempert K. Z. K. and Toht E. P. G. Benzoxadiazocines, benzothiadiazocines and benzotriazocines-III, The synthesis of 2-

(subst.)amino- and 2-(2-subst.hydrazino)-6-(alkylsulfonyl and arylsulfonyl)-5,6-dihydro-4H-3,1,6-benzothiadiazocines. *Tetrahedron*, **1983** (39), 1203.

Billaud, C.; Goddard, J.P.; Gall, T.L. and Mioskowski, C. Preparation of alcohols from sulfones and trialkylboranes. *Tetrahedron Letters*, **2003** (44), 4451-4454.

Biotech, **2004**, http://biotech.embl-ebi.ac.uk:8400/

Blaner, W.S. and Olson, J.A. Retinol and retinoic acid metabolism, In Sporn, M.B., Roberts, A.B. and Goodman, D.S. (eds), *The retinoids: biology, chemistry and medicine*, **1994**, Raven Press, New-York, 229-257.

Blut, S.E. and Weigel, N.L. Vitamin D and prostate cancer. *Proceedings of the Society for Experimental Biology and Medicine*, **1999** (221), 89-98.

Blutt, S.E.; McDonnell, T.J.; Polek, T.C. and Weigel, N.L. Calcitriol-induced apoptosis in LNCaP cells is blocked by overexpression of Bcl-2. *Endocrinology*, **2000** (141), 10-17.

Bohacek, R.S. and Mcmartin, C. Modern computational chemistry and drug discovery: structure generating programs. *Current Opinion in Chemical Biology.*, **1997** (1), 157-161.

Bohlke, K.; Spiegelman, D.; Trichopoulou, A.; Katsouyanni, K. and Trichopoulos, D. Vitamins a, c and e and the risk of breast cancer: Results from a case-control study in Greece. *British Journal of Cancer,* **1999** (79), 23-29.

Bohm, H.J. the computer program LUDI: a new method for the *de novo* design of enzyme inhibitors. *Journal of Computer–Added Molecular Design*, **1992** (6), 61-78.

Bollag, W. The retinoid revolution. *FASEB Journal*, **1996** (10), 938-939.

Boring, C.C.; Squires, T.S. and Tong, T. Cancer statistics. *Cancer Journal for Clinicians*, **1992** (42), 19-38.

Bouillon, R. Okamura, W.H. and Norman, A.W. Structure-function-relationships in the vitamin-D endocrine system. *Endocrine Reviews*, **1995** (16), 200-257.

Bray, F.; Sankila, R.; Ferlay, J. and Parkin, D.M. Estimates of cancer incidence and mortality in Europe in 1995. *European Journal of Cancer*, (**2002**) 38, 99-166.

Brewster, A. and Helzlsouer, K. Breast cancer epidemiology, prevention and early detection. *Current Opinion in Oncology,* **2001** (13), 420-425.

Briest S. and davidson, N.E. Aromatase inhibitors for breast cancer. *Reviews in Endocrine and metabolic disorders*, **2007** (8), 215.

Brinkmann, A.O. Molecular basis of androgen insensitivity. *Molecular and Cellular Endocrinology*, **2001** (179), 105-109.

Britton, J. A.; Gammon, M. D.; Schoenberg, J. B.; Stanford, J. L.; Coates, R. J.; Swanson, C. A.; Potischman, N.; Malone, K. E.; Brogan, D. J.; Daling, J. R. and Brinton, L. A. Risk of breast cancer classified by joint estrogen receptor and progesterone receptor status among women 20-44 years of age. *American Journal of Epidemiology,* **2002** (156), 507-516.

Brodie, A.M.H. Aromatase inhibition and its pharmacologic implications. *Biochemical Pharmacology*, **1985** (34), 3213-3219.

Bugge, T.H.; Pohl, J.; Lonnoy, O. and Stunnenberg, H.G. RXR: a promiscuous partner of retinoic acid and thyroid hormone receptors. *EMBO Journal*, **1992** (11), 1409-1418.

Bundred, N.J. Prognostic and predictive factors in breast cancer. *Cancer Treatment Reviews*, **2001** (27), 137-142.

Buzdar, A.U. Endocrine therapy for breast cancer, In Hunt, K.K.; Robb, G.L.; Strom, E.A.; Tuero, N. (ed), *Breast cancer*, Spinger-Verlag, New-York, **2001**, 366-391.

Buzdar, A.U. Preoperative chemotherapy treatment of breast cancer. A review. *Cancer*, **2007** (110), 2394.

Campbell, M.J. and Koeffler, H.P. Toward therapeutic intervention of cancer by vitamin D compounds. *Journal of the National Cancer Institute*, **1997** (89), 182-185.

Carter, B. S.; Beaty, T. H.; Steinberg, G. D.; Childs, B. and Walsh, P. C. Mendelian inheritance of familial prostate cancer. *Proceedings of the National Academy of Science of U S A*, **1992** (89), 3367-3371.

Catalona, W. J. Prostate cancer. *Current Problems in Surgery,* **1990** (27), 389-461.

Chajes, V.; Hulten, K.; Van Kappel, A. L.; Winkvist, A.; Kaaks, R.; Hallmans, G.; Lenner, P. and Riboli, E. Fatty-acid composition in serum phospholipids and risk of breast cancer: An incident case-control study in Sweden. *International Journal of Cancer,* **1999** (83), 585-590.

Chamberlain, J.; Melia, J.; Moss, S. and Brown, J. Treatment of advanced prostate cancer. *Health Technology Assessment*, **1997** (1), 35-39.

Chambon, P. A decade of molecular biology of retinoic acid receptors. *FASEB Journal*, **1996** (10), 940-954.

Chan, D.M.T.; Monaco, K.L.; Wang, R. and Winters, M.P. New N- and O- arylations with phenyl boronic acids and cupric acetate. *Tetrahedron Letters*, **1998** (39), 2933-2936.

Chan, J. M.; Stampfer, M. J. and Giovannucci, E. L. What causes prostate cancer? A brief summary of the epidemiology. *Seminars in Cancer Biology,* **1998** (8), 263-273.

Chen, K.S.; Prahl, J.M. and DeLuca, H.F. Isolation and expression of human 1,25-dihydroxyvitamin D_3 24-hydroxylase cDNA. *Proceedings of the National Academy of Sciences of the United States of America*, **1993** (90), 4543-4547.

Chen, K.S. and DeLuca, H.F. Cloning of the human 1 alpha,25-dihydroxyvitamin D_3 24-hydroxylase gene promoter and identification of two vitamin D-responsive elements. *Biochimica et Biophysica Acta*, **1995** (1263), 1-9.

Chen, Z.X.; Xue, Y.Q.; Zhang, R.; Tao, R.F.; Xia, X.M.; Li, C.; Wang, W.; Zu, W.Y.; Yao, X.Z. and Ling, B.J. A clinical and experimental study on all-*trans* retinoic acid-treated acute promyelocytic leukemia patients. *Blood*, **1991** (78), 1-12.

Chithalen, J.V.; Luu, L.; Petkovich, M. and Jones, G. HPLC-MS/MS analysis of the products generated from all-*trans*-retinoic acid using recombinant human CYP26A. *Journal of Lipid Research*, **2002** (43), 1133-1142.

Chodak, G.; Sharifi, R.; Kasimis, B.; Block, N.L.; Macramalla, E. and Kennealey, G.T. Single-agent therapy with bicalutamide - a comparison with medical or surgical castration in the treatment of advanced prostate carcinoma. *Urology*, **1995** (46), 849-855.

Chothia, C. and Lesk, A.M. The relation between the divergence of sequence and structure in proteins. *EMBO Journal*, **1986** (5), 823-826.

Christov, K.T.; Moon, R.C.; Lantvit, D.D.; Steele, V.E.; Lubet, R.A.; Kelloff, G.J. and Pezzuto, J.M. 9-cis retinoic acid but not 4-(hydroxyphenyl)retinamide inhibits prostate intraepithelial neoplasia in nobel rats. *Cancer Reaserch*, **2002** (62), 5178-5182.

Clemett, D. and Lamb, H. M. Exemestane: A review of its use in postmenopausal women with advanced breast cancer. *Drugs*, **2000** (59), 1279-1296.

ClustalW WWW Service at the European Bioinformatics Institute http://www.ebi.ac.uk/clustalw.

Coburn, M. C. and Bland, K. I. Surgery for early and minimally invasive breast cancer. *Current Opinion in Oncology*, **1995** (7), 506-510.

Code "scoring svl" obtained from SVL Exchange website http://svl.chemcomp.com Chemical Computing Group Inc Montreal Canada.

Cohen, J.H.; Kristal, A.R. and Stanford, J.L. Fruit and vegetable intakes and prostate cancer risk. *Journal of the National Cancer Institute*, **2000** (92), 61-68.

Colovos, C. and Yeates, T.O. Verification of protein structures: pattern of non-bonded atomic intercactions. *Protein Science.*, **1993** (2), 1511-1519.

Cotter, M. P.; Gern, R. W.; Ho, G. Y.; Chang, R. Y. and Burk, R. D. Role of family history and ethnicity on the mode and age of prostate cancer presentation. *Prostate*, **2002** (50), 216-221.

Culine, S.; Kramar, A.; Droz, J.P. and Theodore, C. Phase II study of all-*trans* retinoic acid administered intermittently for hormone refractory prostate cancer. *The Journal of Urology*, **1999** (161), 173-175.

Cunliffe, W.J. Acne, retinoids and proposed clinical trials. *Retinoids*, **2002** (18), 1.

Curley, R.W. and Robarge, M.J. Retinoid structure, chemistry and biologically active derivatives, In G.V., S. (ed), *Retinoids: their physiological function and therapeutic potential*, **1997**, JAI Press Inc, London, 1-34.

Czeczuqa-Semeniuk, E.; Dzieciol, J. and Anchim, T. The effect of doxorubicin and retinoids on proliferation, necrosis and apoptosis in MCF-7 breast cancer cells. *Folia Histochemica Et Cytobiologica*, **2004** (42), 221-227.

Dahiya, R.; Park, H.D.; Cusick, J.; Vessella, R.L.; Fournier, G. and Narayan, P. Inhibition of tumorigenic potential and prostate-specific antigen expression in LNCaP human prostate cancer cell line by 13-cis retinoic acid. *International Journal of Cancer*, **1994** (59), 126-132.

D'Amico, A.V.; Kantoff, P.W. and Chen, M.H. Aspirin and hormone therapy for prostate cancer. *New England Journal of Medicine*, **2007** (357), 2737-2738.

Dalesio, O.; van Tinteren, H.; Clarke, M.; Peto, R.; Schroder, F.H.; Dechering, I.; Evans, V.; Godwin, J.; Blumenstein, B.A.; Crawford, E.D.; Denis, L.; Hall, R.; Hill, C.; Iversen, P.; Shipley, W.U.; Soloway, M. and Sylvester, R. Maximum androgen blockade in advanced prostate cancer: an overview of the randomised trials. *Lancet*, **2000** (355), 1491-1498.

Dawson, J.H. Probing structure-function relations in haem-containing oxygenases and peroxidises. *Science*, **1988** (240), 433-439.

Debes, J.D. and Tindall, D.J. Mini review: The role of androgens and the androgen receptor in prostate cancer. *Cancer Letters*, **2002** (187), 1-7.

Debruyne, F.J.M.; Murray, R.; Fradet, Y.; Johansson, J. E.; Tyrrell, C.; Boccardo, F.; Denis, L.; Marberger, J.M.; Brune, D.; Rassweiler, J.; Vangeneugden, T.; Bruynseels, J.; Janssens, M. and De Porre, P. *Urology*, **1998** (52),72.

De Coster, R.; Wouters, W.; Vanginckel, R.; End, D.; Krekels, M.; Coene, M.C. and Bowden, C. Experimental Studies with Liarozole (R-75251) - an Antitumoral Agent Which Inhibits Retinoic Acid Breakdown *Journal of Steroid Biochemistry and Molecular Biology*, **1992** (43), 197-201.

Deloukas, P.; Matthews, L.H.; Ashurst, J.L.; Burton, J.; Gilbert, J.G.R.; Jones M.; Stavrides, G.; Almeida, J.P.; Babbage, A.K.; Bagguley, C.L.; Bailey, J.; Barlow, K.F.; Bates, K.N.; Beard, L.M.; Beare, D.M.; Beasley, O.P.; Bird, C.P.; Blakey, S.E.; Bridgeman, A.M. and Rogers, J. The DNA sequence and comparative analysis of human chromosome 20. *Nature*, **2001** (414), 865-871.

DeLuca, H.F. The vitmain-D story - a collaborative effort of basic science and clinical medicine. *FASEB Journal*, **1988** (2), 224-236.

DeMatteis, F. In *iron in biochemistry and medicine, 2nd Ed*, **1980**, Academic Press, London, New York, 5293-324.

Denmark, S.E.; Winter, S.B.D.; Su, X. and Wong, K.T. Chemistry of trichlorosilyl enolates, new reagents for catalytic asymmetric aldol additions. *Journal of the American Chemical Society*, 1996 (118), 7404-7405.

De Vos, S.; Dawson, M.I.; Holden, S.; Le, J.; Wang, A.; Cho, S.; Chen, D. and Koeffler, H.P. Effects of retinoic X receptor (RXR)-class-selective ligands on prostate cancer cell proliferation. *Prostate*, **1997** (32), 115-121.

DiSepio, D.; Malhotra, M.; Chandraratna, R.A.S. and Nagpal, S. Retinoic acid receptor-nuclear factor-interleukin 6 antagonism, a novel mechanism of retinoid dependent inhibition of a keratinocyte hyperprolifertaive differentiation marker. *Journal of Biological Chemistry*, **1997** (272), 2555-2559.

Djikman, G.A.; Van Moorselaar, R.J.A.; Van Ginckel, R.; Van Stratum, P.; Wouters, L.; Debruyne, F.M.J.; Schalken, J.A. and De Coster, R. Antitumoral effects of liarozole in androgen-dependent and independent R3327-Dunning prostate adenocarcinomes. *Journal of Urology*, **1994** (151), 217-222.

Dodds, E.C.; Goldberg, L.; Lawson, W. and Robinson, R. Oestrogenic activity of alkylated stilboestrols. *Nature*, **1938** (142), 34.

Drabel, W. and Regel, E. Process for the production of N-(1,1,1-trisubstituted)-methylazoles. *Germany*, **1975** (117), 161.

Dragnev, K.H.; Freemantle, S.J.; Spinella, M. and Dmitrovsky, E. Cyclin proteolysis as a retinoid cancer prevention mechanism. *Annals of the New York Academy of Sciences*, **2001** (952), 13-22.

Dyrstad, S.W.; Shah, P. and Rao, K. Chemotherapy for prostate cancer. *Current Pharmaceutical design*, **2006** (12), 819-838.

EBI, 2004, http://www.ebi.ac.uk/dali/fssp.

ECCO, 11 and societies, F.o.e.c. Cancer incidence, mortality and survival. **2000**, ECCO 11 The European cancer conference.

Eisen, M.D.; Wiley, D.C.; Karplus, M. and Hubbard, D.E. Hook-A program for finding novel molecular arcitectures that satisfy the chemical and sterric requirements of a molecular binding site. *Proteins*, **1994** (19), 199-221.

Eisenberger, M.A.; Blumenstein, B.A.; Crawford, E.D.; Miller, G.; McLeod, D.G.; Loehrer, P.J.; Wilding, G.; Sears, K.; Culkin, D.J.; Thompson, I.M.; Bueschen, A.J. and Lowe, B.A. Bilateral orchiectomy with or without flutamide for metastatic prostate cancer. *New England Journal of Medicine*, **1998** (339), 1036-1042.

Eldridge, M.D.; Murray, C.W.; Auton, T.R.; Paolini, G.V. and Mee, R.P. Emperical scoring functions: I. The development of fast empirical scoring function to estimate the binding affinity of ligands in receptor complexes. *Journal of Computer-Aided Molecular Design*, **1994** (8), 243.

Elokdah, H.; Gharbia, M.A.; Hennan, J.K.; Mcfarlane, G.; Mugford, C.P.; Krishnamurthy, G. and Crandall, D.L. Tiplaxtinin, a novel, orally efficacious inhibitor of plasminogen activator inhibitor-1: Design, synthesis and preclinical characterization. *Journal of Medicinal Chemistry*, **2004** (47), 3491-3494.

EMBL, **2004**, http://dove.embl-heidelberg.de/Blast2/

Errat, **2004**, http://www.doe-mbi.ucla/Services/ERRAT/

Ettinger, R.A. and DeLuca, H.F. The Vitamin D endocrine system and its therapeutic potential. *Advances in Drug Research.*, **1996** (28), 269-312.

Evans, D.A.; Katz, J.L. and West, T.R., Synthesis of diaryl ethers through the copper-promoted arylation of phenols with aryl boronic acids. An expedient synthesis of thyroxine. *Tetrahedron Letters*, **1998** (39), 2937-2940.

Evans, D.A.; Fandrick, K.R. and Song, H.J., Enantioselective Freidel-crafts alkylations of α,β-unsaturated 2-acyl imidazoles catalysed by bis(oxazolinyl)pyridine-scandium(III) triflate complexes. *Journal of the American Chemical Society*, **2005** (127), 8942-8943.

Evans, D.A.; Scheidt, K.A.; Fandrick, K.R.; Lam, H.W. and Wu, J. Enantioselective indole Freidel-crafts alkylations catalysed by bis(oxazolinyl)pyridine-scandium(III) triflate complexes. *Journal of the American Chemical Society*, **2003** (125), 10780-10781.

Ewing, T. and Kuntz, I.D. Critical evaluation of search algorithms for automated molecular docking and database screening. *Journal of Computational Chemistry*, **1997** (18), 1175-1189.

Expasy server, **2004**, http://ca.expasy.org.

Expasy server, **2004a**, http//us.expasy.org/cgi-bin/niceprot.pl?p43174.

Expasy server, **2004b**, http//us.expasy.org/cgi-bin/niceprot.pl?p08684.

Expasy server, **2004c**, http//us.expasy.org/cgi-bin/niceprot.pl?p11712.

Expasy server, **2004d**, http//us.expasy.org/cgi-bin/niceprot.pl?p10632.

Expasy server, **2004e**, http://ca.expasy.org/cgi-bin/niceprot.pl?Q07973.

Farhan, H.; Wahala, K.; Adlercreutz, H. and Cross, H.S. Isoflavonoids inhibit catabolism of vitamin D in prostate cancer cells. *Journal of Chromatography B*, **2002** (777), 261-268.

Farhan, H.; Wahala, K. and Cross, H.S. Genistein inhibits vitamin D hydroxylase CYP24 and CYP27B1 expression in prostate cells. *Journal of Steroid Biochemistry and Molecular Biology*, **2003** (84), 423-429.

Fechteler, T.; Dengler, U. and Schomberg, D. Prediction of protein three-dimensional structures in insertion and deletion regions: A procedure for searching databases of representative protein fragments using geometric scoring criteria. *Journal of Molecular Biology*, **1995** (253), 114-131.

Feldman, B.J. and Feldman, D. The development of androgen-independent prostate cancer. *Nature Reviews*, **2001** (1), 34-45.

Feldman, D.M.; Zhao, X.Y.; and Krishnan, A.V. Vitamin D and prostate cancer. *Endocrinology*, **2000** (141), 5-9.

Felippe, W.A.B.; Werneck, G.L. and Santoro-Lopes, G. Surgical site infection among women discharged with a drain *in situ* after breast cancer surgery. *World Journal of Surgery*, **2007** (31), 2293-2301.

Fenaux, P.; Wang, Z.Z. and Degos, L. Treatment of acute promyelocytic leukemia by retinoids. *Acute Promyelocytic Leukemia*, **2007** (313), 101-128.

Ferlay, J.; Bray, F.; Pisani, P. and Parkin, D. M. *Globocan 2000: Cancer incidence, mortality and prevalence worldwide,* First ed., 2001, http://www-dep.iarc.fr/globocan/globocan.htmL.

Fletcher, S.G. and andtheodorescu D. Surgery or radiation: what is the optimal management for locally advanced prostate cancer. *Canadian Journal of Urology*, **2005** (12), 58-61.

Fichera, A.; Little, N.; Mustafi, R.; Cedra, S.; Li, Y.C.; Arora, A., Joseph, L., Hart, J. and Bissonneette, M. A vitamin D analogue inhibits colonic carcinogenesis in the AOM/DSS model. *Journal of Surgical Research*, **2007** (142), 239-245.

Fisher, E. R.; Gregorio, R. M.; Fisher, B.; Redmond, C.; Vellios, F. and Sommers, S. C. The pathology of invasive breast cancer. A syllabus derived from findings of the national surgical adjuvant breast project (protocol no. 4). *Cancer,* **1975** (36), 1-85.

Fisher, G.J. and Voorhees, J.J. Molecular mechanisms of retinoid actions in skin. *FASEB Journal*, **1996** (10), 1002-1013.

Fong, C.J.; Sutkowski, D.M.; Braun, E.J.; Bauer, K.D.; Sherwood, E.R.; Lee, C. and Kozlowski, J.M. Effect of retinoic acid on the proliferation and secretory

activity of androgen-responsive prostatic carcinoma cells. *Journal of Urology*, **1993** (149), 1190-1194.

Fontana, J.A.; Daeson, M.I.; Leid, M.; Rishi, A.K.; Zhang, Y.; Hsu, C.A.; Lu, J.S.; Peterson, V.J.; Jong, L.; Hobbs, P.; Chao, W.R.; Shroot, B. and Reichert, U. Identification of a unique binding protein specific for a novel retinoid inducing cellular apoptosis. *International Journal of Cancer*, **2000** (78), 1107-1112.

Franceschi, S. Micronutrients and breast cancer. *European Journal of Cancer Prevention,* **1997** (6), 535-539.

Gann, P. H.; Hennekens, C. H.; Ma, J.; Longcope, C. and Stampfer, M. J. Prospective study of sex hormone levels and risk of prostate cancer. *Journal of National Cancer Institute,* **1996** (88), 1118-1126.

Gao, M.; Ossowski, L. and Ferrari, A.C. Activation of Rb and decline in androgenreceptor protein precede retinoic acid-induced apoptosis in androgen-dependent LNCaP cells and their androgen-independent derivative. *Journal of Cellular Physiology*, **1999** (179), 336-346.

Gasteiger, E.; Gattiker, A.; Hoogland, C.; Ivanyi, I.; Appel, R.D. and Bairoch, A. EXPASY: the proteomics server for in-depth protein knowledge and analysis. *Nucleic Acids Research*, **2003** (31), 3784-3788.

Ghazarian, J.G.; Jefcoate, C.R.; Knutson, J.C.; Orme-Johnson, W.H. and DeLuca, H.F. Mitochondrial cytochrome P450. A componene of chick kidney 25-hydrocholecalciferol-1alpha-hydroxylase. *Journal of Biological Chemistry*, **1994** (249), 3026-3033.

Giguere, V. Retinoic acid receptors and cellular retinoid binding proteins: complex interplay in retinoid signaling. *Endocrine Reviews*, **1994** (15), 61-79.

Gilson, M.K.; Gilson, H.S.R. and Potter, M.J. *Journal of Chemical Information and Computer Sciences*. **2003** (43) (6), 1982-1997.

Giordano, S. H.; Buzdar, A. U. and Hortobagyi, G. N. Breast cancer in men. *Annals of Internal Medicine,* **2002** (137), 678-687.

Giovannucci, E. Tomatoes, tomato-based products, lycopene, and cancer: Review of the epidemiologic literature. *Journal of the National Cancer Institute*, **1999** (91), 317-331.

Gleason, D.F. Histological grading and clinical staging of prostatic carcinoma, *In Urologic Pathology: The prostate*, M. Tannenbaum (ed), **1977**, Philadelphia, Lea and Febiger.

Gollnick, H.; Ehlert, R.; Rinck, G. and Organos, C.E. Retinoids: An overview of pharmacokinetics and therapeutic value. *Methods in enzymology*, **1990** (190), 291-304.

Gomaa, M.S.; Yee, S.W.; Milbourne, C.E.; Barbara, M-C., Simons, C. and Brancale, A. Homology model of human retinoic acid metabolising enzyme cytochrome P450 26A1 (CYP26A1): active site architecture and ligand binding. *Journal of Enzyme Inhibition and Medicinal Chemistry*, **2006** (21), 361-369.

Gomaa, M.S.; Simons, C. and Brancale, A. Homology Model of 1,25-dihydroxyvitamin D_3 24-hydroxylase Cytochrome P450 24A1 (CYP24A1):

Active Site Architecture and Ligand Binding. *Journal of Steroid Biochemistry and Molecular Biology*, **2007**, (104), 53-60.

Gomaa, M.S.; Armstrong, J.L.; Bobillon, B.; Veal, G.J.; Brancale, A.; Redfern, C.P.F. and Simons, C. Novel azolyl-(phenylmethyl)aryl/heteroarylamines: potent CYP26 inhibitors and enhancers of all-*trans* retinoic acid activity in neuroblastoma cells. *Bioorganic and Medicinal Chemistry*, **2008**, in Press.

Goodman and S., L. Goodman and gilman's the pharmacological basis of therapeutics, 10th ed., **2001**, *McGraw-Hill*: New York.

Goodman, D.S. Vitamin A and retinoids in health and disease, *New England Journal of Medicine*, **1984** (310), 1023-1031.

Goss, P. E. and Strasser, K. Aromatase inhibitors in the treatment and prevention of breast cancer. *Journal of Clinical Oncology*, **2001** (19), 881-894.

Gotoh, O. Substrate recognition sites in cytochrome P450 family 2 (CYP2) proteins inferred from comparative analyses of amino acid and coding nucleotide sequences. *Journal of Biological Chemistry*, **1992** (267), 83-90.

Gross, C.; Stamey, T.; Hancock, S. and Feldman, D. Treatment of early recurrent prostate cancer with 1,25- dihydroxyvitamin D_3 (calcitriol). *Journal of Urology*, **1998** (159), 2035-2039.

Gudas, L.J.; Sporn, M.B. and Roberts, A.B. Cellular biology and biochemistry of the retinoids, in *The retinoids: biology, chemistry and medicine* (Sporn MB, Roberts AB and Goodman DS eds, 2nd Ed.), **1994**, Raven Press Ltd., New York.

Guex, N.; Peitsch, M.C. SWISS-MODEL and the Swiss-PdbViewer: An environment for comparative protein modeling. *Electrophoresis* **1997** (18), 2714-2723 (http://wwwexpasyorg/spdbv/).

Guo, Y.; Strugnell, S.A.; Back, D.W. and Jones, G.W. Transfected human liver cytochrome P-450 hydroxylates vitamin D analogs at different side-chain positions. *Proceedings of the National Academy of Sciences of the United States of America*, **1993** (90), 8668-8672.

Guzey, M.; Kitada, S. and Reed, J.C. Apoptosis induction by 1alpha,25-dihydroxyvitamin D_3 in prostate cancer. *Molecular Cancer Therapeutics*, **2002** (1), 667-677.

Hagiwara, H.; Inoguchi, H.; Fukushima, M.; Hoshi, T. and Suzuki, T. Aldol reaction of trimethylsilyl enolate with aldehyde catalysed by pyridine *N*-oxide as a Lewis base catalyst. *Synlett*, **2005** (15), 2388-2390.

Hagiwara, H.; Inoguchi, H.; Fukushima, M.; Hoshi, T. and Suzuki, T. practical aldol reaction of trimethylsilyl enolate with aldehyde catalysed by *N*-methylimidazole as a Lewis base catalyst. *Tetrahedron Letters*, **2006** (47), 5371-5373.

Halgren, T.A. Merk molecular force field.1. Basis, form, scope, parameterization, and performance of MMFF94. *Journal of Computational Chemistry*, **1996** (17), 490-512; 520-552; 553-586; 587-615, 616-641.

Hammond, L.A.; Brown, G.; Keedwell, R.G.; Durham, J. and Chandraratna, R.A.S. The prospects of retinoids in the treatment of prostate cancer. *Anti-Cancer Drugs*, **2002** (13), 781-790.

Hanchette, C.L. and Schwartz, G.G., Geographic patterns of prostate-cancer mortality . Evidence for a protective effect of ultraviolet-radiation. *Cancer*, **1992** (70), 2861-2869.

Hanlon, A.L. and Hanks, G.E. Failure patterns and hazard rates for failure suggest the cure of prostate cancer by external beam radiation. *Urology*, **2000** (55), 725-729.

Hartwig, J. F.; Kawatsura, M.; Hauck, S. I.; Shaughnessy, K. H. and Alcazar-Roman, L.M. Room temperature palladium-catalysed amination of aryl bromides and chlorides and extended scope of aromatic C-N bond formation with a commercial ligand. *Journal of Organic Chemistry*, **1999** (64), 5575-5580.

Hartwig, J.F. Selective functionalisation of alkanes by transition metal boryl complexes. *Synthetic letters*, **1996**, 329.

Hasemann, C.A.; Kurumbail, S.S,; Boddupalli, S.S.; Peterson, J.A. and Deisenhofer, J. Structure and function of cytochrome P450: a comparative analysis of three crystal structures. *Structure*, **1995** (3), 41-62.

Hasemann, C.A.; Ravichandran,K.G.; S.S.; Peterson, J.A. and Deisenhofer, J. Crystal structure and refinement of cytochrome P450terp at 2.3 Å resolution. *Journal of Molecular Biology*, **1994** (236), 1169-1185.

Hayes, D. F. Atlas of breast cancer, Second ed., **2000**, *Mosby*: Barcelona, Spain.

Heinonen, O.P.; Albanes, D.; Virtamo, J.; Taylor, P.R.; Huttunen, J.K.; Hartman, A.M.; Haapakoski, J.; Malila, N.; Rautalahti, M.; Ripatti, S.; Maenpaa, H.; Teerenhovi, L.; Koss, L.; Virolainen, M.and Edwards, B.K. Prostate cancer and supplementation with alpha-tocopherol and beta-carotene: Incidence and mortality in a controlled trial. *Journal of the National Cancer Institute*, **1998** (90), 440-446.

Helewa, M.; Levesque, P.; Provencher, D.; Lea, R. H.; Rosolowich, V. and Shapiro, H.M. Breast cancer, pregnancy, and breastfeeding. *Journal of Obstetrics and Gynaecology of Canada,* **2002** (24), 164-180.

Henon, H.; Anizon, F.; Golsteyn, R.M.; leonce, S.; Hofmann, R.; Pfeiffer, B. and Prudhomme, M. Synthesis and biological evaluation of new dipyrollo[3,4-a:3,4-c]carbazole-1,3,4,6-tetraones, substituted with various saturated and unsaturated side chains via palladium catalysed cross-coupling reactions. *Bioorganic And Medicinal chemistry*, **2006** (14), 3825-3834.

Henry, R. Y. and O'Mahony, D. Treatment of prostate cancer. *Journal of Clinical Pharmacy and Therapeutics,* **1999** (24), 93-102.

Heyman, R.A.; Mangelsdorf, D.J.; Dyck, J.A.; Stein, R.B.; Eichele, G.; Evans, R.M. and Thaller, C. 9-*Cis* retinoic acid is a high affinity ligand for the retinoid X receptor. *Cell*, **1992** (68), 397-406.

Hill, D.L. and Grubbs, C.J. Retinoids and cancer prevention. *Annual Review of Nutrition*, **1992** (12), 161-181.

Hillisch, A.; Pineda, L.F. and Hilgenfeld, R. Utility of homology models in the drug discovery process. *Drug Discovery Today*, **2004** (9), 659-669.

Hong, W.K. and Itri, L.M., Retinoids and human cancer, In Sporn, M.B., Roberts, A.B. and Goodman, D.S. (eds), *The Retinoids: Biology, chemistry and medicine*, **1994**, Raven Press, New York, 597-630.

Hopper, J. L. Genetic epidemiology of female breast cancer. *Seminars in Cancer Biology,* **2001** (11), 367-374.

Hormi-Carver, K.; Feagins, L.A.; Spechler, S.J. and Souza, R.F. All *trans*-retinoic acid induces apoptosis via p38 and caspase pathways in metaplastic Barrett's cells. *American Journal of Physiology-Gastrintestinal and Liver Physiology*, **2007** (292), G18.

Howell, A. Adjuvant aromatase inhibitors for breast cancer. *The lancet*, **2005** (365), 431-432.

Hsieh, K.P.; Lin, Y.Y.; Cheng C.L.; Lai, M.L.; Lin, M.S.; Siest, J.P. and Huang J.D. Novel mutations of CYP3A4 in Chinese. *Drug Metabolism and Disposition*, **2001** (29), 268-273.

Hsing, A.W., Tsao, L. and Devesa, S.S. International trends and patterns of prostate cancer incidence and mortality. *International Journal of Cancer*, **2000** (85), 60-67.

Hulka, B. S. and Moorman, P. G. Breast cancer: Hormones and other risk factors. *Maturitas,* **2001** (38), 103-113.

Hulka, B. S. and Stark, A. T. Breast cancer: Cause and prevention. *Lancet,* **1995** (346), 883-887.

Humphrey, W.; Dalke, A.; Schulten, K. VMD - Visual Molecular Dynamics. *Journal of molecular graphics*, **1996** (14), 33-38.

Hunter, D. J. and Willett, W. C. Nutrition and breast cancer. *Cancer Causes and Control,* **1996** (7), 56-68.

Huynh, C.K.; Brodie, A.M.H. and Njar, V.C.O. inhibitory effects of retinoic acid metabolism blocking agents (RAMBAs) on the growth of human prostate cancer cells and LNCaP prostate tumor xenografts in SCID mice. *British Journal of Cancer*, **2006** (94), 513-523.

Igawa, M.; Tanabe, T.; Chodak, G.W. and Rukstalis, D.B. *N*-(4-Hydroxyphenyl) retinamide induces cell cycle specific growth inhibition in PC-3 cells. *Prostate*, **1994** (24), 127-135.

Iversen, P.; Tyrrell, C.J.; Kaisary, A.V.; Anderson, J.B.; Van Poppel, H.; Tammela, T.L.J.; Chamberlain, M.; Carroll, K. and Melezinek, I. Bicalutamide monotherapy compared with castration in patients with nonmetastatic locally advanced prostate cancer: 6.3 years of follow-up. *Journal of Urology*, **2000** (164), 1579-1582.

Jacobsen, B.K.; Knutsen, S.F. and Fraser, G.E. Does high soy milk intake reduce prostate cancer incidence? The adventist health study (United States). *Cancer Causes and Control*, **1998** (9), 553-557.

Jani, A.B. and Hellman, S. Early prostate cancer: clinical decision-making. *Lancet*, **2003** (361), 1045-1053.

Janssens, F.; Torremans, J.; Janssen, M.; Stokbroekx, R.; Luyckx, M. and Janssen, P. A. J. New antihistaminic N-heterocyclic 4-piperidinamines. 1. Synthesis and antihistaminic activity of *N*-(4-piperidinyl)-1H-benzimidazol-2-amines. *Journal of Medicinal Chemistry*, **1985** (28), 1925-1933.

Jernal, A.; Murray, T. and Ward, E. cancer statistics. *Cancer Journal Clinical*, **2005** (55), 10-30.

John, E.M.; Dreon, D.M. and Koo, J. Residential sunlight exposure is associated with decreased risk of prostate cancer. *Journal of Steroid Biochemistry and Molecular Biology*, **2004** (89-90), 549-552.

Johnson, C.S.; Hershberger, P.A.; Bernardi, R.J.; Mcguire, T.F. and Trump, D.L. Vitamin d receptor: a potential target for intervention. *Urology*, **2002** (60), 123-130.

Jonat, W. Goserelin (Zoladex^{TM}) its role in early breast cancer in pre- and perimenopausal women. *British Journal of Cancer*, **2001** (85), 1-5.

Jones, G.W.; Strugnell, S.A. and DeLuca, H.F. Current understanding of the molecular actions of vitamin D. *Physiological Review*, **1998** (78), 1193-1231.

Jones, G.; Willett, P.; Glen, R.C.; Leach, A.R. and Taylor, R. Development and validation of genetic algorithm for flexible docking. *Journal of Molecular Biology*, **1997** (267), 727-748.

Jordan, V. C. and Koerner, S. Tamoxifen (ici 46,474) and the human carcinoma 8s oestrogen receptor. *European Journal of Cancer,* **1975** (11), 205-206.

Jorapur, Y.R.; Jeong, J.M. and Chi, D.Y. Potassium carbonate as a base for the *N*-alkylation of indole and pyrolle in ionic liquids. *Tetrahedron letters*, **2006** (47), 2435-2438.

Kahraman, M.; Sinishtag, S.; Dolan, P.M.; Kensler, T.W.; Peleg,S.; Saha, U.; Chuang, S.S.; Bernstein, G.; Korczak, B. and Posner, G.H. Potent selective and low calcemic inhibitors of CYP24 hydroxylase: 24-sulfoximine analogues of the hormone 1α,25-dihydroxyvitamin D_3. *Journal of Medicinal Chemistry*, **2004** (47), 6854-6863.

Kalemkerian, G.P.; Susher, R.; Ranalingam, S.; Gandgeel, S. and Mabry, M. Growth inhibition and inductiuon of apoptosis by fenretinide in small-cell-lung-cancer cell lines. *Journal of National Cancer Institute*, **1995** (87), 1674-1680.

Kelly, W.K.; Osman, I.; Reuter, V.E.; Curley, T.; Heston, W.D.; Nanus, D.M. and Scher, H.I. The development of biologic end points in patients treated with differentiation agents: An experience of retinoids in prostate cancer. *Clinical Cancer Research*, **2000** (6), 838-846.

Kessler, L. G. The relationship between age and incidence of breast cancer. Population and screening program data. *Cancer,* **1992** (69), 1896-1903.

Key, T.J.; Forman, D. and Pike, M.C. Epidemiology of cancer, In Franks, L.M. and Teich, N.M. (eds.), *Introduction to the cellular and molecular biology of cancer*, **1997**, Oxford University Press, Oxford, 34-59.

Key, T. J.; Verkasalo, P. K. and Banks, E. Epidemiology of breast cancer. *Lancet Oncolgy,* **2001** (2), 133-140.

Kharkar, P.S. and Kulkarni, V.M. A proposed model of mycobacterium avium complex dihydrofolate reductase and its utility in drug design. *Organic and Biomolecular Chemistry*, **2003** (1), 1315-1322.

Kim, J.H.; Tanabe, T.; Chodak, G.W. and Rukstalis, D.B. In vitro anti-invasive effects of *N*-(4_hydroxyphenyl)-retinamide on human prostate adenocarcinoma. *Anticancer Research*, **1995** (15), 1429-1434.

Kirchhoff, J.H.; Netherton M. R.; Hill I. D. and Fu, G. C. *Journal Of The American Chemical Society*, **2002** (124), 13662-13663

Kirby, R.S.; Brawer, M.K. and Denis, L.J. *In: Fast facts-prostate cancer*, 2nd ed., **1998**, Health press limited, Oxford, 39-61.

Kirby, A.J.; Le Lain, R.; Maharlouie, F.; Mason, P.; Nicholls, P.J.; Smith, H.J. and Simons, C. Inhibition of retinoic acid metabolising enzymes by 2-(4-aminophenylmethyl)-6-hydroxy-3,4-dihydronaphthalene-1(2*H*)-one and related compounds. *Journal of Enzyme Inhibition and Medicinal Chemistry*, **2003** (18), 27-33.

Kirby, A.J.; Le, Lain. R.; Mason, P.; Maharlouie, F.; Nicholls, P.J.; Smith, H.J. and Simons, C. Some 3-(4-aminophenyl) pyrrolidine-2,5-diones as all-*trans*-retinoic acid metabolising enzyme inhibitors (RAMBAs). *Journal of Enzyme Inhibition*, **2002** (17), 321-327.

Kirby, R.S. In: The prostate: small gland, big problem: a guide to the prostate, prostate disorders and their treatments, **2002**, Health press, Oxford, 52-78.

Kirton, S.B.; Baxter, C.A. and Sutcliffe, M.J. comparative modeling of cytochromes P450. *Advanced drug delivery reviews*, **2002** (54), 385-406.

Kliewer, S.A.; Umesono, K.; Mangelsdorf, D.J. and Evans, R.M. retinoid X receptor interacts with nuclear receptors in retinoic acid, thyroid hormone and vitamin D_3 signaling. *Nature*, **1992** (355), 446-449.

Kobayashi, T.; Hashimoto, K. and Yoshikawa, K. Growth inhibition of human keratinocytes by 1,25-dihydroxyvitamin D_3 is linked to dephosphorylation of retinoblastoma gene product. *Biochemical and Biophysical Research Communications*, **1993** (196), 487-493.

Kolonel, L.N.; Hankin, J.H. and Yoshizawa, C.N. Vitamin A and prostate cancer in elderly men: enhancement of risk. *Cancer Research*, **1987** (47), 2982-2985.

Kolvenbag, G.J.; Iversen, P. and Newling, D.W. Antiandrogen monotherapy: a new form of treatment for patients with prostate cancer. *Urology*, **2001** (58), 16-23.

Kolyada, A.Y. Sequence of a human liver cytochrome P-450 cDNA clone. *Nucleic Acids Research*, **1990** (18), 5550-5555.

Konety, B.R.; Johnson, C.S.; Trump D.L. and Getzenberg, R.H. Vitamin D in the prevention and treatment of prostate cancer. *Seminars in Urologic Oncology*, **1999** (17), 77-84.

Koper, P.C.M.; Stroom, J.C.; van Putten, W.L.J.; Korevaar, G.A.; Heijmen, B.J.M.; Wijnmaalen, A.; Jansen, P.P.; Hanssens, P.E.J.; Griep, C.; Krol, A.D.G.; Samson, M.J. and Levendag, P.C. Acute morbidity reduction using 3DCRT for prostate carcinoma: A randomized study. *International Journal of Radiation Oncology Biology Physics*, **1999** (43), 727-734.

Koshiuka, K.; Elstner, E.; Williamson, J.W.; Said, J.W.; Tada, Y. and Koeffler, H.P. Novel therapeutic approach: organic arsenical (melarsoprol) alone or with *all-trans*-retinoic acid markedly inhibit growth of human breast and prostate cancer cells in vitro and *in vivo*. *British Journal of Cancer*, **2000** (82), 452-458.

Kraus, S.; Naor, Z. and Seger, R. Gonadotrophin-releasing hormone in apoptosis of prostate cancer cells. *Cancer Letters*, **2005** (234), 109-123.

Kuerer, H. M.; Buzdar, A. U. and Singletary, S. E. Biologic basis and evolving role of aromatase inhibitors in the management of invasive carcinoma of the breast. *Journal of Surgical Oncology*, **2001** (77), 139-147.

Kuller, L.H.; Cauley, J. A.; Lucas, L.; Cummings, S. and Browner, W. S. Sex steroid hormones, bone mineral density, and risk of breast cancer. *Environmental Health Perspectives*, **1997** (105 Suppl 3), 593-599.

Kumaraswamy, G.; Pitchaiah, A.; Ramakrishna, G.; Ramakrishna, D.S. and Sadaiah, K. Di-μ-hydroxy-bis(N,N,N',N'-tetramethylenediamine)-copper(II) chloride: an efficient practical catalyst for benzylation and allylation of amides. *Tetrahedron Letters*, **2006** (47), 2013-2015.

Kuntz, I.D.; Blaney, J.M.; Oatley, S.J.; Langridge, R.L. and Ferrin, T.E. A geometric approach to macromolecular-ligand interaction. *Journal of Molecular Biology*, **1982** (161), 269-288.

Kurtz, J. M. Factors influencing the risk of local recurrence in the breast. *European Journal of Cancer*, **1992** (28), 660-666.

Lam, P.Y.S.; Clark, C.G.; Saubern, S.; Adams, J.; Winters, M.P.; Chan, D.M.T. and Combs, A. New aryl/heteroaryl C-N bond cross-coupling reactions via aryl boronic acid CuII(OAc)$_2$arylation. *Tetrahedron Letters*, **1998** (39), 2941-2944.

Lane, B.S.; Brown, M.A. and Sames, D. Direct palladium-catalysed C-2 and C-3 arylation of indoles: A mechanistic rationale for regioselectivity. *Journal of the American Chemical Society*, **2005** (127), 8050-8057.

Laufer, S.A.; Domeyer, D.M.; Scior, T.R.F.; Albrecht, W. and hauser, D.R.J. Synthesis and biological testing of purine derivatives as potential ATP-competitive kinase inhibitors. *Journal Of Medicinal Chemistry*, **2005** (48), 710-722.

Le Borgne, M.; Marchand, P.; Nourrisson, M.R.; Loquet, D.; Palzer, M.; Le Baut, G. and Hartmann, R.W. Synthesis and biological evaluation of 3-(azolylmethyl)-1H-indoles and 3-(alpha-azolylbenzyl)-1H-indoles as selective aromatase inhibitors. *Journal of Enzyme Inhibition and Medicinal chemistry*, **2007** (22), 667-676.

Lenz, S. K.; Goldberg, M. S.; Labreche, F.; Parent, M. E. and Valois, M. F. Association between alcohol consumption and postmenopausal breast cancer: Results of a case-control study in montreal, quebec, Canada. *Cancer Causes and Control*, **2002** (13), 701-710.

Leo, M.A. and Lieber, C.S. New pathway for retinol metabolism in liver microsomes. *Journal of Biological Chemistry*, **1985** (260), 5228-5231.

Lesk, A.M. Introduction to bioinformatics, *Oxford university press: New York*, 1st ed., **2002**.

Lesk, A.M. and Chothia, C. The response of protein structures to amino-acid sequence changes. *Philosophical Transactions of the Royal Society of London Series B-Biological Sciences*, **1986** (317), 345-356.

Lesk, A.M.; Levitt, M. and Chothia, C. Alignment of the amino acid sequences of distantly related proteins using variable gap penalties. *Protein Engineering*, **1986** (1), 77-78.

Levitt, M. Accurate modeling of protein conformation by automatic segment matching. *Journal of Molecular Biology*, **1992** (226), 507-533.

Lewis, D.F. Physical methods in the study of the active site geometry of cytochromes P450s. *Drug Metabolisam Reviews*, **1986** (17), 1-66.

Lewis, D.F.V. The CYP2 family: models, mutants and interactions. *Xenobiotica*, **1998a** (28), 617-661.

Lewis, D.F.V. Molecular modeling in drug metabolism: the cytochrome P450, in: *drug metabolism: toward the next millennium (N. Gooderham, ed.)* IOS Press, Amsterdam, **1998b**, 1-12.

Lewis DFV *Guide to cytochromes P450 structure and function,* **2001**, Taylor and Francis, London.

Leze, M.P.; Borgne, M.L.; Marchand, P.; Loquet, D.; Kogler, M.; Baut, G.L.; Palusczak, A. and Hartmann, R.W. 2- and 3-[(aryl)(azolyl)methyl]indoles as potential non-steroidal aromatase inhibitors. *Journal of Enzyme Inhibition and Medicinal chemistry*, **2004** (19), 549-557.

Li, Y.; Hashimoto, Y.; Agadir, A.; Kagechika, H. and Zhang, X.K. Identification of a novel class of RARβ-selective retinoid antagonists and their inhibitory effects on AP-1 activity and RA-induced apoptosis in human breast cancer cells. *Journal of Biological Chemistry*, **1999** (274), 15360-15366.

Liang, J.Y.; Fontana, J.A.; Rao ,J.N.; Ordonez, J.V.; Dawson, M.I.; Shroot, B.; Wilber, J.F. and Feng, P. Synthetic retinoid CD437 induces S-phase arrest and apoptosis in human prostate cancer cells LNCaP and PC-3. *Prostate*, **1999** (38), 228-236.

Limonta, P.; Marelli, M.M. and Moretti, R.M. LHRH analogues as anticancer agents: pituitary and extrapituitary sites of action. *Expert Opinion on Investigational Drugs*, **2001** (10), 709-720.

Lin, F.; Xiao, D.; Kollerai, S.K. and Zhang, X.K. Unique anti-activator protein-1 of retinoic acid receptor β. *Cancer Research*, **2000** (60), 3271-3280.

Lindahl, E.; Hess, B.; van der Spoel, D. GROMACS 3.0: A package for molecular simulation and trajectory analysis. *Journal of molecular modeling*, **2001** (7), 306-317.

Lindley, P.M.; Pincklesimer, L.G.; Evans, B.; Arnold, F.E. and kane, J.J. Arylether sulfone oligomers with acetylene termination from the Ullmann ether reaction. *American Chemical Society Symposium Series*, **1985** (282), 31-42.

Linton, K.D. and Hamdy, F.C. Early diagnosis and surgical management of prostate cancer. *Cancer Treatment reviews*, **2003** (29), 151-160.

Lips, P. Vitamin D deficiency and secondary hyperparathyroidism in the elderly: consequences for bone loss and fractures and therapeutic implications. *Endocrine Reviews*, **2001** (22), 477-501.

Liu, Y.; Lee, M.O.; Wang, H.G.; Li, Y.; Hashimoto, Y., Klaus, M.; Reed, J.C. and Zhang, X.K. Retinoic acid receptor β mediates the growth-inhibitory effect of retinoic acid by promoting apoptosis in human breast cancer cells. *Molecular Cellular Biology*, **2001** (12), 454-494.

Lopez-Pedrera, C.; Torres, A.; Dorado, G. and Velasco, F. Promyelocytic leukemia retinoid signaling targets regulate apoptosis, tissue factor and thrombomodulin expression. *Haematologica*, **2004** (89), 286-295.

Lotan, R. Effects of vitamin A and its analogs (retinoids) on normal and neoplastic cells. *Biochimica Et Biophysica Acta*, **1980** (605), 33-91.

Lovell, S.S.; Davis, I.W.; Arendall III, W.B.; de Bakker, P.I.W.; Word, J.M.; Prisant, M.G.; Richardson, J.S. and Richardson, D.C. Structure validation by Calpha geometry: phi,psi and Cbeta deviation. *Proteins: Structure, Function & Genetics*, **2002** (50), 437-450.

Luthy, R.; Bowie, J.U. and Eisenberg, D. Assessment of protein models with three-dimensional profiles. *Nature*, **1992** (356), 83-85.

Ly, L.H.; Zhao, X.Y.; Holloway, L. and Feldman, D. Liarozole acts synergistically with 1 alpha,25-dihydroxyvitamin D-3 to inhibit growth of DU 145 human prostate cancer cells by blocking 24-hydroxylase activity. *Endocrinology*, **1999** (140), 2071-2076.

Lyne, P.D. Structure-based virtual screening: An overview. *Drug Discovery Today*, **2002** (7), 1047-1055.

Lynn, E.; Hahnfeld, M. D.; Timothy, D. and Moon, M. D. Prostate cancer. *Medical Clinics of North America,* **1999** (83), 1231-1245.

MacLean, G.; Abu-Abed, S.; Dolle, P.; Tahayato, A.; Chambon, P. and Petkovich, M. Cloning of a novel retinoic-acid metabolizing cytochrome P450, Cyp26B1, and comparative expression analysis with Cyp26A1 during early murine development. *Mechanisms of Development*, **2001** (107), 195-201.

Mangelsdorf, D.J.; Thummel, C.; Beato, M.; Herrlich, P.; Schutz, G.; Umesono, K.; Blumberg, B.; Kastner, P.; Mark, M.; Chambon, P. and Evans, R.M. The nuclear receptor superfamily - the 2nd decade. *Cell*, **1995** (83), 835-839.

Marill, J.; Cresteil, T.; Lanotte, M. and Chabot, G.G. Identification of human cytochrome P450s involved in the formatin of all-*trans*-retinoic acid principal metabolites. *Molecular Pharmacology*, **2000** (58), 1341-1348.

Marti-Renom, M.A.; stuart, A.C.; Fiser, A.; sanchez, R.; Melo, F. and Sali, A. Comparative protein structure modeling of genes and genomes. *Annual Review of Biophysics and biomolecular structure*, **2000** (29), 291-325.

Mason, J.S.; Good, A.C. and Martin, E.J. 3D pharmacophores in drug discovery. *Current Pharmaceutical Design*, **2001** (7), 567-597.

Masuda, S. and Jones, G. Promise of vitamin D analogues in the treatment of hyperproliferative conditions. *Molecular Cancer Therapeutics*, **2006** (5), 797-808.

Masuda, S.; Prosser, D.E.; Guo, Y.D.; Kaufmann, M. and Jones, G. Generation of a homology model for the human cytochrome P450, CYP24A1, and the testing of putative substrate binding residues by site-directed mutagenesis and enzyme activity studies. *Archives of Biochemistry and Biophysics*, **2007** (460), 177-191.

Mateus, C.R.; Almeida, w.p. and Coelho, F. Diastereoselective Heterogenus Catalytic Hydrogenation of Baylis-Hillman adducts. *Tetrahedron*, **2000** (41), 2533-2536.

McCormick, D.L.; Rao, K.V.; Steele, V.E.; Lubet, R.A.; Kelloff, G.J. and Bosland, M.C. Chemoprevention of rat prostate carcinogenesis by 9-cis retinoic acid. *Cancer Research*, **1999** (59), 521-524.

McLeod, D.G. Hormonal therapy: Historical perspective to future directions. *Urology*, **2003** (61), 3-7.

McNeal, J.E. and Bostwick, D.G. Intraductal dysplasia: a premalignant lesion of the prostate. *Human Pathology*, **1986** (17), 64-71.

McNeal, J.E.; Villers, A.; Redwine, E.A.; Freiha, F.S. and Stamey, T.A. Microcarcinoma in the prostate: its association with duct-acinardysplasia. *Human Pathology*, **1991** (22), 644-652.

Mestres, J. and Knegtel, R.M.A. Similarity versus docking in 3D virtual screening. *Perspective Drug Design and Discovery*, **2000** (20), 191-207.

Miki, Y.; Swensen, J.; Shattuck-Eidens, D.; Futreal, P. A.; Harshman, K.; Tavtigian, S.; Liu, Q.; Cochran, C.; Bennett, L. M.; Ding, W. and et al. A strong candidate for the breast and ovarian cancer susceptibility gene brca1. *Science,* **1994** (266), 66-71.

Miller, G.J. Vitamin D and prostate cancer: Biological interactions and clinical potentials. *Cancer Metastasis Review*, **1998** (17), 353-360.

Miller, V.A.; Francis, P.A.; Rigas, J.R.; Muindi, J.R.F.; Tong, W.P.; Kris, M.G. and Warrell, R.P. *The cytochrome P-450 inhibitors, ketoconazole and liarozole, modulate all-trans retinoic acid metabolism,* In: 8th NCI/EORTC Symposium on New Drugs in Cancer Therapy, Amsterdam, March **1994**, 15-18.

Miyaura N, Yamada K, Suginome H and Suzuki A Novel and Convenient Method for the Sterospecific and Regiospecific Synthesis of Conjugated Alkadienes and Alkenynes Via the Palladium-Catalyzed Cross-Coupling Reaction of 1-Alkenylboranes with Bromoalkenes and Bromoalkynes. *Journal of the American Chemical Society*, **1985** (107), 972-980.

Miyaura, N.; Yamada, K. and Suzuki, A. *Tetrahedron Letters*, **1979** (36), 3437-3440.

Miyaura N, Yanagi T and Suzuki A The Palladium-Catalyzed Cross-Coupling Reaction of Phenylboronic Acid with Haloarenes in the Presence of Bases. *Synthetic Communications*, **1981** (11), 513-519.

Miyazawa, M.; Shindo, M. and Shimada, T. Metabolism of (+)- and (-)-limonenes to respective carveols and perillyl alcohols by CYP2C9 and CYP2C19 in human liver microsomes. *Drug Metabolism and Disposition*, **2002** (30), 602-607.

Modeller, **2004**, http://guitar.rockefeller.edu/modeller/modeller.htmL.

Modi, S.; Paine, M.J.; Sutcliffe, M.J.; Lian, L.Y.; primrose, W.U.; Wolf, C.R. and Roberts, G.C. A model for human cytochrome P450 2D6 based on homology modeling and NMR studies of substrate binding. *Biochemistry (Moscow)*, **1996** (35), 4540-4550.

Molander, G.A. and Bernardi, G.R. Suzuki-Miyaura cross coupling reactions of potassium alkenyltrifluoroborates. *Journal Of The American Chemical society*, **2002** (67), 8424-8429.

Molecular Operating Environment 2004.03 (MOE) Chemical Computing Group Inc Montreal Quebec Canada http://www.chemcomp.com

Monkawa, T.; Yoshida, T.; Wakino, S.; Shinki, T.; Anazawa, H.; DeLuca, H.F.; Suda, T.; Hayashi, M. and Saruta, T. Molecular cloning of cDNA and genomic DNA for human 25-hydroxyvitamin D_3 1alpha-hydroxylase. *Biochemical and Biophysical Research Communications*, **1997** (239), 527-533.

Moon, R.C.; Mehta, R.G. and Rao, K.V.N. Retinoids and cancer in experimental animals, in *The retinoids: Biology, chemistry and medicine* (Sporn MB, Roberts AB and Goodman DS eds, Ed.), **1994**, Raven Press Ltd., New York, 573-595.

Morris, G.M.; Goodsell, D.S.; Huey, R. And Olson, A.J. Distributed automated docking of flexible ligands to proteins: parallel application of AutoDock 2.4. *Journal of Computer–Aided Molecular Design*, **1996** (10), 293-304.

Morris, M.J.; Kelly, W.K.; Solvin, S.; Ryan, C.; Eicher, C.; Heller, G. and Scher, H.I. A phase II trial of bortezomib and prednisone for castration resistant metastatic prostate cancer. *Journal of Urology*, **2007** (178), 2378-2383.

Moulder, S. and Hortobagyi, G. Advances in the treatment of breast cancer. *Clinical Pharmacology and Therapeutics*, **2008** (83), 26-36.

Moul, J. W.; Wu, H.; Sun, L.; McLeod, D. G.; AmLing, C.; Lance, R.; Kusuda, L.; Donahue, T.; Foley, J. and Chung, A. Epidemiology of radical prostatectomy for localized prostate cancer in the era of prostate-specific antigen: An overview of the department of defense center for prostate disease research national database. *Surgery*, **2002** (132), 213-219.

Moyad, M.A. Disease prevention and prostate cancer. *Seminars in Urologic Oncology*, **1999** (17), 97-102.

Muegge, I and Martin, Y.C.A. General and fast scoring function for protein-ligand interactions: A simplified potential approach. *Journal of Medicinal Chemistry*, **1999** (42), 791-804.

Muindi, J.R.; Young, C.W. and Warrell, J.R.P. Clinical pharmacology of all-*trans* retinoic acid. *Leukemia*, **1994** (8), 1807-1812.

Mulvihill, M.J.; Kan, J.L.C.; Beck, P.; Bittner, M.; Cesario, C.; Cooke, A.; Keane, D.M.; Nigro, A.I.; Nillson, C.; Sith, V.; Srebernak,M.; Sun, F.; Vrkljan, M.; Winski, S.L.; Castelhano, A.L.; Emerson, D. and Gibson, N. Potent and selective [2-imidazol-1-yl-2-(6-alkoxy-naphthalen-2-yl)-1-methyl-ethyl]-dimethyl-amines as retinoic acid metabolic blocking agents (RAMBAs). *Bioorganic and Medicinal Chemistry Letters*, **2005** (15), 1669-1673.

Mulvihill, M. J.; Kan, J. L. C.; Cooke, A.; Bhagwat, S.; Beck, P.; Bittner, M.; Cesario, C.; Keane, D.; Lazarescu, V.; Nigro, A.; Nillson, C.; Panicker, B.; Smith, V.; Srebernak, M.; Sun, F-L.; O'Connor, M.; Russo, S.; Fischetti, G.; Vrkljan, M.; Winski, S. L.; Castelhano, A. L.; Emersonb, D. and Gibsona, N. W. 3-[6-(2-Dimethylamino-1-imidazol-1-yl-butyl)-naphthalen-2-yloxy]-2,2-dimethyl-propionic acid as a highly potent and selective retinoic acid metabolic blocking agent. *Bioorganic and Medicinal Chemistry Letters.* **2006** (16), 2729–2733.

Munz-Seeref, L.; Rosa, E.; Bosch, M.P. and Guerrero, A. A new practical and efficient sulfone-mediated synthesis of trifluoromethyl ketones from alkyl and alkenyl bromides. *Tetrahedron Letters*, **2005** (46), 3311-3313.

Murta, E.F. and Nomelini, R.S. Choices and challenges in endocrine treatment of breast cancer. *International Journal of Clinical Practice*, **2007** (61), 1962-1964.

Nakagawa, T.; Fujisawa, H. and Mukaiyama, T. *Chemistry Letters*, **2003** (32), 462.

Napoli, J.L. Interactions of retinoid binding proteins and enzymes in retinoid metabolism. *Biochimica Et Biophysica Acta*, **1999** (1440), 139-162.

Napoli, J.L. Retinoic acid biosynthesis and metabolism. *FASEB Journal*, **1996** (10), 993-1001.

Narod, S. Genetic epidemiology of prostate cancer. *Biochimica and Biophysica Acta,* **1999** (1423), 1-13

NCBI, 2004, http://www.ncbi.nlm.nih.gov/BLAST/

Needleman, S.B. and Wunsch, C.D. A general method applicable to search for similarities in amino acid sequence of 2 proteins. *Journal of Molecular Biology*, **1970** (48), 443-453.

Nerbert, D.W. and Gonzalez, F.J. P450 genes: structure, evolution and regulation. *Annual Review of Biochemistry*, **1987** (56), 945-993.

Newcomb, P. A.; Storer, B. E.; Longnecker, M. P.; Mittendorf, R.; Greenberg, E. R.; Clapp, R. W.; Burke, K. P.; Willett, W. C. and MacMahon, B. Lactation and a reduced risk of premenopausal breast cancer. *New England Journal of Medicine,* **1994** (330), 81-87.

Nicholson, R. I. Recent advances in the antihormonal therapy of breast cancer. *Current Opinion Investigation Drugs,* **1993** (2), 1259-1268.

Niu, M.Y.; Menard, M.; Reed, J.C.; Krajewski, S. and Pratt, M.A. Ectopic expression of cyclin D1 amplifies a retinoic acid-induced mitochondrial death pathway in breast cancer cells. *Oncogene*, **2001** (20), 3506-3518.

Njar, V.C.O.; Nnane, I.P. and Brodie, A.M.H. Potent inhibition of retinoic acid metabolism enzyme(s) by novel azolyl retinoids. *Bioorganic & Medicinal Chemistry Letters*, **2000** (10), 1905-1908.

Njar, V.C.O. Cytochrome P450 retinoic acid 4-hydroxylase inhibitors: potential agents for cancer therapy. *Mini Reviews in Medicinal Chemistry*, **2002** (2), 261-269.

Njar, V.C.O.; Chopra, P.; Vasaitis, T.S.; Mehta, J.; Huynh, C.; Belosay, A. and Patel, J. Retinoic acid metabolism blocking agents (RAMBAs) for treatment of

cancer and dermatological diseases. *Bioorganic and Medicinal Chemistry*, **2006** (14), 4323-4340.

Novotny, J.; Rashin, A.A. and Bruccoleri, R.E. Criteria that discriminate between native proteins and incorrectly folded models. *Proteins*, **1988** (4), 19-30.

Ogura H., Mineo S. and Nakagawa K. Studies in heterocyclic compounds. Synthesis of 2-substituted aminobenzoxazoles with nickel peroxide. *Chemical and Pharmaceutical Bulletin.*, **1981** (29), 1518-1524.

Oh, W.K. and Kandoff, P.W. Management of hormone refractory prostate cancer: current standards and future prospects. *Journal of Urology*, **1998** (160), 1220-1229.

Ohori, M.; Wheeler, T.M.; Kattan, M.W.; Goto, Y. and Scardino, P.T. Prognostic-significance of positive surgical margins in radical prostatectomy specimens. *Journal of Urology*, **1995** (154), 1818-1824.

Ohyama, Y. and Okuda, K. Isolation and characterization of a cytochrome P-450 from rat kidney mitochondria that catalyzes the 24-hydroxylation of 25-hydroxyvitamin D_3. *Journal of Biological Chemistry*, **1991** (266), 8690-8695.

Okobia, M.; Bunker, C.; Zmuda, J.; Kammerer, C.; Vogel,V.; Uche, E.; Anyanwu, S.; Ezeome, E.; Ferrell,R. and Kuller, L. Case-control study of risk factors for breast cancer in Nigerian women. *International Journal of Cancer*, **2006** (119), 2179-2185.

Omdahl, J.A.; Morris, H.A. and May, B.K. Hydroxylase enzymes of the vitamin D pathway: Expression, function and regulation. *Annual Review of Nutrition*, **2002** (22), 139-166.

Onel, E.; Hamond, C.; Wasson, J. H.; Berlin, B. B.; Ely, M. G.; Laudone, V. P.; Tarantino, A. E. and Albertsen, P. C. Assessment of the feasibility and impact of shared decision making in prostate cancer. *Urology,* **1998** (51), 63-66.

O'Regan, R. M. and Jordan, V. C. The evolution of tamoxifen therapy in breast cancer: Selective oestrogen-receptor modulators and downregulators. *Lancet Oncology,* **2002** (3), 207-214.

Osborne, C. K. Tamoxifen in the treatment of breast cancer. *New England Journal of Medicine,* **1998** (339), 1609-1618.

Osborne, J.L.; Schwartz, G.G.; Smith, D.C.; Bahnson, R.; Day, R. and Trump, D.L. Phase II trial of oral 1,25-dihydroxyvitamin D (Calcitriol) in hormone refractory prostate cancer. *Urologic Oncology*, **1995** (1), 195-198.

Ostrov, D.A.; Prada, J.A.H.; Corsino, P.E.; Finton, K.A.; Le, N. and Rowe, T.C. Discovery of novel DNA gyrase inhibitors by high-throughtput virtual screening. *Antimicrobial Agents and Chemotherapy Journal*, **2007** (51), 3688-3698.

Overberger, C.G. and Bonsignore, P.V. Synthesis of compounds related to segments of synthetic sulfhydryl polymers. *Journal Of The American Chemical Society*, **1958** (80), 5427-5430.

PDB; protein data bank, 2004, http://www.rcsb.org/pdb/

Parker, M.G. and Franks, L.M. Hormones and cancer, In Franks, L.M. and Teich, N.M. (eds), *Introduction to the cellular and molecular biology of cancer*, Oxford University Press, **1997**, Oxford, 274-298.

Pasquali, D.; Rossi, V.; Prezioso, D.; Gentile, V.; Colantuoni, V.; Lotti, T.; Bellastella, A. and Sinisi, A.A. Changes in tissue transglutaminase activity and expression during retinoic acid induced growth arrest and apoptosis in primary cultures of human epithelial prostate cells. *Journal of Clinical Endocrinology and Metabolism*, **1999** (84), 1463-1469.

Pasquali, D. Rossi, V.; Bellastela, G.; Bellastella, A. and Sinisi, A.A. Natural and synthetic retinoids in prostate cancer. *Current Pharmaceutical Design*, **2006** (12), 1923-1929.

Pasquali, D.; Thaller, C. and Eichele, G. Abnormal level of retinoic acid in prostate cancer tissues. *Journal of Clinical Endocrinology and Metabolism*, **1996** (81), 2186-2191.

Pautus, S.; Yee, S. W.; Jayne, M.; Coogan, M. P. and Simons, C. Synthesis and CYP26A1 inhibitory activity of 1-[benzofuran-2-yl-(4-alkyl/aryl-phenyl)-methyl]-1*H*-triazoles. *Bioorganic and Medicinal Chemistry.* **2006** (14), 3643–3653.

Peck, G.L. Retinoids: therapeutic use in dermatology. *Drugs*, **1982** (24), 342-351.

Peck, G.L. and DiGiovanna, J.J. Synthetic retinoids in dermatology, in *The retinoids: Biology, chemistry and medicine* (Sporn MB, Roberts AB and Goodman DS eds, Ed.), **1994**, Raven Press Ltd., New York, 631-658.

Peehl, D.M. and Feldman, D. The role of vitamin D and retinoids in controlling prostate cancer progression. *Endocrine-Related Cancer*, **2003** (10), 131-140.

Peehl, D.M.;Seto, E. and Feldman, D. Rationale for combination ketoconazole/vitamin D treatment of prostate cancer. *Urology*, **2001** (58), 123-126.

Peehl, D.M.; Seto, E.; Hsu, J.Y. and Feldman, D. Preclinical activity of ketoconazole in combination with calcitriol or the vitamin D analogue EB 1089 in prostate cancer cells. *Journal of Urology*, **2002** (168), 1583-1588.

Peehl, D.M.; Wong, S.T.; Cramer, S.D.; Gross, C. and Feldman, D. Suramin, Hydrocortisone and retinoic acid modify inhibitory effects 1,25-dihydroxyvitamin D_3 on prostatic epithelial cells. *Urologic Oncology*, **1995** (1), 188-294.

Peehl, D.M.; Wong, S.T. and Stamey, T. Vitamin A regulates proliferation and differentiation of human prostatic epithelial cells. *Prostate*, **1993** (23), 69-78.

Pelczynska, M.; Switalska, M.; Kutner, A. and Opolski, A. Antiproliferative activity of vitamin D compounds in combination with cytostatics. *Anticancer Research*, **2006** (26), 2701-2705.

Perkins, J. J.; Zartman, A. E. and Meissner, R. S. Synthesis of 2-(alkylamino)benzimidazoles. *Tetrahedron letters*, **1999** (40), 1103-1106.

Petkovich, M.; Brand, N.J.; Krust, A. and Chambon, P. A human retinoic acid receptor which belongs to the family of nuclear receptors. *Nature*, **1987** (330), 444-450.

Petkovich, M. Retinoic acid metabolism. *Journal of the American Academy of Dermatology*, **2001** (45), S136-S142.

Pienta, K.J. and Esper, P.S. Risk-factors for prostate-cancer. *Annals of Internal Medicine*, **1993** (118), 793-803.

Pettersson, F.; Colston, K.W. and Dalgleish, A.G. Retinoic acid enhances the cytotoxic effects of gemcitabine and cisplatin in pancreatic adenocarcinoma cells. *Pancreas,* **2001** (23), 273-279.

Pienta, K.J.; Nguyen, N.M. and Lehr, J.E. Treatment of prostate cancer in rat with the synthetic retinoid fenretinide. *Cancer Research*, **1993** (53), 224-226.

Pili, R.; Kruszewski, M.P.; Hager, B.W.; Lantz, J. and Carducci, M.A. Combination between phenylbutyrate and 13-cis retinoic acid inhibit prostate tumor growth and angiogenesis. *Cancer Research*, **2001** (61), 1477-1485.

Pollard, M.; Luckert, P.H. and Sporn, M.B. Prevention of primary prostate cancer in Lobund-Wistar rats by *N*-(4-hydroxyphenyl)retinamide. *Cancer Research*, **1991** (51), 3610-3611.

Ponzoni, M.; Bocca, P.; Chiesa, V.; Decensi, A.; Pistoia, V.; Raffaghello, L.; Rozzo, C. and Montaldo, P.G. Differential effects of *N*-(4-hydroxyphenyl) retinamide and retinoic acid on neuroblastoma cells: apoptosis versus differentiation. *Cancer Research*, **1995** (55), 853-861.

Posner, G.H.; Crawford, K.R.; Yang, H.W.; Kahraman, M.; Jeon, H.B.; Li, H.; Lee, J.K.; Suh, B.C.; Hatcher, M.A.; Labonte, T.; Usera, A.; Dolan, P.M.; Kensler, T.W.; Peleg, S.; Jones, G.; Zhang, A.; Korczak, B.; Saha, U. and Chuang, S.S. potent low calcemic selective inhibitors of CYP24 hydroxylase: 24-sulfone analogs of the hormone 1α,25-dihydroxyvitamin D_3. *Journal of Steroid Biochemistry and Molecular Biology*, **2004** (89-90), 5-12.

Powell, I.J. Epidemiology and pathophysiology of prostate cancer in African-american men. *The Journal of Urology*, **2007** (177), 444-447.

Prosser, D.E.; Kaufmann, M.; O'Leary, B.; Byford, V. and Jones G. Single A326G mutation converts human CYP24A1 from 25-OH-D3-24-hydroxylase into -23-hydroxylase, generating 1_,25-(OH)2D3-26,23-lactone. *PNAS*, **2007** (104), 12673-12678.

Prufer, K.; Schroder, C.; Hegyi, K. and Barsony, J. Degradation of RXRs influences sensitivity of rat osteosarcoma cells to the antiproliferative effects of calcitriol. *Molecular Endocrinology*, **2002** (16), 961-976.

Qing, F.L.; Wang, R.; Li, B.; Zheng, X. and meng, W.D. Synthesis of 4,6-disubstituted pyrimidines via Suzuki and Kumada coupling reaction of 4,6-dichloropyrimidine. *Journal Of Fluorine Chemistry*, **2003** (120), 21-24.

Quach, T.D. and Batey, R.A. Ligand- and base-free copper (II)-catalysed C-N bond formation: cross-coupling reactions of organoboron compounds with aliphatic amines and anilines. *Organic Letters*, **2003** (5), 4397-4400.

Rampage, **2004**, http://raven.bioc.cam.ac.uk/rampage.php

Rang, H.P.; Dale, M.M. and Ritter, J.M. The reproductive system, In Rang, H.P.; DDale, M.M. and Ritter, J.M. (eds), *Pharmacology*, **1995**, Churchill Livingstone, 454-474.Rao, A.; Woodruff, R.D.; Wade, W.N.; Kute, T.E. and

Cramer, S.D., Genistein and vitamin D synergistically inhibit human prostatic epithelial cell growth, *Journal of Nutrition*, **2002** (132), 3191-3194.

Rao, C. V. Does full-term pregnancy at a young age protect women against breast cancer. *Obstetrics and Gynecology*, **2000** (96), 783-786.

Rarey, M.; Wefing, S. and Lengauer, T. Placement of medium-sized molecular fragments into active sites of proteins. *Journal of Computer–added Molecular Design*, **1996 b**, (10), 41-54.

Rarey, M.; Kramer, B.; Lengauer, T. and Klebe, G. A fast flexible docking method using an incremental construction algorithm. *Journal of Molecular Biology*, **1996 a** (261), 470-489.

Ravaioli, A. and Tassinari, D. Staging of breast cancer: Recommended standards. *Annals of Oncology*, **2000** (11) *Suppl 3*, 3-6.

Ravichandran, K.G.; Boddupalli, S.S.; Hasemann, C.A.; Peterson, J.A. and Deisenhofer, J. Crystal structure of hemoprotein domain of P450BM-3, aprototype of microsomal P450s. *Science*, **1993** (261), 731-736.

Ray, W.J.; Bain, G.; Yao, M. and Gottlieb, D.I. CYP26, a novel mammalian cytochrome P450, is induced by retinoic acid and defines a new family. *Journal of biological chemistry*, **1997** (272), 18702-18708.

Reichel, H.; Koeffler, H.P. and Norman, A.W. The role of the vitamin-D endocrine system in health and disease. *New England Journal of Medicine*, **1989** (320), 980-991.

Reinhardt, T.A. and Horst, R.L. Ketoconazole inhibits self-induced metabolism of 1,25-dihydroxyvitamin D_3 and amplifies 1,25-dihydroxyvitamin D_3 receptor up-regulation in rat osteosarcoma cells. *Archives of Biochemistry and Biophysics*, **1989** (272), 459-465.

Ridderstrom, M.; Masimirembwa, C.; Trump-Kallmeyer, S.; Ahlefelt, M.; Otter, C. and Andersson, T.B. Arginines 97 and 108 in CYP2C9 are important determinants of the catalytic function. *Biochemical and Biophysical Research Communications*, **2000** (270), 983-987.

Roman, S.D.; Clarke, C.L.; Hall, R.E. and Alexander, I.E. Expression and regulation of retinoic acid receptors in human breast cancer cells. *Cancer Research*, **1992** (52), 2236-2242.

Rosenauer, A.; Nervi, C.; Davison, K.; Lamph, W.W.; Mader, S. and Miller, W.H. Estrogen receptor expression activates the transcriptional and growth-inhibitory response to retinoids without enhanced retinoic acid receptor α expression. *Cancer Research*, **1998** (58), 5110-5116.

Ross, A.C. Retnoid production and catabolism: Role of diet in regulation retinol esterification and retinoic acid oxidation. *The Journal of Nutrition*, **2003** (133), 291S-296S.

Sakr, W.A.; Haas, G.P.; Cassin, B.F.; Pontes, J.E. and Crissman, J.D. The frequency of carcinoma and intraepithelial neoplasia of the prostate in young male patients. *Journal of Urology*, **1993** (150), 379-385.

Sali, A. and Blundell, T.L. Comparative protein modeling by satisfaction of spatial restraints. *Journal of Molecular Biology*, **1993** (234), 779-815.

Santos, M.D.L.; Zambrano, A. and Aranda, A. Combined effects of retinoic acid and histone deacetylase inhibitors on human neuroblastoma SH-SY5Y cells. *Molecular Cancer Therapeutics*, **2007** (6), 1425-1432.

Sato, K.; Kira, M.and Sakurai, H. Oxidative Si-C bond cleavage of Organotrifluorosilanes involving organic group migration from hypercoordinate silicon to oxygen. *Tetrahedron Letters*, **1989** (30), 4375-4378.

Scherr, D.; Pitts, W.R. and Vaughn, E.D. Diethylstilbesterol revisited: androgen deprivation, oesteoporosis and prostate cancer. *Journal of Urology*, **2002** (167), 535-538.

Scherr, D.; Swindle, P.W. and Scardino, P.T. National comprehensive cancer network guidelines for the management of prostate cancer. *Urology*, **2003** (61), 14-24.

Schally, A.V.; Comaru-Schally, A.M.; Plonowski, A.; Nagy, A.; Halmos, G. and Rekasi, Z. Peptide analogs in the therapy of prostate cancer. *Prostate*, **2000** (45), 158-166.

Schmidt, A.F. and Smirnov, V.V. Simple method for enhancement of the ligand-free palladium catalyst activity in the Heck reaction with non-activated bromoarenes. *Journal Of Molecular Catalysis A: Chemical*, **2003** (203), 75-78.

Schoch, G.A.; Yano, J.K.; Wester, M.R.; Griffin K.J.; Stout, C.D. and Johnson, E.F. Structure of human microsomal cytochrome P450 2C8. *Journal of Biological Chemistry*, **2004** (279) (10), 9497-9503.

Schuster, I.; Egger, H.; Astecker, N.; Herzig, G.; Schussler, M. and Vorisek, G. Selective inhibitors of CYP24: mechanistic tools to explore vitamin D metabolism in human keratinocytes. *Steroids*, **2001** (66), 451-462.

Schuster, I.; Egger, H.; Nussbaumer, P. and Kroemer, R.T. Inhibitors of vitamin D hydroxylases: structure-activity relationships. *Journal of Cellular Biochemistry*, **2003** (88), 372-380.

Schwab, M.; Claas, A. and Savelyeva, L. Brca2: A genetic risk factor for breast cancer. *Cancer Letters*, **2002** (175), 1-8.

Schwartz, G.G. and Hulka, B.S. Is vitamin-D deficiency a risk factor for prostate-cancer - (hypothesis). *Anticancer Research*, **1990** (10), 1307-1311.

Schwartz, G.G.; Wang, M.H.; Zang, M.; Singh, R.K. and Siegal, G.P. 1 alpha, 25-dihydroxyvitamin D (calcitriol) inhibits the invasiveness of human prostate cancer cells. *Cancer Epidemiology, Biomarkers and Prevention*, **1997** (6), 727-732.

Seewaldt, V.L.; Johnson, B.S.; Parker, M.B.; Collens, S.J. and Swisshelm, K. Expression of retinoic acid receptor β mediates retinoic acid-induced growth arrest and apoptosis in breast cancer cells. *Cell Growth and Differentiation*, **1995** (6), 1077-1088.

Seidenfeld, J.; Samson, D.J.; Hasselblad, V.; Aronson, N.; Albertsen, P.C.; Bennett, C.L. and Wilt, T.J. Single-therapy androgen suppression in men with advanced prostate cancer: A systematic review and meta-analysis. *Annals of Internal Medicine*, **2000** (132), 566-577.

Seidmon, E.J.; Trump, D.L.; Kreis, W.; Hall, S.W.; Kurman, M.R.; Ouyang, P.; Wu, J.M. and Kremer, A.B. Phase I/II dose escalation study of liarozole in patients with stage D, hormone refractory carcinoma of the prostate. *Annals Surgical Oncology.*, **1995** (2), 550-556.

Shao, Z.M.; Dawson, M.I.; Li, X.S.; Rishi, A.K.; Sheikh, M.S.; Han, Q.X.; Ordonez, J.V.; Shroot, B. and Fontana, J.A. P-53 independent G0/G1 arrest and apoptosis induced by a novel retinoid in human breast cancer cells. *Oncogene*, **1995** (11), 493-504.

Sharp, R.M.; Bello-DeOcampo, D.; Quader, S.T. and Webber, M.M. *N*-(4-hydroxyphenyl) retinamide (4-HPR) decreases neoplastic properties of human prostate cells: an agent for prevention. *Mutation Research*, **2001** (496), 163-170.

Sheikh, M.S.; Shao, Z.M.; Li, X.S.; Dawson, M.; Jetten, A.M.; Wu, S.; Conley, B.A.; Garcia, M.; Rochefort, H. and Fontana, J.A. Retinoid-resistant estrogen receptor-negative human breast carcinoma cells transfected with retinoic acid receptor α acquire sensitivity to growth inhibition by retinoids. *Journal of Biological Chemistry*, **1994** (269), 21440-21447.

Shen, J.C.; Wang, T.T.; Chang, S. and Hursting, S.D. Mechanistic studies of the effects of the retinoid *N*-(4-hydroxyphenyl)retinamide on prostate cancer cell growth and apoptosis. *Molecular Carcinogenesis*, **1999** (24), 160-168.

Shipley, W.U.; Thames, H.D.; Sandler, H.M.; Hanks, G.E.; Zietman, A.L.; Perez, C.A.; Kuban, D.A.; Hancock, S.L. and Smith, C.D. Radiation therapy for clinically localized prostate cancer - a multi-institutional pooled analysis. *Jama-Journal of the American Medical Association*, **1999** (281), 1598-1604.

Shirai, T.; Asamoto, M.; Takahashi, S. and Imaida, K. Diet and prostate cancer. *Toxicology*, **2002** (181-182), 89-94.

Silva Idos, S. Alcohol, tobacco and breast cancer: Should alcohol be condemned and tobacco acquitted. *British Journal of Cancer,* **2002** (87), 1195-1196.

Simmons, D.L.; Lalley, P.A. and Kapser, C.B. Chromosomal assignments of genes coding for components of the mixed-function oxidase system in mice: Genetic localisation of the cytochrome P450 PB gene families and the NADPH-cytochrome P450 oxidoreductase and epoxide hydratase genes. *Journal of Biological Chemistry*, **1985** (260), 515-521.

Skinner, S.J.M. and Akhtar M. The stereospecific removal of a C-19 hydrogen atom in estrogen biosynthesis. *Biochemical Journal.*, **1969** (114), 75-81.

Skladanowski, A. and Konopa, J. Mitoxantrone and ametantrone induce interstrand cross-links in DNA of tumour cells. *British Journal of Cancer*, **2000** (82), 1300-1304.

Small, E. J. Prostate cancer, incidence, management and outcomes. *Drugs and Aging,* **1998** (13), 71-81.

Smith, H. J.; Nicholls, P. J.; Simons, C. and Le Lain, R. Inhibitors of steroidogenesis as agents for the treatment of hormone-dependent cancers. *Expert Opinion of Therapeutic Patents,* **2001** (11), 789-824.

Sonneveld, E.; van den Brink, C.E.; van der Leede, B.M.; Schulkes, R.K.; Petkovich, M.; van der Burg, B. and van der Saag, P.T. Human retinoic acid (RA) 4-hydroxylase (CYP26) is highly specific for all-trans-RA and can be induced through RA receptors in human breast and colon carcinoma cells *Cell Growth and Differentiation*, **1998** (9), 629-637.

South calorina prostate cancer institute 2003, URL: http://www.scprostatecancer.com/prostate_cancer/anatomy.htmL, last updated: may 2003, accessed date: 15 July 2005

Sporn, M.B.; Roberts, A.B. and Goodman, D.S. *The retinoids: Biology, chemistry and medicine*, **1994**, Raven Press, New-York.

Srinivasan, J.; Castellino, A.; Bradley, E.K.; Eksterowicz, J.E.; Grootenhuis, P.D.; Putta, S. and Stanton, R. V. Evaluation of a novel shape-based computational filter for lead evolution: Application to thrombin inhibitors. *Journal of Medicinal Chemistry*, **2002** (45), 2494-2500.

Stamey, T.A.; Yemoto, C.M.; McNeal, J.E.; Sigal, B.M. and Johnstone, I.M. Prostate cancer is highly predictable: a prognostic equation based on all morphological variables in radical prostatectomy specimens. *Journal of Urology*, **2000** (163), 1155-1160.

Steele, N.; Zekri, J.; Coleman, R.; Leonard, R.; Dunn, K.; Bowman, A.; Manifold, I.; Kunkler, I.; Purohit, O. and Cameron, D. Exemestane in metastatic breast cancer: effective therapy after third-generation non-steroidal aromatase inhibitor failure. *The Breast*, **2006** (15), 429.

Steinbild, S.; Mross, K.; Frost, A.; Morant, R.; Gillessen, S.; Dittrich, C.; Strumberg, D.; Hochhaus,A.; Hanauske, A. R.; Edler, L.; Burkholder, I. and Scheulen, M. A clinical phase II study with sorafenib in patients with progressive hormone-refractory prostate cancer: a study of the CESAR Central European Society for Anticancer Drug Research-EWIV. *The British Journal of Cancer*, **2007** (97), 1480-1485.

Stoppie, P.; Borgers, M.; Borghgraef, P.; Dillen, L.; Goossens, J.; Sanz, G.; Szel, H.; Van Hove, C.; Van Nyen, G.; Nobels, G.; Vanden Bossche, H.; Venet, M.; Willemsens, G. and Van Wauwe, J. R115866 inhibits all-*trans*-retinoic acid metabolism and exerts retinoidal effects in rodents. *The Journal of Pharmacology and Experimental Therapeutics*, **2000** (293), 304-312.

Sun, S.Y.; Yue, P. and Lotan, R. Induction of apoptosis by *N*-(4-hydroxyphenyl)retinamide and its association with reactive oxygen species, nuclear retinoic acid receptors, and apoptosis-related genes in human prostate carcinoma cells. *Molecular Pharmacology*, **1999** (55), 403-410.

Sung, V. and Feldman, D. 1,25-dihydroxyvitamin D3 decreases human prostate cancer cell adhesion and migration. *Molecular and Cellular Endocrinology*, **2000** (164), 133-143.

Sutcliffe, M.J.; Haneef, I; Carney, D. and Blundell, T.L. Knowledge based modelling of homologous protein, part I: three-dimensional frameworks derived from the simultaneous superposition of multiple structures. *Protein Engineering*, **1987** (1), 377-384.

Sutcliffe, M.J.; Hayes, F.R. and Blundell, T.L. Knowledge based modelling of homologous protein, part II: rules for the conformation of substituted sidechains. *Protein Engineering*, **1987** (1), 385-392.

Suzuki A. Recent advances in the cross-coupling reactions of organoboron derivatives with organic electrophiles. *Journal of Organometallic Chemistry*, **1999** (576), 147-168.

SWISSMODEL, 2004, http://www.expasy.org/swissmod/SWISS-MODEL.htmL.

Swiss-PDB, 2004, http://www.expasy.org/spdbv/

Taimi, M.; Helvig, C.; Wisniewski, J.; Ramshaw, H.; White, J.; Amad, M.; Korczak, B. and Petkovich, M. A novel human cytochrome P450, CYP26C1, involved in metabolism of 9-*cis* and all-*trans* isomers of retinoic acid. *Journal of Biological Chemistry*, **2004** (279), 77-85.

Tallman, M.S.; Nabhan, C.; Feusner, J.H. and Rowe, J.M. Acute promyelocytic leukemia: evolving therapeutics strategies. *Blood*, **2002** (99), 759-767.

Tan, A.R. and Swain, S.M. Adjuvant chemotherapy for breast cancer: an update. *Seminars in Oncology*, **2001** (28), 359-376.

Tang, G. and Russell, R.M. 13-*cis* Retinoic acid is an endogenous compound in human serum. *Journal of Lipid Research*, **1990** (30), 175-182.

Tavassoli, F. A. Ductal intraepithelial neoplasia of the breast. *Virchows Archive,* **2001** (438), 221-227.

Teixeira, C. And pratt, M.A.C. CDK2 is a target for retinoic acid-mediated growth inhibition in MCF-7 human breast cancer cells. *Molecular Endocrinology*, **1997** (11), 1191-1201.

The Prostate Cancer Charity, Treating prostate cancer, **2003**, URL: http://www.prostate-cancer.org.uk.

Thacher, S.M.; Vasudevan, J.; Tsang, K.; Nagpal, S. and Chandraratna, R.A.S. New dermatological agents for the treatment of psoriasis. *Journal of Medicinal Chemistry*, **2001** (44), 281-297.

Thompson, J.D.; Higgins, D.G. and Gibson, T.J. CLUSTAL W: improving the sensitivity of progressive multiple sequence alignment through sequence weighting, position-specific gap penalties and weight matrix choice. *Nucleic Acids Research*, **1994** (22), 4673-4680.

Thompson, W. D. Genetic epidemiology of breast cancer. *Cancer,* **1994** (74), 279-287.

Toma, S.; Isnardi, L.; Raffo, P.; Dastoli, G.; Francisci, E.D.; Riccardi, L.; Palumbo, R. and Bollag, W. Effects of all-*trans*-retinoic acid and 13-cis retinoic acid on breast cancer cell lines: growth inhibition and apoptosis induction. *International Journal of Cancer*, **1997** (70), 619-627.

Tong, A.; Palmer, S.C.; Elder, G. and Craig, J.C. Calcimimetics for secondary hyperparathyroidism in chronic kidney disease patients. *Cochrane Database of Systematic Reviews*, **2006** (4), 521-525.

Tripos SYBYL 7.0, Tripos Inc 1699 South Hanley Rd St Louis Missouri 63144 USA http://www.tripos.com

Trump, D.L.; Hershberger, P.A.; Bernardi, R.J.; Ahmed, S.; Muindi, J.; Fakih, M.; Yu, W.D. and Johnson, C.S. Anti-tumor activity of calcitriol: pre-clinical and clinical studies. *Journal of Steroid Biochemistry and Molecular Biology*, **2004** (89-90), 519-526.

Trump, D.L.; Smith, D.C.; Stiff, D.; Adedoyin, A.; Day, R.; Bahnson, R.R.; Hofacker, J. and Branch, R.A. A phase II trial of all-*trans*-retinoic acid in hormone-refractory prostate cancer: a clinical trial with detailed pharmacokinetic analysis. *Cancer Chemotherapy and Pharmacology*, **1997** (39), 349-356.

Uauy, R. and Solomons, N. Diet nutrition and the life course approach to cancer prevention. *Journal of Nutrition*, **2005** (135) 10-17.

Underwood, B.A. and Arthur, P. The contribution of vitamin A to public health. *FASEB Journal*, **1996** (10), 1040-1048.

Vaishampayan, U.; Hussain, M.; Seren, S.; Sakar, F.H.; Forman, J.D.; Powell, I.; Pontes, J.E. and Kucuk, O. Lycopene and soy isoflavones in the treatment of prostate cancer. *Nutrition and Cancer An International Journal*, **2007** (59), 1-7.

Van der Burg, B.; Van der Leede, B.M.; Kwakkenbos-Isbrucker, L.; Salverda, S.; De Laat, S.W. and Van der Saag, P.T. Retinoic acid resistance of oestradiol-independent breast cancer cells coincides with diminished retinoic acid receptor function. *Molecular and Cellular Endocrinology*, **1993** (91), 149-157.

Van Heusden, J.; Wouters, W.; Ramakaers, F.C.S.; Krekels, M.D.W.G.; Dillen, L.; Borgers, M. and Smets, G. The anti-proliferative activity of ATRA catabolites and isomers is differentially modulated by liarozole-fumarate in MCF-7 human breast cancer cells. *British Journal of Cancer*, **1998** (77), 1229-1235.

Van Heusden, J.; Van Ginckel, R.; Bruwiere, H.; Moelans, P.; Janssen, B.; Floren, W.; Vande Leede, B.J.; Van Dun, J.; Sanz, G.; Venet, M.; Dillen, L.; Van Hove, C.; Willemsens, G.; Janicot, M. and Wouters, W. Inhibition of all-*trans* retinoic acid metabolism by R116010 induced antitumor activity. *British Journal of Cancer*, **2002** (86), 605-611.

Van Wauwe, J.; Coene, M.C.; Goossens, J.; Cools, W. and Monbaliu, J. Effects of cytochrome P450 inhibitors on the *in vivo* metabolism of all-*trans*-retinoic acid in rats. *Journal of Pharmacology and Experimental Therapeutics*, **1990** (252), 365-369.

Van Wauwe, J.; Vannyen, G.; Coene, M.C.; Stoppie, P.; Cools, W.; Goossens, J.; Borghgraef, P. and Janssen, P.A.J. Liarozole, an inhibitor of retinoic acid metabolism, exerts retinoid-mimetic effects in *vivo*. *Journal of Pharmacology and Experimental Therapeutics*, **1992** (261), 773-779.

Verify3D, 2004, http://www.doe-mbi.ucla/Services/Verify_3D/

Vicini, F.A.; Kini, V.R.; Edmundson, G.; Gustafson, G.S.; Stromberg, J. and Martinez, A. A comprehensive review of prostate cancer brachytherapy: Defining an optimal technique. *International Journal of Radiation Oncology Biology Physics*, **1999** (44), 483-491.

Vickers, A. How should we define patients who are at high risk of death from prostate cancer. *Nature Clinical Practice Urology*, **2007** (4), 646-647.

Wakeling, A. E. and Bowler, J. Steroidal pure antioestrogens. *Journal of Endocrinology*, **1987** (112), R7-10.

Wakeling, A.E. and Bowler, J. Development of novel oestrogen-receptor antagonists. *Biochemical Society Transactions*, **1991** (19), 899-901.

Wakeling, A.E. Similarities and distinctions in the mode of action of different classes of anti-oestrogens. *Endocrine-Related Cancer*, **2000** (7), 17-28.

Walters, W.P.; Stahl, M.T.; Murcho, M.A. Virtual Screening-An overview. *Drug Discovery Today*, **1998** (3), 160-178.

Wang, X.; Yin, L.; Rao, P.; Stein, R.; Harsch, K.M.; Lee, Z. and Heston, W.D. Targeted treatment for prostate cancer. *Journal of Cellular Biochemistry*, **2007** (102), 571-579.

Wang, J.; Kollman, P.A. and Kuntz, I.D. Flexible ligand docking: A multistep strategy approach. *Proteins*, **1999** (36), 1-19.

Wang, J.; Eltoum, I. and Lamartiniere, C. Dietary genistein suppresses chemically induced prostate cancer in Lobund-Wistar rats. *Cancer Letters*, **2002** (186), 11.

Warmuth, M. A.; Sutton, L. M. and Winer, E. P. A review of hereditary breast cancer: From screening to risk factor modification. *American Journal of Medicine,* **1997** (102), 407-415.

Waterman, M.R.; John, M.E.; Simpson, E.R. Regulation of synthesis and Activity of cytochrome P-450 enzymes in physiological pathways; In: Ortiz de Montellano, P.R., Ed, *Cytochrome P450: Structure and biochemistry,* **1986**, New York: Plenum Press, 345-386.

Webber, M.M. and Waghary, A. Urokinase-mediated extracellular matrix degradation by human prostatic carcinoma cells and its inhibition by retinoic acid. *Clinical Cancer Research*, **1995** (1), 755-761.

Weindl, G.; Roeder, A.; Schafer-Korting, M.; Schaller,M. and Korting, H.C. Receptor-selective retinoids for psoriasis. Focus on tazarotene. *American Journal of Clinical Dermatology*, **2006** (7), 85-97.

Weiner, S.J.; Kollman, P.A.; Nguyen, D.T. and Case, D.A. An all atom force field for simulations of proteins and nucleic acids. *Journal of Computational Chemistry,* **1986** (7), 230-237.

Weiner, S.J.; Kollman, P.A.; Case, D.A.; Singh, U.C.; Ghio,C.; Alagona, G.; Profeta, S. and Weiner, P. A new force field for molecular mechanical simulation of nucleic acids and proteins. *Journal of the American Chemical Society* **1984** (106), 765-784.

Weiss, G.R.; Liu, P.Y.; Alberts, D.S.; Peng, Y.M.; Fisher, E.; Xu, M.J.; Scudder, S.A.; Baker, L.H.; Moore, D.F. and Lippman, S.M, 13-*cis*-Retinoic acid or all-*trans* retinoic acid plus inteferon-alpha in recurrent cervical cancer: A Southwest Oncology Group phase II randomized trial. *Gynecology and Oncology,* **1998** (71), 386-390.

Weiss, H. A.; Brinton, L. A.; Brogan, D.; Coates, R. J.; Gammon, M. D.; Malone, K. E.; Schoenberg, J. B. and Swanson, C. A. Epidemiology of in *situ* and invasive

breast cancer in women aged under 45. *British Journal of Cancer,* **1996** (73), 1298-1305.

Welsh, W.; Ruppert, J. and Jain, A.N. Hammer-Head: fast, fully automated docking of flexible ligand to protein binding sites. *Chemica. Biol*ogy drug design, **1996** (3), 449-462.

Wessjohann, L. and Gabriel, T. Chromiumm (II) mediated reformatsky reactions of carboxylic esters with aldehydes. *Journal of Organic Chemistry*, **1997** (62), 3772-3774.

Wester, M.R.; Yano, J.K.; Schoch, G.A.; yang, C.; Griffin, K.J.; Stout, C.D. and Johnson, E,F. The structure of human cytochrome P450 2C9 complexed with flubiprofen at 2.0-Å resolution. *Journal of Biological Chemistry*, **2004** (279) (34), 35630-35637.

White, J.A.; Beckett-Jones, B.; Yu-Ding, G.; Dilworth, F.J.; Bonasoro, J.; Jones, G. and Petkovich, M. cDNA cloning of human retinoic acid-metabolizing enzyme (hp450RAI) identifies a novel family of cytochromes P450 (CYP26). *Journal of Biological Chemistry*, **1997** (272), 18538-18541.

White, J.A.; Guo, Y.D.; Baetz, K.; Beckett-Jones, B.; Bonasoro, J.; Hsu, K.E.; Dilworth, J.; Jones, G. and Petkovich, M. Identification of the retinoic acid-inducible all-*trans*-retinoic acid 4-hydroxylase. *Journal of Biological Chemistry*, **1996** (271), 29922-29927.

WHO. *Cancer: Incidence, mortality and survival databases,* updated **2003**, http://www.who.int/mediacentre/news/releases/2003/pr27/en/.

Wilding, G. Endocrine control of prostate cancer. *Cancer Survey,* **1995** (23), 43-62.

Williams, P.A.; Cosme, J.; Sridhar, V.; Johnson, E.F. and McRee, D.E. Mammalian microsomal cytochrome P450 monooxygenase: structural adaptations for membrane binding and functional diversity. *Molecular Cell*, **2000** (5), 121-131.

Williams, P.A.; Cosme, J.; Ward, A.; Angove, H.C.; Matak-Vinkovic, D. and Jhoti, H. Crystal structure of human cytochrome P450 2C9 with bound warfarin. *Nature*, **2003** (424), 464-468.

Wipf, P. Transmetalation reactions in organocopper chemistry. *Synthesis*, **1993**, 537-557.

Wink, M.H.; De la Rosette, J.J.; Grimbergen, C.A. and Wijkstra, H. Transrectal contrast enhanced ultrasound for diagnosis of prostate cancer. *World Journal of Urology*, **2007** (25), 367-373.

Wolf, J.P. and Buchwald, S.L. Room temperature catalytic amination of aryl iodides. *Journal of Organic Chemistry*, **1997** (62), 6066-6068.

Wu, A. H.; Wan, P.; Hankin, J.; Tseng, C. C.; Yu, M. C. and Pike, M. C. Adolescent and adult soy intake and risk of breast cancer in asian-americans. *Carcinogenesis,* **2002** (23), 1491-1496.

Wu, Q.; Chen, Z. and Su, W. Anticancer effect of retinoic acid via AP-1 activity repression is mediated by retinoic acid receptor α and β in gastric cancer cells. *International Journal of Biochemistry and Cell Biology*, **2002** (34), 1102-1114.

Xu, C. and Yuan, C. Candida rugosa lipase catalysed kinetic resolution of β-hydroxy-β-arylpropionates and δ-hydroxy-δ-aryl-β-oxo-pentanoates. *Tetrahedron*, **2005** (61), 2169-2186.

Xue, L.; Lipkin, M.; Newmark. H. and Wang, J. Influence of dietary calcium and vitamin D on diet-induced epithelial cell hyperproliferation in mice. *Journal of the National Cancer Institute*, **1999** (91), 176-181.

Yamamoto, T.; Nishityama, M. and Koie, Y. Palladium-catalysed synthesis of triarylamines from aryl halides and diarylamines. *Tetrahedron Letters*, **1998** (39), 2367-2370.

Yano, J.K.; Wester, M.R.; Schoch, G.A.; Griffin, K.J.; Stout, C.D. and Johnson, E.F. The structure of human cytochrome P4503A4 determined by X-ray crystallography to 2.05-Å resolution. *Journal of Biological Chemistry*, **2004** (279) (37), 38091-38094.

Yee, S.W.; Jarno, L.; Gomaa, M.S.; Elford, C.; Ooi, L.; Coogan, M.P.; McClelland, R.; Nicholson, R.I.; Evans, B.A.J.; Brancale, A. and Simons, C. Novel tetralone-derived retinoic acid metabolism blocking agents: Synthesis and in vitro evaluation with liver microsomal and MCF-7 CYP26A1 cell assays. *Journal of Medicinal Chemistry*, **2005** (48), 7123-7131.

Yee, S.W.; Campbell, M.J. and Simons, C. Inhibition of vitamin D_3 metabolism enhances VDR signaling in androgen-independent prostate cancer cells. *Journal of Steroid Biochemistry and Molecular Biology*, **2006** (98), 228-235.

Ylikomi, T.; Laaksi, I.; Lou, Y.R.; Martikainen, P.; Pennanen, P.; Purmonen, S.; Syvala, H.; Vienonen, A. and Tuohimaa, P. Antiproliferative action of vitamin D. *Vitamin Hormone*, **2002** (64), 357-406.

Yu, V.C.; Delsert, C.; Andersen, B.; Holloway, J.M.; Devary, O.V.; Naar, A.M.; Kim, S.Y.; Boutin, J.M.; Glass, C. and Rosenfeld, M.G. RXRβ: A co-regulator that enhances binding of retinoic acid, thyroid hormone and vitamin D receptors to their cognate response elements. *cell*, **1991** (67), 1251-1266.

Yu, Y.; Zhou, Q.; Hang, Y.; Bu, X. and Jia, W. Antiestrogenic effect of 20s-protopanaxadiol and it's synergy with tamoxifen on breast cancer cells. *Cancer*, **2007** (109), 2374-2382.

Zagars, G.K.; Johnson, D.E.; Voneschenbach, A.C. and Hussey, D.H. Adjuvant estrogen following radiation-therapy for stage-c adenocarcinoma of the prostate - long-term results of a prospective randomized study. *International Journal of Radiation Oncology Biology Physics*, **1988** (14), 1085-1091.

Zagars, G.K.; Pollack, A. and Voneschenbach, A.C. Prognostic factors for clinically localized prostate carcinoma - analysis of 938 patients irradiated in the prostate specific antigen era. *Cancer*, **1997** (79), 1370-1380.

Zandt, M.C.V.; Jones, M.L.; Gunn, D.E.; Geraci, L.S.; Jones, J.H.; Sawicki, D.R.; Sredy, J.; Jacot, J.L.; DiCiocci, A.T.; Petrova, T.; Mitschler, A. and Podjarny, A.D. Discovery of 3-[(4,5,7-trifluorobenzothiazol-2-yl)methyl]indole-*N*-acetic acid (Lidorestat) and congeners as highly potent and selective inhibitors of aldose reductase for treatment of chronic diabetic complications. *Journal Of Medicinal Chemistry*, **2005** (48), 3141-3152.

Zeldin, D.C.; DuBois, R.N.; Falck, J.R. and Capdevila, J.H. Molecular cloning expression and characterization of an endogenous human cytochrome P450 arachidonic acid epoxygenase isoform. *Archives of Biochemistry and Biophysics*, **1995** (322), 76-86.

Zhang, H.; Coville, P.F.; Walker, R.J.; Miners, J.O.; Birkett, D.J. and Wanwimolruk, S. Evidence for involvement of human CYP3A4 in the 3-hydroxylation of quinine. *British Journal of Clinical Pharmacology*, **1997** (43), 245-252.

Zhang, Q.Y.; Dunbar, D. and Kaminsky, L. Human cytochrome P-450 metabolism of retinals to retinoic acids. *Drug Metabolism and Disposition*, **2000** (28), 292-297.

Zhao, J.; Tan, B.K.; Marcelis, S.; Verstuyf, A. and Bouillon, R. Enhancement of antiproliferative activity of 1 alpha,25- dihydroxyvitamin D-3 (analogs) by cytochrome P450 enzyme inhibitors is compound- and cell-type specific. *Journal of Steroid Biochemistry and Molecular Biology*, **1996** (57), 197-202.

Zhao, X.Y. and Feldman, D. The role of vitamin D in prostate cancer. *Steroids*, **2001** (66), 293-300.

Zhao, X.Y.; Ly, L.H.; Peehl, D.M. and Feldman, D. Induction of androgen receptor by 1 alpha,25-dihydroxyvitamin D_3 and 9-cis retinoic acid in LNCaP human prostate cancer cells. *Endocrinology*, **1999** (140), 1205-1212.

Zhuang, S.H. and Burnstein, K.L. Antiproliferative effect of 1 alpha,25-dihydroxyvitamin D_3 in human prostate cancer cell line LNCaP involves reduction of cyclin-dependent kinase 2 activity and persistent G1 accumulation. *Endocrinology*, **1998** (139), 1197-1207.

Zhu, W.Y.; Jones, C.S.; Kiss, A.; Matsukuma, K.; Amin, S. and Luca, L.M.D. Retinoic acid inhibition of cell cycle progression in MCF-7 human breast cancer cells. *Experimental Cell Research*, **1997** (234), 293-299.

Zietman, A.L.; Coen, J.J.; Dallow, K.C. and Shipley, W.U. The treatment of prostate-cancer by conventional radiation-therapy - an analysis of long-term outcome. *International Journal of Radiation Oncology Biology Physics*, **1995** (32), 287-292.

Zincke, H.; Bergstralh, E. J.; Blute, M. L.; Myers, R. P.; Barrett, D. M.; Lieber, M. M.; Martin, S. K. and Oesterling, J. E. Radical prostatectomy for clinically localized prostate cancer: Long- term results of 1,143 patients from a single institution. *Journal of Clinical Oncology,* **1994** (12), 2254-2263.